Material development and characterisation of a functionalised biomaterial to support pancreatic islet viability.

AUTHOR(S)

Liam McDonough

CITATION

McDonough, Liam (2019): Material development and characterisation of a functionalised biomaterial to support pancreatic islet viability.. Royal College of Surgeons in Ireland. Thesis.
https://doi.org/10.25419/rcsi.10764128.v1

DOI

10.25419/rcsi.10764128.v1

RCSI

Material development and characterisation of a functionalised biomaterial to support pancreatic islet viability.

Liam McDonough MPharm MPSI

A thesis submitted to the School of Postgraduate Studies, Royal College of Surgeons in Ireland, in fulfilment of the degree of Doctor of Philosophy.

Supervisors:

Dr. Helena Kelly

Prof. Garry Duffy

July 2019

Candidate Thesis Declaration

I declare that this thesis, which I submit to RCSI for examination in consideration of the award of a higher degree of Doctor of Philosophy is my own personal effort. Where any of the content presented is the result of input or data from a related collaborative research programme this is duly acknowledged in the text such that it is possible to ascertain how much of the work is my own. I have not already obtained a degree in RCSI or elsewhere on the basis of this work. Furthermore, I took reasonable care to ensure that the work is original, and, to the best of my knowledge, does not breach copyright law, and has not been taken from other sources except where such work has been cited and acknowledged within the text.

Signed: _____

Student Number: _____

Date: _____

Table of Contents

List of Abbreviations

- **ATMP** Advanced therapy medicinal product
- **ATP-K^+** Adenosine triphosphate sensitive potassium channel
- **βGP** β-glycerophosphate disodium salt hydrate
- **CaO_2** Calcium Peroxide
- **CAT** Committee for advanced therapies
- **CGM** Continuous glucose monitoring
- **CO_2** Carbon Dioxide
- **DIY APS** Do-it-yourself artificial pancreas
- **DLS** Dynamic light scattering
- **DM** Diabetes mellitus
- **DRIVE** Diabetes reversing implants with enhanced viability and long-term efficacy
- **EC** European Commission
- **ECM** Extracellular matrix
- **EMA** European medicines agency
- **F6H8** Perfluorohexyloctane
- **FBG** Fasting blood glucose
- **FF** Free floating
- **FFI** Free floating islets
- **G'** Storage modulus
- **G''** Loss Modulus
- **GLUT** Glucose transporter
- **GSIS** Glucose stimulated insulin secretion
- **GSX** Glucose stimulation index
- **GTMP** Gene therapy medicinal product
- **h** Hour
- **H_2O_2** Hydrogen peroxide
- **HA** Hyaluronic acid
- **HA-TA** Hyaluronic acid tyramine
- **HCl** Hydrochloric acid
- **HRP** Horse radish peroxidase

- **HUVEC** Human umbilical vein endothelial cell
- **ICH** International Council for Harmonisation
- **IEQ** Islet equivalents
- **IIDP** Integrated Islet Distribution Program
- **iPSCs** Induced pluripotent stem cells
- **ISO** International Organisation for Standardisation
- **kg** Kilogram
- **kGy** Kilogray
- **KRB** Krebs-Ringers Buffer
- **MC** Methylcellulose
- **MCC** Methylcellulose/collagen
- **MgO_2** Magnesium Peroxide
- **mm** Millimetre
- **mM** Milllimolar
- **mL** Millilitre
- **min** Minute
- **MS** Member State
- **µL** Microlitre
- **µm** Micrometre
- **µM** Micromolar
- **natHA** Native HA
- **NHP** Non-human primate
- **O_2** Oxygen
- **OLM** One-layer method
- **PBS** Phosphate buffered saline
- **PDI** Poly dispersity index
- **PDMS** Polydimethylsiloxane
- **PFC** Perfluorocarbon
- **PFD** Perfluorodecalin
- **PFOB** Perfluoro—oxtyl bromide
- **PI** Pseudoislet
- **PLA** Poly-lactic acid

- **PLGA** Poly(lactic-co-glycolic)
- **PP** Pancreatic protein
- **PPBG** Post-prandial blood glucose
- **PTFE** Polytetrafluorethylene
- **PVP** Poly(vinyl pyrrolidone)
- **sCTMP** Somatic cell therapy medicinal product
- **SMBG** Self-monitoring blood glucose
- **sec** Second [time]
- **STZ** Streptozotocin
- **T1D** Type 1 Diabetes
- **T2D** Type 2 Diabetes
- **TE** Tissue engineered
- **TLM** Two-layer method
- **VEGF** Vascular endothelial growth factor
- **WHO** World Health Organisation

List of Figures

List of Tables

Summary (300 words)

Diabetes mellitus is a chronic disease which affects over 425 million people worldwide (2017), a number which is expected to rise to 629 million people by 2045. Diabetes mellitus occurs when the pancreas does not produce enough insulin to meet the demands of the body, due to the malfunction or immune-mediated destruction of the insulin producing β-cells.

The bio-artificial pancreas approach aims to return endogenous insulin production to the patient, by delivering donor pancreatic islets encapsulated in a supportive biomaterial and protected by a semi-permeable immunoisolating shell. The overall objective of the research in this PhD thesis is to develop a novel functionalised biomaterial suitable for use as the extracellular matrix in a bio-artificial pancreas. This functionalised biomaterial would first be assessed *in vitro* with a suitable cell model and then undergo process development and scale-up manufacture for use in pre-clinical small and large animal model *in vivo* testing.

The functionalised biomaterial was formulated as a native hyaluronic acid hydrogel, functionalised with a perfluorodecalin oxygen carrier emulsion. The formulated biomaterial showed rheological characteristics suitable for delivery to a bio-artificial pancreas and improved oxygen storage characteristics compared to non-functionalised hydrogels.

In vitro testing of the biomaterial seemed to show that is was not beneficial to a β-cell line. However it was shown to be biocompatible by an International Organisation for Standardisation (ISO) validated method and also showed biocompatibility with human islets *in vitro*.

Process development of the biomaterial resulted in the development of a protocol for its preparation that was successfully transferred to facilitate the *in vivo* testing. In a large animal model the biomaterial was successfully filled into a semi-permeable immunoisolating shell. In the small animal model the biomaterial showed efficacy when used to deliver primary rat islets cells to the rat model, showing improved fasting and post-prandial blood glucose for up to 8 weeks.

Acknowledgements

Firstly, I would like to give my sincere thanks to my two supervisors, Dr Helena Kelly and Prof. Garry Duffy. Thank you very much for the support and guidance you provided over the past 3 and a bit years. Thank you for the advice that has turned me into a better researcher/pharmacist, and particular thanks for instilling the change in my mind-set that a negative result makes for a good discussion!

Having spent a large portion of time between two labs over the duration of my PhD, I would like to thank the technicians for all there help over that time. In the Pharmacy Research Lab I have to thank Danielle, Eoin, Jim, Colin and Peter for all their help with my strange oxygen requirements and requests to borrow expensive equipment. From TERG I need to thank Johnny and Vinny for their help and patience over the years, particularly with all the work needed to get the hypoxia chamber functional for relatively few experiments. In addition to the technicians, I would also like to thank Dr Brenton Cavanagh for all his help with fluorescent microscopy, Dr Seóna Rossi for her help understanding the rheometer, and Dr Christina Payne for training me to prepare her methylcellulose gel.

I would like to acknowledge the assistance provided to everyone who has been part of the DRIVE team in the RCSI over the years. Thanks to Assist. Prof. Eduardo Ruiz-Hernandez for all his help in the first year of my PhD. I would like to thank Dr Eimear Dolan for all her help in the lab, although particular thanks must be given for all your help with the rat islet isolations. I would like to thank Dr Liam Burke for his help in perfecting presentations. I would like to thank Rita Ibañez for her assistance on the insulin diffusion work. Finally I would like to thank Dr Laura Gallagher for her help in the final stretch in setting up the INS-1E cells and running the final *in vitro* work.

The DRIVE project has been a great experience and I would like to acknowledge everyone who has made the project possible, and in particular I would like to acknowledge the training, assistance and materials provided by different partners of the project. I would like to thank the partners at DCU for providing the MIN6 cell line, and for their assistance and advice in running GSIS assays. I would like to thank the partners in UCD for providing the β-shell samples for preliminary tests and shells that were used in the *in vivo* work. I would like to thank the partners at Boston Scientific for their assistance in developing the oxygenation protocol for the natHA/PFD

emulgels. I would like to thank Abiel srl for providing training on the rat islet isolation and for their work in running the *in vivo* rat experiments. I would like to thank the partners in EXPLORA Biotech for their work with the large animal studies. I would also like to thank the partners at NUIG for their work on the large animal model and also for providing the immunoisolating shells used for the *in vitro* INS-1E testing. I would like to thank DRIVE partners at Oxford for the preliminary human islet data. I would like to thank DRIVE partners at Innocore for providing the VEGF microspheres used in the small animal *in* vivo work. Finally I would like to thank the DRIVE partners at EKUT for hosting me for my Erasmus+ placement for 2 months.

I would like to acknowledge that the INS-1E cell line was provided by Prof. Pierre Maechler, University of Geneva Medical Centre.

Funding Acknowledgement

Funding for this project was provided through the DRIVE project, which received funding from the European Union's Horizon 2020 research and innovation programme under grant agreement number 645991. Additional funding was received for the Erasmus+ placement through the Erasmus Plus Programme of the European Union and the Royal College of Surgeon's in Ireland.

Invention disclosure forms/Presentations

Invention disclosure form

2018 – An inventor on an invention disclosure form, submitted for the invention "*Oxygel: An injectable, crosslinkable hydrogel composed of tyramine derivatised hyaluronic acid and perfluorocarbons for the intramyocardial delivery of oxygen and structural support post myocardial infarction*".

Presentations

L. McDonough, L. Gallagher, B. Cavanagh, G.P. Duffy, H.M. Kelly. *Formulation of a functionalised biomaterial to support cell viability for the treatment of diabetes mellitus*; In: Tissue Engineering International and Regenerative Medicine European Chapter Meeting, Rhodes, 2019. Oral Presentation.

L. McDonough, L. Gallagher, B. Cavanagh, G.P. Duffy, H.M. Kelly. *Formulation of a functionalised biomaterial to support cell viability for the treatment of diabetes mellitus*; In: Royal College of Surgeons Annual Research Day, Dublin, 2019. Poster Presentation.

L. McDonough, E.B Dolan, L.P. Burke, G.P. Duffy, H.M Kelly. *Material development and characterisation of a functionalised biomaterial to support transplanted pancreatic islet viability*; In: Controlled Release Society Meeting, New York, 2018. Poster Presentation.

L. McDonough, E.B Dolan, L.P. Burke, G.P. Duffy, H.M Kelly. *Formulation of a functionalised biomaterial to support cell viability for the treatment of diabetes mellitus*; In: Royal College of Surgeons Annual Research Day, Dublin, 2018. Oral Presentation.

L. McDonough, R. Ibañez, E.B Dolan, B. Cavanagh, M. Salamone, H. Brandhorst, D. Brandhorst, P.R. Johnson, G.P. Duffy, H.M Kelly. *Formulation of a functionalised biomaterial to support pancreatic islet viability in transplantation*; In: International Pancreas and Islet Transplant Association Meeting, Oxford, 2017. Poster Presentation.

L. McDonough, R. Ibañez, E.B Dolan, B. Cavanagh, G.P. Duffy, H.M Kelly. *Formulation of a functionalised biomaterial to support cell viability for the treatment of diabetes mellitus*; In: Royal College of Surgeons Annual Research Day, Dublin, 2017. Poster Presentation.

L. McDonough, H.M Kelly, L.P. Burke, E. Ruiz-Hernandez, G.P. Duffy. *Diabetes Reversing Implants for improved Viability and long-term Efficacy*; In: Royal College of Surgeons Annual Research Day, Dublin, 2016. Poster Presentation.

Chapter 1

Introduction

1.1 Diabetes Mellitus

1.1.1 Impact of diabetes mellitus worldwide

Diabetes mellitus (DM) is a chronic disease which affects over 425 million people worldwide (2017), a number which is expected to rise to 629 million people by 2045 (Figure 1.1) (1). According to the WHO in a 2016 report, prevalence of DM has risen from 4.7% to 8.5% worldwide between 1980 and 2014. Additionally, DM is rising in prevalence in countries of all income levels and is rising faster in low to middle income countries (2). DM is a global disease with impact globally. In 2015 alone more than 5 million deaths were caused by DM worldwide, responsible for more deaths than HIV/AIDS, Tuberculosis and malaria combined (3). There is a substantial economic cost of DM, with a 2016 systematic review published in The Lancet estimating a cost of $825 billion worldwide (4).

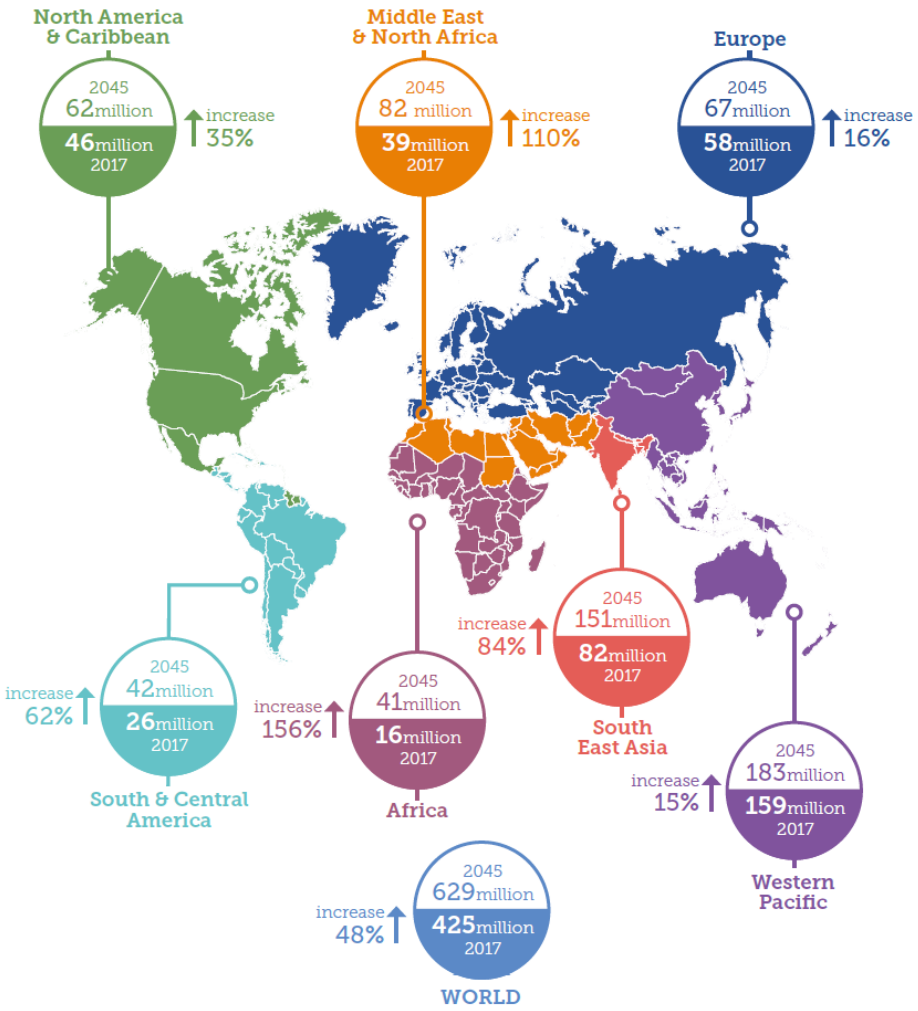

Figure 1.1 *Global incidence of DM (1).*

1.1.2 Pancreas anatomy

The pancreas is an upper abdominal organ situated behind the stomach. The pancreas is an organ of both the gastrointestinal system (the exocrine pancreas), secreting important digestive enzymes into the intestine, and the endocrine system, secreting hormones into the blood to control energy metabolism and storage throughout the body. Anatomically the pancreas is split in three portions, the head, next to the duodenum, the body, and the tail, that extends to the spleen. The pancreas has an extensive arterial blood supply, being supplied by branches of both the celiac trunk and superior mesenteric artery. The exocrine pancreas comprises of more than 95% of the pancreas and is made up of the acinar and duct cells. The acinar cells form pouches throughout the pancreas, which make and secrete the exocrine enzymes to the pancreatic duct system. These ducts branch outwards, eventually feeding into the common bile duct which releases the pancreatic enzymes to the digestive system (5). The endocrine pancreas is the part of the pancreas associated with the management of energy metabolism and is made up of clusters of endocrine cells, the islets of Langerhans.

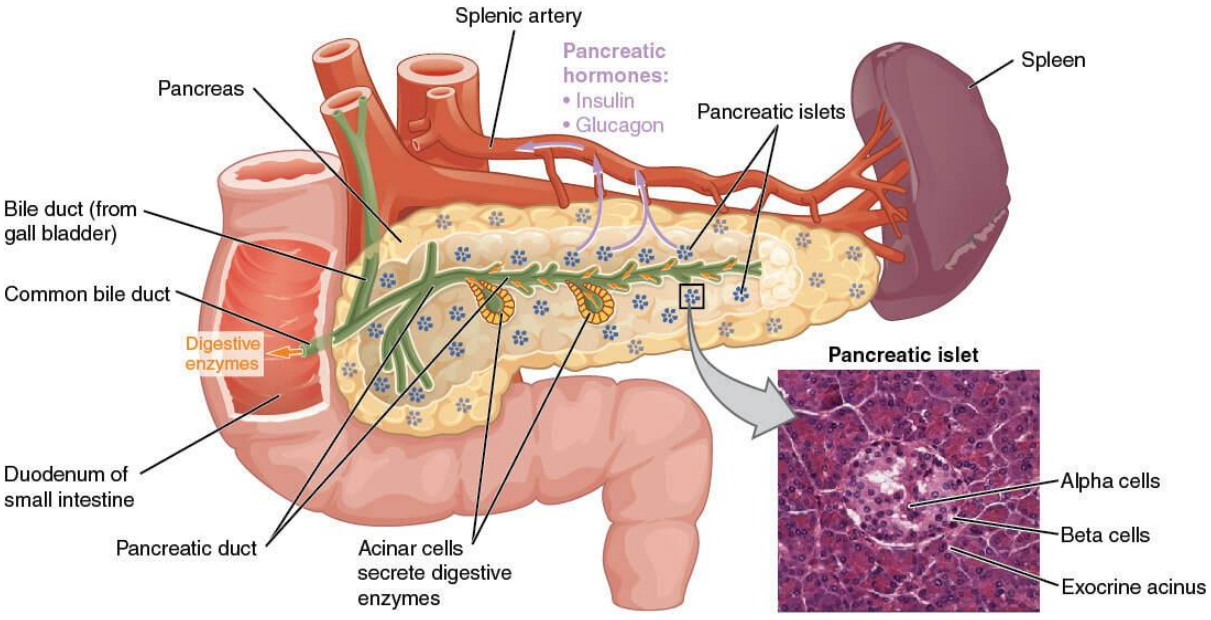

Figure 1.2 *Diagram of the human pancreas and surrounding organs (6).*

1.1.3 Islet anatomy

Pancreatic islets (islets of Langerhans) are structured aggregates of endocrine cells found throughout the pancreas, making up approximately 1% of the total weight of the pancreas. They are complex micro-organs, made up of a number of cell types which contribute to the release of the endocrine hormones and peptides responsible for blood glucose regulation (7, 8). The four distinct cell types making up the islet are the α-cells, δ-cells, pancreatic protein (PP) cells, and β-cells and each islet is also fed with a microvascular network to ensure the cells are sufficiently perfused with nutrients and oxygen.

The α-cells make up 15-20% of the pancreatic islet. They are responsible for the secretion of glucagon, the main peptide hormone which works alongside insulin to regulate blood glucose, by mobilising stored glycogen into glucose to prevent hypoglycaemia in healthy persons. Making up 5-10% of islet mass, the δ-cells release the peptide hormone somatostatin which has a regulatory role in inhibiting the release of glucagon and insulin from the α- and β-cells respectively. The PP cells are the least well studied of the islet cells and are responsible for producing the pancreatic polypeptide. It has shown effects on gastrointestinal motility, as a satiety factor and some metabolic effects, including the suppression of insulin and somatostatin secretion (9). The β-cells form the main bulk of the pancreatic islet making up between 50-80% of pancreatic islet mass. They are responsible for the production and release of insulin into the blood.

Pancreatic islets can vary in size, composition and structure between individuals but there are some common characteristics to most islets. Morphologically human islets are spherical/oval in shape and their size can vary from small to large, 50-500μm in diameter (10). Cell arrangement in pancreatic islets has been studied extensively and human islets are generally considered to comprise of a random intermingling of the α-, β-, and δ-cells (11).However some studies have suggested that islets are organised specifically, with an outer mantle of α- and δ-cells and a core of β-cells, similar to rodent islets (12). There is also disparity in islet cell arrangement between differently sized islets, and islets from different locations in the pancreas; smaller islets are have a higher percentage of β-cells than larger sized islets and islets found in the head of the pancreas have a larger proportion of PP cells. All islets have an

extensive microvasculature (capillary network 5 times more dense the exocrine network) to ensure that sufficient oxygen and nutrients are provided to the highly metabolically active cells, and also ensuring that the cells can respond to the changes in blood glucose levels rapidly (8). Sympathetic fibres, which allow for autonomic innervation of the islets, are also present within the islet.

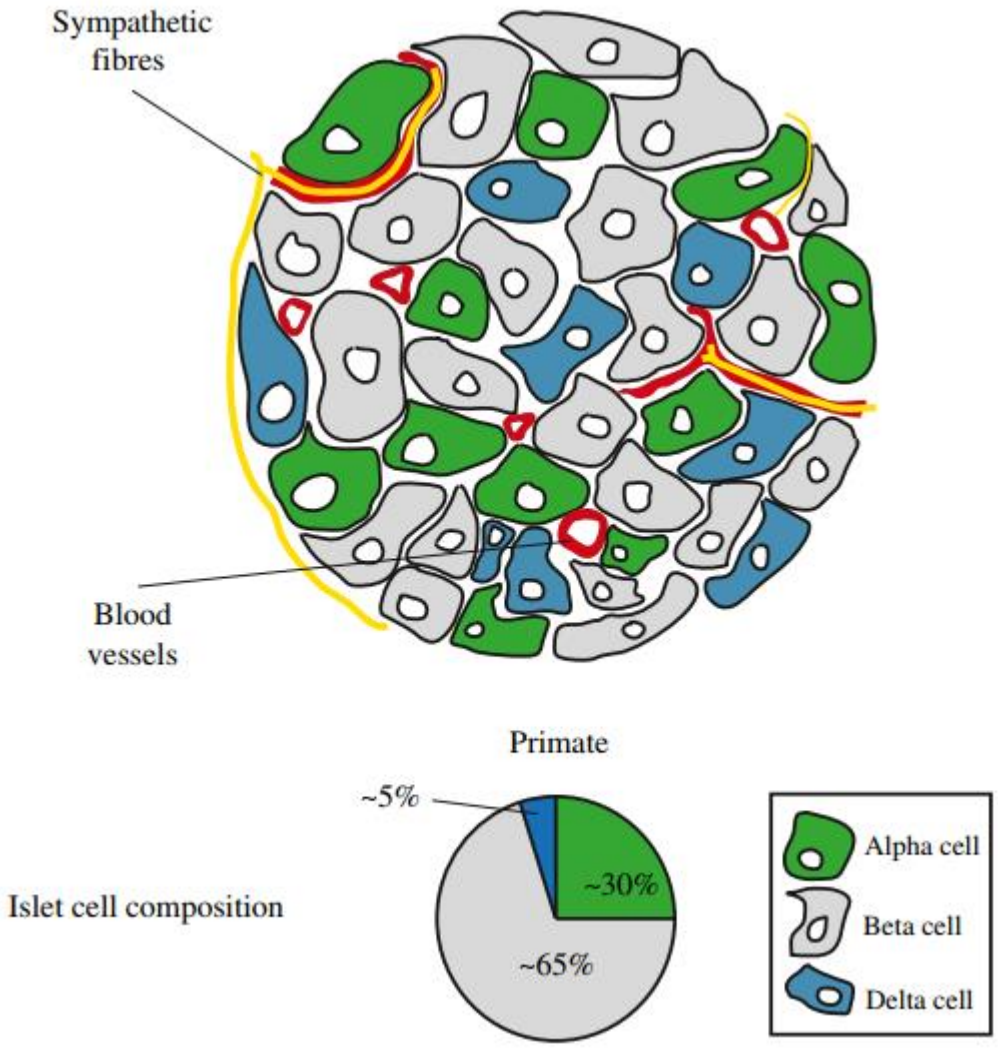

Figure 1.3 *The cell arrangement seen within a human/non-human primate pancreatic islet showing the random intermingling of the cell types, the presence of the microvascular network and the sympathetic fibres (12).*

1.1.4 Pathophysiology of DM

DM occurs when the pancreas does not produce enough insulin to meet the demands of the body. Insulin is a peptide hormone secreted by the β-cells, and it is a key hormone involved in glucose homeostasis in the body, facilitating glucose uptake by cells and regulating carbohydrate, lipid and protein metabolism (13). In DM the failure to produce sufficient insulin results in unregulated blood glucose levels which can lead to high blood glucose, hyperglycaemia. Uncontrolled hyperglycaemia is the primary cause of symptoms of patients presenting with undiagnosed DM; polyuria, polydipsia, increased hunger and unexplained weight loss (14), and, if left undiagnosed and/or unmanaged, uncontrolled high blood glucose can lead to further complications; cardiovascular complications, macro/microvascular degeneration, retinopathy, nephropathy, and lower limb neuropathy (15).

Diabetes UK and the WHO have listed a number of diagnostic criteria that covers the different types of DM; Type 1 (T1D), Type 2 (T2D), and gestational diabetes (16, 17). A patient presenting with any number of the symptoms outlined earlier can be diagnosed for T1D or T2D by:

- Random plasma glucose test ≥ 11.1 mmol/L
- Fasting plasma glucose test ≥ 7.0 mmol/L; or ≥ 5.6 mmol/L in gestational diabetes
- Oral glucose tolerance test, plasma glucose ≥ 11.1 mmol/L two hours after administering 75g anhydrous glucose orally; or ≥ 7.8 mmol/L in gestational diabetes
- Tests in the ranges above without symptoms require an additional blood glucose test on a separate day to confirm a diagnosis
- HbA1c of 48mmol/mol (6.5%) is the recommended cut off point for diabetes diagnosis, however levels below this do not exclude diabetes diagnosed using blood glucose tests.

T2D is the most prevalent type of DM, accounting for up to 90-95% of all cases of DM worldwide.T2D is a progressive disease which is preceded first by impaired glucose uptake, which if left untreated can develop into T2D. The primary mechanism of T2D development is known as insulin resistance, a reduced response

of target tissues to insulin, affecting normal glucose metabolism (18). Insulin resistance develops as result of a combination of factors e.g. weight, age, genetics, and can lead to abnormal insulin secretion, as a result of sustained hyperglycaemia. Poorly managed T2D is progressive, as increased insulin resistance results in higher insulin demand to control blood glucose levels. This demand eventually results in critical oxidative stress to the β-cells (19, 20), leading to cell death and the loss of endogenous insulin production. T2D is considered a manageable disease, and progression can be halted and even reversed with appropriate lifestyle changes, such as diet and exercise (21). In addition to lifestyle changes, T2D may also need to be managed using oral pharmacotherapy that aims to control blood glucose levels (22), however progression of the disease may result in the need for insulin replacement therapy (23).

T1D is less prevalent than T2D, accounting for 5-10% of all cases of DM worldwide (1, 3, 24, 25). T1D is characterised by β-cell autoimmunity leading to the T-cell mediated destruction of β-cells in the pancreas (Figure 1.4). The autoimmunity is caused by a complex relationship between a genetic predisposition to the disease and a number of environmental factors. The majority of these environmental factors have yet to be identified, and as a result the events that trigger the production of autoantibodies which lead to the destruction of β-cells remain largely unknown (24, 26, 27). Research into predicting the development of T1D via biomarkers and subsequent treatment with immunological therapies is ongoing but to date implementing this treatment has been difficult. One of the most significant hurdles to successful treatment is timing. Interventions are typically applied late, after the immune response has already peaked, limiting the effect of potential treatments. Successful pre-diagnosis combined with effective treatment of the autoimmunity are both necessary to treat/prevent the development of T1D (26, 27). There is substantially reduced insulin production in T1D in comparison to T2D and management of the disease is primarily through exogenous insulin treatment.

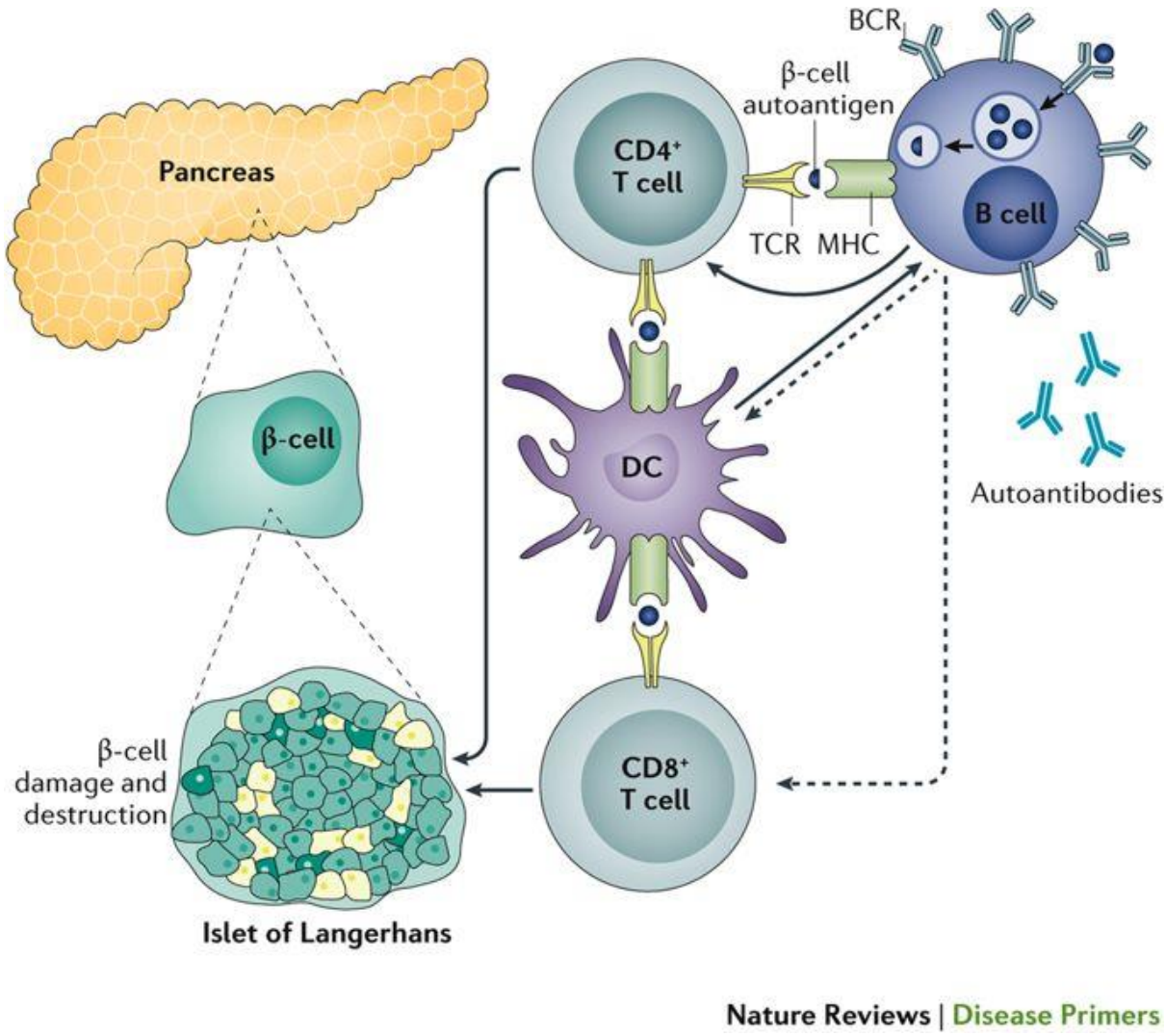

Figure 1.4 *Pathogenesis of T1D. T-cells (CD4+ and CD8+) and dendritic cells (DC) interact with auto antigen presenting β-cells. This leads to the subsequent targeting of pancreatic islets by the T-cells for destruction. BCR, B cell receptor; TCR, T cell receptor; MHC, major histocompatibility complex (25).*

1.1.5 Treatment of T1D

1.1.5.1 Exogenous Insulin

As β-cell mass in T1D patients has been substantially reduced the treatment strategies implemented for T2D patients are not first-line in T1D. In T1D, lifelong insulin replacement therapy is the first-line pharmacotherapy. Insulin analogues have been developed over time to have a range of properties which allow a patient to better control their blood glucose. There are two main classes of insulin analogues available, long acting insulin and short/rapid acting insulin (28). Long acting insulin, such as insulin glargine, acts to provide basal insulin levels throughout the day (29). Insulin glargine is modified to precipitate in the subcutaneous tissue of the injection site. Here it forms a depot which gives prolonged released into the blood over the course of a day (30). Rapid acting insulin, such as lispro and aspart, are used in combination with long acting insulin, to give a bolus dose of insulin before or after a meal to counteract post-prandial blood glucose (PPBG) increases (31, 32).

Self-administration of exogenous insulin is not a set regimen, and insulin requirements change on a daily basis, in response to environmental factors such as diet and exercise. If insulin therapy is not managed correctly and excess insulin is administered blood glucose levels may fall and precipitate hypoglycaemia; blood glucose levels below 3.9mM are considered hypoglycaemic. Symptoms can include autonomic symptoms such as shaking, sweating, anxiety, palpitations and nausea (33). As blood glucose falls further the patient can experience cognitive symptoms/CNS dysfunction like loss of concentration, drowsiness and dizziness, eventually leading to the patient suffering seizures, entering a coma, and even death (34). Most diabetic patients will be educated of the signs and symptoms of hypoglycaemia and will be advised to carry a source of glucose to consume to counteract these symptoms. Repeated hypoglycaemic episodes can impair the body's response to hypoglycaemia, known as hypoglycaemia unawareness. Hypoglycaemia unawareness occurs when a patient's threshold blood glucose for the early adrenergic symptoms, such as shaking and sweating, are the same as or lower than the threshold for cognitive and neurologic symptoms such as confusion, and coma/death (35) (Figure 1.5). This is a serious condition as it can affect a patient's safety and quality of life severely. Additionally, there is a small subset of

patients, with a type of diabetes known as 'brittle' (36, 37) diabetes, who even with a good insulin treatment regimen will still experience large, unpredictable and dangerous fluctuations in blood glucose levels ranging from hyperglycaemia before insulin administration to hypoglycaemic levels after insulin administration.

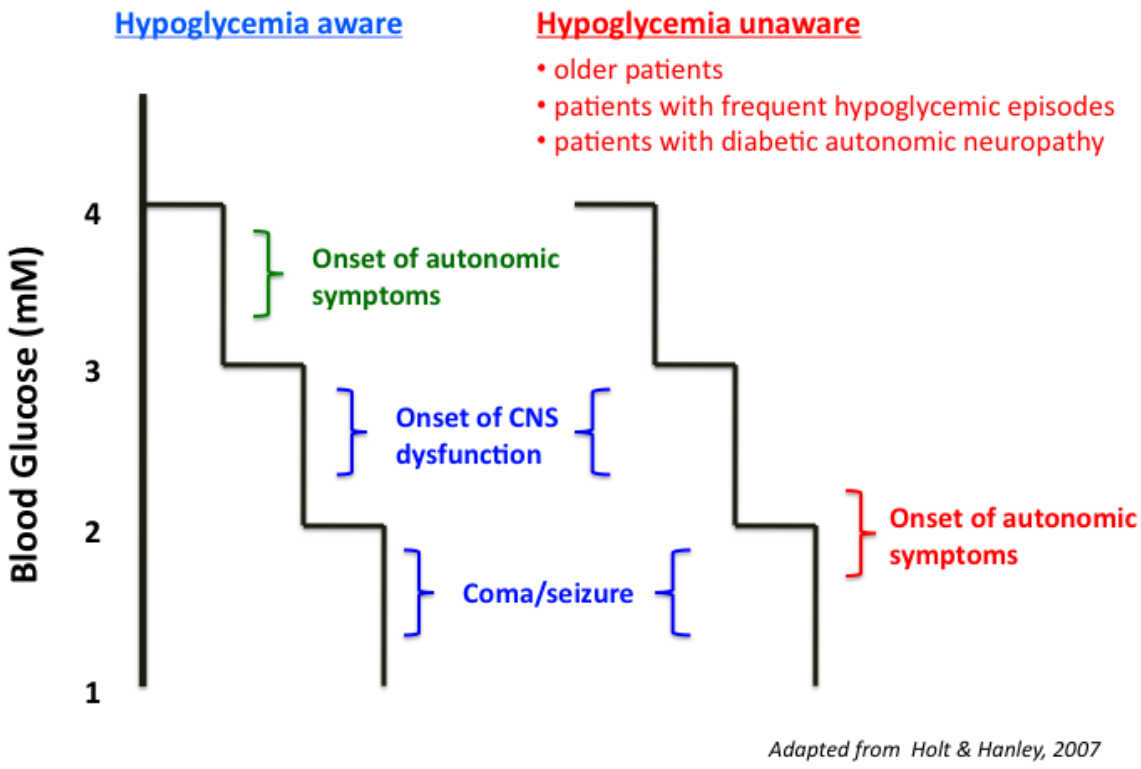

Figure 1.5 *Onset of symptoms of hypoglycaemia in patients who are hypoglycaemia aware or unaware. The onset of the warning autonomic symptoms occurs at lower blood glucose levels in hypoglycaemia impaired patients, increasing the risk of seizures/coma/death in these patients. The onset of cognitive symptoms is unaffected which increases the likelihood autonomic symptoms will go unnoticed (38).*

Despite the relative safety of self-administered exogenous insulin therapy, self-management of multiple injectable medications, multiple times daily injections and the risk of developing life-threatening hypoglycaemia is a significant risk within the population and all of these factors are associated with a large treatment burden to

the patient (39). This has led to the need for and the development of more convenient and effective treatments for insulin dependent DM.

Insulin pumps were the first means of simplifying patient's insulin treatment. Insulin pumps are typically small pocket sized devices which contain a reservoir of insulin and are connected by tubing to an infusion set, a subcutaneous needle/cannula which is held on the skin and allows for the delivery of insulin without changing the needle or injection site for up to 3 days. There are a number of insulin pump manufacturers, developing pumps and needle sets to accommodate different patient body types and lifestyles. These include differences in cannula size/angle for different body types or tubing lengths to account for different infusion sites for example. There are a number of different types of pumps commercially available from different manufacturers such as Medtronic, Insulet, and Roche. Figure 1.6 gives an example of a Medtronic device.

Figure 1.6 *A Medtronic insulin pump. The image on the left shows how an insulin pump would be worn by the patient. The right images shows the (1) Insulin pump, (2) the insulin reservoir that is inserted into the pump, (3) the infusion set, consisting of the needle and cannula and adhesive patch to keep it in place, and (4) the infusion set insertion device, to make it easier to place the cannula correctly (40).*

Pumps typically have two main settings, a basal rate which is programmed to provide a low dose of insulin, which is administered continuously to mimic basal

pancreatic rates, and a bolus dose setting which allows for the administration of a bolus dose of insulin to respond to and limit PPBG spikes or other hyperglycaemic events. Insulin pumps remove a great deal of burden on the patient as infusion sets are changed 2-3 times weekly as opposed to injections being 4 times daily. Bolus dosing is still managed by the patient and blood glucose testing is still required with a pump to ensure blood glucose is adequately controlled. A paper published in 2017 by *Beck et al.* in the Lancet (41) saw that initiating adults with T1D on insulin pumps afforded better glycaemic control but also an increase in biochemical hypoglycaemia (lows in blood glucose which are not noticeable through major side effects but may impair cognitive function) (42).

1.1.5.2 Blood glucose monitoring

As outlined above, monitoring blood glucose levels is an important aspect in the treatment of T1D. The traditional, and still most commonly used, method of measuring blood glucose levels is called self-monitoring blood glucose (SMBG) using a blood glucose monitor. The conventional blood glucose monitor is a small device that the patient carries on their person and requires a small sample of the patient's blood to perform an electrochemical reading to determine blood glucose concentration. Blood is normally let using a small pin-prick and collected on a testing strip and the device provides the result immediately on a screen. The patient can then manage their blood glucose levels with insulin or food as necessary (43).

As outlined, this method for reading blood glucose can be painful and unpleasant, is subject to user error by the patient, and only provides a blood glucose reading at a snapshot in time, meaning it must be repeated multiple times daily to be effective. Continuous glucose monitoring (CGM) is an advancement compared to conventional blood glucose monitoring. CGM uses a fixed sensor placed subcutaneously, that measure glucose concentrations in the interstitial fluid. The first wave of CGM devices required daily calibration by a SMBG reading to function correctly, however newer models do not require any calibration to function. The sensor can then output the readings to the recording device in real-time or/and be saved for viewing later (44). CGM devices perform a reading every 5 minutes, allowing for a near real-time update in the patient's blood glucose levels. CGM devices can also be programmed with alerts that provide warnings through the device or connected apps on the

patient's phone when blood glucose levels rise too high or fall too low, allowing for quicker response times to hyper/hypoglycaemic events (45). CGM provides multiple improvements to SMBG such as reducing the treatment burden associated with multiple times daily pin-prick measurements, allowing for better blood glucose management through real-time updates and recording blood glucose levels for review with a healthcare provider, and through alerts to help better avoid glycaemic events (46, 47).

1.1.5.3 The artificial pancreas

The next step in medical devices to improve the quality of life and care for T1D patients is the artificial pancreas; a medical device which combines the advancements in CGM and exogenous insulin pumps to attempt to imitate a healthy pancreas's role in regulating blood glucose levels in T1D patients (48). The artificial pancreas is a closed loop system of 3 technologies i) infusion pumps for insulin delivery, ii) a continuous blood glucose monitor, iii) a dosing algorithm to ensure insulin is delivered at the correct dose (49) (Figure 1.7). A Lancet paper (50) saw uniformly improved blood glucose control in a multi-centre systematic review and meta-analysis of out-patient randomised control trials using an artificial pancreas.

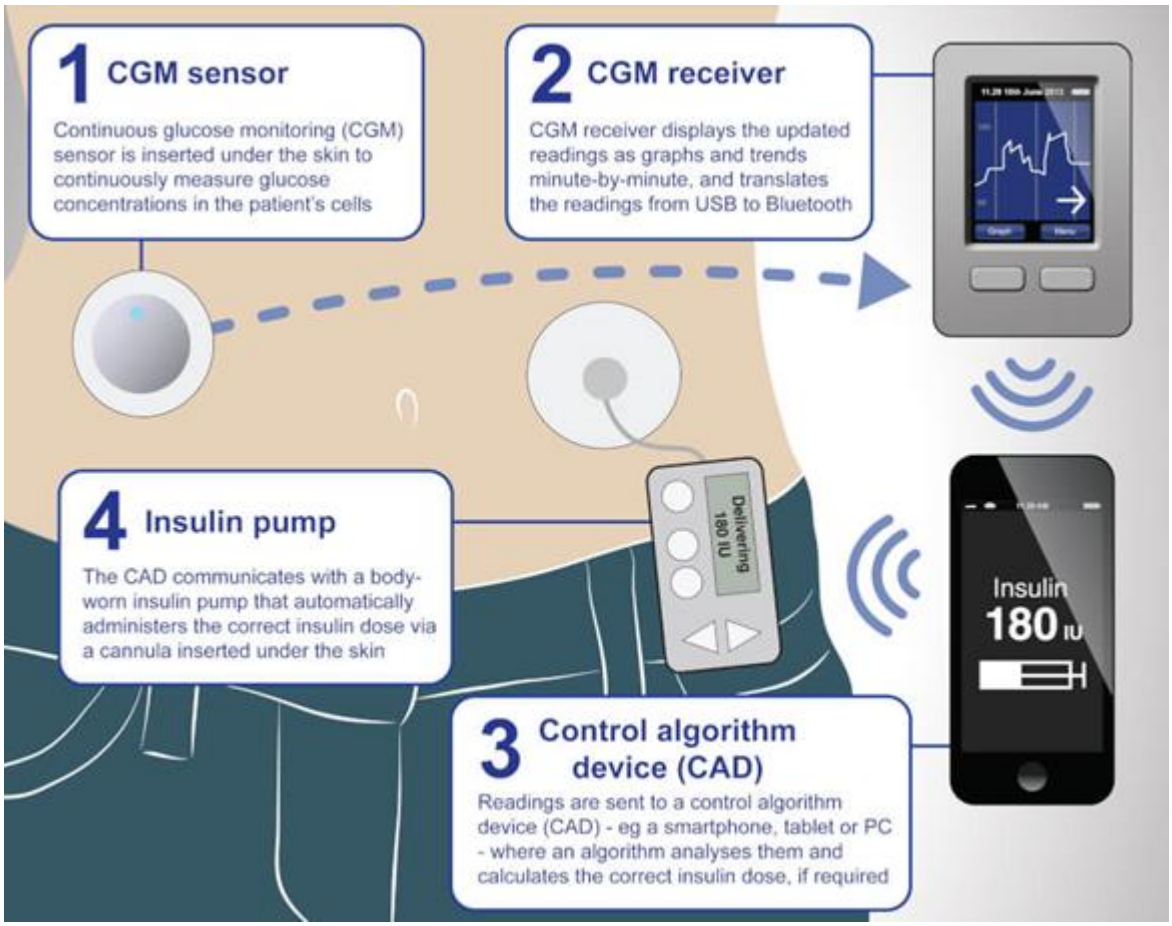

Figure 1.7 *An outline of the function of the closed loop system that makes up the artificial pancreas (51).*

The aim of the artificial pancreas is to require little to no input from the user to maintain glycaemic control, outside of occasional SMBG testing to ensure the system is calibrated. Currently, the technology is limited by the algorithms used in the available devices. In order to ensure accuracy the available devices ask for 2 times daily SMBG for calibration, and require manual input of mealtime carbohydrates and current blood glucose level to provide a bolus dose of insulin. The algorithms are also limited in the blood glucose target levels, where the target levels may be fine for the majority of patients but can be too low for patients who experience post exercise hypoglycaemia, requiring changes to the target levels set in the algorithm to address this issue (52).

There are currently no artificial pancreas systems commercially available. The most advanced systems that are regulated and approved control basal insulin rates only, requiring user input for bolus dosing, and widespread application of these systems is

limited by their high cost. This has led to the concept of the do-it-yourself artificial pancreas (DIY APS). The DIY APS of CGM devices and insulin pump, combined with a communication device, such as a smart phone, and utilising open source publically developed algorithm. Although users of DIY APS systems have reported success with these systems there are a number of concerns and risks associated with the safety of DIY APS due to their being unregulated and untested in clinical trials without formal pathways to report adverse events or distribute safety notices. These issues provide questions as to how healthcare professionals will need to approach managing the care of their patients using DIY APS systems, until commercially available systems become more affordable for widespread use (53).

Although in its early stages, the artificial pancreas remains a promising future system for the treatment of T1D. As the systems and algorithms advance and patient input is further minimised the artificial pancreas may prove to be one of the main competitors to other therapies that aim to return endogenous insulin production to the patient such as transplantation therapies.

1.2 Transplantation in DM

Restoration of endogenous insulin production has been identified as the ideal treatment of T1D where possible. This can be achieved by a whole pancreas transplant or by the transplant of pancreatic islets. The goal of these transplantations is to restore sufficient β-cell mass so that the patient can endogenously produce the insulin required to meet the blood glucose demand. Additionally, this has the potential to reduce the risk of human error associated with the self-administration of insulin and allows for much tighter glycaemic control.

1.2.1 Pancreas Transplantation

Whole pancreas transplantation is a procedure which is successful in the reversal of diabetes, but is a very invasive high risk surgery and as with all transplants requires subsequent life-long treatment with immunosuppressants. The long term risks and side effects of immunosuppressive agents are well established. The general risks associated with immunosuppression are opportunistic infections, an increased risk of malignancies, and bone marrow suppression and cytopenia (54). There are also a number of specific side effects associated with specific drugs. Corticosteroids are commonly used in immunosuppression and chronic corticosteroid use is associated with side effects such as weight gain, osteoporosis, hypertension, hyperlipidaemia, and worsening glucose control (55). Some examples of non-steroidal immunosuppressant and their long-term side effects are: calcineurin inhibitors, tacrolimus and cyclosporines, which are associated with nephrotoxicity and neurotoxicity (56); azathioprine is associated with hepatotoxicity; and there is an increased cancer risk in patients using these agents for immunosuppression long-term (57).

The first whole pancreas transplantation was reported 50 years ago at the University of Minnesota, and pancreas transplantation is the current gold standard for the restoration of β-cell mass today. More than 23,000 transplants have taken place, in both T1D and T2D patients, to date (15). Due to the invasiveness of the procedure, and the requirement for systemic immunosuppression to prevent graft rejection, there are strict criteria which limit the procedure's application to the population of patients with DM (58). The first criteria that is commonly required is that the patient

must have end stage renal disease and plan to or have had a kidney transplant. Pancreas transplantations are commonly performed as simultaneous organ transplantations with the kidney. Diabetic nephropathy and kidney disease are a serious complication of DM, affecting 20-40% of all patients with T2D, and results in a large degree of morbidity and mortality (59). The risk of major complications of two surgeries in minimised by performing the surgeries simultaneously; as a result more than 80% of all pancreas transplants are as part of a simultaneous kidney-pancreas surgery (60). Alternatively, a pancreas transplant may be necessitated without a simultaneous kidney transplant in patients with diabetes with frequent wide fluctuation in glycaemic levels, with a high risk of life-threatening hypoglycaemia (58).

1.2.2 Islet Transplantation

Pancreatic islet transplantation is a promising therapy which has shown the return of endogenous insulin production to the patient (36, 37). In contrast to whole pancreas transplantation, which is a major and invasive surgery, islet transplantation is a minimally invasive procedure. There are ~1 million pancreatic islets in the human pancreas, and β-cell mass makes up about 1-2% the total weight of the pancreas. Thus, isolating the islets which hold the functional, insulin producing cells was seen as an important step in a safe treatment to reverse DM (61). Islet transplantation today consists of two main steps; islet isolation and transplantation of isolated islets.

1.2.2.1 Islet isolation

Isolation and purification of islets from the rest of the pancreatic tissue was a key challenge to ensure the successful translation of islet isolations to the clinic. In 1988 the Ricordi Chamber was developed as an automated and consistent method of isolating quantities of islets from the human pancreas (62). The protocol firstly involves perfusing the pancreas with a digestive enzyme. The pancreas is divided into two main halves which are cannulated individually. The pancreas is then perfused with the digestion solution, after which it is distended. The fat is removed and then the pancreas is cut into smaller pieces to facilitate transfer to the Ricordi Chamber (63).

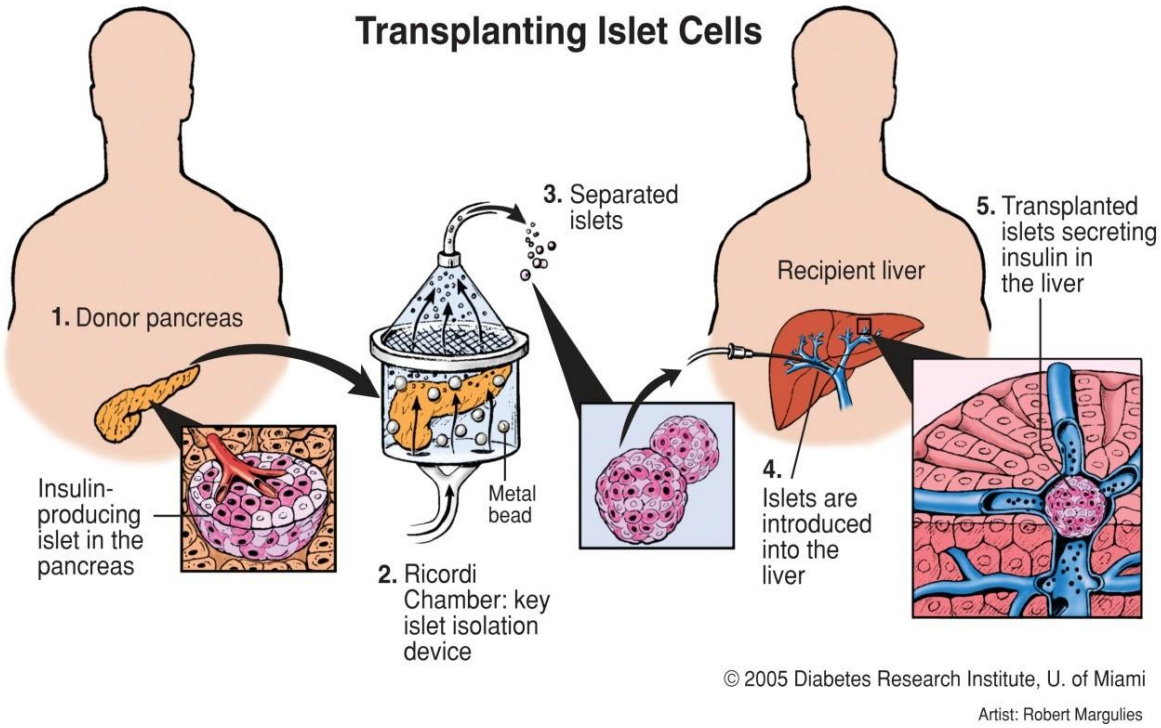

Figure 1.8 *Schematic outlining the process of islet isolation from the human pancreas. The Ricordi Chamber was a key device designed to automate the separation of islets from the bulk of pancreatic acinar tissue.*

The Ricordi Chamber isolator consists of two stainless steel chambers separated by a 280µm mesh and a number of glass marbles are placed in the chamber to aid mechanical digestion. The pancreas and marbles are placed in the bottom of the chamber and additional digestive enzymes are added. The mesh is placed over the top and the Ricordi Chamber is fully assembled by adding the top chamber and closing (64). This is then connected to the digestion circuit. Although the digestion circuit may vary the principle behind the circuit remains the same. A solution is circulated through the entire system to heat the pancreas, gradually dilute collagenases and collect the islets. The islets are then purified further using a gradient method, using specific medias of different density to isolate the islet tissue, such as a Ficoll Gradient (65). Ficoll is a hydrophilic polysaccharide that is dissolved in the media to increase the density to make the gradient. Isolated pancreatic tissue is washed of collagenase solutions and then suspended in heaviest density of the gradient. Subsequently, gradually lower densities are overlaid to form the gradient. Multiple layers of Ficoll are used to separate the islets by purity. The top layer of

Ficoll contains isolated fat and connective tissues. The first layer of gradient will have the most pure isolation of tissue. The next layer will be less pure but is still collected, as many islets remain here. The islets are then washed of Ficoll and suspended in culture media before use.

The site of transplantation of pancreatic islets is important, for supplying oxygen and nutrients to the isolated islets; although isolated islets are functionally intact, they have lost their vascular blood supply. The hepatic portal vein was identified very early as a potential site for a successful islet transplantation (66). The portal vein can be accessed minimally invasively through the use of a percutaneous catheter which helps to minimise the surgical risk of the procedure (36). The vascular transplantation of the islets gives them direct access to the blood for oxygen and nutrient supply.

Isolated islets are measured and counted according to islet equivalents (IEQ). An IEQ is a standardised islet volume, where one IEQ is a perfectly spherical islet of 150µm. Islets are counted within 50µm ranges and correction factors are used to convert the counted islet diameters into IEQs (67, 68). On average, islet yield can range from 250,000 – 400,000 IEQ per pancreas, highlighting that the protocol is not perfect, and a large number of islets are lost throughout the process. The islet transplantation procedure needs 10,000 IEQ/kg of the recipient for successful insulin independence, with a minimum of 5,000 IEQ/kg needed to see improvement in glycaemic control, and 10,000 IEQ/kg needed for insulin independence. As such, in an average 70kg patient, between two and three pancreases are required to provide sufficient IEQ for a successful procedure (69, 70).

1.2.2.2 Transplantation and the Edmonton protocol

The first successful islet transplantation was performed almost 30 years ago, reported by *Najarian et al* and *Largiadér et al* (71). Islet transplantation continued for a number of years with variable success but it was not until 2000 and the development of the Edmonton protocol that the procedure saw real success. In a study with seven T1D patients reported by *Shapiro et al* a new protocol outlined an immunosuppressive regimen which allowed for a significant increase in islet viability after transplantation. The islets were isolated and transplanted as described above. The immunosuppression regimen was glucocorticoid free consisting of sirolimus,

tacrolimus and daclizumab (70). Glucocorticoids are known to have diabetogenic effects (72) and their exclusion from the immunosuppression regimen was key to the increase in islet survival post infusion. A successful transplantation of islets allows the patient to endogenously produce and control blood glucose, with up to 44% of treated patients being insulin free for up to three years (37).

However, application of the protocol is still limited, despite its success. A shortage of organs for transplantation and the risks associated with lifelong systemic immunosuppression mean the transplant is normally only performed on patients who fall into high risk groups of patients with diabetes, such as patients with impaired awareness at risk of hypoglycaemia. Strategies to address these factors have led to a wide range of research to improve islet transplantation outcomes and application of the therapy.

1.3 Extravascular islet transplantation

Two of the biggest challenges facing the intravascular islet transplantation procedure are the need for systemic immunosuppression and the requirements for multiple donor pancreata to reach the 10,000 IEQ/kg body weight for a successful treatment. These issues are directly related to the intravascular site; an allogeneic transplant will require lifelong immunosuppression to prevent graft rejection, and a high amount of IEQ required is due to the loss of islet mass immediately after transplantation into the hepatic portal vein (73). These issues could be addressed by finding new sources of islets or β-cells for these transplantations and/or encapsulation of the islets/cells within an immunoprotective supportive biomaterial and transplantation to an extravascular site. Such an approach is referred to as a ‘bioartificial pancreas’ (74).

1.3.1 Sources of cells for transplantation

Human islets are in short supply for islet transplantations, with the average 70kg male patient requiring upwards of 700,000 IEQ for a successful transplantation. Although a set cut-off point for successful islet isolation has not been decided, a number of authors have determined that a minimum of 250,000 IEQ are required to be isolated to be considered a successful isolation (75, 76). On average a minimum of three donor pancreata are required for a successful islet transplantation using the

Edmonton protocol. In Ireland in 2018, there were a total of 81 deceased organ donors with ~20,000 people having T1D in Ireland (1, 77), showing the degree of scarcity against the potential demand. As a result, a great deal of research into alternative islet and β-cell sources has been carried out, ranging from xenogeneic islet transplantation to induced pluripotent stem cells (iPSCs).

Xenotransplantation of pancreatic islets has been studied as a potential option for the treatment of diabetes for many years, with the first pancreatic xenotransplantation being performed in 1894; pieces of sheep pancreas were implanted subcutaneously and showed some effect in reducing blood glucose levels (78). It was not until 1994 that fetal porcine islet like cell clusters were transplanted to 10 human patients, and although the treatment was not successful in treating diabetes, it was shown that the xenografts could survive for many months (79).

Pig islets have been extensively studied as a potential source of islets for xenotransplantation. Similarities between pig and human insulin are well documented, and pig insulin was used for a number of years prior to the development of conventional manufacturing processes for human insulin (80). Pig islets are similarly sized to human islets and share a similar anatomy with human islets, consisting of a core of β-cells with some islets containing α-cells at the centre (11, 81). Pig islets are an ethically sound source of mammalian islets, as opposed to islets from non-human primates, and a near unlimited supply of pig islets could be made available through controlled farming (78). As with all transplantation, rejection of the xenogeneic pig islets is a risk; however recent advances in genetic engineering have produced transgenic pig islets which can overcome rejection, have improved insulin production, and deactivate the porcine endogenous retrovirus (PERV), to prevent potential transmission of infection from the xenotransplant (82, 83). The advances in and availability of pig islets for xenotransplantation make them a very useful alternative to human islets in the treatment of T1D. Pig islets will likely act as a useful bridge in the islet transplantation therapy, between allogenic donor islets and iPSCs.

Stem cell technologies have been in development for many years, with T1D being a prime candidate for a stem cell therapy as only a single cell type, the insulin producing β-cell, needs to be replaced (84). iPSCs are stem cells which are initially

adult human stem cells that have pluripotency, the ability to differentiate to cells from any germ layer, induced back into the cell, and in theory this can be the patient's own autologous cells (Figure 1.9). There are a number of groups that have successfully differentiated autologous cells into functional β-cells (85, 86), and the results of the first clinical trial of transplanted human partially differentiated endocrine progenitors of β-cells for the treatment will be available later in 2019 (87).

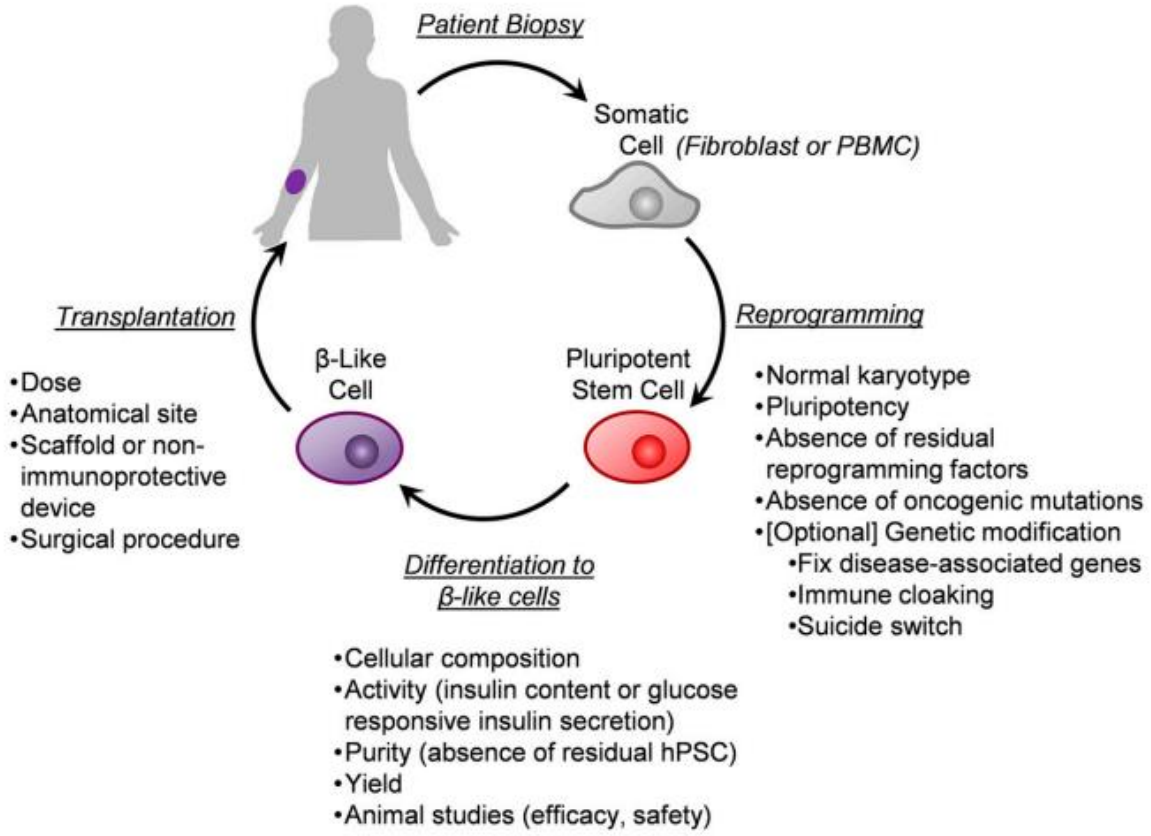

Figure 1.9 *Overview of utilising a patient's own somatic cells for a cell transplantation to treat T1D: the patient's somatic cells are harvested and reprogrammed into iPSCs; these cells are cultured to a suitable yield and differentiated into an insulin producing β-cells; the β-cells can now be transplanted back into the patient (84).*

1.3.2 Biomaterials as an extracellular matrix

1.3.2.1 Biomaterials in islet transplantation

A biomaterial is any material, construct or surface that interacts with biological systems. They may be naturally occurring or synthetic in origin and will be biocompatible with the body's existing tissues. This wide definition of a biomaterial applies to a large number of potential applications, ranging from materials such as metal and ceramics, used in surgical replacements of joints or in stents, to hydrogel and biomaterial scaffolds, used in drug delivery or in implantation.

The purpose of using biomaterials in islet transplantation is to provide protection and support to the encapsulated islets. To this end, a biomaterial that mimics/provides support similar to the extracellular matrix (ECM) of the native islet would be the best biomaterial for islet transplantation. Islets exist within the pancreatic niche, and have a number of interactions with the intra-islet and extra-islet pancreatic tissues for their function. As outlined in the anatomy of the human islet, there is a rich vascular network that supplies each islet individually, and studies with mouse β-cells have shown that the β-cells in the islet interact with these endothelial cells, with the β-cells producing vascular endothelial growth factor (VEGF) to promote vascular development, while benefiting from basement membrane produced by the same endothelial cells that supports insulin gene expression (88). Islets are also innervated by parasympathetic and sympathetic neurons to either promote glucose stimulated insulin secretion (GSIS) or inhibit insulin secretion respectively (89). The tight architecture of the islet and cell-cell contacts between β-cells plays an important role in optimal insulin expression and GSIS (90). In addition to intra-islet interactions, the β-cell also has interactions with the surrounding pancreatic ECM (91) and non-pancreatic tissues, such as the effect of the gut hormones, incretins, on insulin secretion (92). In the process of islet transplantation, the islets are isolated and purified from excess pancreatic tissues. This results in the removal of the ECM, cutting of the vascular blood supply, cutting of innervation from the central nervous system, and removal of the islets from the pancreatic niche and so lose the effect of non-islet tissues. Although a biomaterial that mimics the ECM and pancreatic niche would be the best biomaterial for islet transplantation, implementing a strategy to account for everything that is lost following islet isolation may not be possible, and so

replacing a few key factors while providing a protective biomaterial has been the focus of biomaterial development in islet transplantation to date.

A large number of biomaterials have been investigated for the purpose of transplantation of islets to extravascular sites. Poly-lactic acid polymers (PLA) are an easily manipulated material that can be polymerised to produce materials with varying properties. In particular, poly (lactic-co-glycolic) acid (PLGA) has been used in animal models of islet transplantation. PLGA scaffolds have been used to house islets, and then transplanted to an extravascular/extrahepatic site (93, 94). Another study implanted a commercially available PLA polymer, Ethisorb®, seeded with autologous islets into the omentum of pancreaectomized dogs, and all four animals achieved normoglycaemia for up to 5 months (95). A further study showed successful reversion of diabetes with a PLGA scaffold functionalised with collagen IV, a human ECM protein, in mice (96). A number of other biomaterials such as collagen scaffolds (97, 98), polyhydroxyalkonate polyesters (99), and fibrin scaffolds (100) have also been investigated as potential alternative biomaterials for extravascular islet transplantation, however the role of hydrogels as an ECM are of particular interest in this thesis.

1.3.2.2 Hydrogels in islet transplantation

Hydrogels are three-dimensional polymeric networks based on hydrophilic macromonomers. Hydrogels can be made from virtually any water-soluble polymers and are capable of retaining large amounts of water within their matrix (101). In general, hydrogels exhibit excellent biocompatibility and they have highly tunable mechanical properties, which allows them to be designed in such a manner that they can mimic the mechanical properties of a target tissue (102). There are a number of types of hydrogels, and they can be classified according to different properties associated with their polymer origin (natural or synthetic), polymer network (homopolymeric, copolymeric or multipolymeric interpenetrating polymeric hydrogels), configuration (amorphous, semi-crystalline or crystalline, physical appearance (whether the final hydrogel appears as a matrix, film, or microsphere), electrical charge (nonionic, ionic, zwitterionic) and the different types of crosslinking (103). There are two main types of crosslinking and the type of crosslinking is important to the final properties of the hydrogel. Chemically crosslinked hydrogels

generally refers to hydrogels that have undergone a permanent crosslinking reaction, such as covalent bond forming between the hydrogel polymers. Physically crosslinked hydrogels typically refer to non-covalently linked hydrogels, with crosslinks being formed by transient junctions arising from polymer chain entanglements, or physical interactions such as ionic bonds, hydrophobic interactions or hydrogen bonding between polymer chains (Figure 1.10).

Hydrogels have seen a large number of uses in biomedical applications ranging from the delivery of small and large drug molecules (104), the tunable properties allowing for prolonged or rapid release of a loaded drug in response to *in vivo* stimuli, as a therapeutic agent themselves as a structural component, for structural support in cardia applications (105), and for the encapsulation of therapeutic cells (106). In this thesis, the use of hydrogels for the encapsulation of islets for the treatment of T1D is of particular interest. Table 1.1 gives some examples of the different applications of different hydrogel polymers investigated in islet transplantation in the literature, and shows the number of different methods, transplantation sites, and applications possible using a hydrogel platform.

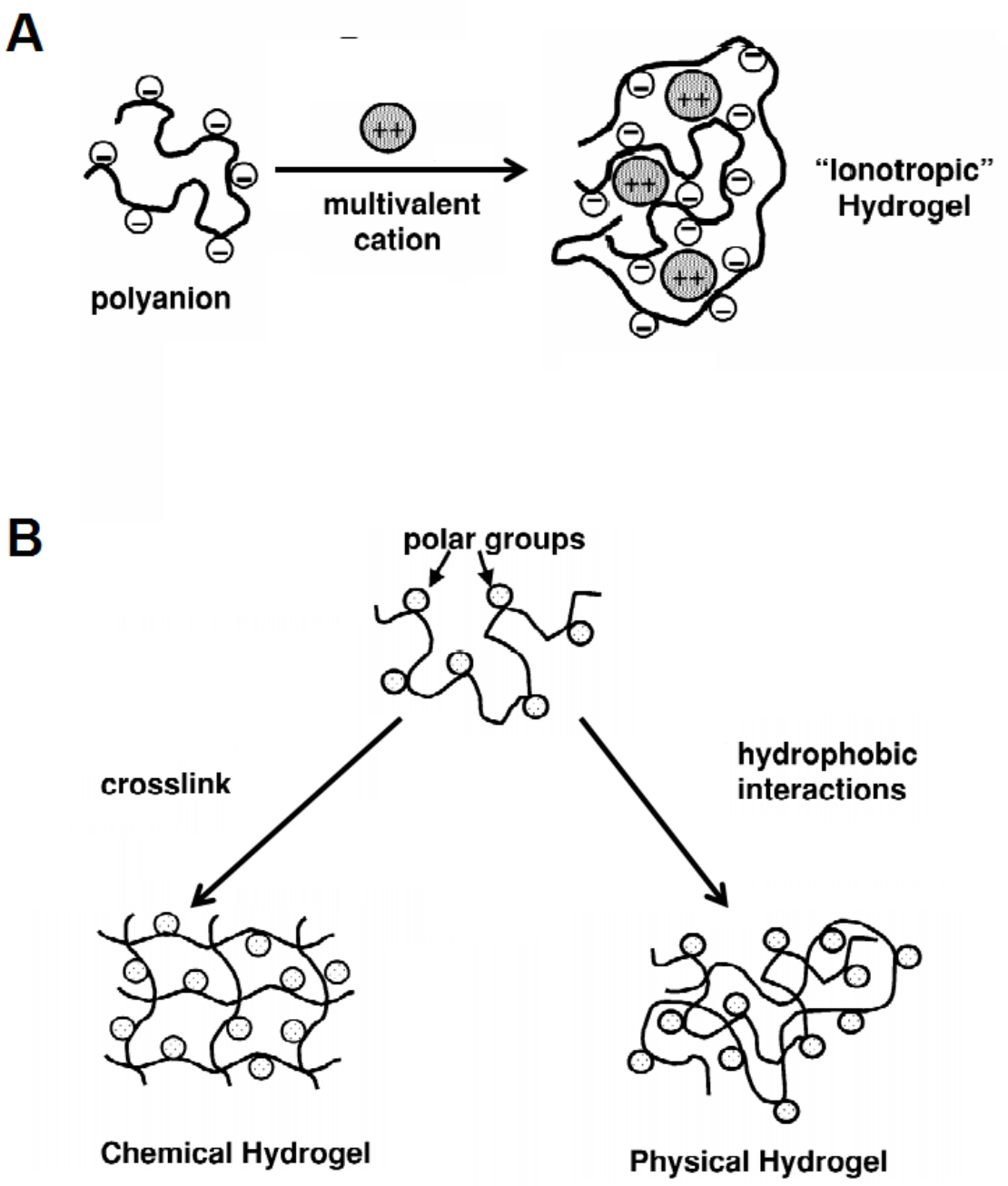

Figure 1.10 *Schematics for the formation of three types of hydrogels.* ***(A)*** *is an example of an 'ionotropic' crosslinked hydrogel, such as calcium alginate. The polyanionic alginate polymer interacts with a multivalent* Ca^{2+} *to give the final crosslinked hydrogel.* ***(B)*** *Schematic for the formation of two types of hydrogel from a single polymer. On the left a chemically crosslinked hydrogel is formed when a crosslinking reaction forms crosslinks between the polymer chains off the functional polar group. On the right a physical hydrogel is formed by physical entanglement of the polymer chains. Adapted from Hoffman et al (107).*

Table 1.1 *Examples of hydrogels investigated in the literature for islet transplantation purposes.*

Hydrogel polymer	Application	Reference
Alginate	Islets seeded at 1,000 IEQ non-human primate islets (NHP) per 1mL of a modified alginate (Z1-Y15). Crosslinked spheres 1.5mm diameters were implanted laparoscopically to bursa omentalis space in NHPs and islets were protected for up to 4 months without immunosupression.	*Bochenek et al (108).*
	iPSCs derived β-cells (SC-β) encapsulated at a density of 2,000 SC-β clusters per 1mL sodium alginate solution ±CXCL12 to enhance GSIS. Crosslinked microspheres were 600-700µm diameter containing >1 SC-β cluster per sphere. Diabetic mice implanted with CXCL12 alginate spheres became normoglycaemic within 72 h without immunosupression.	*Alagpulinsa et al (109).*
	INS-1E cell line cells were encapsulated in alginate microcapsules with or without high molecular weight hyaluronic acid supplementation. The hybrid alginate-HA hydrogel microcapsules enhanced insulin producing cell survival.	*Cañibano-Hernández et al (110).*
	SC-β cells encapsulated in alginate spheres transplanted into mice and treated for 174 days before euthanisation. The implant induced glycaemic correction with immunosuppression for 174 days and the retrieved implants contained viable insulin producing cells.	*Vegas et al (111).*

Hydrogel polymer	Application	Reference
Alginate	Adult pig islets were encapsulated in alginate in a macroencapsulation xenogeneic subcutaneous implant in a primate model and was shown to control diabetes for up to 6 months without immunosupression.	*Dufrane et al (112) .*
Collagen-HA	Rat islets encapsulated in a crosslinked HA/collagen hydrogel and transplanted into the rat omentum without immunosupression. Transplanted rats were followed for 52 weeks before termination and showed normoglycaemia for the duration of the experiment.	*Harrington et al (113).*
Collagen-Chitosan-Laminin	Porcine neonatal islet cells and circulating angiogenic cells were encapsulated in the collagen-chitosan-laminin (CCL) matrix at a density of 300 IEQ/500µL of hydrogel. Islet viability and function was promoted in the collagen-chitosan hydrogel *in vitro*.	*McEwan et al (114).*
Poly (ethylene glycol)	Rat islets were encapsulated in the poly (ethylene glycol)-malemide (PEG-Mal) crosslinked hydrogel at a density of 4,000 IEQ/500µL as the full macroencapsulation device. The PEG-Mal hydrogels were implanted in either the omentum or subcutaneous space of rats, and monitored *in vivo* over 14 weeks.	*Weaver et al (115).*
	Rat islets were encapsulated in a VEGF releasing PEG-Mal hydrogel at a density of 1,500 IEQ/100µL and implanted into the small bowel mesentery for 4 weeks with no immunosupression. The study showed remarkable vascularisation of the PEG-MAL hydrogels.	*Phelps et al (116).*

1.3.3 Macroencapsulation

1.3.3.1 Device consideration

Macroencapsulation involves encapsulation of islets within a single immunoprotective device that additionally can include a biomaterial to support islet viability and function. These devices are typically used to deliver islets extravascularly and essentially act as a bio-artificial pancreas (117). These devices are also typically retrievable or flushable and refillable, which is an important consideration for regulatory purposes. There are three main considerations when designing a macroencapsulation device: the need for a device shell, the use of a biomaterial to support islet viability and an extravascular site for transplantation.

The shell of a macroencapsulation device originated first as a transplantation chamber, membranous bags to hold transplanted cells without providing much function other than retaining the encapsulated cells (118). Research eventually moved towards diffusion chambers that were formulated to be immuno-isolating. By reducing pore sizes in the diffusion chambers researchers found that they could impede the movement of immune cells and immune factors (immunoglobulins) into the device (119). Immune cells can be readily blocked due to their large ~10μm diameter, however large antibodies (IgM) and complement proteins (C1q) could only be hindered at pore diameters of 30nm. To block cytokines the membranes must be even more selective, as Stokes diameters show small differences between factors such as TNF- α (3.80nm) and insulin (2.64nm) (120).

There has been a great deal of research into a suitable biomaterial to support islet graft viability following transplantation. A number of hydrogels have taken the fore-front of this research due to their tunable physical properties, biocompatibility and ability to further functionalise the backbone of the hydrogel to further improve functionality (121).

A number of sites have been investigated for extravascular encapsulation with key factors being to ensure there is sufficient space for the device and access to the vascular network to ensure the encapsulated islets are sufficiently oxygenated and sensitive to changes in blood glucose. The subcutaneous site is popular for macroencapsulation devices due to access to the vascular network and space that

the subcutaneous space provides (122). The intraperitoneal wall has been used in the past for its volume and ease of access in a surgical procedure (123). The omentum has also been researched more recently as a highly vascularised tissue which could support a macroencapsulation device. To date studies have focused on transplanting naked islets to an omental pouch, but it is possible that a macroencapsulation device could be transplanted here also (124).

1.3.3.2 Challenges

While macroencapsulation and delivery to an extravascular site is a promising alternative to the current islet isolation protocol, there are a number of challenges that must be addressed when developing a macroencapsulation device. These challenges primarily arise as a result of the diffusional barriers to nutrients and oxygen into the device and the diffusion of products like insulin and waste out of the device.

Hypoxia is a state of insufficient oxygen for cellular functions resulting in dysfunction and eventual cell death. In macroencapsulation devices the encapsulated islets have been isolated, destroying their complex microvasculature, and encapsulated within a biomaterial and shell. Immediately following transplantation, graft survival is reliant on diffusion of oxygen and nutrients from the surrounding environment or the transplantation site for survival. With a low oxygen pressure (pO_2) the encapsulated islets are at high risk of developing hypoxia induced cell death, necrotic cores and ultimately failure of the graft. Solutions to hypoxia can be built i) into the device through the inclusion of oxygenation technologies, ii) into site choice by choosing a suitably vascular site such that the pO_2 is high enough to provide the encapsulated islets with sufficient oxygen (125) or by iii) techniques such as pre-vascularising the implanted device before filling it with cells (126).

Diffusion of insulin out of a macroencapsulation device is a critical parameter in the design of the device, as failure of insulin to diffuse into the blood in response to raised glucose levels is a failure of the device to adequately treat DM. The diffusion of both glucose into the device and insulin out are time limited factors that must be accounted for in the device permeability (118). Careful device dimension considerations could optimise diffusion across the membrane and biomaterial to address this challenge (127).

Fibrotic tissue forms when fibroblasts attach to the macroencapsulation device. The fibrotic scar tissue is very damaging to the success of the device as it can prevent further vascularisation of the device, compounding the challenges that have previously been discussed (122). Ultimately fibrotic response can be limited by shell design and material selection, where smoother shell surfaces prevent adhesion of fibrotic cells and choice of different materials may not activate fibroblasts and fibrosis can be avoided (123).

1.3.4 Microencapsulation

The primary goal of microencapsulation is the same as macroencapsulation, to protect the islets from the immune system while also allowing the diffusion of beneficial nutrients into the islets and diffusion of insulin and waste away from the islets. Microencapsulation involves the encapsulation of islets on a microsized scale; the encapsulation of 1-3 islets in microsized beads ranging from 200µm to 1000µm. Another method of microencapsulation known as “conformal coating” utilises an interfacial polymerization approach, to allow for the individual covering of islets in very thin layers of hydrogel (Figure 1.11) (128).

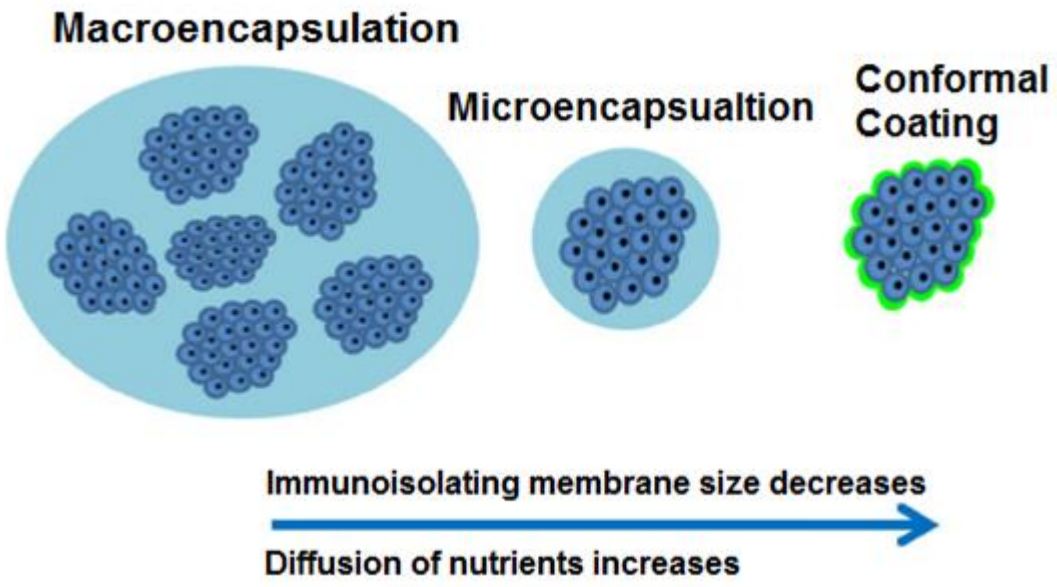

Figure 1.11 *Strategies for encapsulating islets (129).*

As outlined in Table 1.1 above, a number of different hydrogels have been used for the formation of microcapsules for islet transplantation, with alginate proving to be

the most widely researched throughout the years. A review by *Omami et al.* outlines clinical trials that have been performed or are ongoing utilising microencapsulated allo- or xenogeneic transplants. The majority of these trials had no immunosuppression, and showed evidence of islet function for the duration of the trials through detectable C-peptides, reduced exogenous insulin usage, and complete insulin independence in some trials (130).

One of the biggest advantages of microencapsulation in comparison to macroencapsulation is the relatively large diffusion area and small diffusion distance between the transplanted islets and the systemic blood supply after vascularisation. However, a significant disadvantage of a microencapsulation approach is that in practice it is not practical or impossible to retrieve/confirm retrieval of all microcapsules, which is a major regulatory barrier to the translation of microcapsules (122).

1.4 Advances in extravascular macroencapsulation for the treatment of DM

1.4.1 TheraCyte™ and Encaptra® Drug Delivery System

The TheraCyte™ device is a macroencapsulation device, consisting of a planar device design of two semi-permeable membranes, sealed together to form a pouch, with an input port for loading the device. The TheraCyte™ device uses a biocompatible polytetrafluroethylene (PTFE) microporous membrane that promotes neovascularisation (122). The pouch consists of a three layered membrane: an inner layer of 0.4µm PTFE, a middle layer of 5µm PTFE, and an outer layer of polyester mesh (131) (Figure 1.12). The combination of the polyester and PTFE layers promotes vascularisation into the device, and the small 0.4µm pore size acts as an immunoisolating barrier, allowing the diffusion of oxygen, glucose and nutrients into encapsulated cells, and the release of insulin and waste material out of the device.

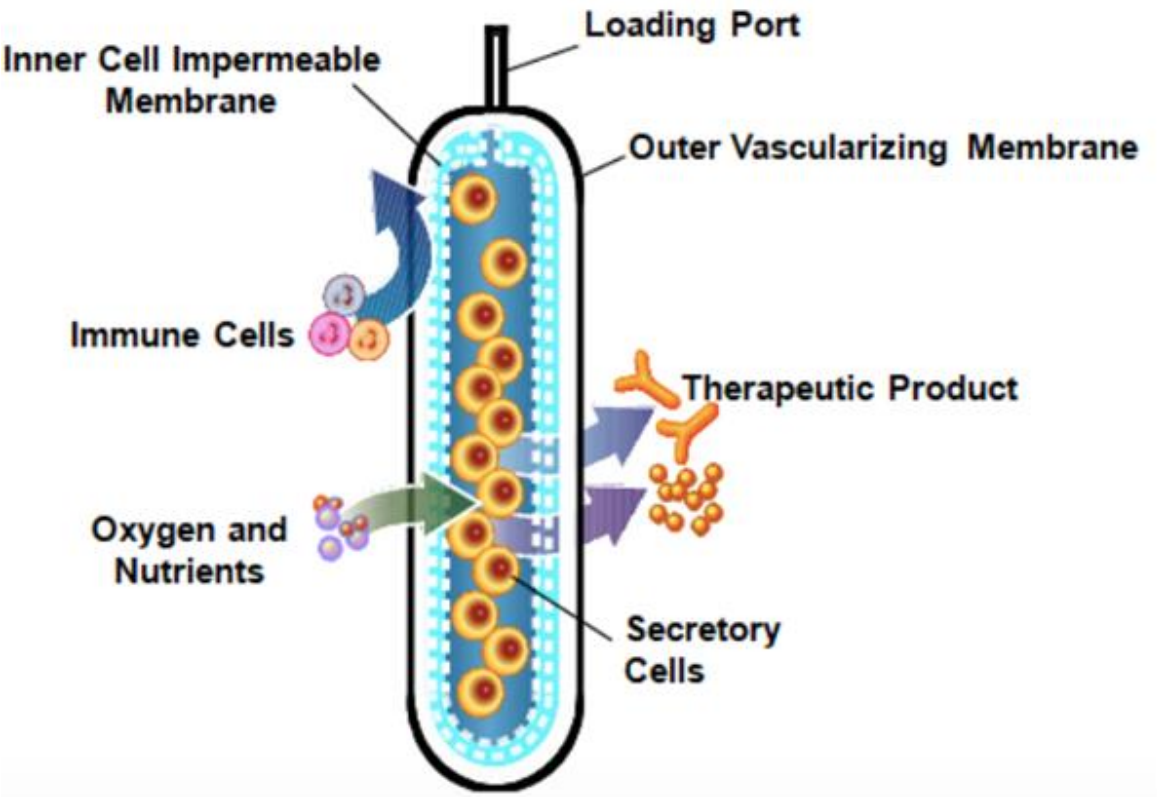

Figure 1.12 *Image outlining the immunoisolation concept of the TheraCyte™ device from the TheraCyte™ website (132).*

Research using the TheraCyte™ device was initiated by Baxter Healthcare Corporation following the discovery of the neovascularisation properties of the PTFE membrane in the late 90s, and was initially researched as a means for delivering gene therapies (133). Though they were unsuccessful with this, they formed Neocrin to investigate using the device for the treatment of diabetes, and to convert the device to be able to be flushed and re-filled, which was unsuccessful due to the capillary overgrowth. The project was downsized and the TheraCyte™ Company was spun-out to sell the devices, allowing academic and corporate entities to research with the device (127). A number of subsequent studies with the TheraCyte™ device have confirmed its potential for use as a macroencapsulation device. The device is immunoisolating and has been shown to reverse diabetes in a number of studies by allogeneic islet transplantation (134-136) and enable the survival of xenogeneic islet grafts in mice for up to 50 days, and up to 8 weeks in non-human primates (137, 138). The TheraCyte™ device has also been studied using differentiated adult human mesenchymal stromal cells to control diabetes in dogs, showing diabetes reversal for up to 18 months in 4 of 7 treated dogs (139) and

human embryonic stem cells in mice, showing glucose-responsive C-peptide levels at 20-30 weeks (140).

The TheraCyte™ device has not progressed further than pre-clinical and experimental work, however when the patent for the technology expired, the company ViaCyte developed the Encaptra® drug delivery system that is similar to the TheraCyte™ technology. The Encaptra® system is a device, that similar to TheraCyte™, consists of a semi-permeable immunoisolating membrane without a filling port (Figure 1.13). ViaCyte has also engineered the PEC-01™ cells, a proprietary pancreatic endoderm cell product. These cells are derived by the directed differentiation of human embryonic stem cells, and are delivered via the Encaptra® system. Following implantation in the Encaptra® device the PEC-01™ pancreatic progenitors mature into functional β-cells following implantation, showing significant GSIS response 8 weeks following implantation (141, 142). The PEC-Encap/VC-01™ product candidate is the combination and the product has shown promising pre-clinical data in small animal studies. In 2014 ViaCyte received approval to evaluate the PEC-Encap product in human clinical trials, NCT02239354, which are ongoing. This is a first-in-human, Phase 1/2 trial to evaluate the safety, tolerability, and efficacy at various doses of the VC-01 product in subjects with T1D. There are two cohorts: Cohort 1 will receive 2 VC-01 product implants and Cohort 2 will receive 4 or 6 VC-01 product implants. The duration of the study is for 2 years, and the primary outcomes are the incidence of all adverse events reported during the study and change in C-peptide from baseline levels to the 6 month check-up visit. No results have been released yet and the trial is estimated to be completed in January 2021 (143).

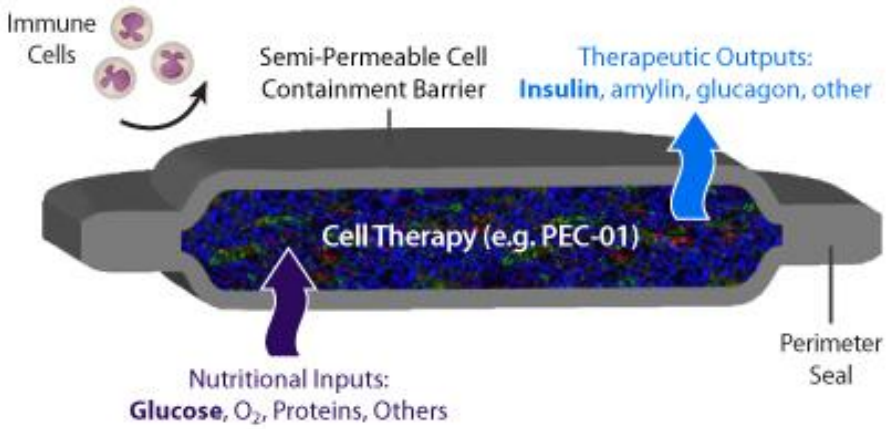

Figure 1.13 *Cross-sectional diagram of the PEC-Encap product (144).*

1.4.2 βair

The βAir bio-artificial pancreas is a macroencapsulation device in development by the company Beta-O_2. The device consists of an immunoisolating semi-permeable membrane, a hydrogel matrix to suspend encapsulated islets, and an air reservoir to supply oxygen to the encapsulated islets. The device has a hard external housing consisting of polyether ketone, and the semi-permeable membrane uses two hydrophilised PTFE membranes with a pore size of 0.45µm. These pores are then impregnated with a high viscosity mannuronic acid alginate, allowing the diffusion of glucose inwards and insulin outwards (145). The PTFE membranes support vascularisation but vascularisation of the βAir device does not provide sufficient oxygen to encapsulated cells, as in the TheraCyte™/Encaptra® devices. βAir employs a novel method of supplying oxygen to the encapsulated cells; an air reservoir. The islets in the device are separated from the oxygen reservoir via a rubber silicone membrane, which facilitates the free diffusion of oxygen gas from the reservoir. The device chamber must be refilled daily with a gas blend (95% oxygen, 5% carbon dioxide) to ensure adequate oxygen supply to the encapsulated islets and can be refilled via a port located externally to the body that is connected to the device by silicone tubing (Figure 1.14) (145).

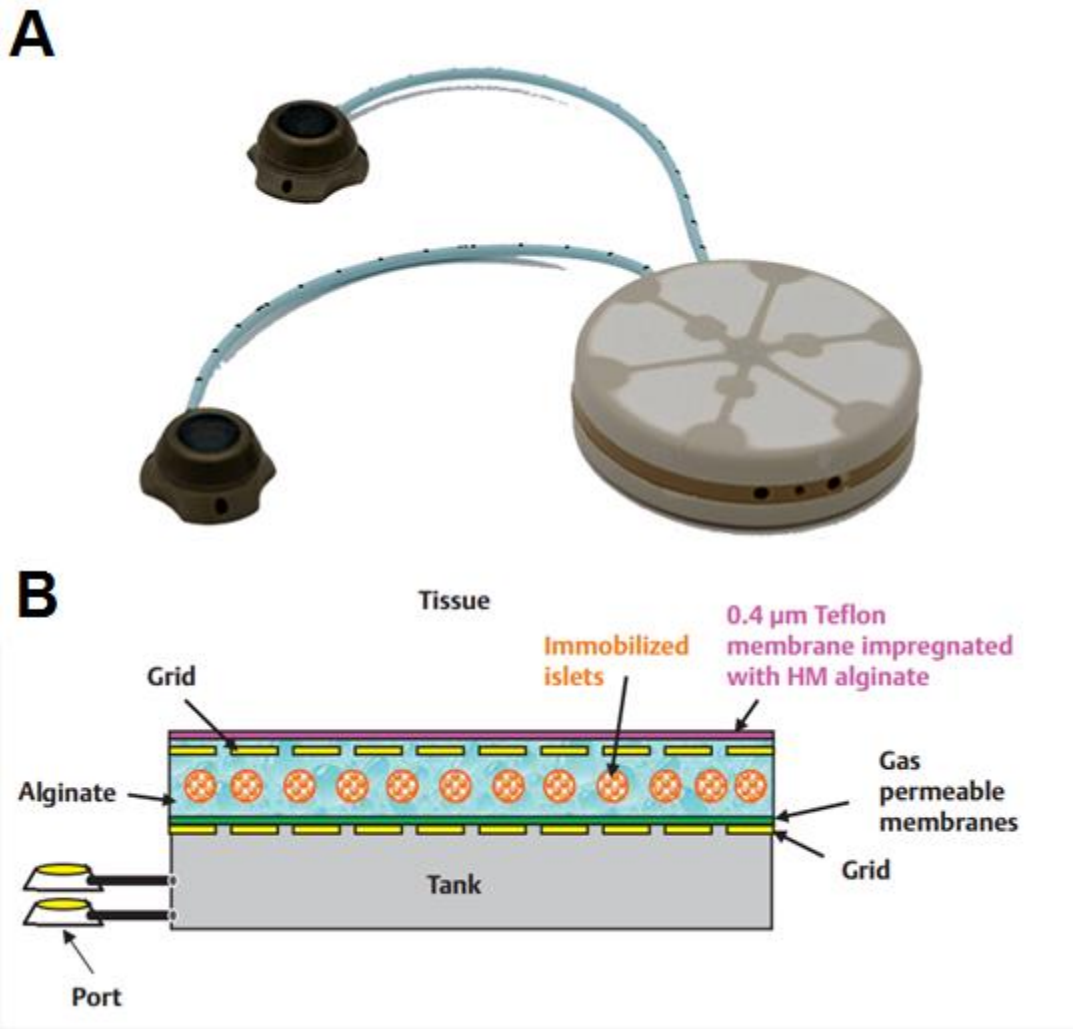

Figure 1.14 (*A)The βAir device and (B) a cross-sectional schematic of the different layers and chambers of the device. Adapted from the Beta-O_2 website and Ludwig et al (146, 147).*

Beta-O_2 first published on the βAir device in 2010, showing allogenic transplantation of pig islets in non-diabetic pigs for up to 13 days, to show islets remained viable after transplantation (147). A follow-up study in 2012 in rats showed that encapsulation in the device improved islet function after 90 days (148). βAir has shown efficacy in xenotransplantation in the treatment of diabetes using rat islets in mini pigs (149), human islets in rats, and pig islets in nonhuman primates (150).

In 2012, a first-in-man trial was performed with a 63 year old man. There was insufficient islets obtained for a standard islet transplantation, and the calculated islet mass transplanted was 2,100 IEQ/kg. The device was implanted into a pre-peritoneal pocket and no discomfort was reported after 2 weeks. The patient was

followed for 10 months and the transplanted islets were functional for the 10 months, but only showed modest improvements to disease management, likely due to the low islet mass transplanted (151). Approval for a Phase 1 clinical safety/efficacy study, NCT02064309, has enrolled 4 patients and was estimated to have completed in May 2019, with no results posted yet. The study is an interventional, single group, open label study. Patients will be implanted with the βair device. The primary outcome is safety of the device, as evaluated by incidence of adverse events within the first year (152).

1.4.3 Sernova Cell Pouch System™

The Sernova Cell Pouch System™ is a macroencapsulation device designed by Sernova Corp. The device consists of a porous polypropylene based matrix, and is designed to be implanted subcutaneously. Vascularisation is promoted into the device by the design of the pouch, and as a result it is not intrinsically immunoisolating. Due to the poor vascularisation of the subcutaneous site, the pouch is designed to first be implanted to the subcutaneous site and pre-vascularised over 30 days before the implantation of therapeutic cells.

An *in vivo* study of the efficacy of the cell pouch system was performed in mice, with islets transplanted to the kidney capsule used as a control. The pouch was implanted 4-5 weeks before transplant of islets to the pre-vascularised device. The device was well tolerated and showed reversal of diabetes comparable to the control kidney capsule transplant recipient for up to 100 days after implantation (153).

To date the Sernova Cell Pouch System™ has received approval for two clinical trials. The first trial, ”A phase I/II study of the safety and efficacy of the Sernova Cell Pouch™ for therapeutic islet transplantation, NCT01652911, was terminated without reason given in July 2016 and no results have been posted (154). Approval for a second clinical trial was granted in May 2018, “A safety, tolerability and efficacy study of Sernova’s Cell Pouch™ for clinical islet transplantation”, NCT03513939, enrolled its first patient in December 2018 and the study is estimated to be completed in July 2021. The study is interventional, with 7 participants and is a prospective, non-randomized, single-arm study. The cell pouch will be implanted under the skin for a minimum of 3 weeks, before initiating immunosuppression for another 3 weeks to ensure sufficient vascularisation of the device. A mass of 3,000

IEQ/kg bodyweight will be transplanted. The primary outcome of the study is to assess the safety of the cell pouch for up to 1 year following implantation, assessed by evaluating the incidence and severity of adverse events (155).

1.4.4 DRIVE project

The Diabetes Reversing Implants with enhanced Viability and long-term Efficacy (DRIVE) project aims to develop an implant for the delivery islets to treat T1D. The implant will consist of a functionalised biomaterial (β-gel), a macroencapsulation device (β-shell), and a surgical tool (β-Cath) and procedure (O-fold) to deliver the implant in a minimally invasive procedure.

The β-Gel will be a hydrogel formulation, loaded with the key components to ensure optimal cell survival. A biocompatible hydrogel will be functionalised with native pancreatic niche proteins and compositional efficacy cues which will encourage islets growth and survival. The β-Gel will also contain an oxygen delivery system; oxygen carriers will be loaded in the hydrogel to improve islet viability and survival in the hypoxic conditions of the delivery site through the first week following transplantation, prior to angiogenesis (Figure 1.15).

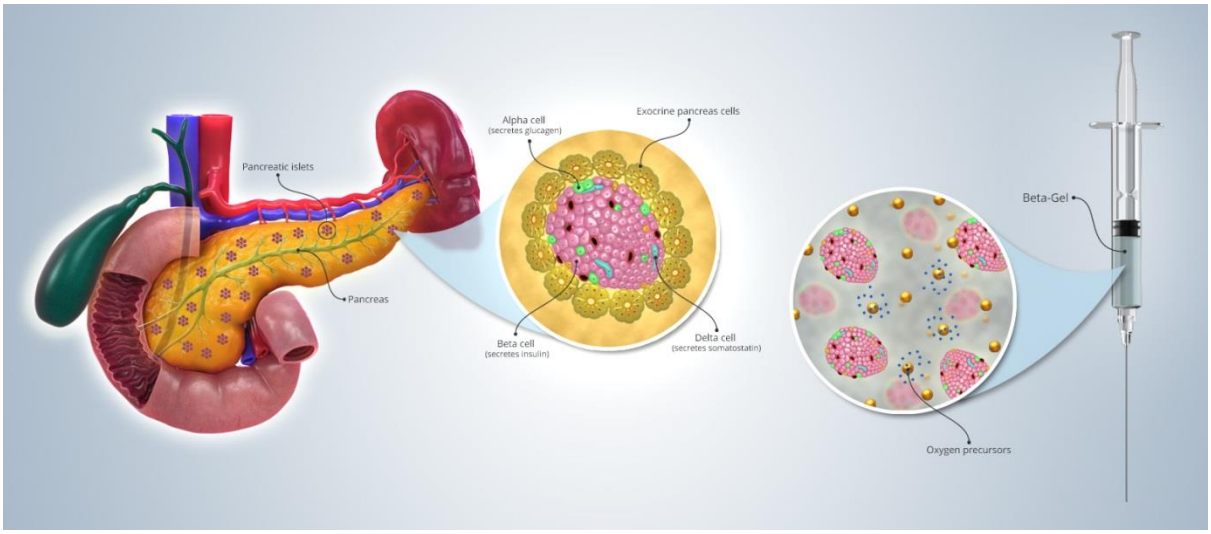

Figure 1.15 *Islets extracted from the pancreas will be included in the β-Gel. The hydrogel will contain a combination of materials including the oxygen carriers which will release oxygen to the islets in vivo.*

The β-Shell is a macroencapsulation device, which will enable the delivery of the β-Gel to an extra-hepatic site. The β-shell will consist of a semi-permeable, immunoisolating, retentive, and protective membrane. The β-shell will additionally support vascularisation onto the surface of the membrane and vascularisation will be further promoted by the inclusion of pro-angiogenic VEGF microparticles in/on the device. The immunoprotective membrane will facilitate the free transfer of glucose, oxygen, and other nutrients into the device while facilitating the release of insulin and clearance of waste back into systemic circulation, while inhibiting immune cells. This will allow for allografted islets to be transplanted without the need for immunosuppression.

The β-Cath will be a minimally invasive, custom designed catheter which will allow for the delivery of the β-shell to an extra-hepatic site, and filling of the device *in situ*.

The DRIVE project is ongoing alongside this thesis project, and the functionalised biomaterial developed for this PhD thesis will be utilised as the lead hydrogel formulation for the DRIVE project. The DRIVE product is currently in pre-clinical biocompatibility and efficacy trials in small and large animal models.

1.5 Thesis Objectives

While there has been much advancement in conventional diabetes management, returning endogenous insulin production to the patient with diabetes will remain the best treatment option for patient health outcomes and quality of life. Current treatment methodologies, such as the Edmonton protocol, although successful in reversion of diabetes in the short-term and improving patient outcomes, still require the use of systemic immunosuppression, meaning the treatment is not suitable for all patients. The scarcity of human islets and the number of islets required for a successful transplantation also greatly limit the application of the current procedure to a greater patient population. Islet encapsulation and the bioartificial pancreas are a potential solution to all of these problems, by improving transplanted islets viability and function without the need for systemic immunosuppression.

The overall objective of the research in this PhD thesis is to develop a novel functionalised biomaterial suitable for use as the ECM in a bio-artificial pancreas. Our central hypothesis was that hydrogels would act as a suitable ECM, to provide mechanical support and protection to the encapsulated islets, and that functionalisation with an oxygenation technology would overcome the hypoxia associated with macroencapsulation which is one of the key challenges of extravascular implantation of cells. These factors, in combination with the immunoprotective macroencapsulation device and a system to promote vascularisation i.e. the DRIVE technology, have the potential to overcome challenges faced by previously investigated approaches. In order to test this hypothesis the following objectives were pursued:

1. Formulation of a perfluorocarbon oxygen carrier functionalised hydrogel using hyaluronic acid and methylcellulose polymers, and assessment of their properties for inclusion in a bio-artificial pancreas. (Chapter 2)
2. Assessment of the lead fuctionalised hydrogels *in vitro* with a suitable β-cell line and primary pancreatic islets. (Chapter 3)
3. Process development and scale-up manufacture of the functionalised hydrogels for small and large animal *in vivo* testing. (Chapter 4)

Chapter 2

Formulation and physiochemical characterisation of a functionalised biomaterial to improve viability of transplanted islets

2.1 Introduction

2.1.1 Oxygen precursors for tissue engineering

Oxygen is an essential molecule required for the survival and function of most cells in the body. Therefore ensuring that there is a sufficient oxygen supply available to cells in tissue engineering applications is a key challenge that must be addressed; the development of hypoxia within bioengineered scaffolds remains one of the most pressing issues to date (156, 157). There have been a number of successful grafts of engineered tissue constructs without the addition of a supplementary oxygen supply, but these have mainly concerned tissues with low oxygen requirements due to their low metabolic activity (158). The development of a device containing pancreatic islets, an exceptionally metabolically active tissue with a high oxygen demand (159, 160), requires an adequate oxygenation technology to minimise the development of hypoxia and to protect the efficacy and viability of the islets.

There are a number of novel and established technologies being investigated in the literature to supplement oxygen supplies for bioengineering purposes. Oxygen generating biomaterials are one of the most heavily investigated areas in delivering oxygen to bioengineered scaffolds. The mechanism involves the decomposition of hydrogen peroxide (H_2O_2) to produce oxygen by the following reaction (161):

$$2H_2O_2 \longrightarrow O_2 + 2H_2O$$

This mechanism can reliably and sustainably provide oxygen release with only water generated as an easily eliminated by-product. Liquid hydrogen peroxide itself has been studied as an oxygen generating material however it does not provide oxygen sustainably; the decomposition into its products occurring rapidly within 5 h (162). As a result a great deal of research has been focused on improving this release rate by formulating the liquid hydrogen peroxide to retard its decomposition and prolong oxygen release. Strategies range from encapsulating hydrogen peroxide in PLGA microspheres (163), encapsulation in d-poly (methyl methacrylate) microcapsules (164) and generating a H_2O_2/poly (vinyl pyrrolidone) (PVP) complex (165). These approaches have seen varying levels of success, ranging from sustained oxygen release for >7 h in the case of the PLGA microspheres and up to two weeks of

sustained, physiologically relevant oxygen release in the case of the H_2O_2/PVP complex.

Solid/metal peroxides are in a similar class of oxygen generating materials as liquid hydrogen peroxide, functioning by generating hydrogen peroxide when allowed to react with water which will then decompose into oxygen and water as described above. By limiting the solid peroxides interaction with water through hydrophobic encapsulation, oxygen release can be more finely tuned with solid than liquid peroxides. Two such solid peroxides are calcium peroxide and magnesium peroxide which interact with water by the following reactions (161):

$$CaO_2 + 2H_2O \longrightarrow Ca(OH)_2 + H_2O_2$$

$$MgO_2 + 2H_2O \longrightarrow Mg(OH)_2 + H_2O_2$$

Calcium peroxide is a much more prolifically studied solid peroxide, due to its relatively higher solubility in water and thus faster reaction and oxygen release rate. *Pedraza et al* have investigated a polydimethylsiloxane (PDMS)-CaO_2 scaffold as a means of oxygenating β-cells and islets in hypoxic conditions *in vitro* (166). The highly hydrophobic nature of PDMS allowed for prolonged release of >40 days from the scaffold. *Coronel et al* have investigated a PDMS-CaO_2 disk for the supplementation of oxygen to pancreatic islets *in vivo* (167). Streptozotocin induced diabetic rats were implanted with the scaffold and were normoglycaemic within 5 days up to 40 days when the study was voluntarily terminated. Although solid peroxides provide a promising outlook on the supply of oxygen to cells in bioengineered scaffolds there are still a number of concerns which may limit their use *in vivo.* The solid peroxides are a limited oxygen source which once depleted adds no additional benefit to the bioengineered scaffold. The oxygen release of these materials is also not limited by the surrounding environment which can lead to super saturated oxygen systems, the loss of O_2 from a scaffold by diffusion and also the risk of generating cytotoxic oxygen radicles (161, 166, 168, 169).

A novel technology to provide a renewable supply of oxygen to a site is the use of photosynthetic organisms such as microalgae. In theory these organisms could recycle waste CO_2 into fresh oxygen to be utilised by the cells they are co-cultured with. Microalgae have been successfully co-cultured with human cells (170), and

have been successfully implanted in hydrogel (171) and collagen (172) scaffolds. Although studies have had interesting results a clear limitation of this novel technology is the need for light within the scaffold, limiting its placement to the skin or potentially subcutaneous tissue.

Microtanks are another novel technology, consisting of hollow polymer microspheres which can be loaded under hyperbaric conditions with 100% oxygen. The spheres are commercially available and are melt-mixed into polycaprolactone, spread into sheets and punched into disks of microtank-loaded constructs. By varying the concentration of microtanks loaded into the constructs oxygen delivery can be varied to prolonged times of up to 6 days and may be used to support cell viability in anoxia for this length of time (173).

2.1.2 Perfluorocarbons

The perfluorocarbons (PFCs) are a group of chemically inert compounds with properties that make them interesting for oxygen delivery. They are an easily manipulated group of compounds as they are mostly liquid at room temperature and are very chemically and thermally stable (174, 175). Structurally, the PFCs are made up of long chain fluorinated or semi-fluorinated carbon molecules. The C-F bond is a very strong intramolecular bond, leading to the low reactivity and chemical inertness of the PFCs. Fluorinated carbon molecules also result in very low intermolecular forces, Van der Waals forces (176). It is the weak intermolecular forces that allow for the PFCs high gas solubility, with the gas molecules “fitting” into the cavities between molecules (177). This gives the PFCs a relatively simple mechanism of action for delivering oxygen to a target site compared to the other strategies discussed. Due to their high solubility for oxygen the PFCs can be pre-loaded with oxygen before use with cells. As it is not independently driven by a catalyst or other mechanism, the release of this oxygen payload is dependent on the diffusion gradient of the surrounding environment. This ensures that there is an oxygen supply available in surplus of what may be available in culture media, scaffold materials or blood plasma. This limits the risk of hyperoxygenation and the production of free oxide radicals (178). Additionally, once an initial oxygen payload has been delivered the PFCs can remain *in situ* as part of a scaffold, effectively enhancing oxygen transport within the scaffold. The use of PFC emulsions for this purpose has been explored in

alginate hydrogels (179-181), chitosan based hydrogels (182, 183), and fibrin scaffolds (184). Finally, PFCs can act as a scavenger molecule for the waste product CO_2 (185), effectively oxygenating and removing waste gases simultaneously. A wide range of PFCs have been synthesised to date and their physical properties vary based on their molecular weight and chemical structure, existing primarily as either a liquid or gas. Their biological and chemical stability makes them interesting for use in biological and medical processes which includes uses such as biomedical imaging (186, 187), tamponades in ophthalmological surgeries (188, 189), biocompatible drug delivery agents (190) and their most studied uses as an oxygen carrier for use with cells *in vivo* and *in vitro*.

PFCs have been manipulated for use as an oxygen carrier to enhance oxygen transport for a wide range of purposes in the biomedical field. PFCs have been investigated for their potential to enhance cells growth and viability in 2D/floating culture. The first strategy that is employed is to culture in a 2 phase system, where the hydrophobic PFC is immiscible with the aqueous culture medium. A second strategy is using a PFC emulsion with the aqueous media. Aeration and suitable oxygenation is a potential limiting step in commercial bioreactors, limiting cell concentrations and thus products. *Damiano et al* used perfluoromethyldecalin (Flutec PP9) to oxygenate a bioreactor, aerating the PP9 and spraying it into the bioreactor vessel where it fell to the bottom for collection and recirculation. When compared to standard bubbling, growth was up to 6.2 times greater when PP9 was used (191). *Pilarek et al* cultured adherent cell lines at the interface formed between oxygenated PFD and DMEM culture media, to study growth and morphology. The cells had the potential to grow as 3D aggregates as they were not limited by vessel shape and oxygen requirements of a 3D aggregate were met by the PFD (192).

PFCs have also been used as a means of enhanced organ preservation for transplantation with hearts, kidneys, livers, lungs, small bowels, and pancreases all being stored in or with PFCs prior to transplantation (193). There are a number of techniques which can be used to preserve the organs however the most common method used with the pancreas is cold static storage. This sees the reduction of the temperature of the organ to 4°C to reduce metabolic activity. The PFCs can be used as part of a two-layer (TLM) or one-layer method (OLM). TLM sees a double layer of PFC and preservation solution prepared, and the organ is then placed floating

between the two layer (194). The PFC layer can then be oxygenated continuously. OLM removes the need for a preservation solution layer allowing the use of PFC alone, which further simplifies the procedure. *Brandhorst et al* found that OLM was a viable method for pancreas preservation (195).

The use of PFCs as a component of a potential blood substitute has also been studied. Fluosol-DA was the first commercially available PFC emulsion based blood substitute. It had a strong safety profile but did not show suitable efficacy as it could not meet the oxygen demands required. Subsequently further research was done to make a better blood substitute product, so called 2nd generation PFC emulsions. These emulsions used PFCs with higher oxygen capacities and greater concentrations of PFC. Oxygent is one such 2nd generation emulsion, containing 60% w/v of Perfluoro-octyl bromide (PFOB) with a phospholipid emulsifier. It was shown to be effective when used in lieu of a blood transfusion intraoperatively (196) and was found to enhance standard treatment of haemorrhagic shock (197).

Table 2.1 *Examples of PFCs used for oxygenation in cell culture, organ preservation and blood substitution.*

Perfluorocarbon	Function	Reference
Flutec P99	Liquid-liquid oxygenation of submerged cultures in a bioreactor.	*Damiano et al (191)*
Flutec P11	Enhancement of oxygen transfer in hybridoma cell culture in a bioreactor.	*Cho et al (198)*
Perfluoro-tripropylamine	Component of Fluosol-DA blood substitute.	*Mitsuno et al (199)*
	Oxygenating calcium alginate encapsulated insulinoma cells.	*Goh et al (200)*
Fluorinert FC-40 Fluorinert FC-70	Enhancing oxygen transfer in a bioreactor as PFC emulsion.	*Ju et al (201)*
Perfluoro-octylbromide (PFOB)	PFC emulsion for guinea pig heart preservation.	*Isaka et al (202)*
	Component of Oxygent used in blood transfusion intraoperatively	*Keipert (196)*
	Component of Oxygent used in resuscitation from haemorrhagic shock.	*Kemming et al (197)*
	PFOB emulsion used to prevent hypoxia in pancreatic β-cells prior to transplantation	*Maillard et al (203)*

Perfluorocarbon	Function	Reference
Perfluorodecalin (PFD)	Optimising oxygen mass transfer in a multiphase bioreactor.	*Amaral et al (204)*
	Growth of cells at a liquid-liquid interface of culture media and oxygenated PFD.	*Pilarek et al (192)* *Lowe et al (205)*
	TLM for pancreas preservation	*Witkowski et al (194)* *Scott et al (206)*
	OLM for human pancreas preservation.	*Brandhorst et al (178, 207)*
	TLM for canine bowel preservation.	*Tsujimura et al (208)*
	Endobronchial administration for porcine lung preservation	*Loehe et al (209)*
	Component of Fluosol-DA blood substitute	*Mitsuno et al (199)*
Perfluorohexyloctane (F6H8)	An alternative to PFD in OLM for human pancreas preservation.	*Brandhorst et al (178, 207)*
	Used to as a HTK-F6H8 emulsion to flush porcine kidneys during cold ischaemia.	*Asif et al (210)*
	Used for long-storage of rat pancreata for subsequent islet isolation	*Brandhorst et al (211, 212)*

2.1.3 PFD and F6H8

Two PFCs that have been widely explored and which were chosen for further study as part of this project are F6H8 and PFD. PFD was chosen due to its long history of use, having an established safety and efficacy record for a wide variety of uses. F6H8 is the second PFC chosen due to the work performed by *Brandhorst et al* which specifically showed F6H8 to have promise for organ preservation of donor pancreata.

F6H8 is a semi-fluorinated PFC consisting of six fluorinated carbon molecules with a non-fluorinated octane tail ($C_{14}F_{13}H_{17}$). It is a liquid at room temperature and has a lower specific gravity of 1.35g/cm^3 than other PFCs. This property has led to its traditional use as a temporary vitreous tamponade (213) in retinal surgery, and it is available commercially as F6H8-Vitreous Substitute (Fluoron). Its lower specific gravity allows it to be used without risking further mechanical damage to the eye. It has previously been studied as a long term tamponade (214) but evidence suggests that it may induce some structural modifications over longer periods of time (215). It is the lower density of F6H8 that benefits it in organ preservation also. PFD was traditionally used as part of TLM and later OLM for organ preservation. The use of PFD is somewhat limited by its high density (1.92g/cm^3), as it is unable to penetrate deeper tissues of the pancreas. F6H8s lower density allows for deeper tissue permeation and its similar carrying capacity to PFD results in better oxygenation. When compared with PFD, F6H8 had higher intrapancreatic pO_2 than PFD treated pancreata (178) and another study found that F6H8 preparations allowed for increased cold ischaemia time (216). Although there is currently limited data available for F6H8 usage in tissue engineering, the efficacy and safety established through its use as a tamponade with a delicate organ such as the eye and proven efficacy with pancreatic cells makes strong candidate molecule for use with the hybrid HA/PFC hydrogel.

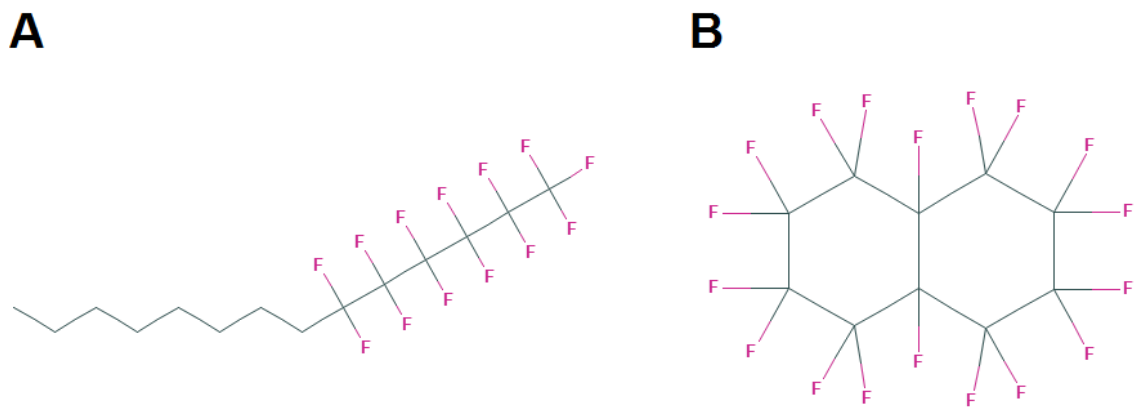

Figure 2.1 *(A) Structure of F6H8, a semi-fluorinated PFC. (B) Structure of PFD, a fully fluorinated PFC.*

PFD has a long history of use as an oxygen carrier. PFD is an extremely stable and inert molecule, consisting of two fully fluorinated carbon rings ($C_{10}F_{18}$). It is a liquid at room temperature and has a high density of 1.92g/cm^3. It is favoured for its long history of use in biological systems, with one of its first reported uses being as part of Fluosol-DA, a blood substitute from a Japanese manufacturer (217). It was a component of the first blood substitute product to receive FDA approval (218), which indicates that there is a comprehensive safety profile attached to all components of the preparation. Although the product was ultimately pulled from the market it was not as a result of safety associated with the product but poor efficacy of the treatment identified in post marketing research. Efficacy of PFD is seen with higher concentrations, with this particularly clear with PFDs use in TLM of organ preservation. Entire organs meant for transplant can now be excised, flushed with preservation solution, partially immersed in oxygenated PFD (219) and maintain viability for prolonged periods of cold storage.

PFD has also started to see some use in tissue engineering purposes to make oxygenated scaffolds. *Douglas et al* reported supplementing a chitosan hydrogel with PFD to improve adipose derived stem cells viability and reduce cell death (183) while *Tamimi et al* investigated the use of integrating PFD into an engineered bioceramic with bone marrow to enhance bone regeneration (220). *Maillard et al* have reported the use of PFD emulsions for the culture of pancreatic islets in a fibrin-based matrix prior to islet transplantation; storage of isolated islets in the fibrin/PFD emulsion

matrix improved islet viability, function and morphology and helped to reduce hypoxia in encapsulated islets (184). There is a large body of evidence surrounding safety and efficacy of PFD *in vivo* making PFD a suitable choice as one of the primary PFCs to be investigated for this project.

2.1.4 Hyaluronic acid

Hyaluronic acid (HA) or hyaluronan is a naturally occurring polysaccharide polymer found widely distributed in all mammalian tissues as a major component of the ECM (221). The HA polymer is an uncomplicated polysaccharide, consisting of linear repeating units, a disaccharide of alternating D-glucuronic acid and D-N-acetylglucosamine connected by β-linkages (Figure 2.2) (222) and has a high molecular weight of up to 1 x 10^7 DA (223, 224).

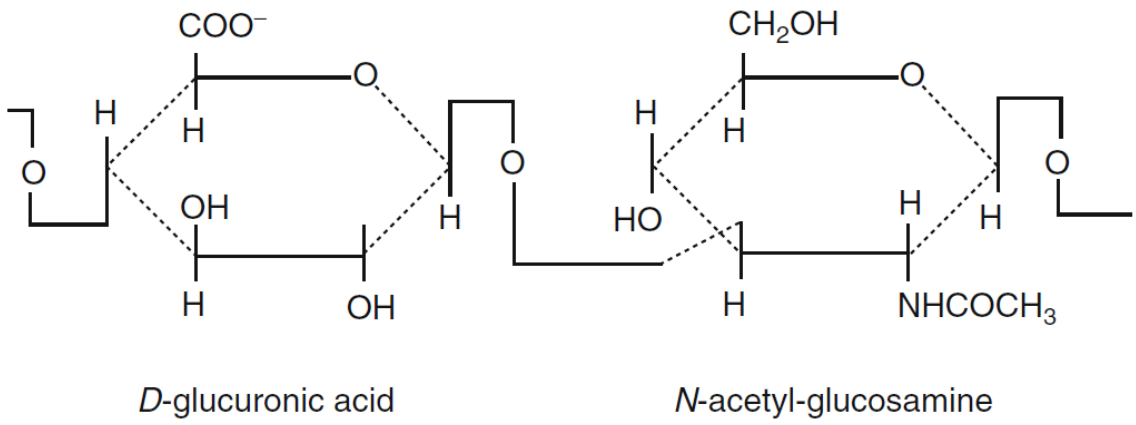

Figure 2.2 *The structure of HA repeating subunit (225).*

It is synthesised by a group of plasma membrane proteins called the hyaluronan synthases and subsequently degraded by another enzyme group the hyaluronidases (226, 227). HA has a number of functions as part of the ECM ranging from: interactions with proteins in the ECM and on the cell surface, modulating functions ranging from immune inflammatory response to tumour progression; as a hydrophilic filler protein, maintaining tissue hydration and lubrication in joints and other mechanically active tissues; and in wound healing (228, 229). Although HA is found throughout the body it's prevalence in mechanically active sites has led to a great deal of research, such as; the synovial fluid of joints and cartilage, used in osteoarthritis as a treatment and to provide symptomatic pain relief (230, 231); and

the skin, HA is used in popular “anti-ageing” cosmetics (232). An unmodified or “native” HA (natHA) does not form a chemically crosslinked hydrogel, instead making a physical matrix network with transient junctions caused by polymer chain entanglement (103). As a result, research into using a natHA as a biomaterial by itself is limited, and it is more frequently used to supplement other formulations for its modulatory functions. However due to the natHA’s high molecular weight and chain length, its biocompatibility, and safety in use it shows potential to be used as part of this project. By functionalising a natHA hydrogel with an oxygen precursor with/without another bioactive element could provide a suitable biomaterial to improve islet viability following transplantation.

Although HA shows promise as a biomaterial in its native state, HA also has a highly modifiable polysaccharide backbone. The hydroxyl and carboxylic groups are the two primary sites on the saccharide monomers, that facilitate the substitution of side-chains/groups (233). Substitutions can be made to add favourable characteristics to the HA such as adding side groups to facilitate crosslinking and hydrogel formation, or improving cell adhesion to improve by adding bioactive side groups like RGD (234). For this project we also investigated a tyramine modified HA (HA-TA) which allows for the formation of a rigid solid hydrogel by covalent bonding of the phenol on the tyramine groups. Horseradish peroxidase (HRP) and H_2O_2 are the catalysing agents for this reaction. The heme group on the HRP and the H_2O_2 form an intermediate oxidated heme on the HRP (Compound I). Compound I converts back to HRP in its initial state in 2 steps. Compound 1 first reacts with the first substrate, the phenol group (Ph-OH) of the HA-TA, to give Compound II and a phenol radicle (Ph-O•). Compound-II then reacts with a second Ph-OH group to return back as HRP, releasing a H_2O molecule and giving a second Ph-O•. The two Ph-O• can now dimerise giving a covalent bond. In the correct conditions this allows the formation of crosslinks across separate HA chains to form a solid hydrogel (235). This reaction is outlined in Figure 2.3 (236).

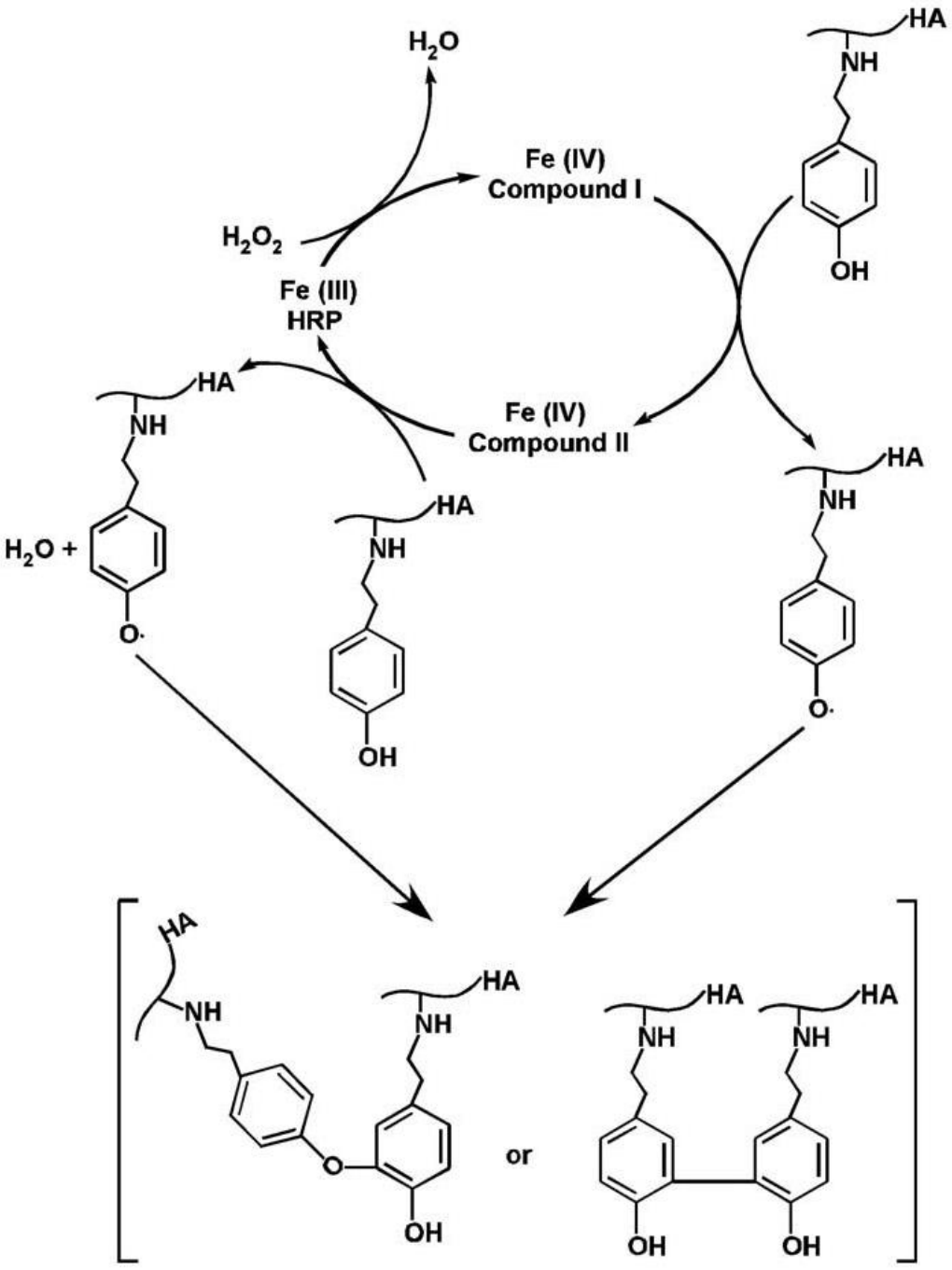

Figure 2.3 *Crosslinking reaction of the HA-TA hydrogel (236).*

Gelation can be finely controlled by the degree of substitution of the HA and by changing the concentration of the HRP and H_2O_2. HA-TA hydrogels have previously been studied for a number of purposes such as drug and/or cell delivery. *Lee et al* (236) and *Xu et al* (237) investigated the use of the HA-TA hydrogel as an injectable vehicle for protein delivery, with drug release being mediated by hyaluronidase degradation of the hydrogel. Other groups have investigated similar hydrogels as cell

delivery vehicles (238, 239). The primary challenge of functionalising a HA-TA hydrogel is ensuring the physical characteristics of the crosslinked hydrogel are maintained.

2.1.5 Methylcellulose

Methylcellulose (MC) is a water soluble, biodegradable cellulose polysaccharide derivative. It is commonly used in the pharmaceutical industry as a filler in tablets and capsules, stabilising agent in emulsions (240), as a therapeutic agent by itself as a bulk laxative (241), in encapsulation (242), and as a gelling agent (243). When looking at MC for use as a biomaterial, pure MC undergoes a thermoresponsive crosslinking reaction at ~50-70°C. Although this high temperature is unsuitable for use as a biomaterial a number of studies have identified different salts that can reduce the gelation temperature to lower levels within physiological levels (244). Work done previously in the Duffy-Kelly Lab has identified a formulation for a MC hydrogel using β-glycerophosphate (βGP) to reduce the gelation temperature (245). This hydrogel forms a crosslinked hydrogel at physiological levels. This hydrogel has also been formulated with a type I collagen to act as a bioactive ECM adhesion molecule for encapsulated cells. Our aim is to further functionalise this methylcellulose/collagen (MCC) hydrogel with an oxygen precursor while ensuring the sol-gel transition at physiological temperatures is not lost.

2.1.6 Aims

The overall aim of this Chapter is to formulate and characterise a functionalised biomaterial to improve the viability of transplanted cells.

Three biomaterials formulations were assessed using two base polymers, HA, using both a native natHA (natHA) and a crosslinked HA (HA-TA), and a thermoresponsive MC hydrogel.

To address the challenge of hypoxic conditions in transplanted cells in extravascular scaffolds and device as discussed in Chapter 1 we wanted to look at improving the oxygen supply to encapsulated islets in the initial period immediately following implantation, when the transplanted cells have an increased oxygen demand.

PFCs were chosen due to their established safety and biocompatibility profile, mechanism of action and high oxygen solubility, allowing them to store higher concentrations and improve the rate of diffusion through the material.

The specific aims of this chapter were:

- To formulate the hydrophobic PFCs as a stable emulsion to facilitate their incorporation into the hydrogels.
- To functionalise the hydrogel biomaterial with the PFC emulsion.
- To characterise the oxygen loading and storage properties of the functionalised hydrogel biomaterial to assess whether they improve the oxygen supply.
- To rheologically characterise the functionalised hydrogel biomaterial to determine their suitability for delivery to an extravascular device.

2.2 Materials and Methods

2.2.1 Materials

PFD, MC (88k Da, 400 centiposes), H_2O_2, βGP, glacial acetic acid, hydrochloric acid (HCl) and phosphate buffered saline (PBS) were purchased from Sigma-Aldrich (Ireland). F6H8 was obtained from Novaliq GmbH (Germany). Lipoid E80 was purchased from Lipoid AG (Switzerland). natHA polymer (~1.2-1.3M Da chains), HA-TA (~200-250K Da chains) and HRP were obtained from Contipro a.s. (Czech Republic). Bovine type I fibrillar collagen was purchased from Southern Lights Biomaterials (New Zealand). Oxygen (99.5% purity) was purchased from BOC gases (Ireland).

2.2.2 Experimental Outline

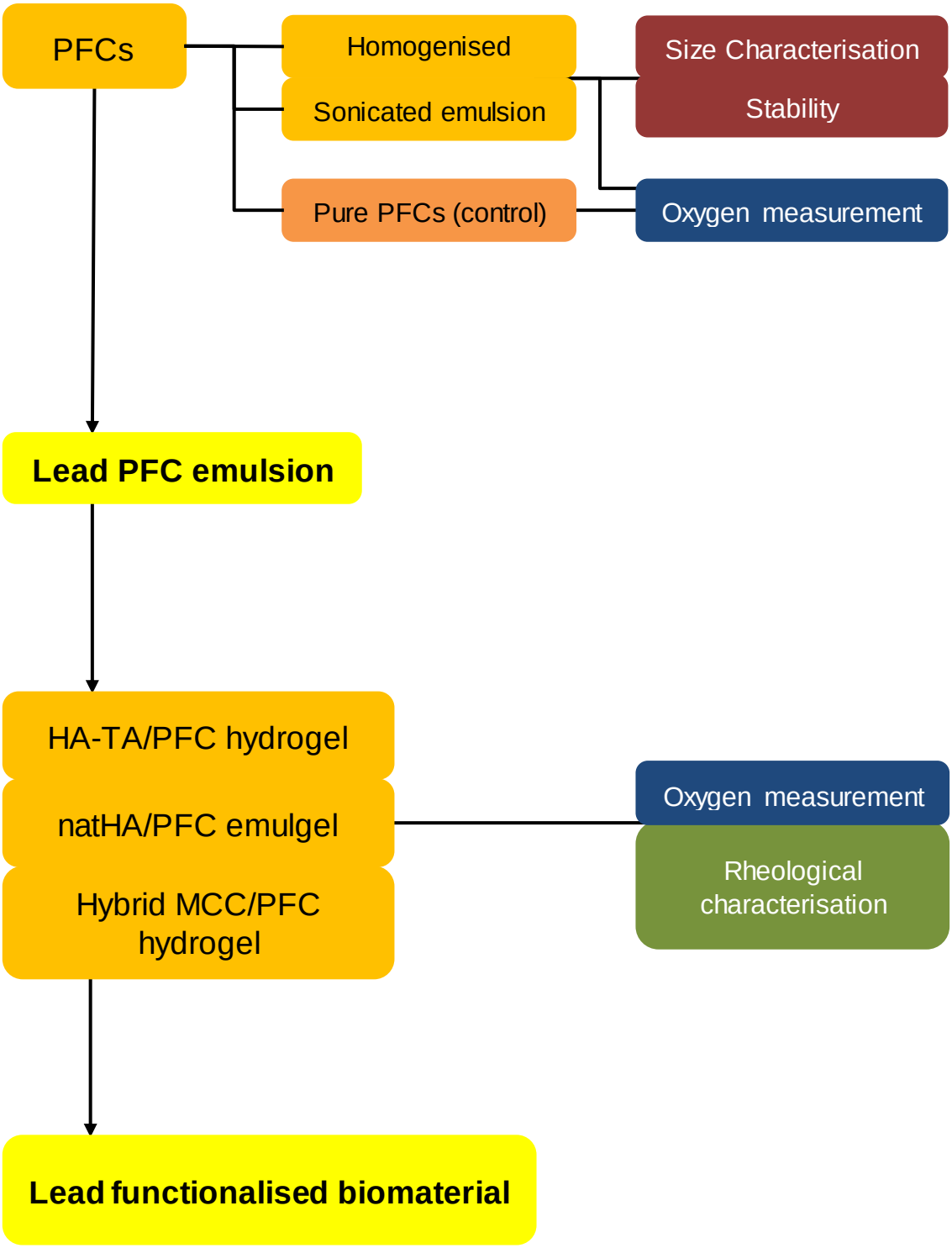

Figure 2.4 *Outline of the formulation and characterisation activities perform for selection of the lead functionalised biomaterial.*

2.2.3 PFC emulsion formulation

As PFCs are a hydrophobic class of compounds the PFCs of choice, PFD and F6H8, were formulated as an emulsion to enable incorporation into a hydrophilic polymer matrix. The PFC emulsion formulation was adapted from a protocol outlined by *Sanchez et al* (246) at concentrations of ~70%w/v of the PFC in PBS, using Lipoid E80 as the emulsifier, by two methods, homogenisation and sonication. The final composition of the two emulsions is shown in Table 2.2.

Table 2.2 *Formulation composition for the PFC emulsions.*

PFC	PFC density	Lipoid E80	PFC	PBS
PFD	1.908g/mL	160mg	0.7mL	1.3mL
F6H8	1.33g/mL	160mg	1mL	1mL

2.2.3.1 Preparation of the homogenised PFC emulsions

Homogenised PFC emulsion was prepared using the Ultraturrax T25 homogeniser. For 2mL of the final emulsion, lipoid was weighed into a 10mL beaker and PBS added. The lipoid was gradually dispersed in the PBS using the homogeniser at 9500RPM until fully dispersed and the liquid was an opaque milky white. Under continuous mixing at 9500RPM the PFC was added dropwise and once added completely the homogeniser speed was increased to 17500RPM and mixed on ice for 10 min (PFD) or 20 min (F6H8). All mixing was done on ice to minimise heat generation.

2.2.3.2 Preparation of the sonicated PFC emulsions

Sonicated PFC emulsions were prepared using the Branson SLPt sonicator (150 watts) with a 0.125" microtip. For 4mL of the final emulsion, lipoid was weighed into a 50mL tube and PBS added. The lipoid was dispersed at 50% amplitude for 30 sec. The 50mL tube was transferred to an ice bath and PFC added. The sonic probe tip was positioned at the layer of lipoid dispersion and the PFC mixture was sonicated for a further 7 min at 50% amplitude.

2.2.4 Emulsion characterisation

2.2.4.1 Size and stability characterisation

PFC emulsions were characterised for their droplet size by dynamic light scattering (DLS) using the Zetasizer NanoZs (Malvern). 2mL of the emulsions were stored in 15mL tubes at three temperatures: 20-25°C, 37°C and 4°C. Samples for size measurements were taken periodically to assess emulsion stability.

2.2.4.2 Oxygen loading and oxygen release

Oxygen storage properties of PFC emulsions were characterised by measuring oxygen release profiles, using PBS and pure PFCs as a control. Emulsions were first diluted to 30% w/v PFC. This concentration was identified as the working concentration for the PFCs during preliminary testing with the HA-TA hydrogel; concentrations >30% w/v of PFD resulted in poorly formed hydrogels (Figure 2.5A). Samples were then oxygenated by bubbling 99.5% purity oxygen through the liquid for 7 min/mL; this was identified as sufficient to saturate the sample (Figure 2.5B).

The oxygen concentration over time was measured using the Firesting O_2 optical oxygen meter (Pyroscience GmbH, Denmark) (Figure 2.6A). 1mL oxygenated samples were placed in identical vials and the probes were placed equal depths into each vial. A 1mL layer of PBS was carefully overlaid onto the emulsion to prevent evaporation directly affecting the emulsion concentration (Figure 2.6C). The results were recorded using the Pyroscience proprietary software and the graphs were generated using Microsoft Excel.

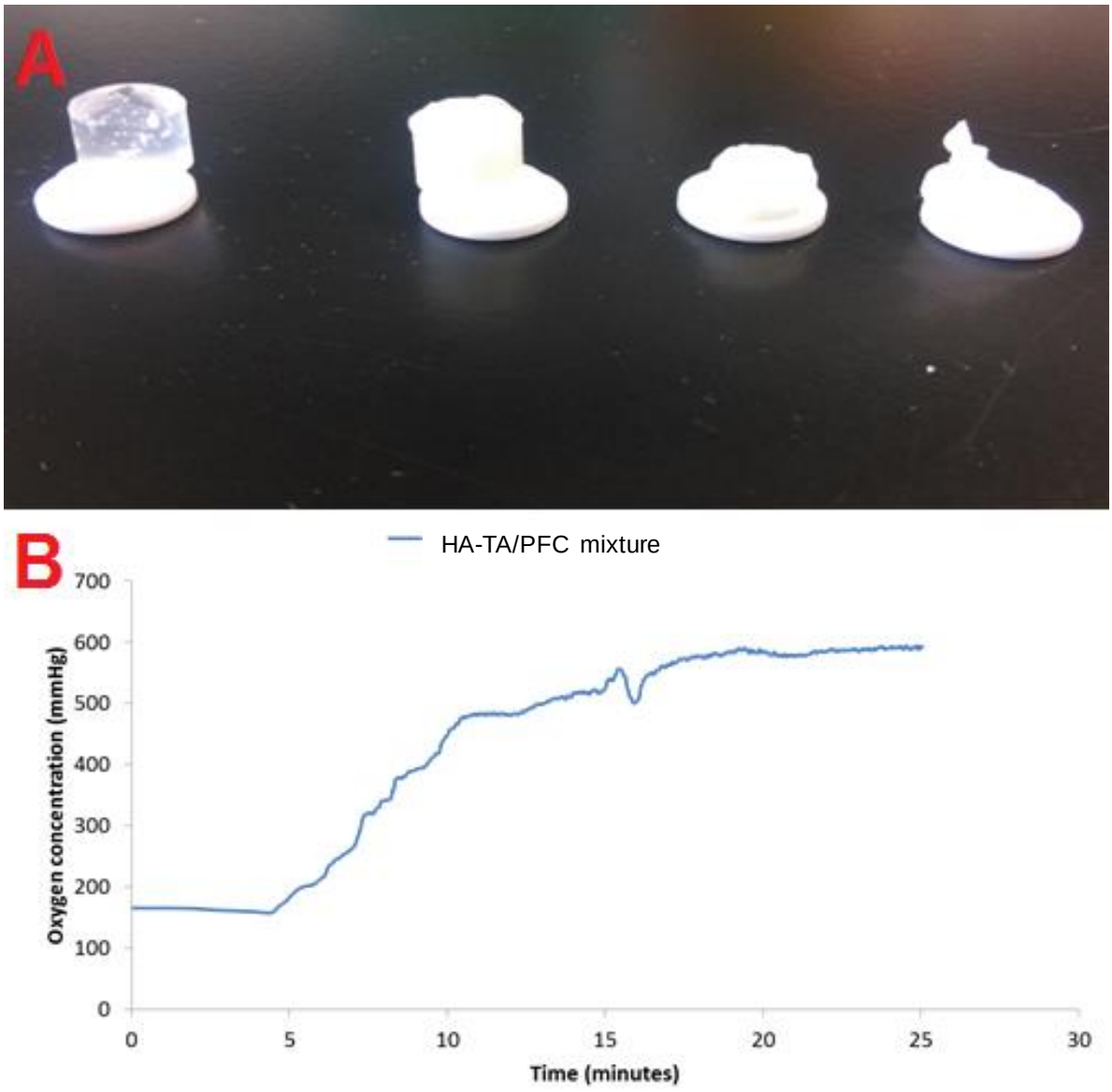

Figure 2.5 *Preliminary experiments used to inform formulation and methods used in Chapter 2. (A) Structure of HA-TA hydrogels with differing PFC concentrations; from left to right 0/30/35/45% w/v. (B) Oxygenation of 3mL of a HA-TA/PFC mixture; oxygen concentration plateaus after ~20 min.*

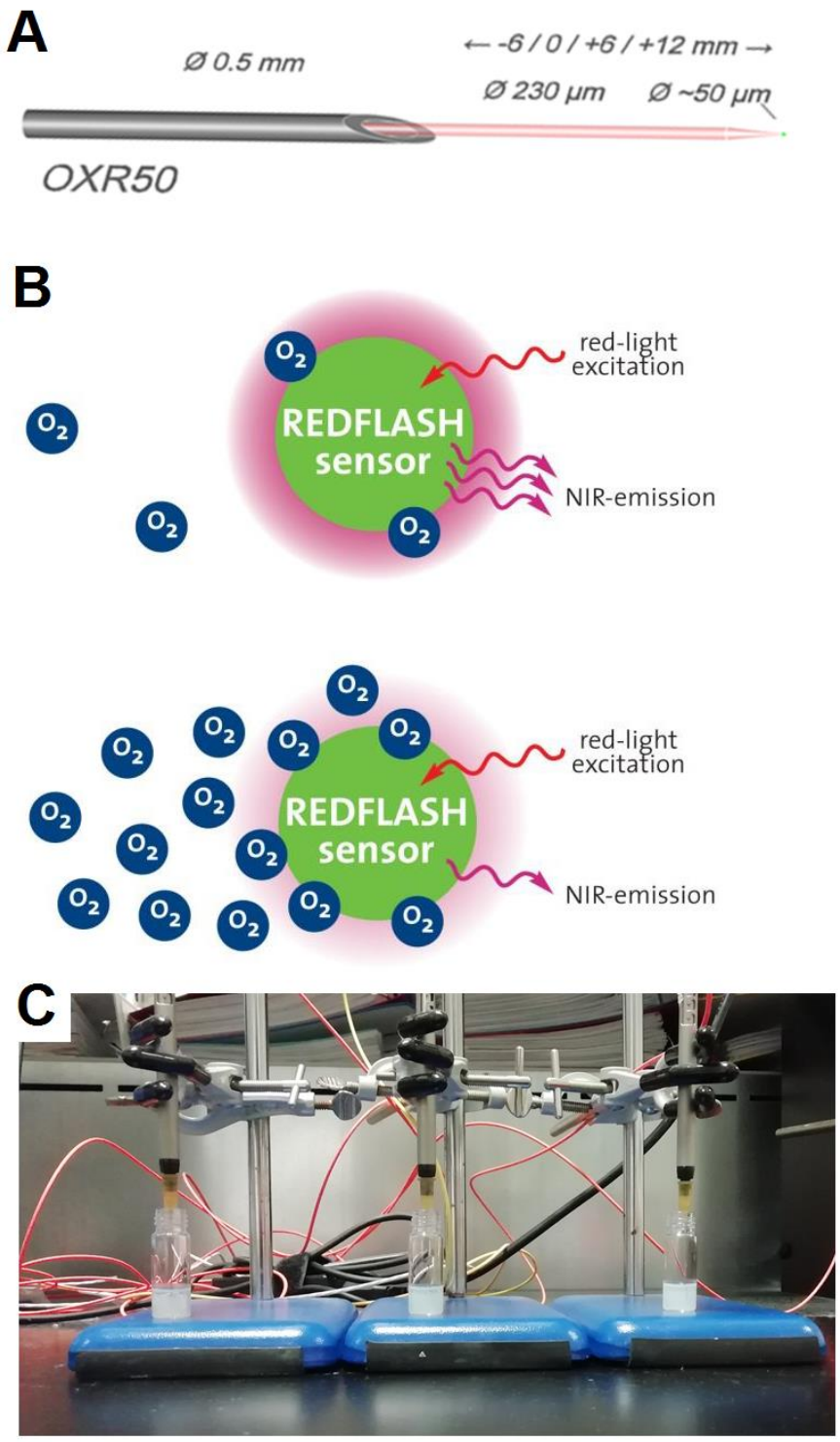

Figure 2.6 *(A) The Pyroscience OXR50 retractable probe tip. The fine needle houses the fibre optic probe. The tip is coated in a REDFLASH dye which detects the oxygen based on the principle illustrated. (B) The REDFLASH dyes show near infrared luminescence which is quenched in the presence of high oxygen concentration (247). (C) Oxygen probe setup with tips placed equal distances into the sample I identical vials.*

Table 2.3 *Formulation composition evaluated using a HA-TA, natHA or MCC as base polymers.*

	% w/v					
Gel formulation (GF)	**HA-TA**	**HRP + H_2O_2**	**NatHA**	**MC**	**Collagen**	**PFD**
1a	1	-	-	-	-	-
1b	1	V	-	-	-	-
2a	1	-	-	-	-	30
2b	1	V	-	-	-	30
3	-		2	-	-	-
4	-		1.5	-	-	-
5	-		1	-	-	-
6	-		1	-	-	28
7	-		0.615	-	-	28
8	-		-	2.5	0.1	-
9	-		-	2.5	0.1	30

2.2.5 Formulation of a PFC functionalised biomaterial

Three base polymers, HA-TA, natHA, and MCC, were investigated to identify a lead functionalised biomaterial formulation. Table 2.3 outlines the general formulation for the gel formulations discussed in subsequent sections.

2.2.5.1 Formulation of a hybrid HA-TA/PFD hydrogel

A short-chain HA substituted with tyramine side chains was supplied by Contipro. This material can form a covalently crosslinked hydrogel via an enzyme catalysed reaction, outlined in Figure 2.3. Table 2.3 (GF 1-2) outlines the composition of the different HA-TA formulations.

HA-TA hydrogel acted as a control. To prepare the hydrogel, lyophilised HA-TA was hydrated in PBS (conc. 1% w/v) overnight on a roller to ensure the HA-TA was fully hydrated. The HA-TA polymer solution was sterile filtered using a 0.2µm syringe filter. The crosslinking agent HRP was provided aliquoted at 8 U/mL and H_2O_2 was prepared fresh at 0.1% w/w for each preparation. The HA-TA polymer solution was divided into two parts, Part A and Part B, and one crosslinking agent was added to each part; 30µL/mL HRP solution to Part A; 30µL/mL H_2O_2 to Part B. Both solutions were drawn into separate syringes and attached to the gel mixing rig (Figure 2.7). As the solutions are pushed through the rig they pass through the static mixer which ensured homogenous mixing. After mixing the hydrogel take ~30-60 sec to form a solid shape and can be collected into different containers or a mould depending on the characterisation being performed. The hydrogels were given sufficient time to fully gel before manipulation. The HA-TA hydrogels are a solid clear colourless hydrogel.

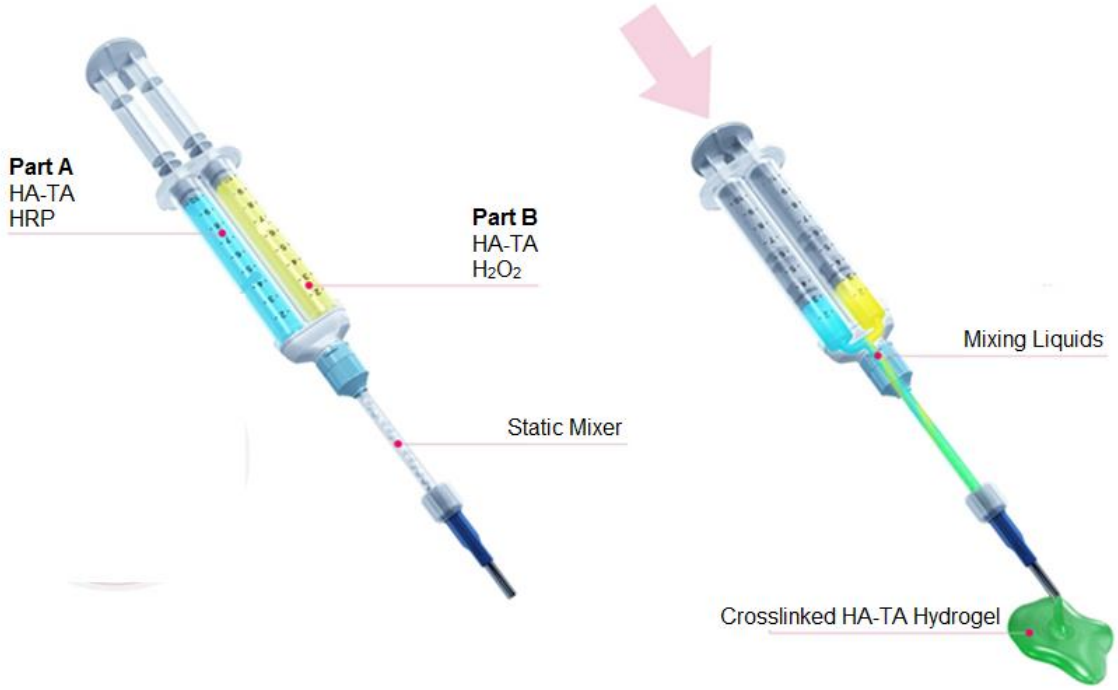

Figure 2.7 *Schematic showing HA-TA hydrogel preparation and the gel mixing rig.*

A hybrid HA-TA/PFD hydrogel was prepared using the HA-TA and the sonicated PFD emulsion (66.78% w/v) from Section 2.2.3.2 above. Lyophilised HA-TA was hydrated in PBS at a 1.818% w/v and was vortexed with PFD emulsion at a 0.55:0.45 ratio to give a mixture with the final concentrations of 1% w/v HA-TA and 30% w/v PFD. The same mixing protocol for forming the HA-TA hydrogel from above was followed using the HA-TA/PFD mixture (Figure 2.7). After mixing the hybrid HA-TA/PFD hydrogel took longer (~1-2 min) to fully gel.

2.2.5.2 Formulation of a natHA/PFD emulgel

The natHA used for this study was a long chain, high molecular weight (~1.2-1.3MDa) with no side chain substitution. When hydrated the natHA forms a concentration dependant viscous liquid hydrogel. Table 2.3 (GF 3-7) outlines the different compositions of the natHA formulations.

Control natHA was prepared at a number of different concentrations for rheological assessment. Lyophilised natHA was hydrated in PBS in a 50mL tube over 1-2 days on a roller to ensure it was fully hydrated. Hydrogels ranging from 1-2% were prepared for assessment (GF3-5).

NatHA/PFD emulgel was prepared using the natHA and the sonicated PFD emulsion (66.78% w/v) from Section 2.2.3.2. NatHA was hydrated in PBS up to concentrations of 3% w/v for dilution with PFD emulsion to give the final concentrations in Table 2.3 (GF 6-7). Due to the high viscosity of the natHA hydrogels, the PFD emulsion was incorporated into the natHA by passing the natHA and the PFD emulsion between two syringes connected by a female-female coupler to give a homogenous natHA/PFD emulgel.

2.2.5.3 Formulation of a hybrid MCC/PFD hydrogel

MCC wafers were prepared according to the protocol outlined in the paper by *Payne et* al (245). A stock solution of 4% w/v MC was prepared by stirring in deionised water. The collagen slurry was prepared by blending bovine type I collagen into a solution of 0.05M acetic acid at 15,000RPM for at least 90 min. The slurry was added dropwise into the 4% w/w MC polymer solution, and deionised water was added, to give final concentration of 2.5% w/v MC and 0.1% w/v collagen. This was allowed to mix for 1 h and then equilibrated at 4°C overnight. The equilibrated solution was aliquoted into 30mL aliquots in 50mL falcon tubes and centrifuged at 3500 G to degas the polymer solution. The polymer solution was transferred to metal moulds and freeze-dried using an optimised freeze drying protocol to prepare MCC wafers. The MCC wafers were sterilised by gamma irradiation at 25 kGy, in accordance with sterilisation standards in the European Pharmacopeia (248).

The control MCC hydrogel was prepared by rehydrating an MCC wafer in 30mL of a 5.6% w/v βGP salt solution, by stirring for up to 3 days on ice. The pH was adjusted to 7.0-7.4 using 1M HCl. This gave the final MCC polymer solution which is a translucent/clear colourless liquid. When heated above 37°C this forms an opaque solid hydrogel.

The hybrid MCC/PFD hydrogel was prepared by rehydrating an MCC wafer in 16.5mL of a 10.18% w/v βGP salt solution, by stirring for up to 5 days on ice. The pH was adjusted to 7.0-7.4 using 1M HCl. Once the wafer had been fully hydrated the resulting MCC polymer solution was diluted with sonicated PFD emulsion to give the final concentrations in Table 2.3.

2.2.6 Rheological characterisation of functionalised biomaterials

The rheological characteristics of all formulations were measured on either the AR-1000 constant stress rheometer (TA instruments, USA) or the Discovery Hybrid Rheometer HR-2 (TA instruments, USA). Temperature control was provided by a peltier plate and a LAUDA Ecoline 003 E100 water-bath (Lauda-Konigshofen, Germany) was used as the heat-sink. All measurements were performed using the same cone shaped geometry (40mm diameter, 4.013° cone angle, 112µm gap), and solvent trap of the geometry was filled with water to minimise evaporation during testing. Prior to commencing testing, the rheometer was calibrated by setting the geometry gap and performing rotational mapping of the geometry. Approx. 1.3mL of the sample was loaded on to the temperature controlled peltier plate and the geometry was lowered to the gap. Analysis of rheometry data was processed using TA Data Analysis software, if using the AR-1000, or TRIOS Software, if using the HR-2 (TA instruments, USA). All samples were run in triplicate with presented results being indicative of the norm.

Flow procedures (steady state flow and peak flow hold) were used to measure the viscosity (Pa.s) of the hydrogel in response to changes in shear stress (Pa). Oscillatory procedures (time sweep and temperature sweep) were used to measure the storage modulus (G') and the loss modulus (G'') to measure gelation over time for the HA-TA based hydrogels, and thermoresponsive gelation for the MCC based hydrogels. Rheological assessments performed on the hydrogel formulations in this chapter are outlined in Table 2.4.

Table 2.4 *Experimental parameters for rheological characterisation of the formulations of the HA-TA, natHA and MCC base polymers.*

GF	Test	Stress	Time	Temperature	Frequency	Strain
1b, 2b	Steady State Flow Sweep	5-25 Pa	-	20°C	-	-
1a, 2a	Time Sweep	-	30 min	20°C	1 Hz	1%
3, 4, 5, 6	Steady State Flow Sweep	1-50 Pa	-	25°C	-	-
6	Peak Hold Recovery	1-50-1 Pa	5-5-10 min	25°C	-	-
7	Steady State Flow Sweep	1-35 Pa	-	25°C	-	-
7	Peak Hold Recovery	1-35-1 Pa	5-5-10 min	25°C	-	-
8, 9	Steady State Flow Sweep	1-50 Pa	-	25°C	-	-
8	Temperature sweep	5 Pa	20 min	25-45°C @1°C/min increments	1Hz	-
9	Temperature sweep	-	20 min	25-45°C @1°C/min increments	1Hz	0.5%

2.2.7 Oxygenation and characterisation of oxygen storage properties of the functionalised biomaterials

Different oxygenation protocols were developed for the different biomaterials, based on their viscosity. The oxygen storage properties of the functionalised biomaterials were characterised by measuring their oxygen release profiles.

2.2.7.1 Oxygenation of HA-TA hydrogels

The oxygen storage properties of the HA-TA and hybrid HA-TA/PFD hydrogels were characterised by measuring their oxygen release profiles. The HA-TA polymer solution and HA-TA/PFD mixture were oxygenated by bubbling 99.5% purity oxygen at 1L/min flow rate through Part B (Figure 2.7) in a syringe for 7 min/mL. Part B was exclusively oxygenated as when encapsulating cells the cells would be mixed into Part A to reduce their contact with H_2O_2, as this is cytotoxic to cells.

Part B was oxygenated in a syringe to minimise the loss of oxygen. This approach is the result of preliminary work that was performed to identify where oxygen was being lost when preparing HA-TA hydrogels. GF1a was oxygenated by bubbling in a glass vial, at a rate of 7 min/mL. Once oxygenated the oxygen concentration in the GF1a was measured in the vial and recorded. GF1a was then drawn up through an 18g needle into a syringe and transferred to a fresh vial, where the oxygen concentration was measured again. It was identified that the vacuum generated to draw liquids into a syringe partially degassed oxygenated samples, reducing the oxygen concentration in the sample (Figure 2.8).

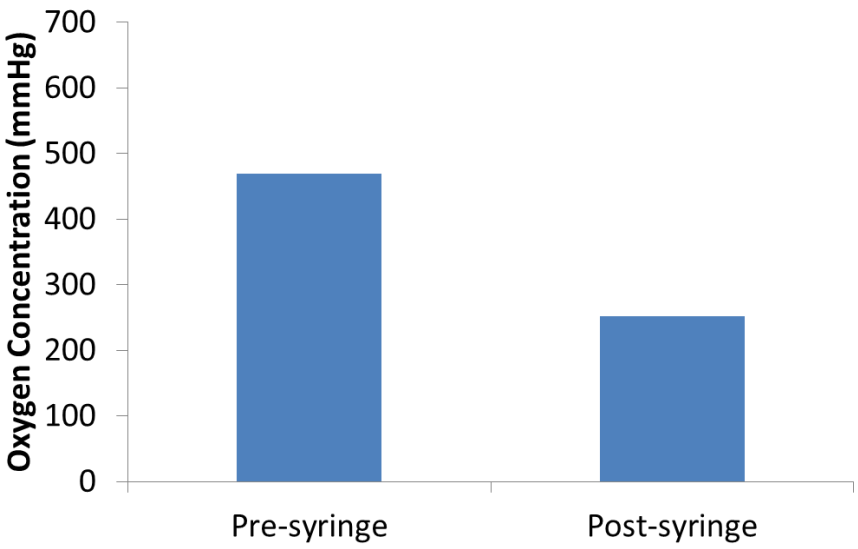

Figure 2.8 *Before drawing into the syringe the hybrid HA/PFC polymer mixture was oxygenated by bubbling up to 500mmHg oxygen. Post-drawing into the syringe the hybrid HA/PFC polymer mixture into the syringe 280mmHg oxygen remained in the mixture.*

2.2.7.2 Oxygenation of natHA hydrogels and MCC hydrogels

Due to the high viscosity of the natHA and MCC hydrogel and emulgels, oxygen could not be bubbled through the liquid as was done with the HA-TA polymer solutions.

Therefore a new method for oxygenation was developed in conjunction with collaborators in Boston Scientific Ireland as shown in Figure 2.9. A Y-mixer, a y-linker for two syringes with a static mixer element designed into the output, was 3D printed by BSCI. The natHA or MCC hydrogels were connected to one of the Y-mixer inputs and a second syringe connected to a supply of 99.5% pure oxygen was connected to the other input. An open ended syringe is connected to the output of the Y-mixer for collection of the oxygenated material. The syringe with the material to be oxygenated is set up on a syringe pump at a pumping rate of 50µL/min and the oxygen is turned on to 1.5L/min flow rate. The static mixer element creates a high surface area for oxygen diffusion into the material being oxygenated and the low pumping rate provides sufficient time for diffusion to occur. Once the material has stopped pumping through the setup the plunger can be put back into the collection syringe and used immediately (Figure 2.9).

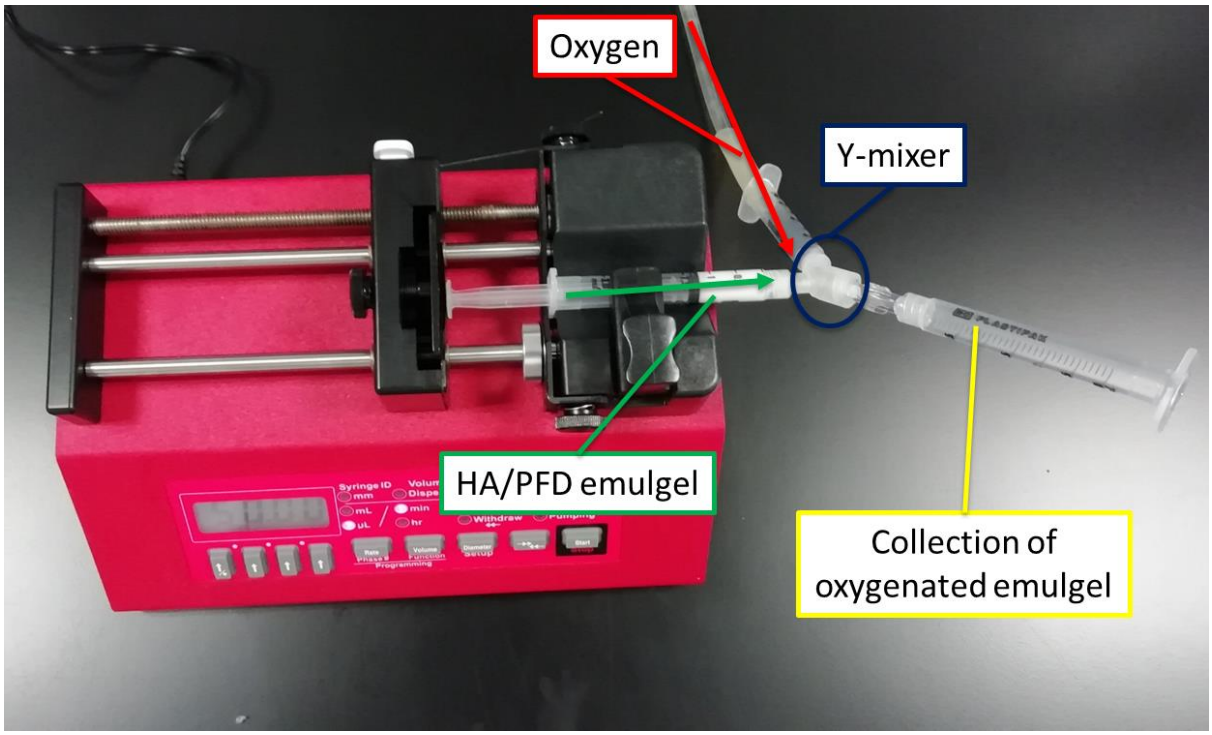

Figure 2.9 *Oxygenation protocol setup to oxygenate highly viscous natHA hydrogel and natHA/PFD emulgels.*

2.2.7.3 Oxygen release testing

The oxygen storage properties of the oxygenated hydrogels were characterised by measuring their oxygen release profiles. The oxygen concentration over time was measured using the Firesting O_2 optical oxygen meter. 1mL of oxygenated hydrogel was transferred to identical vials. A 1mL layer of PBS was laid onto the samples to prevent evaporation dehydrating the hydrogels and the probes were placed equal depths into each vial. The results were recorded using the Pyroscience proprietary software and the graphs were generated using Microsoft Excel.

2.3 Results

2.3.1 PFC emulsions droplet size and stability

Table 2.5 shows the droplet size and stability for the homogenised PFD and F6H8 emulsions over 48 h at room temperature (20-25°C) and 4°C. Both PFC emulsions exhibited micro-sized droplets with a high (>0.6) polydispersity index with an average increase in droplet size over 48 h. The PFD emulsion showed a larger average droplet size of >2000nm and the F6H8 showed a smaller droplet size ranging from ~600-900nm over the 48 h. The homogenised PFD and F6H8 emulsions were an opaque milky liquid and both emulsions were visibly unstable, with phase separation occurring within 24 h (Figure 2.10).

Droplet size and stability of sonicated PFC emulsions was measured over 21 days after storage at room temperature, 4°C, and at 37°C. Table 2.6 shows the size characterisation and stability data for the sonicated PFD and F6H8 emulsions. The sonicated emulsions are a nano-sized emulsion with a lower (<0.4) PDI than their homogenised counterparts. The emulsions are shown to be stable over the 21 days on the bench and in the fridge with little change in the droplet size and PDI. The sonicated PFD emulsion was an opaque milky liquid and the sonicated F6H8 emulsion was a translucent yellow liquid.

Table 2.5 *Dynamic light scattering data showing the average size (d.nm) and polydispersity index (PDI) of the PFD and F6H8 emulsions prepared by homogenisation after storage at room temperature and 4°C for up to 48 h.*

		0 h		24 h		48 h	
		Z-Average (d.nm)	**PDI**	**Z-Average (d.nm)**	**PDI**	**Z-Average (d.nm)**	**PDI**
Bench (20-25°C)	**PFD**	2204.33	0.763	2376.33	0.818	1891.33	0.714
	F6H8	579.1	0.625	918.93	0.643	865.9	0.663
Fridge (4°)	**PFD**	2204.33	0.763	2262.66	0.829	2580.67	0.944
	F6H8	579.1	0.625	747.16	0.635	769	0.619

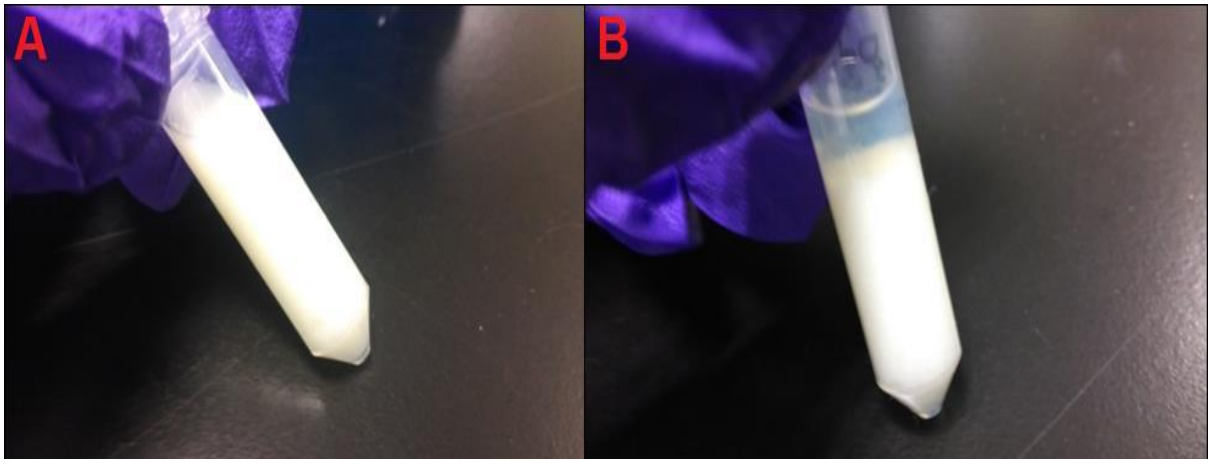

Figure 2.10 *Visible phase separation in the homogenised PFD emulsions. (A) 0 h after preparation. (B) 24 h after preparation. PFD emulsion shown is representative of what was seen after 24 h in F6H8 emulsion.*

Table 2.6 *Dynamic light scattering data showing the average size (d.nm) and polydispersity index (PDI) of the PFD and F6H8 emulsions prepared by sonication. The samples were stored at room temperature, 4°C, and at 37°C for 21 days.*

		0 days		7 Days		21 days	
		Z-Average (d.nm)	PDI	Z-Average (d.nm)	PDI	Z-Average (d.nm)	PDI
Bench (20-25°C)	PFD	129.4	0.361	166.63	0.338	146.13	0.277
	F6H8	179.47	0.334	144.8	0.304	139.63	0.242
Fridge (4°)	PFD	129.4	0.361	148.53	0.306	212.17	0.335
	F6H8	179.47	0.334	162.9	0.369	132.43	0.252
Incubator (37°C)	PFD	129.4	0.361	189.1	0.451	132.5	0.418
	F6H8	179.47	0.334	129.73	0.237	137.2	0.234

The sonicated PFD emulsion was selected as the lead emulsion due to it's history of use *in vivo* compared with the F6H8 and a longer stability study for 2 months was performed. Table 2.7 shows the size characterisation data for the sonicated PFD and Figure 2.11 shows the DLS intensity distribution of the 3 time-points. The sample kept at 4°C showed the greatest stability showing a monomodal size distribution and no discolouration at 60 days. The sample kept at 37°C which showed a large increase in PDI, a shift to a tri-modal size distribution and substantial discolouration.

Table 2.7 *Stability study of the lead PFD emulsion prepared by sonication. Dynamic light scattering measurements showing the average size (d.nm) and polydispersity index (PDI).*

	0 days		30 days		60 days	
	Z-Average (d.nm)	**PDI**	**Z-Average (d.nm)**	**PDI**	**Z-Average (d.nm)**	**PDI**
Bench (20-25°C)	147.88	0.242	148.1	0.297	146.82	0.285
Fridge (4°)	147.88	0.242	146.82	0.273	146.83	0.288
Incubator (37°C)	147.88	0.242	140.68	0.393	149.61	0.566

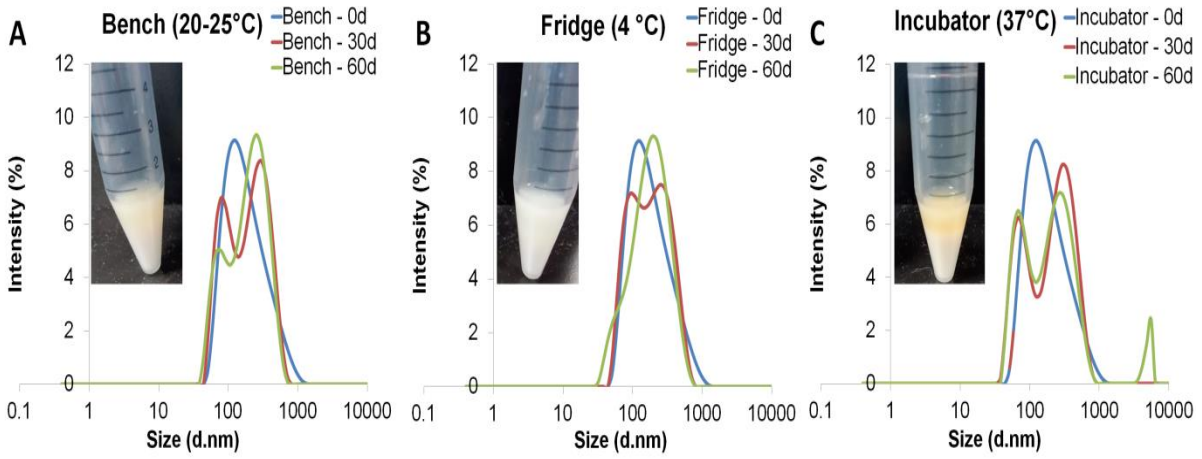

Figure 2.11 *DLS intensity distribution for the sonicated emulsion at 0 h, 1 month and 2 months and corresponding images to show appearance of emulsion in each condition after 60 days. A - Sample kept on the bench at room temperature, B – sample kept in the fridge, and C – sample kept in an incubator at 37°C.*

2.3.2 Oxygen release profiles from PFC emulsion

The oxygen release profiles of PBS, PFD, F6H8, and the homogenised and sonicated PFC emulsions were measured after bubbling with oxygen (Figure 2.12). PBS showed oxygen loading at 555mmHg and release to 160mmHg over 6 h, PFD showed loading at 512mmHG and release to 160mmHg over ~1.1 h, and F6H8 showed release from 639mmHg to 160mmHg over ~0.9 h (Figure 2.12A). The homogenised F6H8 emulsion showed loading to 512mmHg and release to 160mmHg in ~64 h and the homogenised PFD emulsion showed loading at 464mmHg release too 160mmHg in ~24 h. The sonicated F6H8 emulsion showed loading at 670mmHg and release to 165mmHg in 72 h, and the PFD emulsion showed loading at 700mmHg and release to 168mmHg in 72 h (Figure 2.12B).

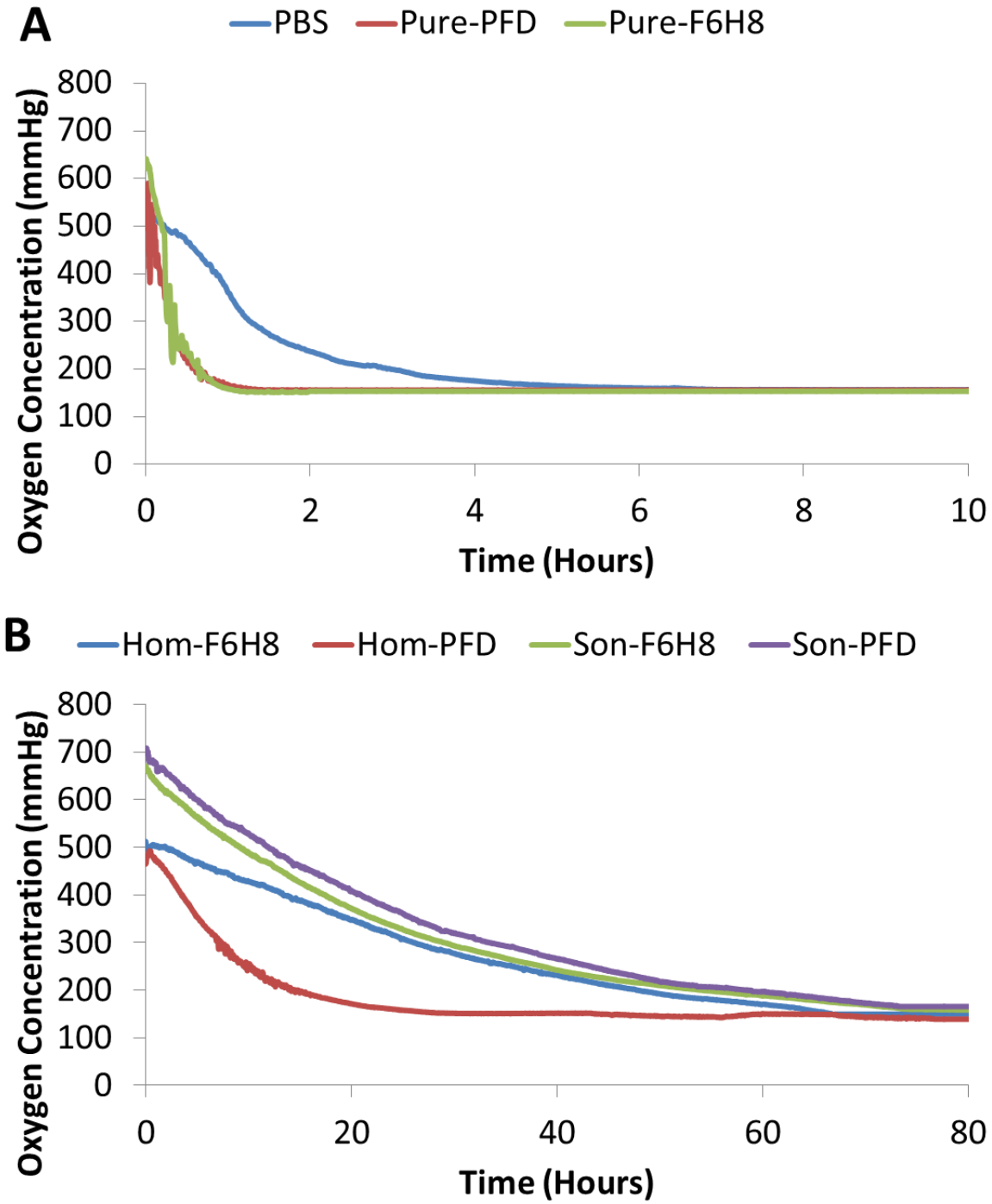

Figure 2.12 *Oxygen release profiles of the PFCs, the PFC emulsions and PBS as a control to atmospheric levels (155-160mmHg). (A) The PFD and F6H8 samples were open to air and showed release of loaded oxygen in <1 h and PBS showed release of loaded in <6 h. (B) The emulsions showed a more prolonged release of oxygen compared to pure PFCs, the sonicated emulsions showed the most prolonged for up to 80 h. Data shown representative of the norm (n=3).*

2.3.3 Rheological properties of the functionalised biomaterials hydrogel

2.3.3.1 HA-TA hydrogels

A steady state flow sweep was performed in order to evaluate the viscosity of the HA-TA polymer solution and polymer/PFD mixture without crosslinkers, GF1a and GF2a (Table 2.3), under increasing shear stress. These formulations were low viscosity liquids, GF1a was a colourless clear liquid and GF2a was an opaque milky liquid. The steady state flow sweep rheogram (Figure 2.13) below shows that GF2a mixture has a higher viscosity than the GF1a. GF2a showed shear thinning, decreased viscosity with increasing shear stress, thinning from 0.25 Pa.s at 5 Pa shear stress down to 0.088 Pa.s at 25 Pa.

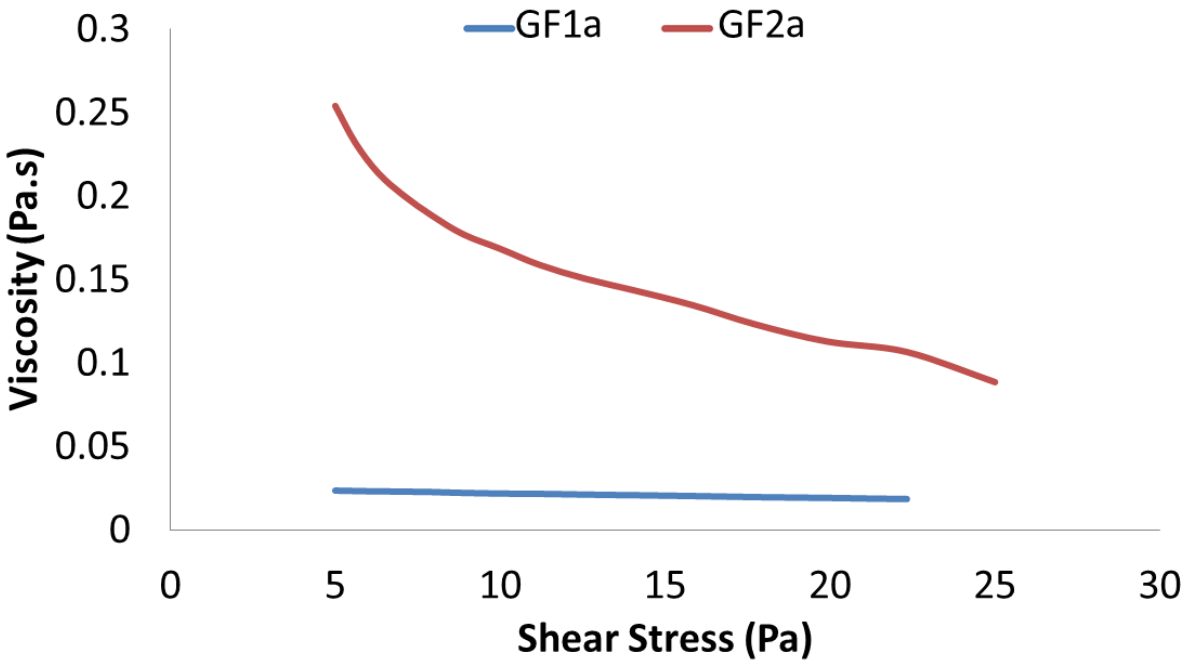

Figure 2.13 *Rheogram of steady state flow from 5-35 Pa of the HA-TA polymer solution (GF1a) and HA-TA/PFD mixture (GF2a), demonstrating that the addition of the PFD emulsion increases the viscosity of the mixture compared to the polymer solution alone and shows shear thinning under increasing shear stress. Data shown representative of the norm. (n=3)*

An oscillatory time-sweep was performed on the crosslinked HA-TA hydrogels, GF1b and GF2b (Table 2.3), to measure gelation over time and the final strengths of the hydrogels measured by the storage modulus (G'') relative to the loss modulus (G'). GF1b formed a clear colourless solid hydrogel, and GF2b formed an opaque white solid hydrogel. Figure 2.14 shows the rheograms of the oscillatory time-sweep of both the GF1b (Figure 2.14A) and GF2b (Figure 2.14B). Gelation has occurred when the storage modulus (G') surpasses the loss modulus (G'') and both samples gelled before the rheometer could be started, indicating the crosslinking reaction is rapid. The final storage modulus of GF1 is 912.6 Pa and the final storage modulus of GF2b is 278.2 Pa.

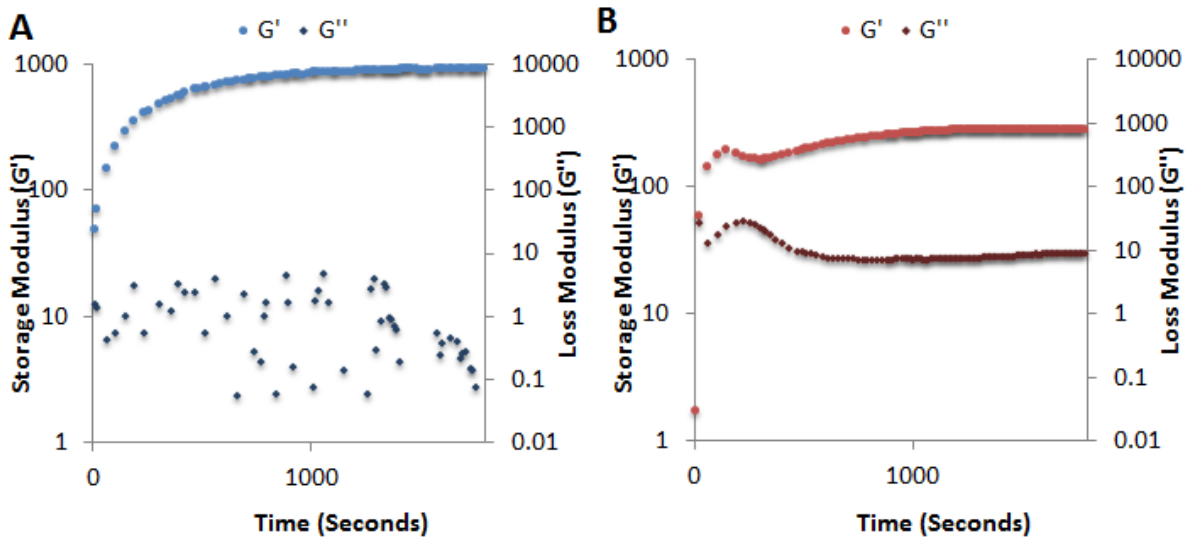

Figure 2.14 *Rheological characterisation of the HA hydrogel (GF1b) and hybrid HA/PFD hydrogel (GF2b) Gelation occurs when G' exceeds G". (A) Rheogram of oscillatory time sweep of GF1b. (B) Rheogram of the oscillatory time sweep of GF2b. Data shown representative of the norm. (n=3)*

2.3.3.2 NatHA hydrogels

A steady state flow sweep was performed in order to evaluate the viscosity of the natHA hydrogels, GF3-GF7 (Table 2.3), under increasing shear stress. GF3-5 were clear colourless viscous liquids and GF6-7 were opaque white viscous liquids. Figure 2.15 shows the steady state flow sweep rheograms for the natHA formulations, GF3-GF7. GF3-GF5 shows that increasing the concentration of natHA gave a non-linear increase in the resting viscosity of the natHA hydrogels. The rheograms for GF6 and GF7 show that the addition of the PFD emulsion to the natHA hydrogels gave the resulting natHA/PFD emulgels relatively high standing viscosities, in comparison to the natHA hydrogels alone (GF5). All of the natHA hydrogels showed shear thinning, with the emulgels, GF6 and GF7, showing substantially increased shear thinning, in comparison to the natHA hydrogel counterparts with similar resting viscosities.

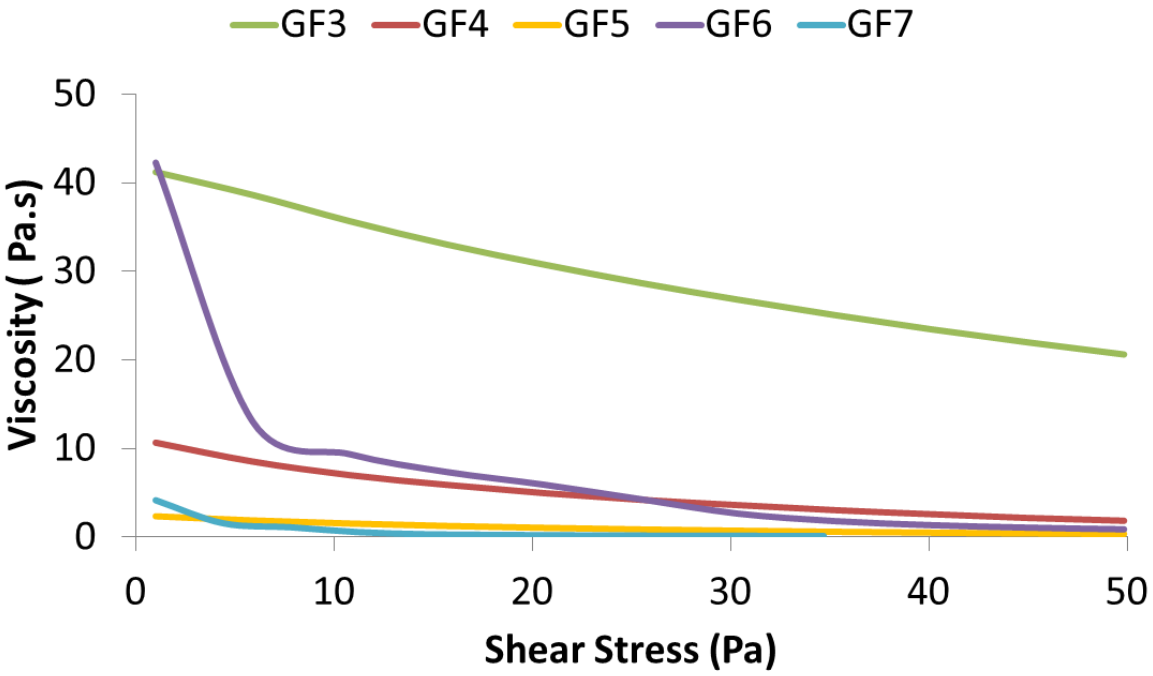

Figure 2.15 *Rheograms of steady state flow from 1-50 Pa of the natHA hydrogels and emulgel (GF3-6) and 1-35 Pa (GF7), showing increasing viscosity with increasing natHA concentration, increased viscosity with the addition of the PFD emulsion, and shear thinning with increased shear stress. Data shown representative of the norm. (n=3)*

A peak flow hold recovery test was performed to by holding a sample at a low (resting) stress for 5 min, applying a stress for 5 min, and removing the stress to the resting stress for an additional 10 min. The rheograms in Figure 2.16 and Figure 2.17 show the peak flow hold recovery measurement of GF6 and GF7 respectively, and show that when the shear stress is removed from the emulgel that the initial rheological characteristics before applying the shear stress are recovered.

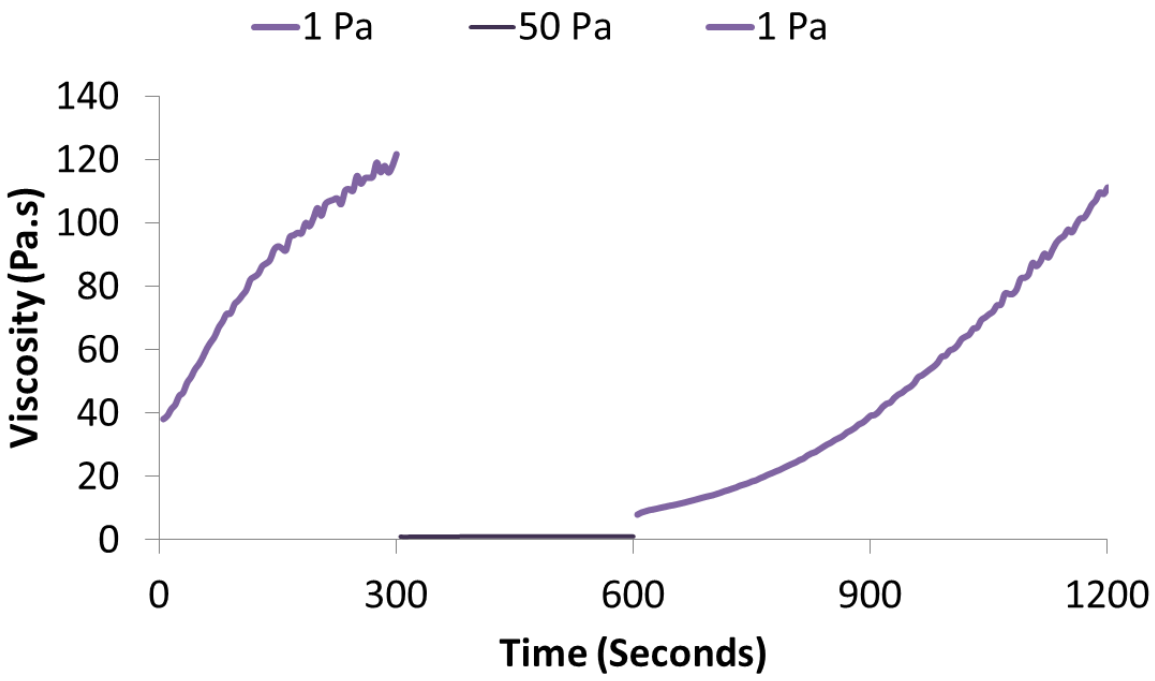

Figure 2.16 Rheogram of the peak flow hold recovery of the 1%/30% natHA/PFD emulgel (GF6). *The sample demonstrates low viscosity when put under higher shear stress and then recovery over 10 min when the shear stress is removed. Data shown representative of the norm. (n=3)*

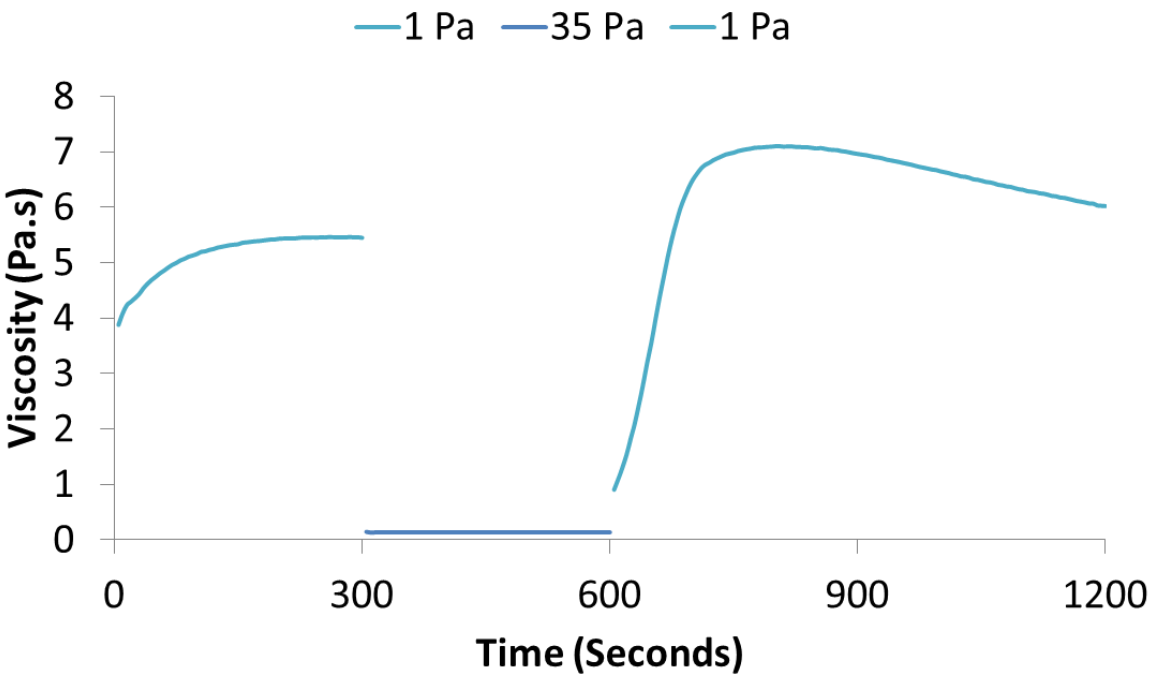

Figure 2.17 *Rheogram of the peak flow hold recovery of the 0.615%/30% natHA/PFD emulgel (GF7). The sample demonstrates low viscosity when put under higher shear stress and then recovery over 10 min when the shear stress is removed. Data shown representative of the norm. (n=3)*

2.3.3.3 MCC hydrogels

A steady state flow sweep was performed in order to evaluate the viscosity of the MCC hydrogels (GF8 and GF9) (Table 2.3), under increasing shear stress. Figure 2.18 shows the steady state flow sweep rheograms for the MCC formulations. The addition of the PFD emulsion increased the standing viscosity of the GF9 compared to GF8. GF9 showed substantial shear thinning.

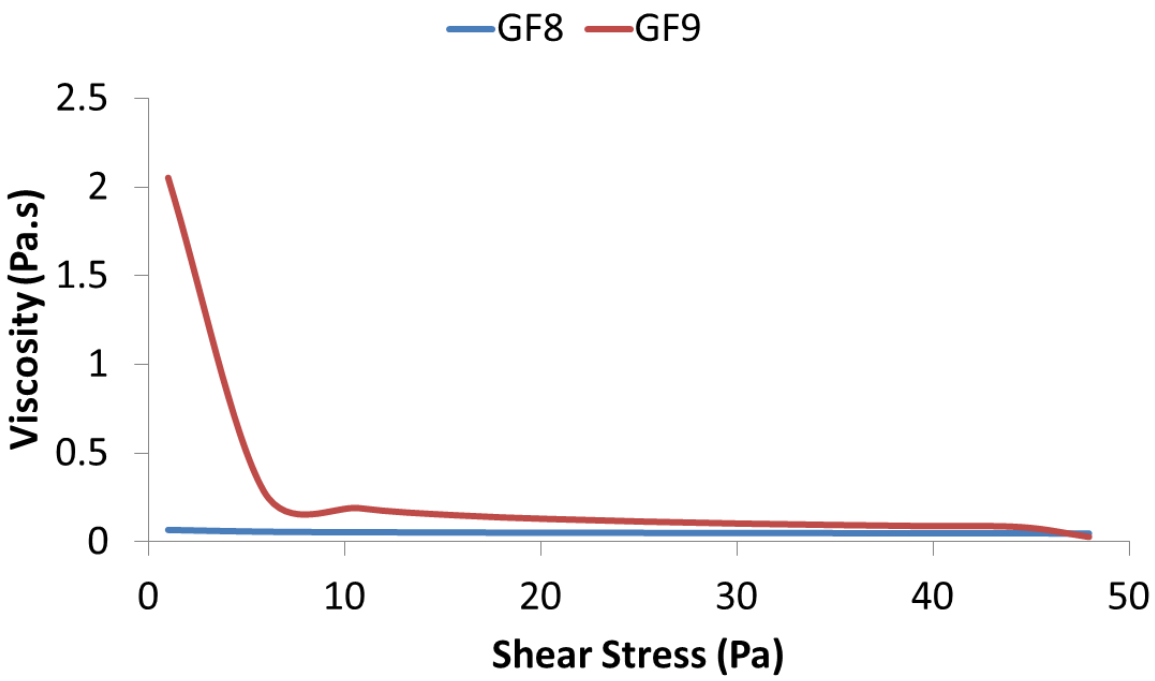

Figure 2.18 *Rheograms of steady state flow from 1-50 Pa of the MCC hydrogels, showing increased viscosity with the addition of the PFD emulsion to GF9, and shear thinning with increased shear stress. Data shown representative of the norm. (n=3)*

Temperature sweeps were performed to confirm the sol-gel temperature, when the storage modulus (G') is greater than the loss modulus (G''), of the MCC hydrogels using oscillatory rheological testing (Table 2.4). Figure 2.19 shows the oscillatory rheograms for the temperature sweep performed. GF8 showed sol-gel transition at 35°C with increasing gel strength (G') with increasing temperature. GF9 shows sol-gel transition at 30°C and increasing gel strength up to 39°C, and a subsequent drop in strength at higher temperatures. GF9 remained gelled at the temperatures tested.

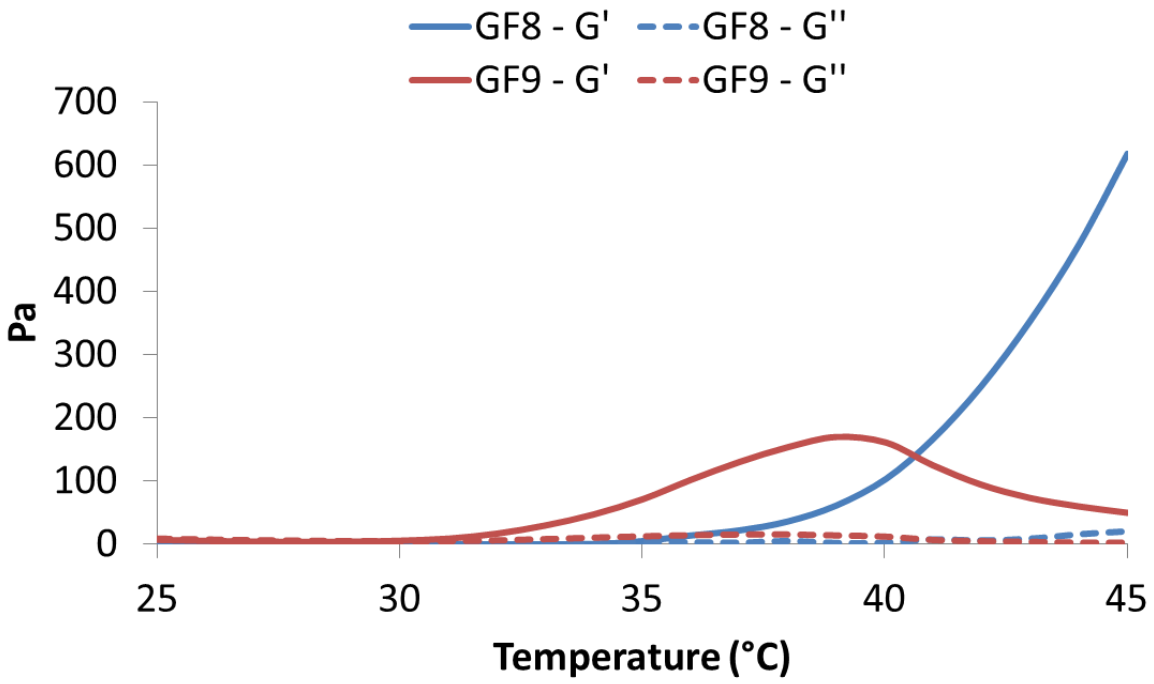

Figure 2.19 *Rheograms of oscillatory temperature sweep from 25-45°C of the MCC hydrogels, GF8 and GF9. GF8 shows sol-gel transition at 35°C and increasing strength at higher temperatures, whereas GF9 shows sol-gel transition at 30°C and decreasing strength at higher temperatures. Data shown representative of the norm. (n=3)*

2.3.4 Oxygen release profiles of the functionalised biomaterials hydrogel

2.3.4.1 HA-TA hydrogels

The oxygen release profiles of GF1b and GF2b after loading with oxygen by bubbling Part B (Figure 2.7) for 10 min (Figure 2.20). GF1b showed oxygen loading to 469mmHg and release to 160mmHg in ~20 h, and GF2b showed loading at 545mmHg and release to 160mmHg in ~47 h.

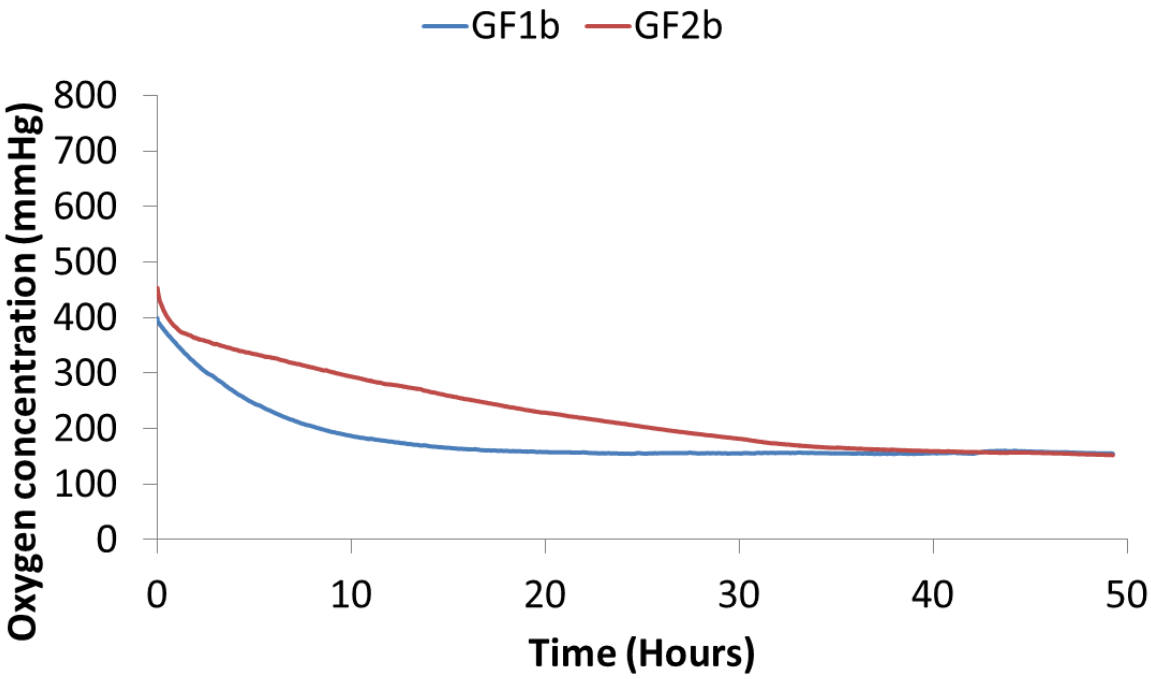

Figure 2.20 *Oxygen release profiles of the HA-TA hydrogel (GF1b) and the hybrid HA-TA/PFD hydrogel (GF2b). Inclusion of the PFD increased the loaded oxygen of the hydrogel and showed a more prolonged release of oxygen to atmospheric levels (155-160mmHg) over 45-50 h. Data shown representative of the norm. (n=3)*

2.3.4.2 natHA hydrogels

The oxygen release profiles of GF3, GF5, GF6 and GF7 after loading with oxygen by using the oxygenation setup from Section 2.2.7.2 (Figure 2.21). GF3 and GF5 showed oxygen loading to 380mmHg and 599 mmHg respectively and release to 160mmHg over ~26 h. GF6 showed oxygen loading to 567mmHg and release to 160mmHg over ~50 h. GF7 showed oxygen loading at 621 mmHg and release to 160mmHg over 58 h.

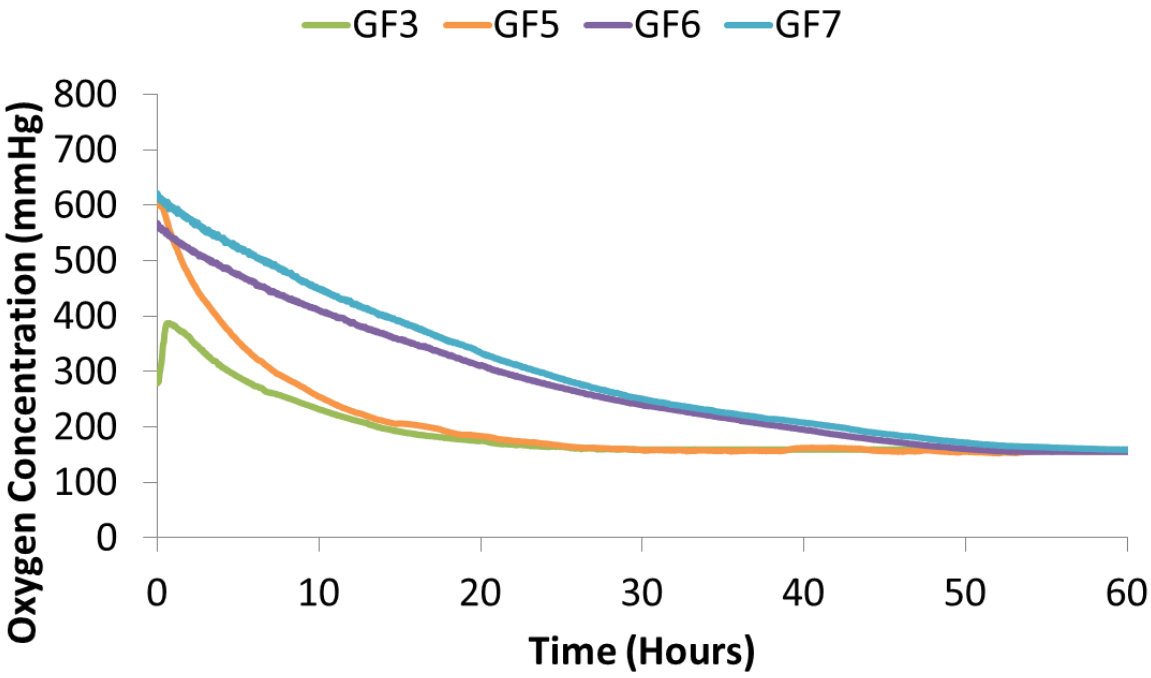

Figure 2.21 *Oxygen release profiles of natHA hydrogels 2% w/v (GF3) and 1% w/v (GF5) and the natHA/PFD emulgels 1%/28% and 0.615%/28% (GF6 and GF7 respectively). Results shown representative of the norm. (n=3)*

2.3.4.3 MCC hydrogels

The oxygen release profiles of GF8 and GF9 after loading after loading with oxygen by using the oxygenation setup from section 2.2.7.2 (Figure 2.22). GF8 showed oxygen loading to 600mmHg and release to 160mmHg in ~55 h, and GF9 showed loading at 545mmHg and release to 160mmHg in ~100 h.

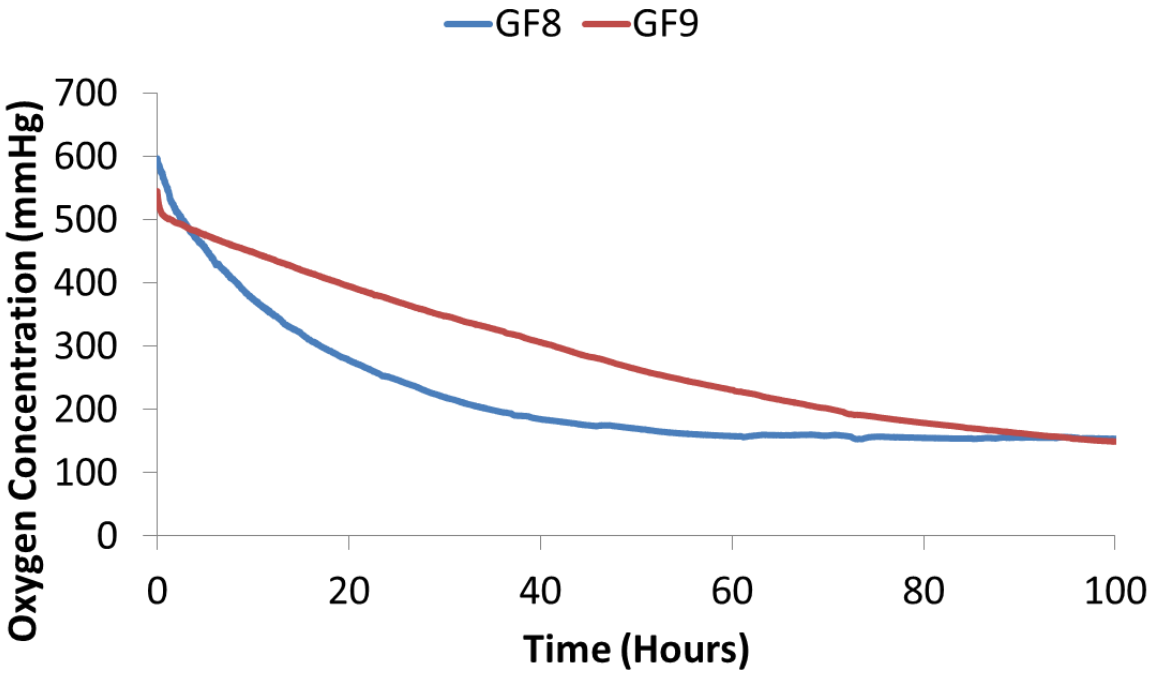

Figure 2.22 *Oxygen release profiles of MCC hydrogels (GF8) and the MCC/PFD emulgels (GF9). Results shown representative of the norm. (n=3)*

2.4 Discussion

The aim of this chapter was to formulate and characterise a functionalised biomaterial with the aim of improving the viability of transplanted cells to an extravascular site in an implant. There were two key challenges to this: firstly, finding a material that adequately mimics the ECM to support islets *in vivo*; and secondly supplying oxygen to implanted islets to prevent the development of hypoxia in the biomaterial which damages cells, leading to cell death. To address these challenges a biomaterial which could be functionalised with improved supplemental oxygen supply was formulated. A panel of lead biomaterials, HA-TA, natHA, and MCC, were selected for functionalisation with PFCs as the oxygenation technology. In the formulation stage, the key characteristics identified for the final biomaterial were stability, rheological characteristics to allow for successful delivery to a device for implantation, and oxygen carrying capacity of the functionalised biomaterial.

PFCs were chosen for delivery of a supplemental oxygen supply due to their high oxygen solubility and inert nature. The main challenge associated with incorporating the PFCs into a hydrophilic biomaterial is that they are a highly hydrophobic class of chemicals, due to the fluorination of the carbon backbone. Consequently, preparation of the PFCs as an o/w emulsion is required for their incorporation into a hydrophilic hydrogel (176). Two approaches to the formation of the PFC emulsions were explored; preparation by homogenisation and sonication, and their size and stability characteristics were investigated.

The homogenised PFC emulsions were prepared first and were shown to be very unstable. Both the homogenised PFD and F6H8 emulsions were characterised for their size over a 48 h period on the bench and in the fridge, and both showed physical instability and an increase in droplet size in both storage conditions. This can be explained by one of two mechanics; creaming and coalescence (249). Creaming is caused by flocculation of emulsion droplets into larger collection of droplets, loosely bound together by intermolecular forces, and is reversible through resuspension of the flocculated droplets through agitation of the sample. Following from flocculation, coalescence is a physical change in droplet size, whereby flocculated droplets combine together to form a single bigger droplet, this is irreversible and the sample must be re-homogenised to reverse coalescence. The

increase in Z.average droplet diameter suggests that the settling has resulted in some coalescence of the emulsion, indicating the homogenised emulsions are not stable.

In addition to homogenisation we also identified that using direct sonication via a sonic probe allowed for the rapid and effective formation of PFC emulsions without modifying the emulsion composition. The parameters for emulsifying the PFCs, 50% amplitude for 5 min run time while immersing the container in ice water to minimise the effect of heat generated, resulted in promising emulsions. The sonicated PFD emulsion appeared visually similar to the homogenised emulsions and the sonicated F6H8 appearing as a translucent, yellow dispersion, the optical change suggesting the formation of a colloidal nanoemulsion. The formation of the colloidal nanoemulsion in the sonicated F6H8 sonicated emulsion but not the sonicated PFD emulsion is likely due to the differences in the molecular weights of the PFCs (PFD 1.908g/mL and F6H8 1.33g/mL), with *Daik et al* showing a similar property with lower molecular weights resulting in smaller droplets in a liquid natural rubber emulsion (250).

The sonicated PFC emulsions are made up of a narrow range of droplet sizes, leading to a substantially lower Z-average d.nm in comparison with the homogenised emulsions as seen in Table 2.5. This small <200nm droplet size gives rise to a very stable set of emulsions, as described by the DLVO theory. The DLVO theory describes the balance between the electrostatic repulsive forces and attractive Van der Waal's forces and kinetic energy of Brownian motion of the nano-droplets. The stable colloid has larger repulsive forces than the Brownian motion kinetic energy can overcome, preventing coagulation and coalescence (251). The improved stability can be seen when comparing the two techniques employed to emulsify the PFCs; there are substantial changes in droplet size in the homogenised emulsions over 48 h, whereas the sonicated emulsions maintain their droplet sizes for up to 21 days (Table 2.6). After the sonicated PFD emulsion was selected as the lead emulsion due to it's history of use *in vivo* compared with the F6H8 a longer stability study for 2 months was performed. In Figure 2.11 the intensity distribution profiles show that there are some changes in the size populations over the 60 day period, the degree of which is dependent on storage conditions, where after 30 days the emulsion droplet size starts to show a shift from a monomodal to a bimodal distribution, with

increasing droplet size. In the samples stored on the bench and at 37°C there is also evidence of a split with yellow discolouration indicating oxidation of the lipoid. This has affected the stability in the sample stored at 37°C substantially, with an increase in the PDI to >0.5 after 60 days and the formation of a peak >1000nm on the intensity distribution graph. In comparison the sample stored at 4°C shows creaming of larger droplets, with smaller droplets remaining in suspension, without discolouration and the creamed droplets can be readily resuspended by vortexing.

PFC emulsion oxygen release profiles compared to the oxygen release profiles of the unmodified PFCs show substantial differences. The homogenised emulsions loaded a relatively lower oxygen concentration than the pure PFCs but saw a substantially longer release profile; the pure PFD and F6H8 dropped to atmospheric oxygen concentrations within 1 h (Figure 2.12A) whereas the homogenised PFD and F6H8 emulsions dropped to atmospheric levels within ~25 h and 65 h respectively (Figure 2.12B). Additionally, the sonicated emulsions saw even higher loading oxygen concentrations, with longer release profiles than both of the homogenised emulsions of ~70-80 h. This difference in release profiles can be explained by the high diffusion co-efficient for oxygen of the PFC family. The unmodified PFCs have a higher diffusion co-efficient for oxygen than water (252). As a result, the rate of diffusion of oxygen from the pure PFCs into the air is more rapid than from the PFC emulsions as they also must diffuse through the continuous phase of the emulsion i.e. water, which acts to limit the rate of diffusion of the oxygen from the PFCs in the emulsion. Additionally, the lecithin component of the emulsion acts as a barrier impeding oxygen diffusion (253). Fundamentally, an o/w emulsion is a droplet of hydrophobic liquid, covered in a layer of an emulsifier, dispersed homogenously within an aqueous continuous phase. The oxygen must first diffuse from the hydrophobic droplet, the PFC, through the emulsifier, the lecithin, into the aqueous phase of the emulsion and finally released to the air. This retards the diffusion of oxygen from the PFC compared to the pure PFC alone.

This can be briefly explained by Fick's First Law of Diffusion: Fick's First Law is written as $J = -D \frac{d\varphi}{d x}$, where J is the diffusion flux, D is the diffusion coefficient, and $\frac{d\varphi}{d x}$ is the concentration gradient.

A decrease in the diffusion coefficient, such as between the PFC and the lecithin, would decrease the flux of the oxygen. This explains the rapid release of oxygen from the pure PFCs, the high diffusion co-efficient results in a rapid release of oxygen. In contrast, as the diffusion co-efficient through the lecithin, and then water, is lower, a more prolonged oxygen release is seen. This beneficial characteristic of the emulsions prevents the rapid diffusion and loss of oxygen. The more prolonged oxygen release profile is due to the smaller droplet size as the thickness of the lecithin layer is proportionally larger to the smaller volume of encapsulated PFC. A proportionally larger barrier to oxygen diffusion acts to further decrease the rate of diffusion relative to the larger droplet sizes.

Based on the above stability data and oxygen release profiles the sonicated emulsions were clearly superior to the homogenised emulsions; however neither the PFD nor F6H8 emulsions were shown to have better characteristics to support inclusion of one over the other. PFD was selected as the lead component as it has more data to support *in vivo* use, having previously been a component of an FDA approved product, and chemically can hold more oxygen than F6H8, which is of critical importance in the initial period following islet delivery when cells are under the highest stress. The 2 month stability data for the sonicated PFD emulsion shows suitable stability for short-term use for the *in vitro* an *in vivo* work and for on demand manufacture of a final product.

The PFD emulsion, as the lead oxygen carrier was then progressed to incorporation and evaluation in the hydrogel biomaterials. The lead biomaterial must have properties that allow for the delivery to a macroencapsulation device while also being able to suspend and protect transplanted islets once delivered. The device will likely be filled *in situ* so properties that facilitate delivery via a catheter would be beneficial. Preliminary work done identified that a concentration of 30% w/v PFD was the maximum concentration at which the hybrid HA/PFD hydrogel could still form a solid hydrogel (Figure 2.5A). The lead HA-TA formulation selected was GF2b, 1% HA-TA and 30% w/v PFD hydrogel as it formed a visibly solid hydrogel. The non-crosslinked polymer mixture for this formulation (GF2a) was characterised rheologically by a steady state flow sweep. The GF2a mixture flows readily and was shown to have a low viscosity of <0.3 Pa.s at a shear stress of 5 Pa, and shows shear thinning (Figure 2.13). The GF2a mixture was also shown to have a higher viscosity than a

1% HA-TA polymer solution (GF1a). The presence of the PFD emulsion droplets and flocculated droplets increases the viscosity by disrupting flow through the mixture, and shear thinning occurs as a result of the suspended droplets being forced to align with the flow under increased shear stress and breaking up the floccs that further improves flow (254). An oscillatory timesweep of both formulations following the addition of the crosslinkers (GF1b and GF2b) indicated a rapid crosslinking reaction for sol-gel transition. The GF2b hydrogel showed a lower G' than the GF1b hydrogel indicating that the incorporation of the emulsion reduces the overall strength of the HA-TA/PFD hydrogel, or as seen in Figure 2.5A can prevent the formation of a hydrogel entirely. We hypothesise that this is due to the emulsion droplets sterically hindering the crosslinking reaction; that the physical presence of the emulsion droplets blocks the formation of crosslinks between the HA-TA chains. A similar effect has been seen in the literature where PEG functionalisation sterically blocked covalent crosslinking in a heparin hydrogel (255) and *Maillard et al* saw a similar effect when supplementing a fibrin matrix with a PFD emulsion (184). The final strength of hydrogel is not a critical parameter for the success of the biomaterial, as it is intended for use in a macroencapsulation device, but some crosslinking to form a matrix to keep islets suspended is beneficial.

NatHA was the second biomaterial investigated. In contrast to the HA-TA hydrogel, the natHA hydrogel functions by chain entanglement to give a high viscosity liquid (256). The rheograms of the natHA hydrogels in Figure 2.15 show that this viscosity scales non-linearly with concentration with GF3 (2% w/v HA) showing a viscosity substantially more than double the viscosity of GF5 (1% w/v HA) and in all cases shear thinning behaviour. Preliminary work performed by DRIVE partners in DCU showed that GF3 was able to maintain pseudoislets in suspension for >3 days (data not shown). As a result this resting viscosity (viscosity at 1 Pa shear stress) was targeted for the functionalised biomaterial.

Incorporation of the emulsion into natHA (GF6 and GF7) increased the resting viscosity of the resultant emulgel in comparison to the natHA hydrogel counterparts, which is in line with the results seen with the HA-TA polymer solutions and mixtures (GF1a and GF2a). This can also be seen in when comparing the viscosities of GF5 hydrogel and GF6 emulgel. Both GF5 and GF6 have 1% w/v natHA polymer, but the standing viscosity of the GF6 emulgel is 10-20 times higher than the GF5 hydrogel.

GF6 emulgel matches the resting viscosity of the GF3 hydrogel (2% w/v natHA) which was the target viscosity. The GF6 emulgel also showed significant shear thinning behaviour. As outlined above shear thinning is a useful property when developing a biomaterial for delivery via a catheter, however unlike the HA-TA hydrogels which could crosslink into a solid hydrogel after shear thinning to retain the islets in suspension, the natHA/PFD emulgels could not. Therefore it is important that these hydrogels are able to recover their structure on removal of shear stress. A recovery protocol showed that upon removal of the stress the hydrogel gradually recovers its viscosity over 10 min. This result is positive; it shows the GF6 emulgel does recover its viscosity over time, but not immediately, which gives the emulgel time to spread homogenously throughout the device after delivery. The GF7 emulgel was formulated as a lower viscosity biomaterial to overcome some of the challenges of working with a higher viscosity biomaterial, such as the shear stress being applied to and damaging the cells when mixing them into the GF6 emulgel, and issues identified with filling the devices which will be discussed in Chapter 3 and Chapter 4 respectively. The GF7 emulgel showed similar properties to the GF6 emulgel, showing both shear thinning and recovery, but with a lower overall viscosity.

The MCC hydrogels were the final biomaterial investigated for this project. The MCC hydrogels were considered for the project as they are liquid at lower temperatures, but are thermoresponsive and can be modified to undergo sol-gel transition at physiological temperatures to form a solid hydrogel. These properties align with the target characteristics of the ECM biomaterial for this project, as the MCC gel in liquid state could be delivered via a catheter and then form a solid biomaterial to suspend the islets *in situ*. In line with the results seen above, the addition of the PFD emulsion in GF9 greatly increases the resting viscosity of the hydrogel, compared to GF8 (Figure 2.18). As a follow-up, an oscillatory temperature sweep test was performed to identify the sol-gel transition temperatures of the hydrogels to ensure they were within physiological limits. The GF8 hydrogel underwent sol-gel transition at 35°C, which is suitable for gelling *in situ.* The addition of the PFD emulsion (GF9) resulted in a substantial decrease in sol-gel transition temperature (Figure 2.19) to 30°C, which creates a risk of gelation in the catheter. *Douglas et al* hypothesised that the inclusion of the hydrophobic PFD decreases the aqueous content of the final hydrogel. This in turn increases the incidence of interactions facilitating the formation

of a gel at lower temperatures (183). This also applies to the βGP concentration, where lower aqueous phase volume leads to an increase in βGP concentration in the aqueous phase. The mechanism of action of the βGP is to alter the ionic environment to lower the sol-gel transition temperature (245). The effective increase in the aqueous concentration of the β-GP by the presence of the PFD emulsion is likely to have contributed to the reduced the sol-gel transition temperature of GF9. Additionally, the GF9 hydrogel is unstable relative to the GF8 formulation. GF8 shows an increase in hydrogel strength (increasing G') with increasing temperature, up to 45°C. In comparison, the GF9 increases in strength up to 39°C and subsequently begins to break back down as the G' decreases.

The GF1a polymer solution and GF2a mixture were oxygenated by bubbling oxygen through the liquid in the syringe. In both cases only Part 2 (Figure 2.7) of the formulation was oxygenated. This was done as Part 1 contains the cells of the hydrogel and the cells were mixed into Part 1 by syringing the polymer solution up and down. Comparing the oxygen release profile of the GF1b hydrogel in Figure 2.20 and the oxygen release profile of PBS from Figure 2.12A shows that formulation of a hydrogel substantially prolongs the diffusion of oxygen. The GF1b hydrogel had half of its total volume oxygenated but showed a more prolonged diffusion of the loaded oxygen to atmospheric levels from the hydrogel over 20 h, in comparison to the PBS which saw diffusion to atmospheric levels within 6 h. This is a well-documented mechanic of a number of biomaterials that can be explained by the matrix of the biomaterial reducing the rate of diffusion of oxygen through it. In our case, this effect lowers the diffusion rate of the oxygen out of the material but in practical applications this is one of the primary mechanisms that causes of the formation of necrotic cores in biomaterials (257). The oxygen release profiles from Figure 2.20 show that the inclusion of the PFD emulsion in the GF2b hydrogel improved both the loaded oxygen and gave more prolonged release of oxygen from the hydrogel, up to 47 h, when compared with the GF1b hydrogel. The prolonged oxygen release matches the results seen with the PFD emulsion and PBS, and the improved oxygen loading can be explained by the inclusion of the PFD emulsion increasing the diffusion of oxygen into the biomaterial.

The high viscosity of the natHA formulations did not facilitate oxygenation by bubbling. This is due to an effect caused by the shear thinning of the materials.

When oxygenating the high viscosity hydrogel or emulgel a bubble of oxygen shear thins through the viscous liquid, creating a “path” behind it. The continuous flow of oxygen then follows this shear thinned path through the highly viscous liquid, and in place of a stream of bubbles with a collective large surface area there is a single low surface area channel of oxygen passing through the liquid (258). To address this issue, in collaboration with Boston Scientific a method using a Y-linker with a static mixing element to increase surface area for diffusion to improve oxygen loading was developed. The oxygen loading into GF3 hydrogel shows the lowest loaded oxygen of any of the investigated materials, 380mmHg, but it shows a prolonged release of oxygen for up to ~26 h, the same as GF5 hydrogel which loaded more oxygen (Figure 2.21). This can be explained by the higher viscosity matrix of the GF3 hydrogel retarding the diffusion of oxygen more than the lower viscosity matrix in the GF5 hydrogel, affecting both the diffusion into the material and diffusion out. In comparison, the GF6 emulgel has a similar resting viscosity to the GF3 hydrogel but shows improved oxygen loading. Additionally, the viscosity of the suspending medium also affects the diffusion co-efficient according to the Stokes-Einstein equation, which would affect the rate of diffusion according to Fick’s First Law. The GF6 emulgel shear thins substantially under increasing shear stress and this decrease in viscosity would result in a subsequent increase in diffusion of oxygen into the emulgel in comparison to the GF3 hydrogel. The improved loading seen in the lower viscosity GF7 emulgel provides additional data to support this hypothesis. Both the GF6 and GF7 emulgels load at high levels of 567mmHg and 621 mmHg, showing release to atmospheric levels in 50 and 58 h respectively, giving the most prolonged oxygen release profiles of the HA based biomaterials.

The MCC hydrogels, GF8 and GF9, were oxygenated by the same method as the natHA formulations, due to the high viscosity of the GF9 formulation. The GF8 and GF9 formulations show high initial oxygen loading similar to the lower viscosity natHA hydrogels. However, the MCC hydrogels show substantially more prolonged release of oxygen than the natHA hydrogels. GF8 shows oxygen loading at ~580mmHg, similar to the GF6 and GF7 hydrogels, but shows release to atmospheric levels over 50 h, despite having no PFD component in the hydrogel (Figure 2.22). In line with this, the GF9 hydrogel shows loading at ~550mmHg, and shows the most prolonged release of oxygen compared to any other hydrogel tested

of ~100 h to reach atmospheric levels. We hypothesise that the substantial prolonged release of oxygen is the result of a partial or total sol-gel transition during the experiment at room temperature as the sol-gel transition temperature of the gel had been reduced, as seen in Figure 2.19. If this had occurred, this would be in line with the results seen in the GF1b crosslinked HA-TA hydrogel showing a substantially more prolonged release of oxygen than PBS alone.

Out of the three biomaterials investigated in this chapter, the natHA/PFD emulgels show the greatest promise as a suitable biomaterial to provide oxygen to encapsulated cells due to their rheological characteristics allowing for delivery via a catheter and their prolonged oxygen release profiles. Although the MCC hydrogels showed the most prolonged oxygen release profiles, the instability of the final GF9 hydrogel, and risk of sol-gel transition during delivery blocking the catheter precludes it for this project. In comparing the natHA/PFD emulgels with the sonicated PFD emulsion itself, the emulsion alone shows higher oxygen loading (700mmHg) and a more prolonged release of oxygen (72 h to atmospheric levels) than in the emulgels. This indicates that oxygen loading into the GF6 and GF7 emulgels is being limited by the oxygenation method used for these experiments due to the viscosity of emulgels, and it is possible that substantially greater oxygen loading could be achieved. The protocol currently in use (preparing volumes of 1-3mL) may not be scalable to larger volumes needed for human sized devices (~140-300 mL), and future work should focus on developing a new oxygenation method for these hydrogels. Ultimately, the natHA/PFD emulgels fulfil the material characteristics desired for the ECM of an artificial pancreas, showing shear thinning facilitating delivery via a catheter to an *in situ* device, and an improved oxygen supply for encapsulated cells following transplantation.

Chapter 3

Development of an *in vitro* model to determine glucose responsivity and evaluation of lead formulations

3.1 Introduction

In Chapter 2 the formulation and characterisation of a number of biomaterials for use as an extra-cellular matrix in a bio-artificial pancreas based on their physical properties was discussed. This Chapter focuses on the assessment of these lead biomaterials with a suitable *in vitro* model to investigate their potential efficacy and biocompatibility, before moving into *in vivo* studies.

3.1.1 An *in vitro* cell model for translation to human applications

When investigating novel therapeutics for use with human islets the relative scarcity and difficulty of sourcing human islets for research use is a major challenge. An estimate on donor pancreases in the United States estimated that there was 1 donor pancreas available for every 333 T1D patients (259). With whole pancreas transplantation and islet transplantations (which require up to 2 donor pancreases per patient) taking priority over research, there is evidently a need for alternative cell sources to perform preliminary testing.

3.1.1.1 Cell lines as an *in vitro* model in T1D

Cell lines are cells which have been modified to proliferate indefinitely. This allows for the continued study of the cell type without the need to continually source primary cells from a new organism. There has been a great deal of research aimed at creating cell lines for many purposes, with many popular cell lines in use in labs worldwide including CACO-2 (human Caucasian colon adenocarcinoma), Calu-3 (human lung adenocarcinoma) and the HeLa (the first immortalised cell line studied, human cervical cancer).

For diabetes research a number of β-cell lines have been produced and researched. The key challenge with developing a β-cell line is producing a proliferating, immortalised cell line which does not differentiate from the original functionality of the β-cells over a number of proliferations (260), most specifically responsiveness to glucose and release of insulin.

The MIN6 cell line is a mouse insulinoma cell line produced in 1990 by *Miyazaki et al.* The MIN6 cell line was established from pancreatic tumors taken from the SV40 T-antigen transgenic mouse *(261)*. The cell line has been well regarded as an *in vitro*

model for T1D research as it is glucose responsive at physiological levels, and the cell line shows GSIS at levels similar to an isolated pancreatic islet (262, 263). A number of groups have looked at the encapsulation of MIN6 cells in biomaterials or for encapsulation in a bioartificial pancreas device (119, 264-272). *Skrrzypek et al* investigated MIN6 and MIN6/HUVEC (human umbilical vein endothelial cells) aggregates in flat poly (ether sulfone)/polyvinylpyrrolidone devices compared to free-floating aggregates, and showed that the encapsulated MIN6 aggregates were similar to free-floating, indicating the encapsulation device did not affect glucose response (273). *Hayashi et al* investigated the MIN6 cell line in a three-layer agarose microcapsule and a mesh reinforced polyvinyl alcohol hydrogel tube and the encapsulated MIN6 were shown to function glucose responsively in a static incubation after encapsulation (264).

The INS1 cell line was established in 1992 by *Asfari et al.* INS-1 cells are a rat insulinoma cell line that is glucose responsive within physiological glucose levels *(274)*. *Johnson et al* have used the INS-1 cells encapsulated in alginate as a means of developing assays for use with islets (275). The INS-1 cells are limited in that they produce only 20% the amount of insulin that would be produced by native cells (276) The INS-1E cell line was differentiated by *Maechlar et al* in 2004 from the parental INS1 cell line. The INS-1E cell is a very stable cell line that can be used over a wide range of passages while remaining glucose responsive. INS-1Es show secretory responses to amino acid and sulphonylurea similar to isolated islets (277). The INS-1E cells have been less extensively studied for encapsulation in biomaterials (278-280).

Pseudoislets (PIs) are islet-like structures produced by a method which allows cells to be cultured in a morphology that resembles natural islets (281). This way of culturing the cell increases the cell-cell contact needed by the majority of insulin-producing cell lines, as it helps to mimic the architecture of the islet unit that is lost when culturing in 2D on plastic, ultimately improving cell function (282). There is a range of literature detailing the different methods of forming PIs; ranging from static incubation of cells on non-adherent plastics, the use of hanging droplet methods (283), microencapsulation of cells in alginate microspheres (284), and the use of magnetic microparticles to encourage formation (285), to outline a few.

3.1.1.2 Mammalian islets as an *in vitro* model in T1D

Mammalian islets are the logical choice when investigating technologies for islet encapsulation. There are a number of different animal models which are widely used for islet research and identifying the most suitable islet source is important from a scientific and ethical viewpoint.

As outlined above, although human islets would be the preferred islet source for study, availability is limited and time-dependent. The second best choice of an islet source is NHP islets. NHP islets closely resemble human islets anatomically, sharing the intermingling endocrine cells and general morphology (286, 287). Ethically, NHP should only be considered for research purposes if no other suitable species or alternatives could be used (288) and NHP cannot be used for research in the Republic of Ireland.

Pig islets have been studied as an alternative to human islets for many years, due to the traditional usage of pig insulin in diabetes treatment. Pig islets are also being investigated by a number of groups as a source of xeno-islets for human transplantation (289). The usage of pig islets is ethically sound due to their long history as farmed animals, and as a source for pancreases are readily available. Pig islets are similarly sized to human islets and share a similar anatomy with human islets, consisting of a core of β-cells with some islets containing α-cells at the centre (11, 81). Pig islets are difficult to isolate however, as they have no islet capsule which leads to fragmentation and irregular borders following isolation. As the pig pancreas is a well-defined organ the techniques for islet isolation are difficult and have a high skill and equipment requirement (290).

Rat islets are a suitable alternative to human islets for research purposes. Rat islets have been used for a number of research purposes in diabetes research, ranging from the first allogenic islet transplantations to encapsulation in novel devices with oxygen carriers (291). Rat islets are a similar size to human islets and consist of a core of β-cells with a border of α- and δ-cells (11, 81). Relative to pig islet isolations, the skill and equipment requirement for isolating rat pancreatic islets is low and the technique is easily transferable.

3.1.2 Glucose stimulated insulin secretion (GSIS)

The function of the β-cells in the homeostasis of blood glucose is controlled by the secretion of the hormone insulin into the blood. Blood glucose control and the release of insulin is predominantly controlled by β-cells responding to the blood glucose level itself but it is further modulated and affected by other nutrients, neural and hormonal factors.

Central to the understanding of GSIS is the adenosine triphosphate sensitive potassium channel (ATP-K^+). When plasma glucose levels increase, glucose enters the β-cells through the glucose transporter (GLUT) on the cell membrane. The glucose is metabolised by the cell, first undergoing phosphorylation by glucokinases, followed by glycolysis to generate pyruvate. Pyruvate metabolism by pyruvate dehydrogenase and pyruvate carboxylase in the cytosplasm, and further metabolism in the mitochondria produces ATP. The ATP-K^+ channel is one of the primary determinants of cell membrane potential and closure of the channel leads to membrane depolarization. Membrane depolarization opens L-type voltage dependant Ca^{2+} channels, leading to an influx of Ca^{2+} and a rise in Ca^{2+} concentration in the cell which stimulates insulin exocytosis (Figure 3.1).

The ATP-K^+ model alone describes a mono-phasic GSIS mechanism, whereby the increased plasma glucose results in the fast release of insulin over 5-6 min to maintain normoglycaemic levels. However, it was established by Grodsky in 1972 (292), that GSIS is biphasic, showing both the rapid release of insulin described by the ATP-K^+ model as the first phase and an additional increase in insulin over the following 60 min. A mechanism for an ATP-K^+ independent model of GSIS was established in 1992 by showing that increased plasma glucose still resulted in insulin secretion even if the ATP-K^+ was permanently closed, preventing the membrane polarization necessary for Ca^{2+} influx. Insulin exocytosis without Ca^{2+} increase established the ATP-K^+ channel independent GSIS (293). The exact mechanism of action for this ATP-K^+ channel independent GSIS has not yet been identified. It is theorized however that pyruvate metabolism and TCA cycle intermediates could be potential key components.

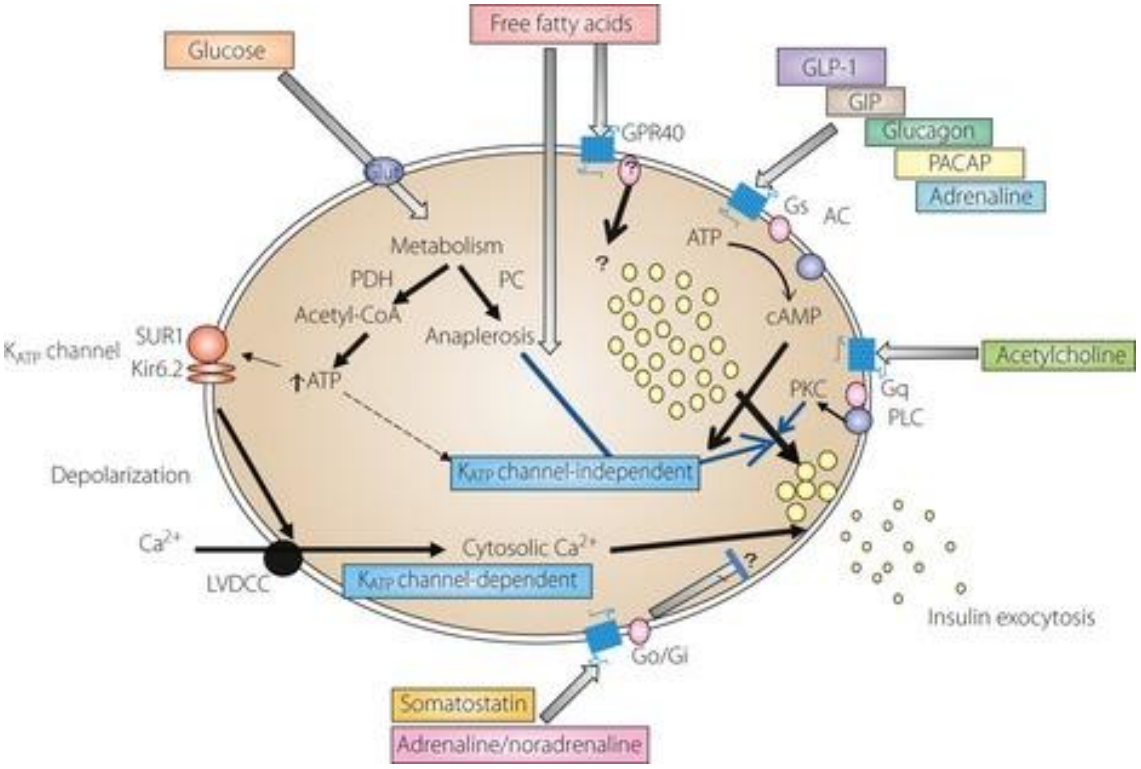

Figure 3.1 *The GSIS pathways, outlining the ATP-K+ dependent and independent pathways (294).*

GSIS, primarily second phase ATP-K^+ channel independent, is further modulated and enhanced by a number of nutrients, endogenous hormones, and neural factors. Glucose itself causes a time-dependent potentiation of insulin secretion, where glucose exposure actually increases response to another glucose stimulus applied at a later time (295). Metabolizable amino acid and glyceraldehyde show similar effects. Free fatty acids and the parasympathetic nervous system may also play a role in time-dependent potentiation. The incretins, gastrointestinal hormones, enhance nutrient induced insulin secretion by binding to G protein coupled receptors and increasing cAMP production, which elevates GSIS *(294)*. *In vivo* insulin secretion is controlled by a number of interrelated systems, and is finely tuned and modulated by nutrients, hormones and neural inputs, the implications of which may not be fully elucidated.

3.1.3 Aims

The overall aim of this Chapter is to assess the formulated biomaterials from Chapter 2 using *in vitro* cell models with a glucose responsive, insulin secreting cell line.

The specific aims of this Chapter are:

- To establish *in vitro* models using both a cell line and a primary cell source
- To evaluate the suitability of the *in vitro* models for use in testing the lead gel formulations
- To assess the functionality of cells after gel encapsulation

3.2 Methods

3.2.1 Materials

The MIN6 cell line was acquired from DRIVE partner DCU (Ireland). The LIVE/DEAD kit for mammalian cells was purchased from Thermo-Fisher (Ireland). Lewis rats were purchased from Envigo (United Kingdom) weighing 150-200g and kept for up to a maximum of 4 weeks before euthanisation and islet isolation. The enzymes, Collagenase G (ColG) and Collagenase H (ColH), were provided by DRIVE partner Abiel (Italy). Thermolysin, DMEM media (D5671), RPMI 1640 (R8758) media, Histopaque-1119 and Histopaque-1077 were obtained from Sigma (Ireland). The rat insulin ELISA kit was obtained from Mercodia (Switzerland). The INS-1E cell line was acquired from Prof. Pierre Maechler, University of Geneva Medical Centre (Switzerland). Immunoisolating shells were obtained from DRIVE partner NUIG (Ireland).

3.2.2 Experimental outline

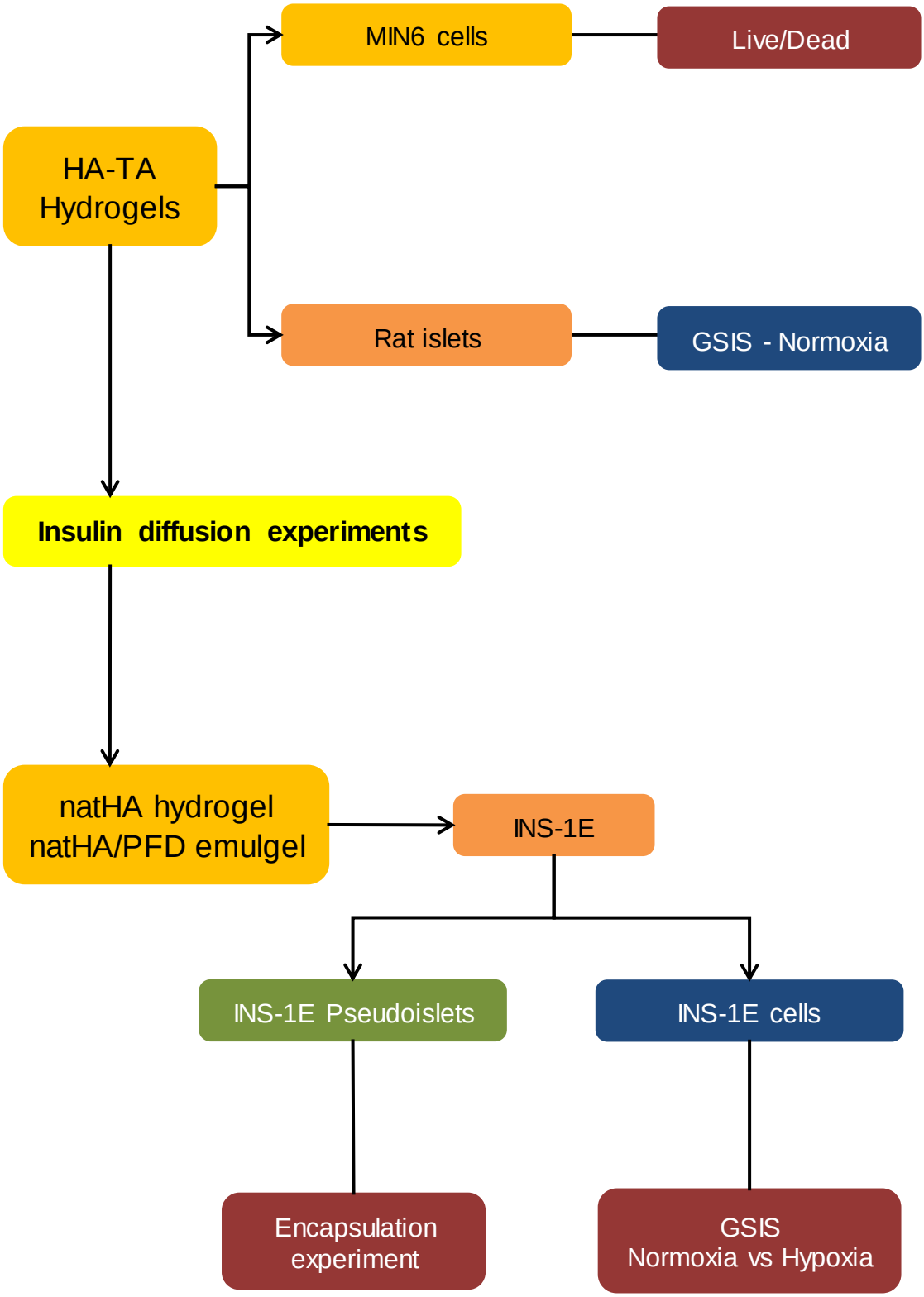

Figure *3.2* *Outline of in vitro work performed on candidate biomaterials.*

3.2.3 MIN6 cell line

The MIN6 cell line was cultured in T75 flasks at 37°C in 5% CO_2 and fed with a high glucose DMEM (D5671), supplemented with 2% L-glutamine, 10% fetal bovine serum (FBS), and 1% Pen-Strep. Cells ranging from passage number of 42 to 47 were used. The cells were cultured up to 70-80% confluence in the flasks and split 1:3 as required. MIN6 cells do not tolerate higher confluence, losing glucose responsiveness at higher confluences, and do not have sufficient cell-cell interactions at lower confluences to be successfully cultured.

3.2.3.1 Encapsulation of the MIN6 cell line in the HA-TA hydrogels

The HA-TA and hybrid HA-TA hydrogels were prepared as detailed in Table 2.3 and Section 2.2.5. MIN6 cells were mixed into Part A, the HA-TA + HRP portion, to minimise their exposure to the free H_2O_2 in Part B, at a concentration of 10 million cells/mL to give a final concentration of 5 million cells/mL when mixed with Part B. This cell concentration was identified as suitable by preliminary work performed by DRIVE partner DCU. The hydrogels and encapsulated cells were filled into 200µL cylindrical moulds (8mm diameter, 4mm depth) and were given sufficient time to fully gel (>2 min) before being transferred to a 24 well plate with DMEM for culture.

3.2.3.2 Live/dead staining of encapsulated MIN6 cells

At the endpoint of the experiment, the encapsulated cells were stained using a LIVE/DEAD kit for mammalian cells (Thermofisher). Cell staining was carried out using a modified version of the manufacturer's protocol. 2.5µL Calcein AM and 10µL ethidium homodimer-1 were added to 5mL of PBS to give the staining solution. The hydrogels were washed with PBS before transferring to the staining solution and incubating for 30 mins. The hydrogels were washed again with PBS.

The HA-TA hydrogels were clear/slightly turbid and the confocal laser could easily visualise up to 300µm into the hydrogel. In contrast, the hybrid HA-TA/PFD hydrogels were completely opaque and the laser could only penetrate 30µm into the hydrogel before complete loss of resolution. To overcome this and to investigate cells closer the centre of the hydrogel, the solid hydrogel was bisected to give a flat surface that runs throughout the hydrogel.

3.2.4 Rat islets

Rat islets were isolated from rat pancreata as needed for each experiment. Rats were purchased from Envigo and kept for at least 1 week before euthanisation and islet recovery. For each experiment performed, islets were isolated from 6 rats over 3 days; 2 rat pancreases were harvested each day and the islets were isolated from the pancreases within 1 hr. This work was carried out under AREC approval no. 1236bbbb.

3.2.4.1 Rat pancreas collection

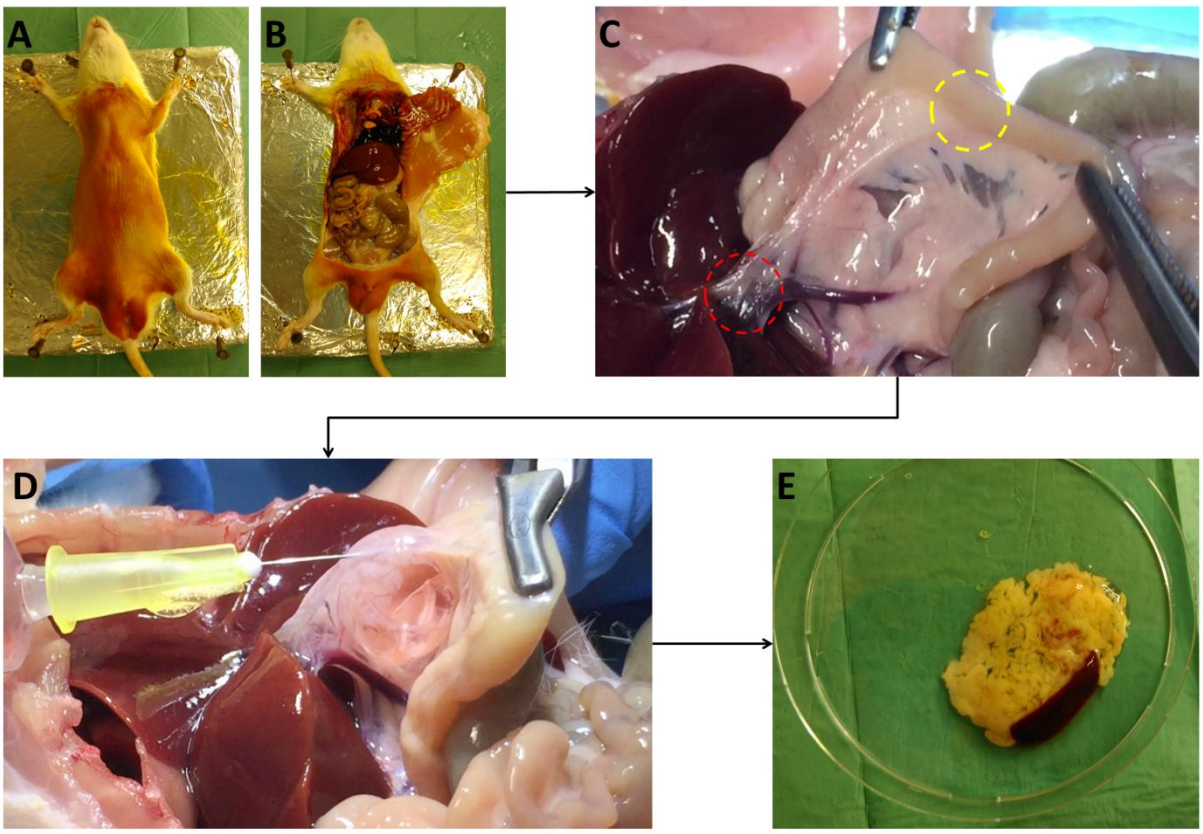

Figure 3.3 *(A) Rat is fixed supine and skin sterilised with ethanol and iodine. (B) Door shaped incision exposing abdominal organs. (C) Small intestine identified and pancreas is stretched between intestines. Areas outlined in circles were clamped to block flow into the liver (red) and flow into the duodenum (yellow) (D) Bile duct cannulated and the digestion solution is perfused into pancreas, the tissue distends and spreads throughout the pancreas. (E) The perfused pancreas is collected with the spleen (red-brown) attached. The spleen and fat tissue are removed at this stage.*

The protocol was adapted from the long standing protocol for rodent islet isolation (296) by DRIVE partner Abiel srl for use with their collagenase enzymes. Training on this protocol was provided by Abiel.

10mL of collagenase solution containing 40U of ColG and 170U ColH was prepared per rat and placed on ice before use. Each rat was individually euthanized by CO_2 asphyxiation and cervical dislocation to confirm death. The rat was prepared for the procedure by shaving the hair from the abdomen and sterilising the skin using ethanol 95% and iodine. The rat was fixed supine on a styrofoam board and transferred to a sterile work surface prior to incision (Figure 3.3A).

A door shape incision was cut into the abdomen of the rat and the ribs were removed to better facilitate access to the bile duct (Figure 3.3B). Abdominal organs were moved and the liver was repositioned against the thoracic cavity to expose the common bile duct. The duodenum was identified and gently stretched to expose the pancreatic tissue and the common bile duct. The bile duct runs from the liver and into the duodenum (Figure 3.3C); both sides of the duct were blocked using a clamp to prevent flow into the liver and duodenum.

Immediately before perfusion, 100µL of thermolysin was added to the 10mL collagenase solution to make the Digestion solution. 5mL of Digestion solution was drawn into a syringe and using a 30g needle, the bile duct was cannulated. The Digestion solution was perfused into the pancreas and after 1-2mL the pancreas should begin to noticeably distend (Figure 3.3D). Once the full volume was perfused the needle was removed followed by the removal of the clamps.

The pancreas was extracted first by pulling it away from the organs it is attached to, the duodenum and the small intestine, the stomach, large intestine and liver. The pancreas was then transferred to a petri dish (Figure 3.3E) where the spleen and fat were removed. The pancreas was then transferred to the remaining 5mL of Digestion solution and placed on ice for up to 1 h. Two pancreases were collected in ~1 h and then transferred to a laminar flow hood for islet purification.

3.2.4.2 Rat islet purification

The pancreata were agitated in the Digestion solution at 100RPM at 37°C for 10 min to digest the tissue further. The digestion was halted by adding 20mL of media containing serum, and the tissue was further dissociated by vigorous shaking, 40 shakes 20-30 sec, to free the islets from the surrounding tissue. The tubes were centrifuged at 800RPM and the media was removed. The pellet was resuspended in 10mL of media. The resuspended slurry was passed through a 0.419mm wire sieve into a fresh petri dish to separate out non-digested tissue, fat and lymph. The sieved material was collected and the tube and dish were washed with fresh media to bring the final volume to 25mL. The sieved material was now centrifuged at 800RPM. The media was poured off and the pellet allowed to dry.

The pellet was resuspended in 15mL ice-cold heavy Histopaque-1119 (1.119g/mL) and transferred to a new 50mL tube. 20mL ice-cold light Histopaque-1077 (1.077g/mL) was carefully layered to make a sharp interface. Finally, 15mL of media was layered on top of the Histopaque-1077 with another sharp interface. The tube containing the gradient was centrifuged at 800G for 5 min, using the slowest acceleration and deceleration. The islets formed a visible ring (Figure 3.4A) at the interface and were collected using a pasteur pipette. The islets were washed 3 times, and then transferred to a 10cm petri dish. Prior to encapsulation the rat islets were pooled into a 5mL volume and 4 x100µL samples were taken for counting. The islets were imaged using a Leica System microscope and the islets sizes were measured using the ImageJ program (Figure 3.4B). The islets were measured by their diameter and this was compared to table for calculating IEQ for human islets from the Integrated Islet Distribution Program (IIDP) (Figure 3.4C).

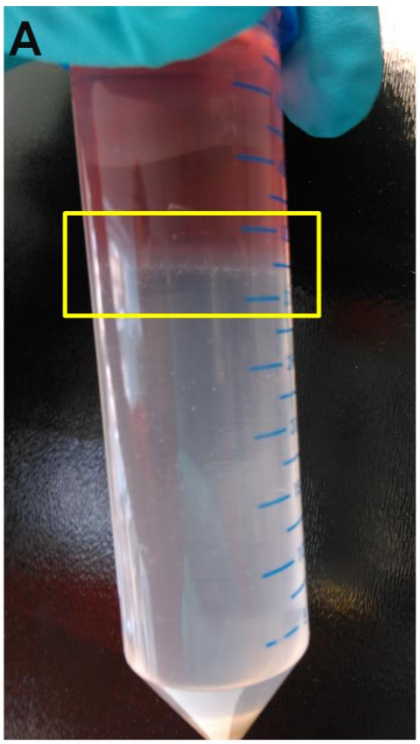

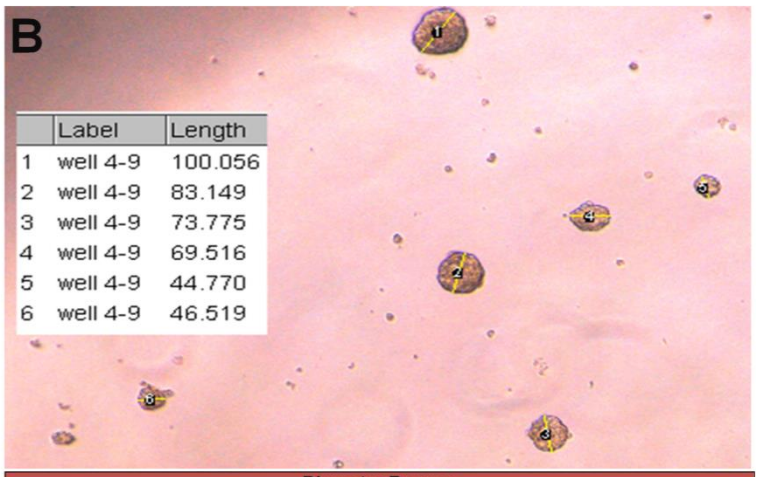

C

Diameter Ranges								
µm	50-100	101-150	151-200	201-250	251-300	301-351	351-400	>400
Calculated Conversion Factors								
Multiply by Column total to get IEQ	0.167	0.667	1.685	3.5	6.315	10.352	15.833	22.75

Figure 3.4 *Rat islet purification (A) Islets forming a ring at the interface between Histopaque-1077 and RPMI1640. (B) Islet count in a 96 well plate showing ImageJ software output. (C) Table for calculating IEQ from the IIDP.*

3.2.4.3 Encapsulation of rat islets in the HA-TA hydrogels

Rat islets were encapsulated in the HA hydrogels at a density of 5,000 IEQ/mL. This islet concentration is based on the current practice of 10,000 IEQ/kg of the patient's weight. An average weight for an adult patient with diabetes of 70kg was taken as a reference value, giving a required number of islets to be 700,000 IEQ total. As there is a large loss of approximately 50% of the transplanted islets in a hepatic portal vein islet infusion this means that ~350,000 IEQ are required to reverse T1D. At 5,000 IEQ/mL this would give a final fill volume of approximately 70ml.

The rat islets were encapsulated according to the same protocol used for the MIN6 cells, Section 3.2.3.1. The formulations tested with the islets are outlined in Table 3.1. The prepared gels were transferred to a 24 well plate with RPMI 1640 media (11mM glucose concentration) at 37°C for culture before testing.

Table 3.1 *HA-TA hydrogel formulations tested with islets at 5,000 IEQ/mL*

Hydrogel	Lipoid E80	PFD	Oxygenated	Repeats
HA-TA hydrogel (GF1b)	X	X	X	n=3
HA-TA/Lipoid hydrogel	3.5% w/v	X	X	n=2
HA-TA/PFD hydrogel (GF2b)	3.5% w/v	30% w/v	¨H	n=3

3.2.4.4 GSIS assay of encapsulated islets

At set time-points of 24 h, 96 h and 168 h a GSIS assay was performed to determine the insulin secretion of islets encapsulated within the hydrogels.

Krebs-Ringers Buffer (KRB) was prepared according to *Appendix 1* and the pH was brought to 7.4. Glucose was added to the KRB to give a low glucose buffer (3.3mM glucose) and a high glucose buffer (16.7mM glucose), based on a protocol provided by DRIVE partner Abiel.

Hydrogels were first washed in low glucose media for 30 min, changing the media every 10 min. Hydrogels were incubated in low glucose media for 1 h after which media was collected and stored at -20°C for ELISA. Following this hydrogels were incubated in high glucose media for 60 min and media collected and stored at -20°C. Mercodia rat insulin ELISA was used to determine the concentration of insulin released by the encapsulated islets.

As a control to test baseline insulin secretion, free floating islets (FFI) were treated to the same GSIS protocol at the 24 h time-point only. Encapsulated islet results were normalized against FFI results.

3.2.5 Insulin diffusion experiments

Two protocols were used to characterise insulin diffusion properties through the HA-TA and hybrid HA-TA/PFD hydrogels.

Insulin release from HA-TA hydrogels was tested using FITC-labeled insulin. HA-TA and hybrid HA-TA/PFD hydrogels were made up with 50mg/mL FITC-insulin, injected into custom cylindrical moulds (8mm diameter, 4mm height) and allowed to

set. The hydrogels were then transferred to a 24-well plate and incubated at 37°C in 1mL of PBS. The PBS was collected after 0.5/1/2/3/4/24 h time-points and replaced with fresh PBS. The supernatant was measured with a fluorescent plate reader at 495/515nm ex/em.

Insulin diffusion through the HA-TA hydrogels was visualized and measured by confocal microscopy. HA-TA and hybrid HA-TA/PFD hydrogels were prepared using the same custom mould as above. Hydrogels were transferred to a 24-well plate incubated in 50mg/mL FITC-insulin solution of PBS. After 1 h hydrogels were removed from the FITC-insulin solution and washed in PBS, bisected vertically, and a tile scan of the bisected surface was performed using confocal microscopy. The images were analyzed using image j, to determine a measurement of fluorescent intensity in relative light units (RLUs) across the surface.

3.2.6 INS-1E cell line

The INS-1E cell-line was selected at this point as MIN6 cells at a low enough passage number to ensure function were not available.

The INS-1E cell line was cultured in Falcon® T75 flasks, specifically Falcon® brand as it is preferred by the cell line, at 37°C in 5% CO_2 and fed with RPMI 1640 (R8758), supplemented with 5% FBS, 1mM pyruvate, 10mM HEPES and 50µM β-mercaptoethanol. The cells were cultured up to a 70-80% confluence in the flasks and split 1:6 once weekly.

3.2.6.1 INS-1E PIs

INS-1E cells were also prepared as PIs to assess the effect of gel mixing during encapsulation on islet integrity. PIs were prepared according to the following protocol. INS-1E cells were cultured to 70-80% and were trypsinised and counted. The INS-1E cells were suspended at a density of 500 cells/100µL and, using a multichannel pipette, were seeded into a U-bottom 96-well plates at a density of 500 cells/well. The cells were incubated for 72 h to allow the formation of a single PI/well. When needed, the PIs were pooled and immediately encapsulated in a hydrogel at the desired density to minimise the risk of hypoxia and clumping of the pooled PIs.

3.2.6.2 Encapsulation of INS-1E cells in natHA hydrogels and natHA/PFD emulgels

As outlined in Section 2.2.5.2, the natHA based hydrogels were too high a viscosity to mix by stirring or passing up and down in a syringe. As a result INS-1E cells and PIs were mixed into the natHA hydrogel and natHA/PFD emulgel by passing a cell/PI suspension over and back between two syringes. NatHA hydrogel or natHA/PFD emulgel was prepared at higher concentrations of their components. These were then diluted down to their final concentrations using an INS-1E cell or PI suspension.

For these experiments the INS-1E cells were prepared at a density of 5 million cells/mL of final gel; this density was selected based on a paper by *Cañibano-Hernández et al* (110). Following encapsulation, the hydrogels/emulgels were filled into a 30µL immunoisolating shell (Figure 3.5) using a syringe pump at a slow rate (50µL/min) to minimise the risk of bursting. The shells were filled through the port using a 23G needle and heat sealed.

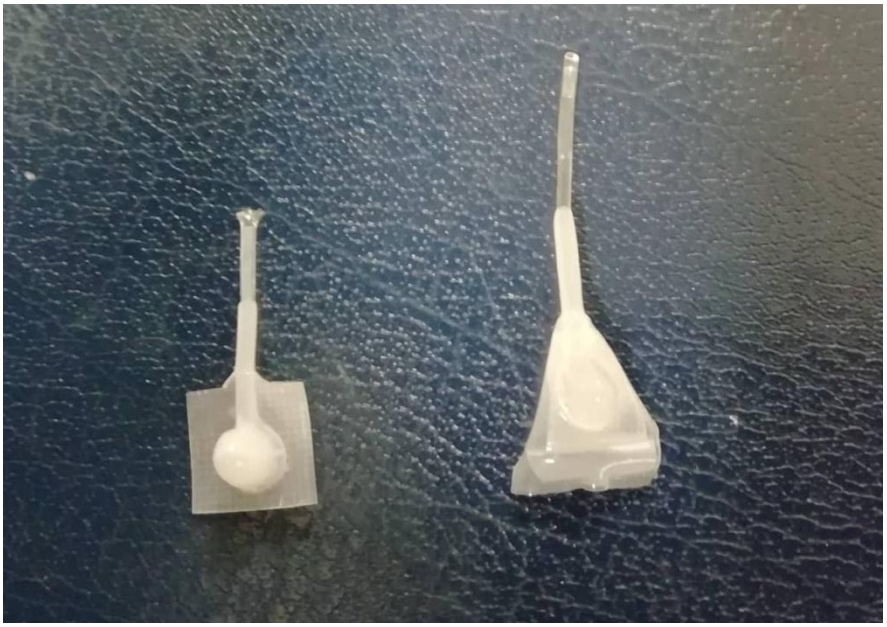

Figure 3.5 *The immunoisolating shell design used for in vitro experiments with INS-1E cells and PIs. The shells have a round hemispherical 30µL chamber (~5mm diameter). The flat surface on the underside is a semi-permeable immunoisolating membrane (~10-15mm wide).*

3.2.6.3 Assessment of encapsulation PI morphology

The morphology of PIs after encapsulation in natHA hydrogels of different viscosities was measured. PIs were encapsulated at a density of 100 PIs/mL in natHA at final concentrations of 2%/1.5%/1%/0.75% w/v natHA.

100µL volumes of encapsulated PIs in natHA were transferred to 96 well plates, and 100µL of a live/dead staining solution, prepared as outlined in Section 3.2.3.2, was placed on top and was incubated for 30 mins. PIs were then imaged using fluorescent microscopy to give a qualitative assessment of PI morphology.

3.2.6.4 GSIS assay on encapsulated INS-1E cells

At set time-points of 24 h, 72 h and 168 h the GSIS was used to determine the insulin secretion of the INS-1E cells and their PIs that were encapsulated in GF5 hydrogel or GF7 emulgel in the immunoisolating shells from Figure 3.5.

KRB was prepared according to *Appendix 1.2* and the pH was brought to 7.4 to ensure full dissolution of all components. Glucose and theophylline were added to the KRB to give a low glucose buffer (3.3mM glucose) and a high glucose buffer (16.5mM glucose). A wash buffer of a low glucose concentration (3.3mM glucose) without theophylline was also prepared. Theophylline was added to enhance the GSIS response of the encapsulated cells, to better mimic glucose responsiveness seen in primary cells in the INS-1E cell-line (297).

The shells were transferred to a fresh 48 well plate and were then washed in wash buffer for 30 min, changing the buffer every 10 min. The shells were then incubated in low glucose buffer for 1 h, to normalize the conditions that may have developed between wells. Following this incubation, the shells were washed 3 times again and incubated for 2 h in low glucose buffer. The supernatant from this incubation was collected and stored at -20°C. The shells were washed 3 times, and incubated in the high glucose media for 2 h. This supernatant was collected, the shells were washed a final 3 times and incubated in low glucose media once again. This supernatant was collected and the shells were transferred back to RPMI 1640 media until the next time-point. The Mercodia rat insulin ELISA was used to analyze the amount of insulin released by the encapsulated INS-1E cells.

The INS-1E cells were encapsulated in both a 1% w/v natHA hydrogel and the natHA/PFD emulgel (GF7) in the immunoisolating shell. These samples were incubated as two separate groups. The normoxia group was incubated at 37°C at 5% CO_2 and the hypoxia group was incubated at 37°C at 5% CO_2 in a hypoxia chamber set at 1% O_2. GSIS assays were run at 24 h/72 h/168 h after encapsulation.

3.2.6.5 Statistical analysis

Statistical analysis of this data was performed with GraphPad PRISM software, version 8.1.2. Data was expressed means ± standard deviation (SD), and differences were considered significant between groups using one-way ANOVA and Tukey's Post Hoc Test when $p<0.05$.

3.3 Results

3.3.1 Live/dead viability imaging of encapsulated MIN6 cells

Figure 3.6A and 3.6B show cells encapsulated within a HA-TA hydrogel, and 3.6C and 3.6D show cells encapsulated within a hybrid HA-TA/PFD hydrogel. The cells encapsulated in HA-TA hydrogels show approximately equal live cells (green) and dead nuclei (red). Additionally a number of live cells are associated with dead nuclei i.e. red nuclei are present within the green live cells. In Figure 3.6C and 3.6D the majority of nuclei are dead, and a large proportion of living cells are also associated with a dead nucleus, indicating that encapsulated cells are staining for both are permeable to both the live (Calcein AM) and dead (ethidium homodimer-1) stains. Ethidium homodimer-1 is excluded by intact cell membrane, indicating that cells staining for both dyes are non-viable.

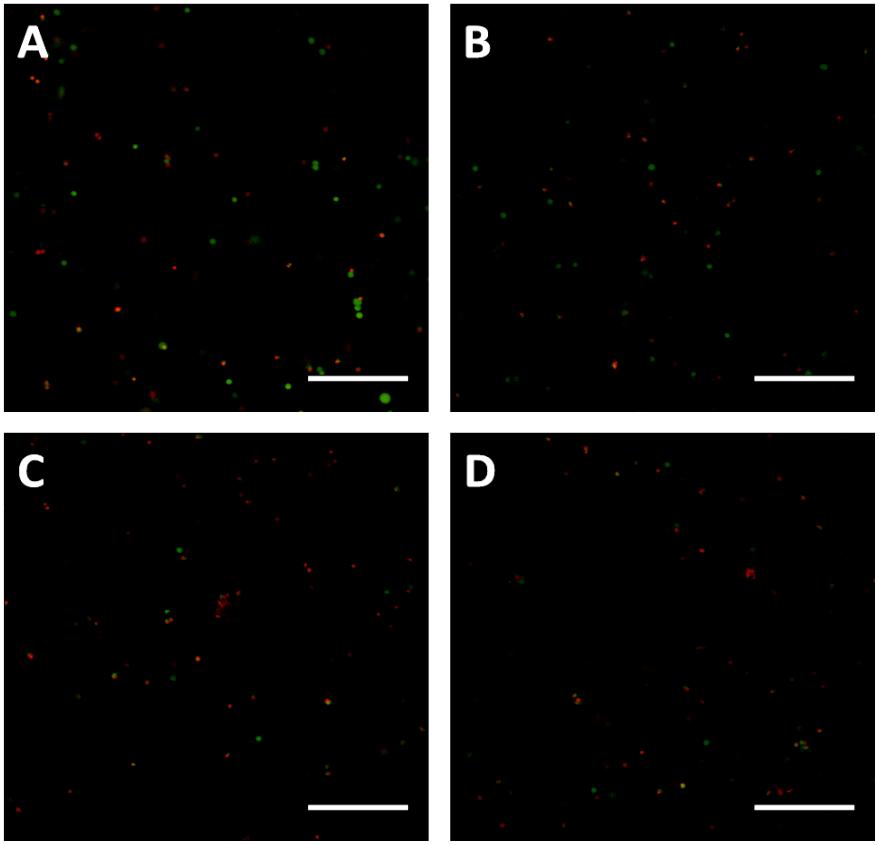

Figure 3.6 *Live/dead confocal imaging of encapsulated MIN6 cells. Green indicates living cells and red indicates dead nuclei. (A+B)Showing cells encapsulated in a HA-TA hydrogel. (C+D) showing cells encapsulated in a hybrid HA-TA/PFD hydrogel. Scale bars show 200µm length.*

3.3.2 Rat islets

3.3.2.1 Islet isolation yields

In total there were 66 rats and 11 weeks of islet isolations over 7 months dedicated to the preparation of a hydrogel. 6 additional rats were used over a number of weeks to practice the isolation and purification techniques and to optimize process parameters with the equipment in the RCSI.

The selected islets density of 5,000 IEQ/mL meant that for a 200µL hydrogel, the size of the moulds that were used, a minimum of 1,000 IEQ was needed per gel. In addition to this, the static mixer used to mix the hydrogels for crosslinking had a dead volume of approximately 150-200µL. This meant that a minimum of ~1,500-1,700 IEQ were required for a single hydrogel per experiment. As a result, this meant that two of weeks (Figure 3.7) did not yield enough IEQ from the rat islet isolation protocol to prepare a single hydrogel at the selected density. In total, eight HA-TA based hydrogels were prepared at the selected islet encapsulation density and GSIS was performed on these hydrogels.

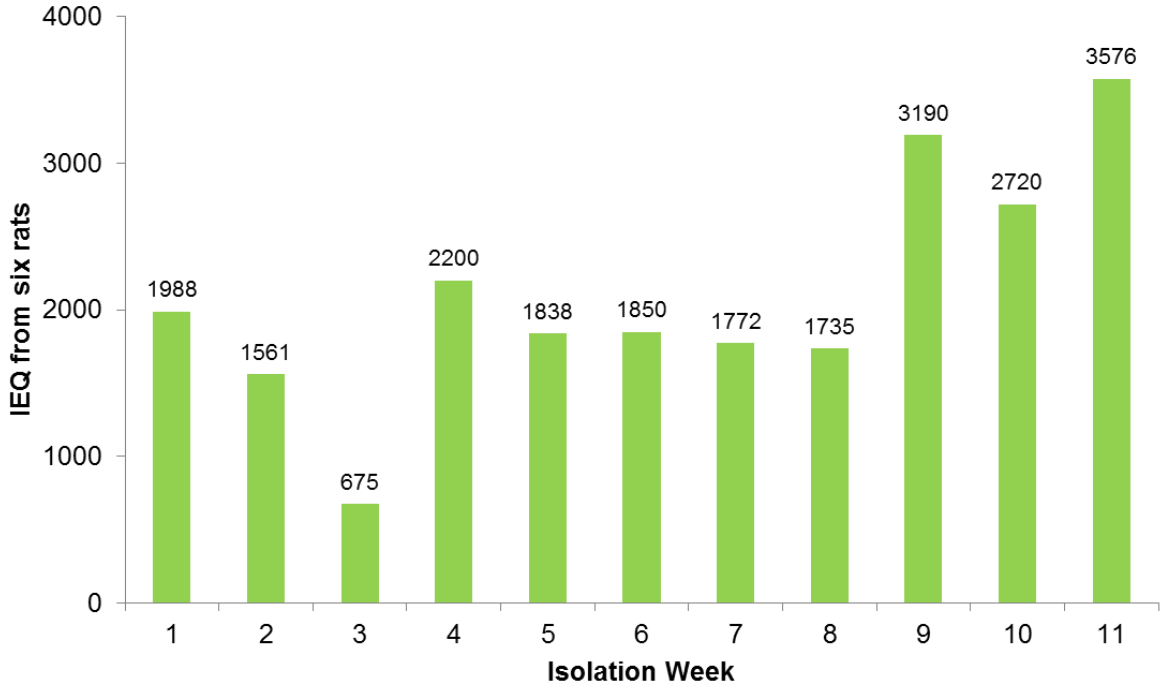

Figure 3.7 *IEQ from six rats over 11 weeks of isolations. This is the total number of IEQ isolated each week from 6 x >200g male Lewis rats.*

3.3.2.2 Insulin secretion from HA-TA encapsulated rat islets

For the purposes of these studies, a group will be considered to show glucose responsive behaviour when the ratio between insulin release at high glucose stimulation (16.7mM) and low glucose stimulation (3.3mM), referred to as the glucose stimulation index (GSX) is >3 (298).

We saw that rat islets encapsulated in HA-TA (Figure 3.8A) and HA-TA/PFD (Figure 3.8C) hydrogels were not glucose responsive (GSX <3) and showed high standard deviations at all time-points. Although neither group was glucose responsive, HA-TA/PFD showed GSX values of <1 at all time-points compared to the HA-TA which showed GSX of ~1 at 24 h and 168 h. The HA-TA/Lipoid (Figure 3.8B) hydrogels were glucose responsive at 24 h and 96 h however showed the highest standard deviations, increasing the margin of error.

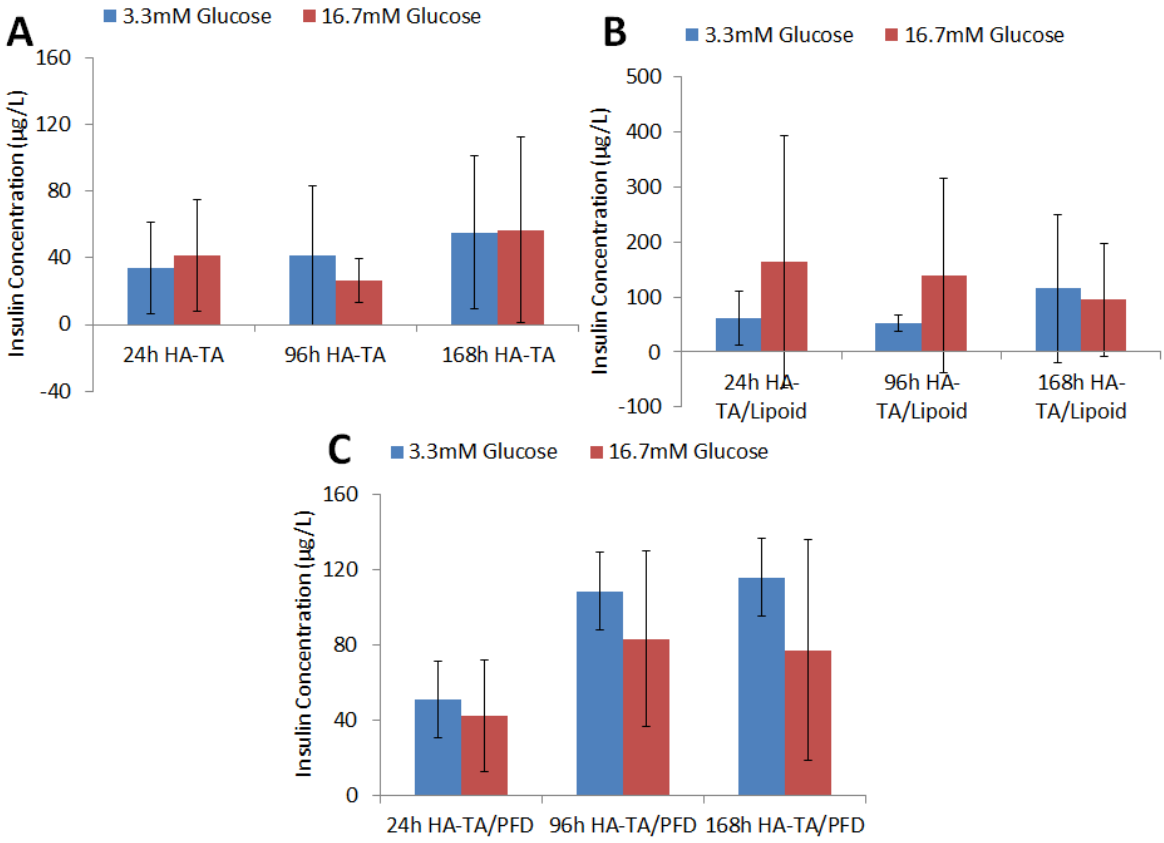

Figure 3.8 *Insulin secretion by encapsulated rat islets in response to low (3.3mM) and high (16.7mM) glucose stimulation. (A) HA-TA hydrogel, showing no GSIS (n=3) (B) HA-TA/Lipoid hydrogel, showing GSIS (n=2) (C) HA-TA/PFD hydrogel, showing no GSIS (n=3). Values shown represent the mean ± SD.*

The GSIS results of the encapsulated rat islets were also compared to FFI that were used as a control. This was done by normalising the insulin secretion of the encapsulated islets at low (3.3mM) glucose stimulation at each time-point with the low glucose stimulation of the FFI at 24 h (Figure 3.9). The GSIS results are presented as the insulin secretion per IEQ from the encapsulated islets normalised as a ratio against the results of the GSIS for the FFI islet at 24 h, where FFI is 1. All results were compared to FFI at 24 h instead of FFI at their respective time-points as FFI viability is reduced over long term culture. The encapsulated rat islets show low insulin release from the HA-TA hydrogels, with the highest insulin release being one fifth (0.2) the release seen from the FFI and the lowest release being less than one tenth (<0.1). This indicates that substantially less insulin is released from encapsulated islets than FFI.

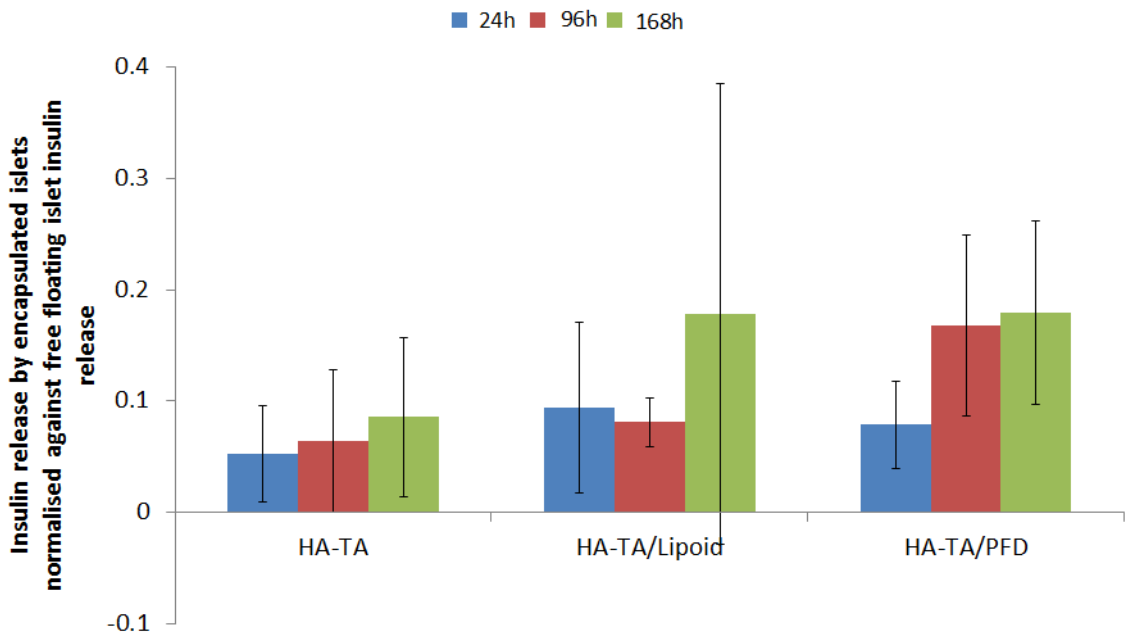

Figure 3.9 *Insulin secretion by encapsulated islets in HA-TA hydrogels normalised against FFI controls, where FFI would be 1. The encapsulated rat islets show low insulin release from the HA-TA hydrogels, with the highest insulin release being one fifth (0.2) the release seen from the FFI and the lowest release being less than one tenth (<0.1).*

3.3.3 Insulin diffusion through the HA-TA hydrogels

Release of encapsulated insulin from the HA-TA based hydrogels was slow, showing <20% of encapsulated insulin being released after 1 h incubation, and <80% after 24 h. Insulin diffusion through the HA-TA hydrogel was also slow, taking ~2 h to diffuse to the centre of a 200µL HA-TA hydrogel and taking >2 h to diffuse to the centre of a HA-TA/PFD 200µL hydrogel.

Figure 3.10 shows the release of FITC-insulin from GF1b and GF2b over 24 h. GF2b released more of the loaded FITC-insulin than GF1b in the time studied, however neither released all loaded insulin by 24 h.

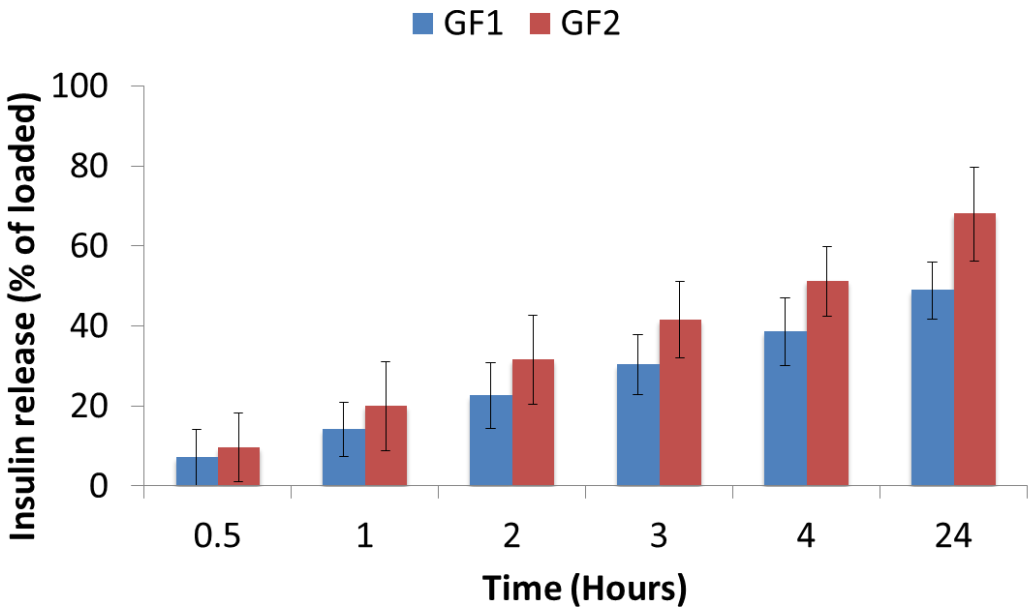

Figure 3.10 *Release of loaded FITC-insulin from the HA hydrogel (GF1b) and hybrid HA/PFD hydrogel (GF2b). Graph shows cumulative percentage of loaded insulin at 0.5, 1, 2, 3, 4, and 24 h.*

Figure 3.11 and Figure 3.12 show the diffusion of the FITC-insulin through GF1b and GF2b respectively. FITC-insulin diffuses completely throughout the GF1b within 2 h whereas the FITC-insulin only diffuses ~2mm into the GF2b in the same timeframe.

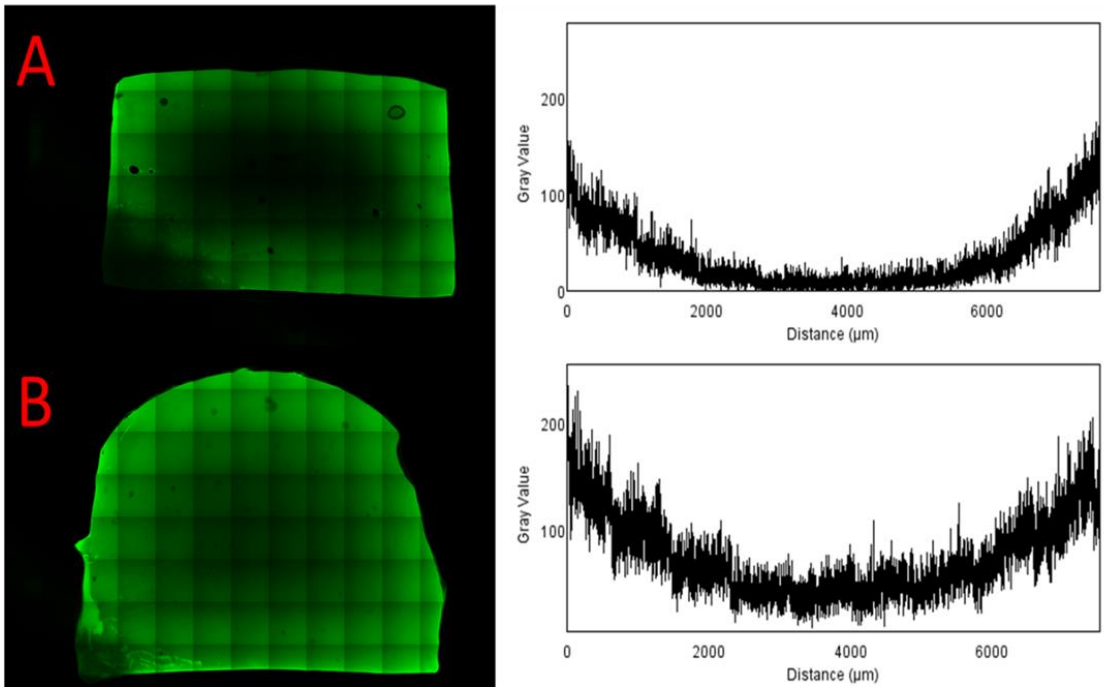

Figure 3.11 *FITC-insulin diffusion through the HA hydrogel (GF1b) using a confocal microscopy tile scan to visualise the FITC-insulin diffusion through the hydrogel and ImageJ to analyse the intensity of the response throughout the hydrogel. (A) Diffusion through GF1b after 1 h. (B) Diffusion through GF1b after 2 h.*

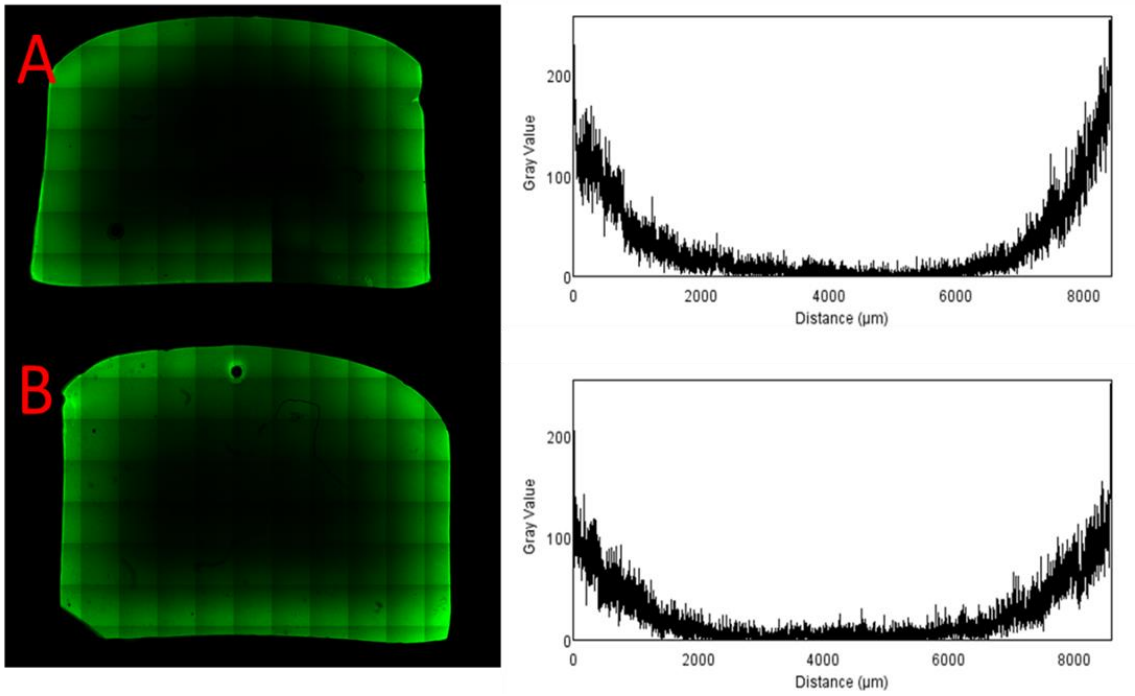

Figure 3.12 *FITC-insulin diffusion through the HA hydrogel (GF2b) using a confocal microscopy tile scan to visualise the FITC-insulin diffusion through the hydrogel and ImageJ to analyse the intensity of the response throughout the hydrogel. (A) Diffusion through GF2b after 1 h. (B) Diffusion through GF2b after 2 h.*

3.3.4 PI morphology after mixing in natHA hydrogels

The viscosity of the higher concentration natHA hydrogels had a significant effect on the morphology of the PIs after mixing as shown in Figure 3.13. The control PIs refer to PIs that were not mixed and are in PBS, and they show the characteristic round morphology expected of PIs. The PIs in 2% w/v natHA are completely broken and have lost all PI morphology. The PIs in 1.5% w/v natHA show some damage to their morphology, but there is still evidence of their characteristic morphology. The PIs in 1% w/v and 0.75% w/v natHA show morphology comparable to the control. The viability of the cells is unchanged in all natHA hydrogels.

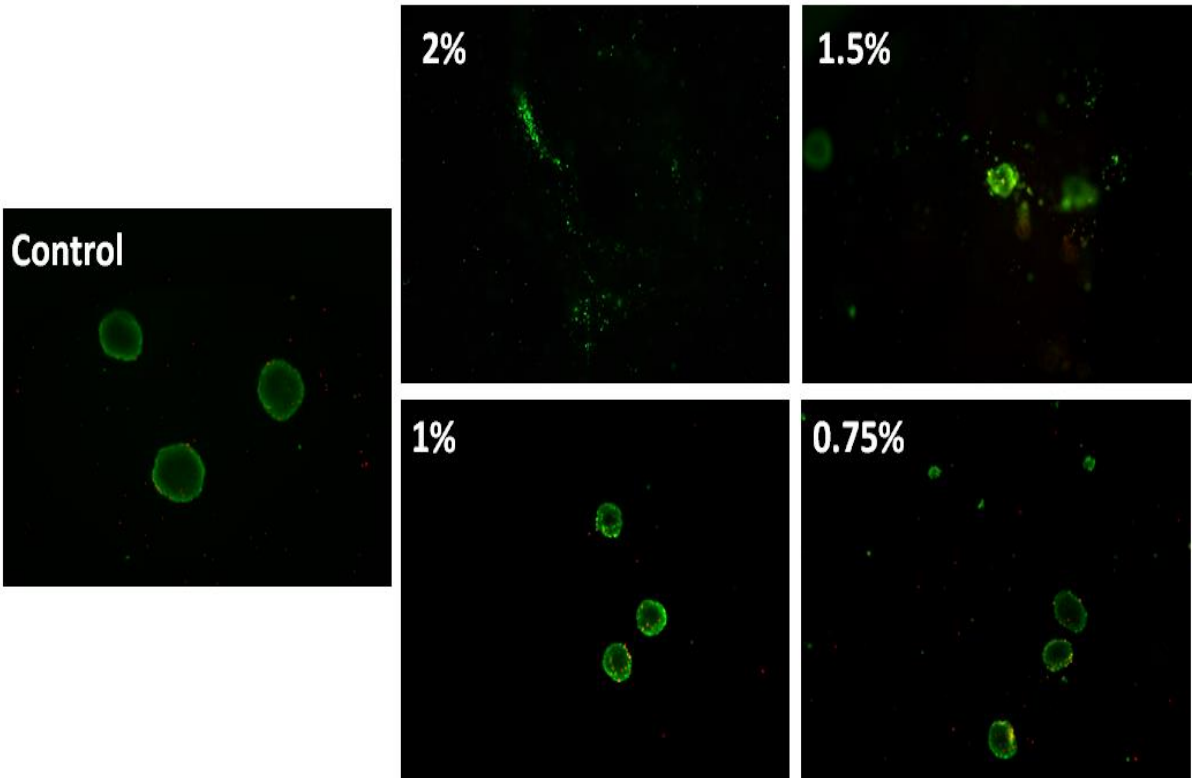

Figure 3.13 *Islet morphology imaged by fluorescent microscopy with live/dead staining after encapsulation in different concentrations of a natHA hydrogel. The control refers to islets suspended in PBS.*

3.3.5 Comparison of insulin secretion by encapsulated INS-1E cells in normoxia and hypoxia in a natHA hydrogel and natHA/PFD emulgel

Figure 3.14 shows the GSIS results for the INS-1E cells encapsulated in the natHA hydrogels in both normoxia and hypoxia. The graph shows that the cells encapsulated in natHA hydrogel in normoxia were glucose responsive at all time-points, with a GSX >3 and a statistically significant increase between insulin secretion after the first low glucose (3.3mM) stimulation and high glucose (16.5mM) stimulation. This indicates the cells within the natHA hydrogels in normoxia are functional. In comparison, cells encapsulated in natHA hydrogel in hypoxia showed lower insulin secretion at 24 h and little to no insulin secretion at 72 h and 168 h time-points, indicating the cells were not functional in hypoxia.

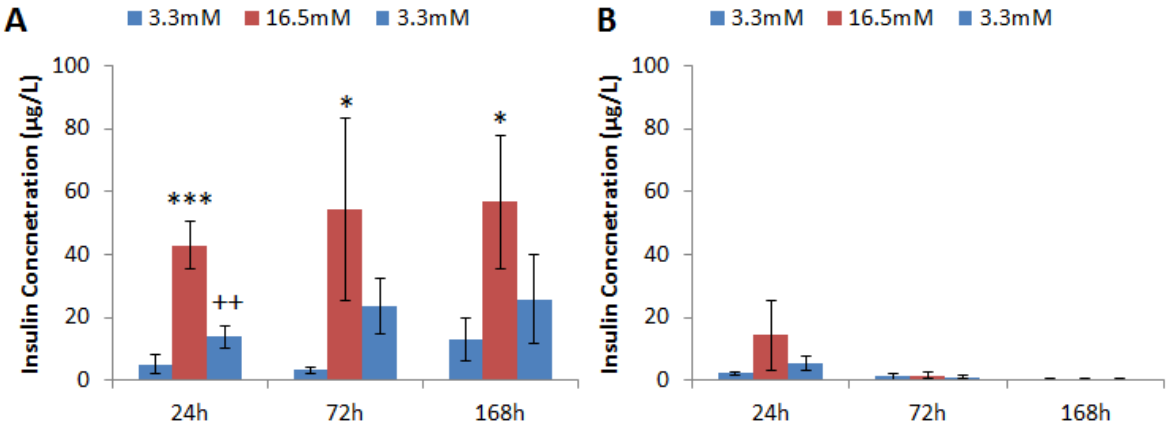

Figure 3.14 *GSIS by INS-1E cells encapsulated in natHA hydrogels in an immunoisolating shell in normoxia or hypoxia for up to 168 h. (A)INS-1E cells encapsulated in natHA hydrogel in normoxia (B) INS-1E cells encapsulated in natHA hydrogel in hypoxia. Values represent the mean ± SD. *: p<0.05, ***: p<0.001 compared to the first low glucose stimulation. ++: p<0.01 compared to the high glucose stimulation.*

Figure 3.15 shows the GSIS results for the INS-1E cells encapsulated in the natHA/PFD emulgels in both normoxia and hypoxia. The graph shows that the encapsulated cells were not glucose responsive in normoxia, showing no significant differences in insulin secretion between stimulation with low or high glucose at any time-point. In general, the insulin secretion by the natHA/PFD emulgel encapsulated cells was lower than cells encapsulated in the natHA hydrogels.

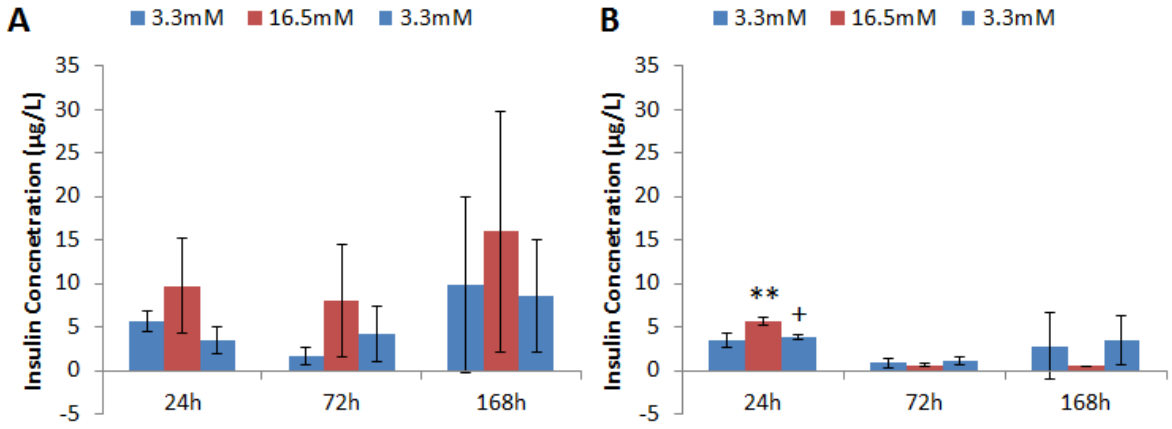

Figure 3.15 *GSIS by INS-1E cells encapsulated in natHA/PFD emulgels in an immunoisolating shell in normoxia or hypoxia for up to 168 h. (A)INS-1E cells encapsulated in natHA/PFD emulgel in normoxia (B) INS-1E cells encapsulated in natHA/PFD emulgel in hypoxia. Values represent the mean ± SD. **: p<0.01 compared to the first low glucose stimulation. +: p<0.05 compared to the high glucose stimulation.*

3.4 Discussion

The overall aim of this Chapter was to assess the formulated biomaterials from Chapter 2 with a suitable *in vitro* model to identify which biomaterial should be brought forward for further pre-clinical *in vitro* and *in vivo* testing. One of the key challenges with this was identifying suitable *in vitro* models for the different formulations that were being assessed, and throughout the testing a number of cell lines and primary islet cells were used.

The first formulation that was assessed was the HA-TA/PFD hydrogel, with rat islets. A primary cell type was used instead of a cell line because a cell line with a suitable insulin secretion profile could not be optimised for use with the HA-TA hydrogels. Initially, some preliminary work was performed with the MIN6 cell line, due to its documented high insulin secretion and GSIS. However preliminary testing showed they were not suitable for use with the HA-TA hydrogels as they were particularly sensitive to the H_2O_2 used to crosslink the HA-TA hydrogels. Although β-cell sensitivity to H_2O_2 is well documented in the literature (299), it was thought that the low concentration (0.1% w/w), in conjunction with the relatively low residence time due to the H_2O_2 molecule being catalysed to form the HA-TA crosslinks on the backbone, would be sufficient to prevent toxicity. *Inberg et al* identified that a concentration of 200µM H_2O_2 caused 17% of MIN6 cells to be identified as necrotic (300). 0.1% w/w converts to be ~30mM H_2O_2; it is likely that this high concentration resulted in the large proportion of dead nuclei observed. This could also explain why there are a higher proportion of dead cells in the HA-TA/PFD hydrogels (Figure 3.6C and 3.6D) compared to the HA-TA hydrogels (Figure 3.6A and 3.6B). As previously noted HA-TA/PFD hydrogels take longer to gel than the HA-TA hydrogels and are weaker than the HA-TA hydrogel counterparts. This indicates that the H_2O_2 has a higher residence time to damage the encapsulated cells, and less is used overall in the crosslinking reaction increasing the damage to encapsulated MIN6 further.

The primary challenge with using primary rat islets was sourcing a sufficient number for the target density of 5,000 IEQ/mL. This density was necessary to ensure a sufficient quantity of islets within a volume of hydrogel that was feasible for implantation.

Results from the rat islet encapsulation experiments showed limited glucose responsivity and high standard deviations. Comparison with FFI at 24 h showed that the insulin release by encapsulated islets is substantially lower than FFI.

We had two lead hypotheses on the cause of the reduced release. Firstly, that the physical properties of HA-TA hydrogels were responsible for the lack of insulin release was considered. Similarly to oxygen diffusion out of the HA-TA hydrogels, by Fick's First Law of diffusion "J = -D $\frac{d\varphi}{d\ x}$", where J refers to the diffusion flux, which describes the amount of a substance/molecule/atom that will flow through unit area over a specific period of time. This law may describe the low insulin release, if the flux of glucose and insulin is limited by HA biomaterial it is possible we would see a large lag time on insulin production and release into the media being tested compared to the FFI. Alternatively, we considered that the insulin molecule, which is negatively charged at physiological pH (301), may be binding to the components of the hydrogel. It is unlikely that this is the case, as the low insulin was consistent between the HA-TA and HA-TA/PFD hydrogels. HA-TA itself also has an overall negative charge indicating it should not be binding the insulin molecules, and *Lee et al* investigated a HA-TA hydrogel system for protein delivery and saw that negatively charged alpha-amylase could be sustainably released, in comparison to positively charged lysozymes that were electrostatically bound to the hydrogel. Finally we considered the possibility that the insulin was physically retained within the crosslinks of the hydrogel, preventing diffusion outwards.

To investigate the hypothesis that the physical properties of the HA-TA hydrogels were reducing insulin release, a FITC labelled insulin was used to measure release from HA-TA hydrogels and to image the diffusion of insulin into the hydrogels. FITC-insulin loaded into the HA-TA and HA-TA/PFD hydrogels was released very slowly, with only ~15% and ~25% being released respectively after 1 h. This correlates with the release of approximately 10% and 20% from the islets encapsulated in the same hydrogels when compared with the FFI. Additionally the full insulin payload had not been fully released after 24 h. Figures 3.11 and 3.12 show the diffusion through the HA-TA hydrogel and HA-TA/PFD hydrogel respectively. It took 2 h of incubation for the FITC-insulin to diffuse to the centre of the HA-TA hydrogel. The FITC-insulin did not diffuse to the centre of the HA-TA/PFD hydrogel within the same time-frame. It is

clear from these results that the diffusional barrier from the HA-TA matrix retarded the diffusion of insulin through the hydrogels. This is a significant issue in the translation of the device to the clinic due to the potential “lag” period

Therefore further evaluation focused on the natHA based hydrogels. Due to issues relating to ethics, cost and time management it was decided to revert to the use of a cell line in place of continuing with the primary rat islets. MIN6 cells at the correct passage were not available therefore an alternate cell line was identified for use; the INS-1E cell line (Pierre Maechler, Geneva, Switzerland). This cell line is well established as discussed in Section 3.1.1 and was being used by other partners in the DRIVE consortium (EKUT, Tubingen)

INS-1E PIs were used to assess structure and morphology after mixing into the high viscosity natHA based hydrogels. We looked at the PIs structure, morphology, and viability after mixing and encapsulation in the natHA hydrogels. This was performed to ensure that shear stresses imparted on the PIs during the mixing step would not damage them. Shear stress is a concern for cells that undergo hydrodynamic stresses (302-304). While the islet capsule is likely to provide greater protection to primary islet cells than a PI, evaluation of the impact of mixing to a PI provides an important indicator of the effect of mixing. 2% natHA resulted in destruction of the PI, with both 1% natHA and 0.75% natHA showing undamaged PIs, providing a boundary viscosity within which testing could be performed. As it was desirable to maximise the viscosity of the encapsulating emulgel to assist with islet suspension, a viscosity that mimicked the 1% natHA hydrogel was preferable. GF7 (0.615% natHA/28% PFD) showed comparable viscosity and was selected as the lead emulgel for further evaluation.

The cells were encapsulated in the natHA based hydrogels, and the natHA based hydrogels were then encapsulated in a pouch, to prevent the hydrogel from dispersing completely. This pouch was acquired from DRIVE partners in NUIG, who had designed an immunoisolating pouch (Figure 3.5) that facilitated the diffusion of insulin through its semi-permeable membrane. From Figure 3.14 and Figure 3.15 we saw that the presence of the PFD emulsion in the natHA/PFD emulgel does not show to be beneficial in hypoxia, showing no glucose responsiveness at any time-point. NatHA/PFD emulgel also appears to negatively affect INS-1E cell function in

normoxia, with the encapsulated cells showing no significant glucose responsiveness at any time-point, in contrast to INS-1E cells in the natHA hydrogels.

There are a number of reasons that this may be the case. A clear consideration is that the inclusion of the PFD emulsion is cytotoxic to the encapsulated cells, however this is not supported by the literature, as the PFD and emulsifier were selected for their history of use as biocompatible components, and biocompatibility testing will be performed in Chapter 4 to investigate this further. Alternatively, it is possible that the PFD emulsion retarded the diffusion of secreted insulin. The presence of the PFD emulsion increases the viscosity of the natHA/PFD emulgel, and as discussed previously, according to Fick's First Law, increased viscosity leads to decreased diffusion. Alternatively insulin may be binding to the PFD emulsion droplets by some interaction. Insulin has been shown to be strongly attracted to negatively charged lipid interfaces (301), and other groups have investigated lecithin emulsifiers as a component of oral insulin formulations (305, 306). Finally, the aim of the natHA/PFD formulations is to provide oxygen to encapsulated cells immediately after transplantation. As the devices cannot be vascularised *in vitro* the effect of hypoxia on the cells encapsulated in both the natHA hydrogel and natHA/PFD emulgel was the same after the loaded oxygen was depleted.

In conclusion, this Chapter allowed the exclusion of the HA-TA hydrogels from further evaluation due to challenges with insulin diffusion. The natHA formulations were therefore identified as the lead formulations. PIs were used to assess the effect of the mixing protocol on islet structure and morphology, and it was identified that a lower viscosity natHA formulation was favourable to maintaining islet morphology after encapsulation. The *in vitro* testing of the natHA formulations showed contradictory results, with the natHA/PFD emulgel showing to not be beneficial to INS-1E cell function in hypoxia. The natHA/PFD emulgel also showed to be detrimental to INS-1E cell function in normoxia, compared to the natHA hydrogel alone.

Chapter 4

Translational reality of the DRIVE technology

4.1 Introduction

The aim of this project is to formulate and design a biomaterial suitable for use as a component in a bio-artificial pancreas which has undergone pre-clinical evaluation with a view to clinical translation.

This bio-artificial pancreas will encapsulate pancreatic islets in an immune-isolating membrane enabling implantation. These islets after implantation will be able to replace endogenous insulin production in T1D patients. In Chapter 2 we discussed the formulation of the natHA/PFD emulgel; the biomaterial component made of natHA to suspend the islets and the PFD emulsion to improve oxygen supply to encapsulated islets. In Chapter 3 we evaluated the emulgel *in vitro* with an insulin secreting glucose responsive cell line. In this Chapter we look at combining the emulgel with an immunoisolating "β-shell" to give the bio-artificial pancreas, and its evaluation *in vitro* with human islets, *in vivo* in small animal studies and scale-up the formulation for preliminary acute large animal *in vivo* studies.

These preliminary preclinical studies are an important stepping-stone in clinical translation. In pharmaceutical manufacturing, process development is the complex stage in the development of a pharmaceutical product that starts after the product formulation has been determined and ends when the manufacturing process has been optimised. Successful process development results in an established process with a known endpoint, that successfully translates the results of research conducted in a lab into an industrial product. Figure 4.1 below outlines the medicinal product development pathway (307). The work outlined in this chapter represents the start of the process development stage, and will focus on the steps required to enable generation of the non-clinical and preclinical data required to translate the product from the bench to the clinic.

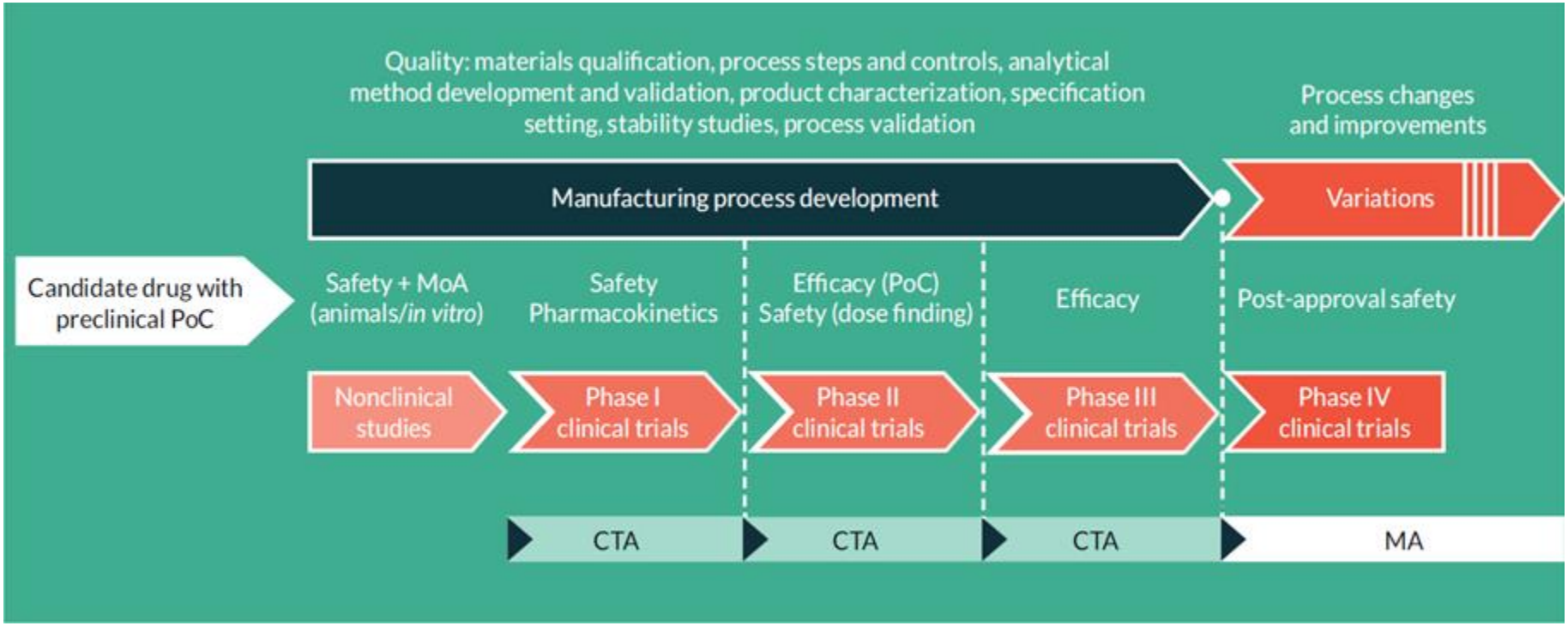

Figure 4.1 *Outline of the medicinal product development pathway, from clinical trials to marketing authorisation (307).*

4.1.1 Regulatory Framework

A bio-artificial pancreas as a single implantation device, with multiple components, offers a complex product from a regulatory standpoint. In 2007 the European Commission (EC) amended the Directive 2001/83/EC (308) on the "*Community code relating to medicinal products for human use*" with Regulation (EC) No 1394/2007 "*on advanced therapy medicinal products* (ATMP)" (309). This regulation laid down the specific rules regarding the classifications, authorisation, supervision, and pharmacovigilance of ATMPs and established the Committee for Advanced Therapies (CAT) (310) to draft an opinion on ATMP applications and to provide recommendations and guidance regarding prospective ATMPs. The CAT is a committee of the European Medicines Agency (EMA). The EMA is a decentralised agency in the EU responsible for the scientific evaluation, supervision and safety monitoring of medicines in the EU. The EMA provide central authorisation for ATMPs, meaning ATMPs benefit from a single evaluation and authorisation procedure through the EMA.

The ATMP regulation came into being due to the development of increasingly complex advanced therapies not covered by existing directives and regulations. The ATMP regulation lists three types of medicinal products for human use as ATMPs: gene therapy, somatic cell therapy, and tissue-engineered products. In addition to the three primary types a definition is also given for a 'Combined ATMP'.

A gene therapy medicinal product (GTMP) is defined as containing/consisting of an active substance of a recombinant nucleic acid for use in humans to regulate, repair, replace, add or delete a genetic sequence. The therapeutic, prophylactic or diagnostic effect must relate directly to the recombinant nucleic acid sequence or the product of its expression. Both of these characteristics are needed for classification as a GTMP, and vaccines as prophylaxis against infectious disease are specifically excluded from this definition.

A somatic cell therapy medicinal product (sCTMP) is a biological product that contains cells or tissue that have been subject to substantial manipulation so that the biological characteristics, functions or structure have been altered for the intended clinical use or that they will not be used for the same essential function as in the donor. This allows the cells to be used in humans to treat, prevent or diagnose a

disease through pharmacological, immunological or metabolic action. The list of manipulations that are not considered substantial included in the ATMP regulation include, but are not limited to: cutting, centrifugation, sterilization, separation, concentration or purification, and filtering.

A tissue engineered (TE) product is a product that consists of engineered cells or tissues that are administered to human beings to regenerate, replace or repair human tissue. Engineered cells or tissues are cells that have undergone substantial manipulation to change the biological functions or structure needed for the intended purpose. Additionally, a TE product can have human or animal cell products that are either viable or non-viable, with or without additional substances such as cellular products, biomolecules, chemicals, biomaterials, scaffolds or matrices. The CAT has provided a decision tree for determining if a product can be classified as a sCTMP or TE product (Figure 4.2).

A combined ATMP is a product that that utilises both a medical device and a viable cellular/tissue or non-viable cellular/tissue that act on the human body to give the primary effect of the combined ATMP. The medical device or active implantable medical device must be an integral part of the product for the product to be considered a combined ATMP. The decision tree (Figure 4.2) also outlines if a product can be considered a combined ATMP.

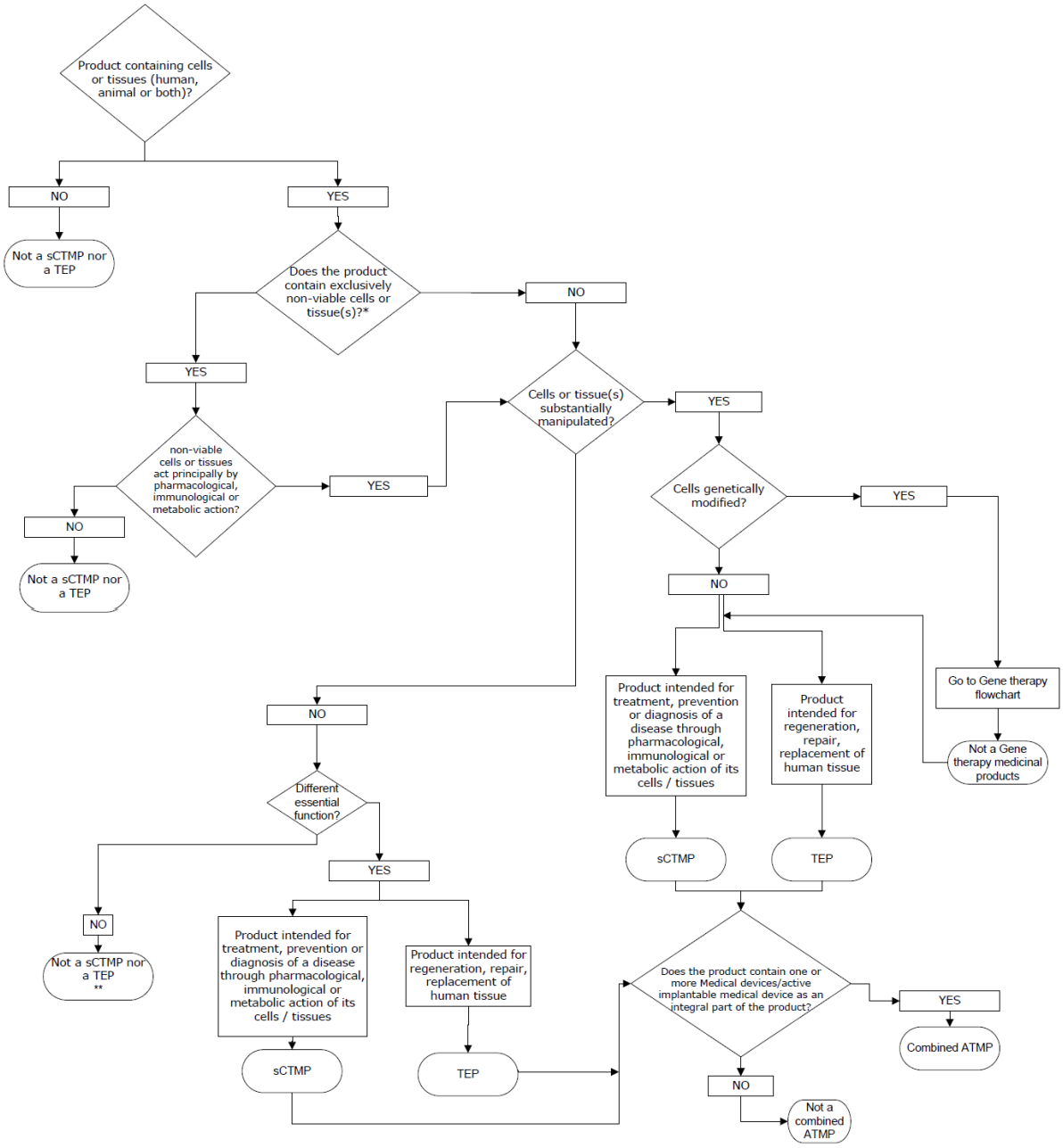

Figure 4.2 *Decision tree for sCTMP and TE (311).*

4.1.2 DRIVE technology as an ATMP?

In 2011 human islets were classified as non-ATMP (312). The steps taken to isolate and purify human islets from the pancreatic tissue were not considered a substantial manipulation and that the functional islet unit was unaltered following isolation. Additionally, in 2018 an application of "*allogeneic pancreatic islets encapsulated by elastin-like recombinamers"* was classified as non-ATMP for the same reason (313),

the cells were not substantially manipulated and the cells are intended to be used for the same essential function in the recipient as in the donor.

While these classifications may suggest that the DRIVE product would not be classified as an ATMP, these applications do not include a medical device, alongside the viable cellular component of the donor human islets. Additionally, the carrier system/islet delivery system as a functionalised biomaterial aligns with the descriptions defined in the TE classification.

From June 2009 - December 2018 the CAT has classified 316 applications (314). 8 of these applications were specifically related to the treatment of T1D, and 4 of these aimed to utilise β-cell populations as a treatment modality (Table 4.1).

The first of these applications from 2010 referred to a "*mixture of porcine β-cell and accompanying endocrine cell populations in an alginate matrix*" was classified as a sCTMP (314). A similar application in 2013 referred to "*alginate encapsulated porcine pancreatic islets cells"* and was classified as a sCTMP combined product (315). From the 2013 application, the islet cells were harvested from neonatal piglets and subsequent growth and differentiation during cell processing was deemed to be substantial manipulation. The mechanism of action was claimed to be the metabolic production of porcine insulin to replace endogenous insulin, which was sufficient to be classified as a sCTMP. Additionally, the alginate present as an alginate microcapsule was integral to the product as a barrier between the human body and the porcine islet cells while allowing free diffusion of nutrients, waste and products. In a 2014 reflection paper (311), clarification was provided on why these treatments were not classified as a TE product. The primary mechanism of action claimed was the treatment of T1D by the metabolic production of porcine insulin, a replacement of the function of the endogenous islets, as opposed to a TE product where the mechanism must be to regenerate, repair, or replace the human tissue itself. Although this sets a precedent regarding the classification of human islet therapies, these classifications do not fully encompass the scope and complexity involved in a bio-artificial pancreas product. By utilising a biomaterial ECM, pancreatic niche proteins, human islets as a cell component, and a medical device (immunoisolating shell), it is likely that the bio-artificial pancreas product would be classified as a combined therapy.

Table 4.1 *CAT scientific recommendations on classification of ATMPs for the treatment of T1D. None of these products have received approval as an ATMP.*

Product Description	Therapeutic area	Classification	Uses β-cell populations for treatment	Date of adoption of recommendation
Mixture of porcine beta cell and their accompanying endocrine cell populations in an alginate matrix	Endocrinology: intended for the treatment of diabetes	sCTMP – not combined	yes	02/07/2010
Human islets of Langerhans	Intended for: Autologous: Post pancreatectomy for benign pancreatic pathologies. Allogenic: Treatment of severe forms of T1D	Not an ATMP	yes	29/07/2011
Autologous $CD4^+$ T cells targeted to cells presenting class II restricted epitopes	Intended for autoimmune diseases with MHC restricted specific immunity e.g. multiple sclerosis, T1D or graft rejection	sCTMP	no	23/11/2011
Alginate encapsulated porcine pancreatic islet cells	Intended for treatment of T1D	sCTMP	yes	28/02/2013

Product Description	Therapeutic area	Classification	Uses β-cell populations for treatment	Date of adoption of recommendation
Bone marrow-derived autologous non-hematopoietic stem cells	Intended for treatment of T1D	sCTMP	no	21/12/2015
Autologous *ex vivo* expanded polyclonal $CD4^+$, $CD25^+$, $CD127^{low/-}$, $FOXP3^+$ regulatory T-cells	Intended for treatment of T1D	sCTMP	no	04/04/2016
Autologous ex vivo expanded regulatory T lymphocytes with the cell marker profile of CD3+. CD4+, CD25high, CD127-, FoxP3+	Intended for treatment of T1D	sCTMP	no	30/05/2016
Allogeneic pancreatic islets encapsulated by elastin-like recombinamers	Intended for the treatment of severe forms of T1D	Not an ATMP	yes	28/03/2018

4.1.3 ICH guidelines

The International Council for Harmonisation of Technical Requirements for Pharmaceuticals for Human Use (ICH) mission is to bring together regulatory authorities and pharmaceutical industry to discuss the scientific and technical aspects of drug registration and authorisation. In doing so they aim to improve harmonisation in the drug development process to ensure safe, effective, and high quality medicines are developed and registered as efficiently as possible (316). This is done through the development and publishing of the ICH Guidelines which are divided into three main categories;

- ***Quality guidelines*** that cover areas such as product testing, and approaches to quality by design through Good Manufacturing Practice and pharmaceutical development;
- ***Safety guidelines*** that aim to uncover potential risks such as carcinogenicity and other elements of the products toxicology profile; and
- ***Efficacy guidelines*** to guide on performing clinical trials.

One key quality guideline is the guideline for Pharmaceutical Development Q8 (R2) which defines the aim of pharmaceutical development as '*design of a quality product and its manufacturing process to consistently deliver the intended performance of the product*' (317). It provides guidance and raises considerations for the entire pharmaceutical development process, from the components of the drug product down to the container closure system. Many of these factors were relevant for the process development of the natHA/PFD emulgel as part of the pre-clinical studies.

4.1.4.1 Components of the Drug Product

The ICH guideline provides considerations for the effect of the physiochemical and biological properties of the drug substance and excipients on manufacturability e.g. solubility, water content, particle size. Table 4.2 below outlines the formulation of the natHA/PFD emulgel, and the considerations in providing these components as a final product.

Table 4.2 *Formulation and considerations for components of the natHA/PFD emulgel.*

Active Component	Excipients	Considerations
natHA	PBS – hydrating the natHA	What form to provide natHA in? – powder or hydrated viscous liquid
		What storage conditions for the provided natHA?
		An expiry date?
PFD emulsion	Lipoid E80 - emulsifier	What storage conditions for the supplied PFD emulsion?
	PBS – continuous phase of emulsion	An expiry date?

4.1.4.2 Drug Product

This section of the guideline looks at the formulation of the final drug product as a whole, and focuses on highlighting the entire formulation process from initial concept to final formulation, for inclusion in the CTD. This includes the choice of drug products, the manufacturing process and knowledge gained from the development of similar products. If excipient ranges are listed they must be justified. In addition to this, a summary of the different formulations used in clinical safety and efficacy

studies or relevant bioavailability or bioequivalence studies should be noted, and deviations from the proposed commercial formulation should be noted.

Therefore in developing a protocol for multiple pre-clinical studies in small and large animals, a system to efficiently track the formulations used for the different pre-clinical studies is important for eventually developing a final CTD.

Overages are discussed in this section as something that should be discouraged if used to compensate for degradation during manufacture or shelf-life. If overages do need to exist in the manufacturing process they should be fully accounted for and justified.

4.1.4.3 Manufacturing process development

The guidelines for the manufacturing process development focus on developing and choosing the manufacturing processes while considering the critical formulation attributes, appropriateness of components, and appropriateness of equipment used. It outlines that during the process development stage a basis for improvement, validation, continuous verification, and process control requirements should be included and accounted. In addition, studies to investigate and address the microbial, physical, and chemical attributes of the product should be identified and designed into the process. This stage should also identify critical process parameters that need to be monitored or controlled.

4.1.3.4 Container closure system

The container closure system of the product should be given consideration in relation to the intended use of the product and suitability of the container for storage and shipping. The container closure system should also be compatible with the components, provide sufficient protection from environmental factors such as moisture and light,

4.1.3.5 Sterilization

The EMA has published guidelines on sterilisation including detailing methods of sterilisation and required outcomes for methods to ensure product sterility. Terminal sterilisation methods are preferred over filtration or aseptic processing as sterility

assurance levels can be calculated and tightly controlled. This is not possible in aseptic processing where accidental contamination due to poor technique cannot be reliably controlled. The guidelines account for sensitive products, detailing that aseptic processing under controlled conditions can provide satisfactory quality for the end product (318). A summary of the sterilisation methods detailed in the guidelines and further specifications as outlined in the European Pharmacopeia is shown in Table 4.3.

The EMA has also provided guidelines on the selection of an appropriate sterilisation method and has included two decision trees for sterilisation of aqueous (Figure 4.3) and non-aqueous products.

The selection of appropriate sterilisation methods for the components of the natHA/PFD emulgel is necessary to ensure pre-clinical studies are not affected by microbial contamination or infection in animal models.

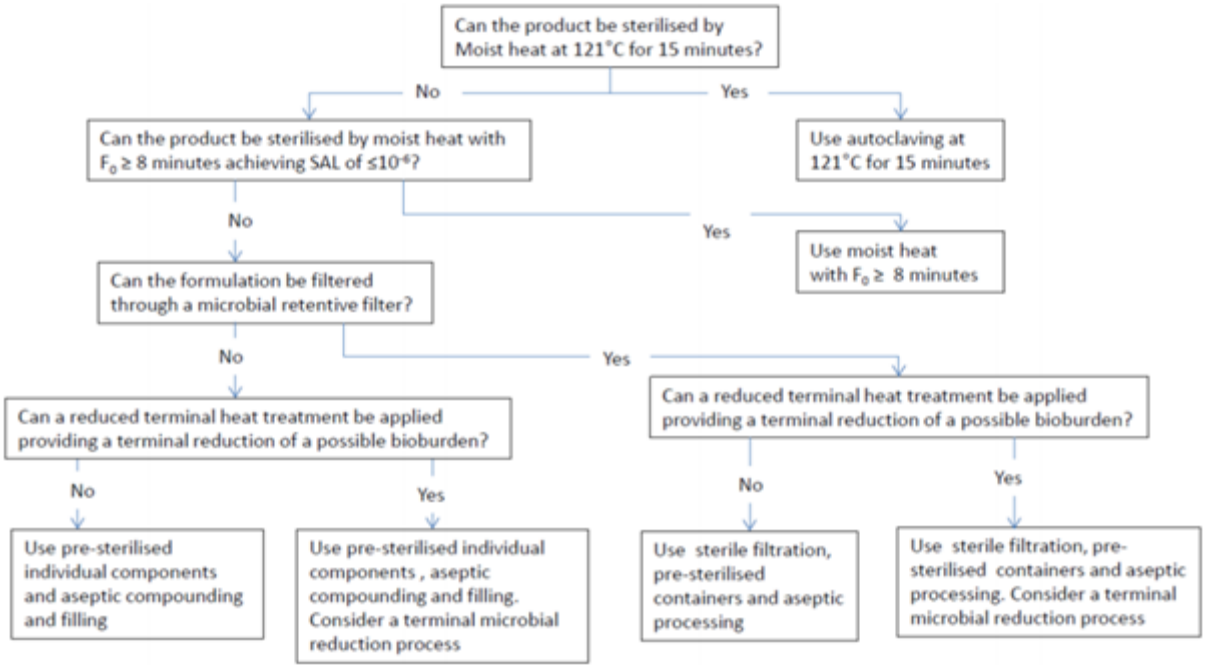

Figure 4.3 *Decision tree for sterilisation of aqueous products (318).*

Table 4.3 *Summary of sterilization methods outlined by the European Pharmacopeia.*

Method	Details of method	Reference condition
Steam Sterilisation	Sterilisation of products in an autoclave or similar piece of equipment, using hot saturated steam under pressure. Preferred method of sterilisation for aqueous preparations.	≥121 °C for ≥15 min
Dry Heat sterilisation	Sterilisation of products in an oven or similar piece of equipment, using dry heat.	≥160 °C for ≥120 min
Ionization radiation sterilisation	Use of a source of ionising radiation e.g. gamma irradiation from radioisotope cobalt 60.	≥25 kGy absorbed dose
Gas sterilisation	Use of a chemical capable of forming a gas to sterilise surfaces e.g. ethylene oxide. Provides surface sterilisation of the product only so not suitable for many medicinal products e.g. liquids or powders.	No specified reference condition
Sterile filtration	Sterile filtration using a microbial retentive filter of a bulk solution. Sterile filtration should be performed immediately prior to filling into final product containers.	Filter pore sizes less than 0.22µm
Aseptic processing	Not considered a sterilisation process but concerns techniques to maintain sterility e.g. aseptic processing units.	No specified reference condition

4.1.4 Preclinical studies

Preclinical studies are performed after the drug discovery stage and before the drug enters clinical studies in humans. The aim of preclinical studies is to provide information about the safety of the drug or treatment, and also provide evidence of treatment efficacy, utilising both *in vitro* and *in vivo* studies (319). Preclinical research is invaluable in gathering the pharmacodynamics, pharmacokinetic and toxicology data required for a CTD or investigational new drug (IND) application, required to move a new treatment forward to clinical trials.

To obtain relevant and usable results, an appropriate preclinical model that can be compared with the target patient population must be selected. While *in vitro* studies are typically considered a fast and efficient method of testing the efficacy and toxicology of a treatment a significant limitation is the fact that cells are cultured "on plastic" and so are unlikely to behave as they do *in vivo,* with no visibility *of* off-site effects.

Therefore reliable animal models for *in vivo* preclinical studies are of great importance. A reliable animal model is one which has a strong predictive potential for therapy success when translated from animal model to the human patient (320). There are a significant number of animal models of DM available, and can be classified based on the types of DM they mimic and the onset of the DM. The two categories of induction of DM in animal models are spontaneous onset diabetes models and induced onset DM.

Spontaneous onset diabetic models are models of diabetes whereby T1D develops spontaneously, typically via an autoimmune process. This type of induction is very useful for research into and treatment of the autoimmune processes involved in the development of T1D, and can also be used for research into anti-diabetic agents and glucose management through insulin delivery (321). Some of the most commonly used spontaneous onset DM models include Biobreeding (BB) rats, the non-obese diabetic (NOD) mouse, Akita mice, and the LEW 1AR1/iddm rats (322).

However induced diabetic models are the most frequently used type of diabetic model as they are easier to generate than spontaneous models. They are commonly used where research is less focused on the autoimmune processes and more on the

treatment of the hyperglycaemia itself (321). Two methods to induce onset of T1D are through surgical induction, either by total or partial pancreatectomy, or chemical induction of diabetes, most commonly using streptozotocin (STZ) (322). STZ induced diabetes models are one of the most commonly used models for islet transplantation research, as the mechanism of action, uptake by the β-cells by glucose transporter GLUT2 and subsequent toxicity, leads to reliable diabetes induction across a number of animal models (323).

The NHP model has been identified as the ideal candidate for performing pre-clinical trials for islet transplantation. This is due primarily to their evolutionary similarities to humans, longer lifespan than other animal models allowing for longitudinal studies and multiple procedures over longer periods and clinically present with similar features of diabetes as in humans (324, 325). However, the use of NHP for preclinical research is limited greatly by ethics considerations, and according to the 3Rs should only be used where there are no viable alternatives available (326).

Rodent models are useful for transplantation research in T1D due to the availability of different rat and murine models and the high availability, relatively low cost, and relevant acceptability of rats and mice for research. As the primary outcome in transplantation research is the reversion of T1D, the importance of differences in the pathology of T1D between rodent models and humans is lessened, allowing greater focus on the efficacy of the treatment (327).

Pigs do not spontaneously develop diabetes; however protocols for induction of diabetes using STZ or pancreatectomy have been developed. The primary advantage of using pig models for islet transplantation research is that they are relatively anatomically and physiologically similar to humans (328). In addition to this, pigs have a moderately low cost for a large animal model, and are more ethically acceptable than nonhuman primates.

Finally, the bio-artificial pancreas is an extra-vascular device, meaning a suitable implantation site must be investigated. There are a number of considerations when selecting an implantation site ranging from: surgical considerations e.g. access to the site, or if the device needs to be fixed in place; physical and physiological considerations e.g. access to a blood supply for blood glucose control, vascularisation potential of the site, and maximum available volume; and finally

issues which could affect acceptance of the treatment by a patient cohort e.g. palpability. Two potential sites identified for the DRIVE project are the anterior abdominal wall (AAW) and the omentum. The AAW is a space with a potentially large volume and has access to vascularisation and systemic blood supply via abdominal blood supply. Alternatively, the omentum is a highly vascularised tissue attached to the stomach that extends down to cover the intestines. Although it exists as a continuous sheet of tissue, it could be folded into a pouch into which a device could be fixed, giving extensive access to the systemic blood supply (329).

4.1.5 Aims

The overall aim of this Chapter is to develop a process to facilitate the successful combination of the individual elements of the bio-artificial pancreas enabling transfer of the process to different collaborators to allow for *in vivo* pre-clinical studies in both small and large animal models.

The specific aims of this Chapter are:

- To develop a defined process and supporting protocol for preparing the natHA formulations for use in pre-clinical studies.
- To assess the biocompatibility of the natHA/PFD emulgel formulation *in vitro* and *in vivo*.
- To formulate a natHA based radiopaque gel for use in acute large animal model studies to enable imaging of delivery of the natHA formulations.

4.2 Material and Methods

4.2.1 Materials

VEGF microspheres were obtained from DRIVE partner Innocore (Netherlands). Visipaque® 320mg iodine/mL was purchased from Synapse Medical (Dublin, Ireland). Sterile natHA hydrogel (~1.2-1.3M Da chains), was obtained from Contipro a.s. (Czech Republic). The β-shells tested in this Chapter were provided by UCD (Ireland).

4.2.2 Protocol development for the preparation of the natHA/PFD emulgel

A protocol was developed to ensure the natHA/PFD emulgel formulation could be reproducibly and repeatedly prepared at multiple partner sites for:

- biocompatibility studies,
- *in vivo* rat and pig studies, and
- *in vitro* human islet studies.

There were a number of factors to consider in the preparation of this protocol including:

- The supply and preparation of the components of the emulgel
- Development of a robust process for oxygenation and transfer of the oxygenation protocol to partners
- Specific alterations to the protocol needed for the different studies

4.2.2.1 NatHA preparation

natHA was supplied as a non-sterile powder. As outlined in Chapter 2, Section 2.2.5.2, rehydrating natHA to achieve a homogeneous gel takes over 48 h. Following rehydration, the high viscosity of natHA gel does not facilitate sterilisation by filtration through a 0.2µm filter.

Following discussion with the project partner and supplier of the natHA, Contipro, two methods to sterilise HA were identified:

- The natHA could be provided as a sterile lyophilised wafer to be hydrated at the correct concentration with PBS on site in sterile conditions in a laminar flow hood. Using a non-ISO method the natHA was filter sterilised at a low concentration and freeze dried into the lyophilised material. This material would then be hydrated, transferred to a syringe and filled to the correct level and either capped for future use or used immediately. This is not a validated method for pre-filled syringes and each batch was tested for sterility.
- Contipro could also provide pre-filled syringes of natHA gel at the correct concentration and volume that had been sterilised in compliance with EN ISO

17665-1 and 2, *Sterilisation of health care products by moist heat*. Each batch was tested for sterility.

4.2.2.2 PFD emulsion supply

As detailed in Chapter 2, Section 2.2.3, the PFD emulsion is made up of three main components, PFD (Sigma), Lipoid E80 (Lipoid Gmbh), and PBS (Sigma).

The PFD emulsion was prepared as described in Section 2.2.3 with sterile components and under aseptic conditions.

- Lipoid E80 was supplied as a sterile component by the manufacturer.
- PBS was supplied as a sterile component by the manufacturer.
- The PFD was filter sterilised under a laminar flow hood using a 0.2µm filter.
- The sonic probe tip was sterilised by steam sterilisation in an autoclave.
- The emulsion was manufactured under laminar airflow in a cell culture hood.
- The 4mL emulsion batches were pooled, mixed and aliquoted in sterile containers to an appropriate volume for each study.

Aliquots of PFD emulsion were provided to partners in sealed sterile containers and were re-suspended by vortexing prior to use.

4.2.2.3 Preparation of the natHA/PFD emulgel

As detailed in Chapter 2, Section 2.2.5.2, a method to mix the high viscosity natHA with the PFD emulsion by passing over and back between two connected syringes was identified as an easy and consistent method to mix the components. In addition to ease of use, by using sterile consumables, syringes and female-female luer connectors, the process can also be performed aseptically with the sterile consumables, minimising contamination risk.

4.2.2.4 Oxygenation protocol

The oxygenation protocol and setup from Chapter 2, Section 2.2.7.2, was used to oxygenate the emulgel due to the high viscosity of the emulgel. This protocol was included as an Appendix to the final protocols sent to partners and was developed to ensure ease of implementation and consistency between the different sites. To facilitate this, critical process parameters (CPP's) were strictly controlled: the infusion

rate of the gel was set at 50µL/min to allow sufficient time for the gel to oxygenate; and the oxygen flow rate was controlled between partners by providing and using an inline oxygen flow meter (Oxy-view™, Qosina).

4.2.2.5 Considerations for incorporating islets and VEGF microspheres

As outlined in Chapter 3, the high viscosity of the emulgel makes it difficult to mix cells into the emulgel by pipetting or syringing up and down.

To address this issue in the protocols the islets were mixed into the emulgel using the same method used for the cells and PIs. The islets were first re-suspended in a volume of PBS or media which was then mixed into the oxygenated emulgel by mixing between syringes.

VEGF was included in the final emulgel of the *in* vivo small animal studies, to help promote vascularisation of the implanted devices. The VEGF was available in a sustained release formulation of VEGF microspheres, provided by DRIVE partner Innocore.

The VEGF microspheres were incorporated into the emulgel at the same step as the islets. This was based on concerns from Innocore that inclusion at an earlier step would result in excess mixing that could damage the spheres leading to large bolus releases of encapsulated VEGF. To minimise the mixing and ensure a homogenous distribution of the microspheres in the final emulgel, a suspension of VEGF microspheres was prepared. This VEGF microsphere suspension could then be used in place of PBS or media to resuspend collected islets and then mixed into the oxygenated emulgel.

4.2.2.6 Kit preparation for natHA/PFD emulgel studies

To minimise variability between consumables, sites, and human input in preparing for the studies, kits containing the materials i.e. natHA, PFD emulsion, β-shells, and consumables e.g. syringes, needles, female-female luers, were assembled by a single operator from RCSI and sent for each study in addition to the protocol (Figure 4.4).

Figure 4.4 *Example of a natHA/PFD emulgel preparation kit prepared for use in in vivo biocompatibility studies.*

4.2.2.7 Protocols developed

Throughout this project a number of different protocols were developed for different gel formulations, *in vitro* and *in vivo* studies, and different shells. The list of protocols developed is shown in Table 4.4.

Table 4.4 *Sample list of protocols developed as part of the project and the purpose of the protocol.*

Protocol	Gel Type	Purpose
Emulgel protocol for biocompatibility testing	NatHA/PFD (GF6)	Sent to Fraunhofer-Institute IGB for biocompatibility testing (Section 4.2.3)
β-gel preparation procedure for rat studies – UCD shell	NatHA/PFD (GF7)	Sent to Abiel Srl for *in vivo* rat efficacy studies with the lead UCD designed β-shell (Section 4.2.6)
β-gel preparation procedure for human islet studies – UCD shell	NatHA/PFD (GF7)	Sent to Oxford for *in vitro* biocompatibility studies with human islets (Section 4.2.4)
Protocol for acute Pig study – UCD shell	Radiopaque gel (RGF1) (July 2018)	Radiopaque gel mimicking GF6 viscosity sent to EXPLORA for filling study (Section 4.2.5.2).
Protocol for acute Pig study – UCD shell	Radiopaque gel (RGF2) (December 2018)	Radiopaque gel mimicking GF7 viscosity sent to EXPLORA for filling study (Section 4.2.5.3).
β-gel preparation procedure for chronic pig study	NatHA/PFD (GF7)	Sent to EXPLORA for *in vivo* chronic biocompatibility study
β-Gel preparation procedure for Human Islet study – UCD Shell	NatHA/PFD (GF 7)	Sent to Oxford for *in vitro* GSIS studies.

4.2.3 *In vitro* biocompatibility testing of natHA/PFD emulgel

A kit and protocol to prepare GF6, without islets and without VEGF microspheres was sent for biocompatibility testing to the Fraunhofer-Institute for interfacial Engineering and Biotechnology IGB (Stuttgart, Germany).

The emulgel was tested for cytotoxicity on a sub-confluent monolayer culture of the HACaT cell line, a keratinocyte cell line from adult human skin commonly used for ISO biocompatibility and cytotoxicity evaluations (330). The emulgel was prepared on-site at the Fraunhofer Institute by following the provided protocol and materials for testing.

An extraction method in accordance with the DIN EN ISO 10993-12: 2012 procedure (331) was performed on the final B-gel formulation. The extract was applied to the HACaT cells and cytotoxicity testing was performed according to DIN EN ISO 10993-5: 2009 procedure (332). Cell proliferation was measured against controls that were negative (DMEM with 10% FCS) and positive (DMEM with 10% FCS and 1% SDS) for cytotoxicity.

A control sample of cells treated using an extract from an extraction vessel with no β-gel formulation was also performed.

4.2.4 *In vitro* human islet studies

All human islet studies were carried out by DRIVE partners in University of Oxford, Nuffield Dept. of Surgical Sciences, England. Due to a scarcity of islets usable for research, only a pilot study of experiments (n=2) was completed. The aim of this study was to evaluate the biocompatibility of the emulgel and also the optimal islet density of human islets in the β-shell.

Two formulations of natHA/PFD emulgel (HA-gel low and HA-gel high) were tested, the difference being the density of human islets in the emulgel. The final formulations of the two gels were based on GF7 and the final formulations can be found in Table 4.5.

Table 4.5 *Formulations of the HA-gel low and HA-gel high used for the in vitro human islet studies.*

Component	Concentration	
	HA-gel low	HA-gel high
NatHA	0.615% w/v	0.615% w/v
PFD (as emulsion)	28% w/v	28% w/v
Islets (Wistar rats)	1,500 IEQ/mL	3,000 IEQ/mL
Oxygenation	yes	yes

There were a number of encapsulation conditions;

- No encapsulation of FFI in CMRL-1066 media (FF low and FF high) as a control,
- Islets suspended in CMRL-1066 encapsulated in a UCD small animal study β-shell (CMRL Low and CMRL High),
- Islets suspended in natHA/PFD emulgel (HA-gel low and HA-gel high) encapsulated in a UCD small animal study β-shell, at two different islet densities; 1,500 IEQ/mL (low) and 3,000 IEQ/mL (high).

Islets were kept in culture for 5 days and islet yield, ROS production, fragmentation index, and viability were measured, and islet morphology was examined by light microscope.

4.2.5 *In vivo* large animal studies (pig model)

Large animal studies with female Landrace pigs, 25-30kg body weight, were carried out by DRIVE partner EXPLORA in Rome, Italy. These studies consisted of two acute animal studies performed in July 2018 and December 2018.

A key aim for these studies in relation to the natHA/PFD emulgel component was to evaluate filling of the shell devices. To enable this, a gel that could be imaged but retained similar material characteristics to the emulgel formulation was required.

4.2.5.1 Formulation and characterisation of radiopaque HA gels

A radiopaque gel enabled visualisation of gel under x-ray/CT imaging. Visipaque®, a commercially available imaging agent which contains an iodinated contrast agent at a concentration of 320mg Iodine/mL, has been previously used for the purposes of creating a radiopaque hydrogel. A concentration of ~20% w/w Visipaque® was sufficient to produce a radiopaque gel for *in vivo* use (333, 334).

Similar rheological behaviour to the natHA/PFD emulgels was required to ensure that the gel was representative of the filling process. Table 4.6 below details the radiopaque gel formulations assessed.

RGF 1 and 2 were assessed using the rheological techniques described in Chapter 2, Section 2.2.6, Table 2.4.

Table 4.6 *Formulation composition for the radiopaque gels.*

Radiopaque gel formulation (RGF)	**NatHA**	**Visipaque®**	**Viscosity**
	% w/v	**% w/w**	**Pa.s**
1 (July 2018)	1.9	21	40-50
2 (December 2018)	1.1	21	3-5

4.2.5.2 Acute *in vivo* pig studies – filling studies (July 2018)

A protocol for the preparation of RGF1 for filling into 20ml devices (Figure 4.5A) was developed. In brief

- 18mL of 2.43% w/v natHA was filled into a 20mL syringe;
- Visipaque® 320mg Iodine/mL was provided in its original packaging;
- 4mL of Visipaque® was filled into another syringe
- The Visipaque and natHA were mixed until homogeneous by passing the contents of the syringes over and back
- β-shells were implanted by laparoscopic procedure to the anterior abdominal wall
- Once in position RGF1 was filled into the shell manually at a slow rate via a filling port from the top of the shell
- Visualisation of the filling was performed via 2D x-ray images using a C-arm

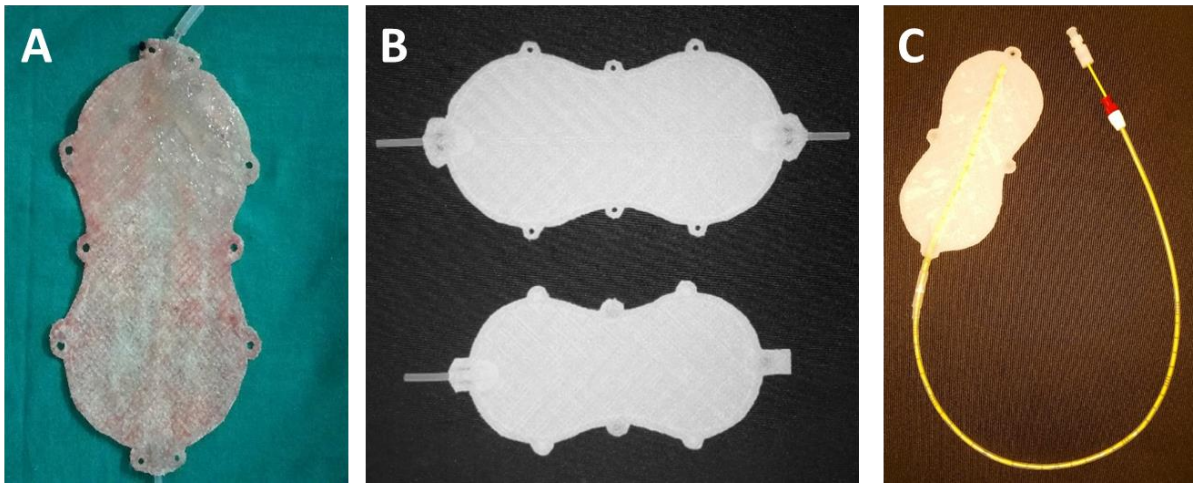

Figure 4.5 *(A) The 20mL UCD β-shell. (B) Size comparison of the 20mL UCD β-shell (top) and the 10mL UCD β-shell (bottom). (C) The 10mL UCD β-shell with the filling catheter extended through the shell.*

4.2.5.3 Acute *in vivo* pig studies – filling studies (December 2018)

Following the results of the July 2018 acute study, the β-shell was redesigned to a 10mL volume (Figure 4.5C).

- The protocol was modified accordingly for the new volume and RGF2 gel formulation.
- The mixing protocol remained unchanged
- The shell was implanted laparoscopically to the anterior abdominal wall and filled using a new technique; a filling catheter extending through the length of the shell (Figure 4.5 C) fills the shell from the bottom to the top sequentially in 5x2mL infusions.
- Visualisation of the filling was also via 2D x-ray images using a C-arm.

4.2.6 *In vivo* small animal (rat) studies

Rat studies were carried out using wistar rats by the DRIVE partner Abiel in Sicily, Italy. The aim of these studies was to:

a) evaluate biocompatibility, of the natHA/PFD emulgel and
b) determine viability and efficacy of transplanted islets.

The protocol and formulation outlined and developed in Section 4.2.2, and detailed in the results in Section 4.3.1, was modified for this study. The final natHA/PFD emulgel (rat-βgel) formulation used for this study was based on GF7 and the final formulation is detailed in Table 4.7.

Table 4.7 *Formulation of the rat-β gel used for the small animal in vivo studies.*

Component	Concentration
NatHA	0.615% w/v
PFD (as emulsion)	28% w/v
Islets (Wistar rats)	12,500 IEQ/mL
VEGF microspheres	6.25mg/mL
Oxygenation	yes

This study was performed using a miniaturized β-shell developed by DRIVE partner UCD (Figure 4.6A). Each shell was filled with 160µL of the rat-βgel formulation from Table 4.7. Shells were implanted to the omentum, fixed against the ventral wall with sutures, in 12 STZ-induced diabetic wistar rats. Controls consisted of 3 healthy rats (no STZ induced diabetes) and 4 STZ induced diabetic rats, without any shell/islet implantations. The glycaemic response of the control healthy and STZ induced rats was tested for 4 weeks after implantation.

The glycaemic response of the implanted rats was tested for 4 weeks after implantation. Following this 4 non-responder rats were euthanized and their implants were removed. The remaining 6 responder and 2 non-responder rats were maintained for a further 4 weeks. 2 non-responder and 2 of the responder rats were euthanized at this point and had their implants removed. The remaining 4 responder rats then had their implants removed and were maintained for a final 4 weeks.

According to the IPGTT protocol, rats were fasted for 8 h and baseline blood glucose was measured, before administering 2g/kg glucose. Blood glucose was then tested at 30/60/120/180 min following administration.

Before terminating the experiment, a CT scan of the shell was taken (Figure 4.6B).

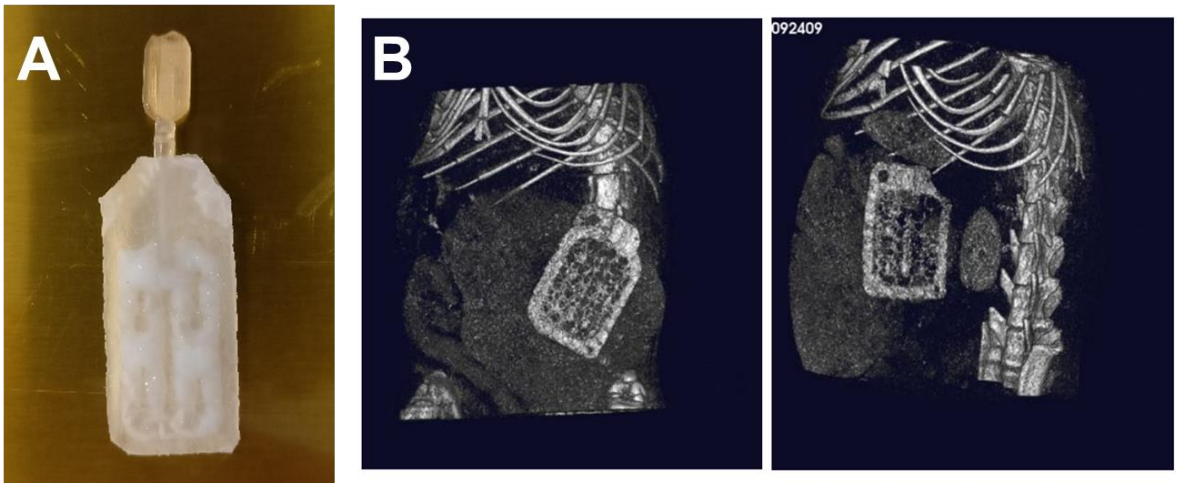

Figure *4.6* *The UCD β-shell designed for small animal studies. (A) A sample β-shell filled with natHA/PFD emulgel. The rounded plastic top is used to seal the shell with a small plug and can be snapped off, leaving the plug intact. (B) CT scanner images showing the implanted β-shells in vivo in the rats used in this study.*

The VEGF microspheres used as part of this study were manufactured and provided by DRIVE partner Innocore as aliquots that could be suspended to facilitate their inclusion into the final emulgel. The VEGF microspheres release up to 50% of loaded VEGF for up to 21 days in a sustained manner of 150ng/day (Figure 4.7).

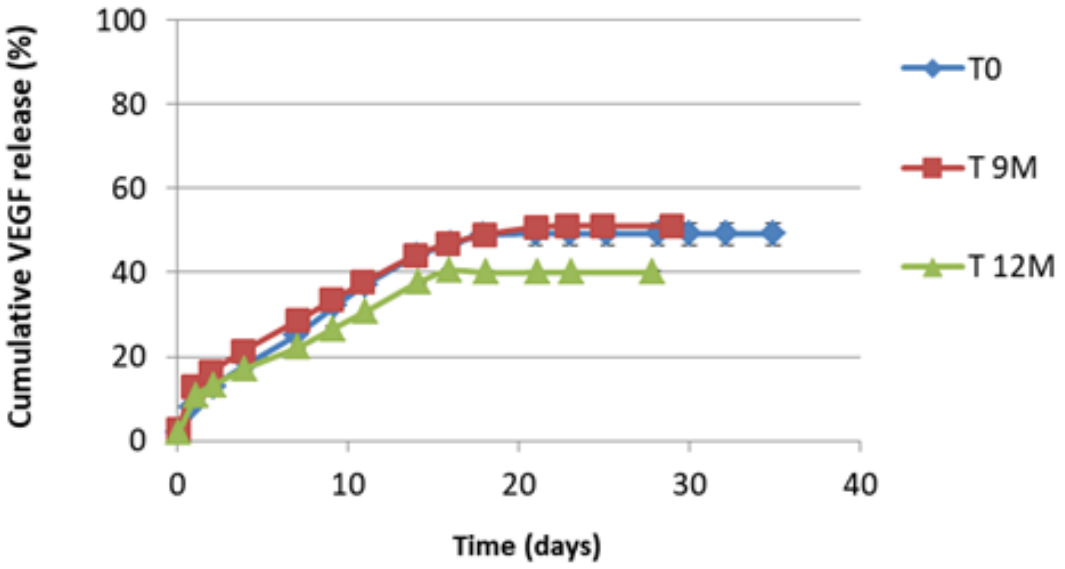

Figure *4.7* *The cumulative release profile of the VEGF from the VEGF microspheres. The VEGF microspheres used in the small animal in vivo studies show a sustained release of up to 50% of loaded VEGF for up to 21 days at a rate of 150ng/day. The release profile is stable after freezer storage for up to 9 months, with a decrease in released VEGF at 12 months. Figure provided by Innocore.*

4.3 Results

4.3.1 Protocol development for the preparation of the natHA/PFD emulgel

One of the primary outputs from this project was the development of the kit and protocol to facilitate the transfer of the β-gel formulation to the different partners. Following the development of the base protocol it was modified and transferred on seven occasions to 4 different partners and collaborators to facilitate the biocompatibility and *in* vitro and *in* vivo work as part of the DRIVE project.

In this results section we have broken down and explained the different components of one of the final protocols provided as part of the DRIVE project for future *in vitro* human islet work. The full protocol as provided to the DRIVE partner is also provided as Appendix 2 for readability.

4.3.1.1 Kit contents and preparative actions

For the purpose of record keeping, the first page of the protocol detailed the name of the study, and included a section to fill in the operator and date. The first page also detailed the materials, the form they were provided in, and the partners that provided them. (Figure 4.8)

β-Gel preparation procedure for Human Islet study – UCD Shell

To be completed by operator;

Operator & date.	Initials: ⌊_⌋⌊_⌋⌊_⌋ Paraph: _____ ⌊_⌋⌊_⌋/⌊_⌋⌊_⌋/⌊_⌋⌊_⌋ (dd/mm/yy)

Kit contents

Materials

Material description	Supplied by :	Delivery date (dd/mm/yy)
Component A • 1x 1.2mL Native-HA (1.845% w/v) solution in CMRL-1066 in capped 3mL syringe (**Syringe A**) Lot No:	RCSI	⌊_⌋⌊_⌋/⌊_⌋⌊_⌋/⌊_⌋⌊_⌋
Component B • 1x 2mL PFD emulsion (66.78% w/v) in 15mL Falcon tube (**Component B**) Lot No:	RCSI	⌊_⌋⌊_⌋/⌊_⌋⌊_⌋/⌊_⌋⌊_⌋
8x UCD β-shells + 8x Shell caps • Lot no: Jan2019	UCD	⌊_⌋⌊_⌋/⌊_⌋⌊_⌋/⌊_⌋⌊_⌋

Figure 4.8 *Page 1: Allowing the recording of operator details and details the materials included in the kit.*

The second page of the protocol details the consumables provided as part of the kit (Figure 4.9), including the brand, expiry date and QC status of the consumables provided. The QC status refers to whether or not they have undergone sufficient QC for use as a medicinal product. In these preliminary studies the consumables obtained from manufacturers e.g. BD needles and syringes, conform to the QC and sterilisation standards detailed in EMA guidelines.

Consumables

Consumable description	Product/ lot reference	Expiry date (dd/mm/yy)	QC status
8x 3mL Syringe Luer-lok tip BD	8140553 CAV04	30/04/23	Conform ☐ Not conform ☐ R&D use only ☐
4x Combifix Adapter (female-female luer)	18L02A8151	01/10/23	Conform ☐ Not conform ☐ R&D use only ☐
5x 18G 1.2x40mm needles BD Microlance	1807 05	01/01/23	Conform ☐ Not conform ☐ R&D use only ☐
3x Luer lock cap UHS (RED)	32362354	01/08/19	Conform ☐ Not conform ☐ R&D use only ☐

Figure 4.9 *Page 2: Detailing the plastic consumables included in the kit for traceability and to minimise variability.*

Preparative actions are also detailed on the second page (Figure 4.10). These actions include ensuring that the correct facilities are available e.g. laminar flow hood, oxygen is available, and materials or components that cannot be included in the kit are available e.g. media, islets.

Preparative actions

A Laminar Air Flow is available	yes / no
CMRL 1066 complete medium available (40% serum)	yes / no
8400 IEQ available	_____ IEQ used
Syringe pump available	yes / no
Oxygenation syringe available	yes / no
Qosina Oxyview oxygen flow meter	yes / no
BSL Y-mixer available	yes / no
UCD bracket available	yes / no
All materials stored at 4°C before use	yes / no
VEGF microspheres available (stored at -20°C)	yes / no

Figure 4.10 *Page 2: Detailing preparative actions for equipment or components not included in the kit*

4.3.1.2 Preparing the oxygenated natHA/PFD emulgel

The first part of the gel preparation protocol details mixing the materials provided in the kit i.e. the natHA and the PFD emulsion, to give the emulgel that will be further diluted to the final concentration (Figure 4.11). These steps detail the initial mixing method to mix the materials and refer to the oxygenation protocol, detailed separately in an Appendix to the protocol. A larger volume than needed is prepared, to give sufficient overage when accounting for loss of volume during the mixing process. Critical process parameters include final volumes used, vortexing time and emulgel mixing time. The base formulation of the natHA/PFD emulgel is detailed in Appendix 3.1, and overages are detailed in Appendix 3.2.

Gel Preparation

To prepare β-gel for 4 UCD shells	
1. Vortex **Component B,** the PFD emulsion, for 30 seconds **Confirm Component B selected []**	yes / no Time vortexed : _____
2. Draw 1.5mL PFD emulsion into a 3mL syringe using an 18G needle– **Syringe B**	yes / no PFD emulsion volume :_____ mL
3. Remove the red cap from **Syringe A** and connect it to the female-female luer connector. Fill the air volume of the connector with **Native-HA** from **Syringe A.** **Confirm Syringe A selected []**	yes / no
4. Connect **Syringe B** to the other end of the female-female luer connector.	yes / no
5. Vigorously mix the contents of **Syringe A** into **Syringe B** and then transfer the contents back to **Syringe A.** Repeat this 20-30 times until the mixture appears homogenous and milky.	yes / no Times mixed : _____ Volume **Syringe A** : _____
6. Remove **Syringe B** and the female-female luer connector from **Syringe A.**	yes / no
7. **Oxygenate the emulgel by the oxygenation protocol (Appendix A)**	yes / no
8. Transfer 0.6mL to two fresh syringes: **Syringe C1** and **Syringe C2**	yes / no Volume **Syringe C1** : _____ Volume **Syringe C2** : _____

Figure 4.11 *Page 3: Part 1 of the protocol, detailing the first mixing steps and referencing the oxygenation protocol included as an appendix.*

4.3.1.3 Incorporating islets/VEGF microspheres into the natHA/PFD emulgel

This stage of the protocol (Figure 4.12) includes steps to prepare the final emulgel with and without VEGF microspheres as this particular protocol was intended for use in a comparative study with and without VEGF. The oxygenated natHA/PFD emulgel intermediate is mixed with the islets with or without VEGF to give the final emulgel, using the same mixing technique as has been used previously. Critical process parameters include final volumes, and emulgel mixing times. The overages and calculations for the IEQ, VEGF, and final emulgel volumes are detailed in Appendix 3.3.

To prepare β-Gel WITH VEGF	
15. Prepare a suspension of 25mg/mL VEGF microspheres in the eppendorf using complete media.	yes / no
16. Resuspend 2400 IEQ in 0.2mL of the VEGF microsphere suspension and transfer to a 3mL syringe – **Syringe D2**	yes / no _____ IEQ used Volume of islet suspension : _____
17. Connect **Syringe C2** to a female-female luer connector and fill the air volume with oxygenated emulgel.	yes / no
18. Connect **Syringe D2** to the female-female luer connector with **Syringe C2.**	yes / no
19. First mix the contents of **Syringe C2** into **Syringe D2** and then transfer the contents back to **Syringe C2.** Repeat this 15-20 times, until homogenous +5 additional mixes.	yes / no Times mixed : _____
20. Disconnect the empty **Syringe D2** from the female-female luer.	yes / no Volume **Syringe C1** : _____
21. **Syringe C2** can now be used to fill 2 UCD shells **(Appendix B).**	yes / no

Figure 4.12 *Page 3-4: Part 2 of protocol, after oxygenation. The oxygenated emulgel is mixed and diluted with the human islet/VEGF microsphere suspension to the final emulgel that can be used to fill the shells.*

4.3.1.4 The oxygenation method protocol

This protocol is provided as a separate Appendix A to the full protocol (Figure 4.13) for ease of presentation and as the method employed is separate to the rest of the protocol. The protocol is not intended for a specific syringe pump but is intended for the specific consumables provided for the kit i.e. the BD 3mL luer-lok syringe diameter is 8.66mm. An image of the setup is provided and the protocol refers to the image for guidance when setting up the protocol to ensure it is easily translated. The oxygen flow rate was standardised at 1.5L/min using a flow rate meter, to ensure consistency between operators, and the pump rate was set at a sufficiently low rate to ensure oxygenation. These parameters were selected based on the parameters used for oxygenation data from Chapter 2.

Appendix A:

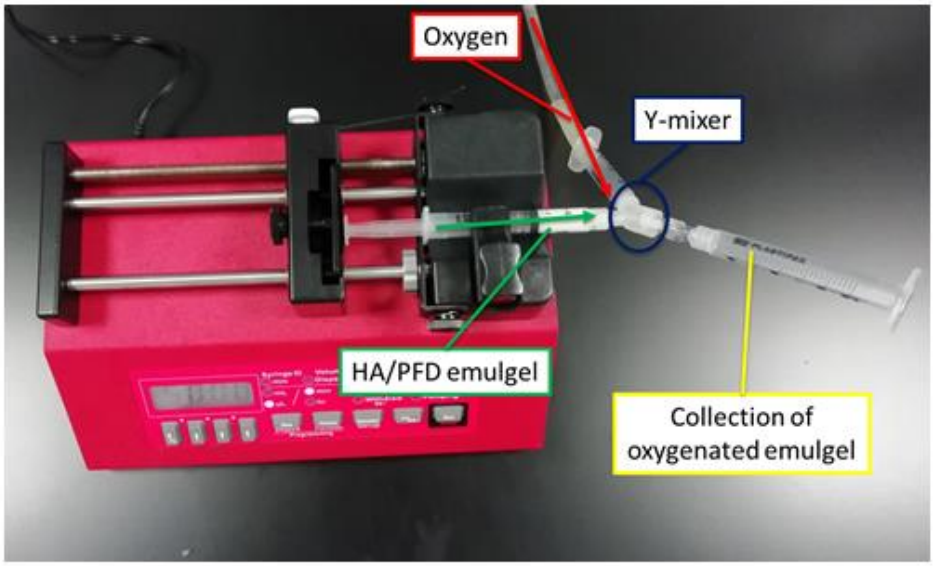

Oxygenation Method	
1. **Syringe A** is connected to the BSL Y-mixer.	yes / no
2. The oxygen supply is connected to the other input of the Y-mixer using a 3mL syringe and tubing	yes / no
3. Remove the plunger from a 3mL syringe (**Syringe C**). Connect a female-female luer to **Syringe C** and connect it to the static mixer opposite the oxygen supply and **Syringe A.**	yes / no
4. Setup in the syringe pump as shown in the image above. **Syringe C** should be angled upwards to prevent the gel from flowing out.	yes / no
5. Set the syringe diameter to 8.66mm on the syringe pump.	yes / no
6. Set the oxygen flow to 1.5L/min	yes / no
7. Start the syringe pump at a rate of 50uL/minute until the content of the syringe is depleted or you have collected ~1.5mL of oxygenated gel (minimum).	yes / no
8. Replace plunger in **Syringe C** and remove remaining air gaps. Return to Step 8 of Gel Preparation protocol.	yes / no

Figure 4.13 *Appendix A: Oxygenation protocol for the natHA/PFD emulgel detailed clearly and with an image to aid in setup.*

4.3.1.5 Additional protocols and appendices

Finally, additional protocols were amended to the final protocol, based on the study they were being provided for. The additional protocols were specific for the study being performed, and may or may not be included depending on the study e.g. testing new protocols to fill the large shells for large animal studies. In this protocol the methods to fill the small animal UCD shells was provided as Appendix B (Figure 4.14) as the operators of this protocol were not familiar with their configuration.

Appendix B:

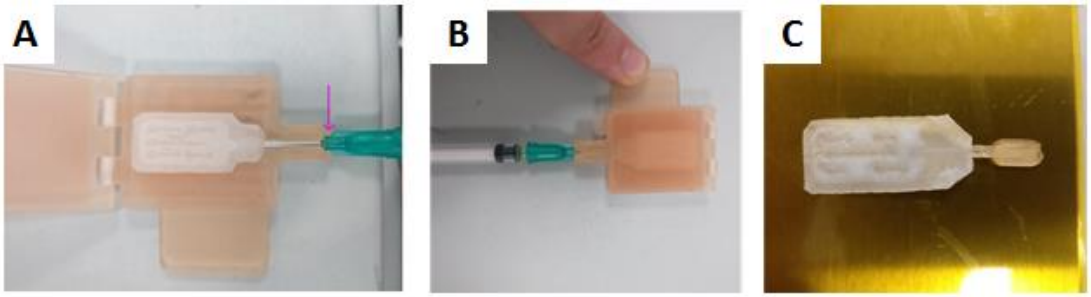

Filling the UCD Shell	
1. Set the syringe diameter to 8.66mm on the syringe pump.	yes / no
2. Set the volume to be dispensed to 0.2mL	yes / no
3. Attach a UCD shell to **Syringe C.**	yes / no
4. Attach the UCD bracket to the green luer lock and close. The bracket should grip the green luer as indicated by the arrow in Figure A	yes / no
5. Start the syringe pump at a rate of 100uL/minute	yes / no
6. When the 0.2mL of gel has been dispensed ensure the syringe pump has stopped.	yes / no
7. Detach the shell from the **Syringe C**, and remove the filling tip. Seal the inlet port with the UCD Shell cap. Once sealed the tab can be snapped off (Figure C).	yes / no
8. Place in a 6 well plate with enough media to cover the body of the shell (6mL).	yes / no
9. Mix the gel in **Syringe C** 5-10 times before filling another shell.	yes / no
10. Repeat Steps 2 – 9 for each shell.	

Figure 4.14 *Appendix B: An example additional appendix that was provided; this protocol details the filling protocol used for the UCD immunoisolating shell.*

4.3.2 *In vitro* biocompatibility

Biocompatibility of the natHA/PFD emulgel was confirmed according to the ISO standards, DIN EN ISO 10993-5: 2009, using MTS to measure proliferation. Figure 4.15 shows the results as a % of proliferation of the HACaT cell line vs the control that was negative for cytotoxicity.

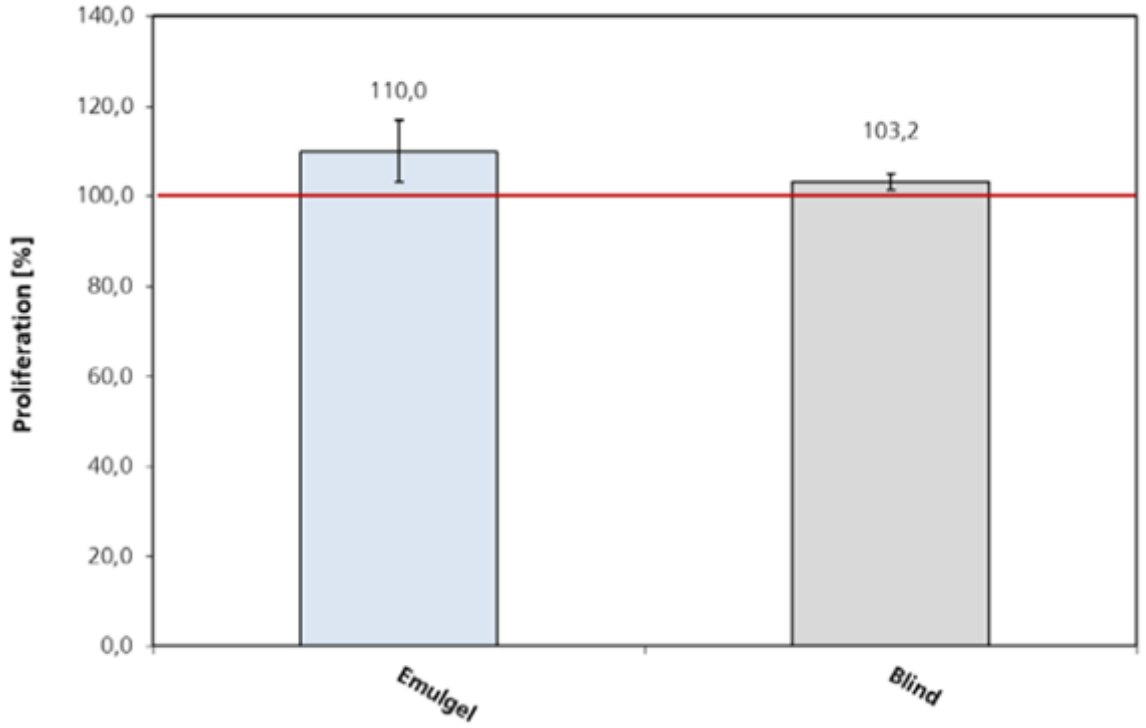

Figure 4.15 *The cytotoxic potential of the natHA/PFD emulgel and a blind control. Proliferation of 81-100% relative to the control is non-cytotoxic. Blind control refers to cells treated by an extract from an extraction vessel with no material.*

4.3.3 Pilot *in vitro* human islet biocompatibility studies

90-100% of islet yield was retained in the free floating (FF) Low/High control islets. However islets encapsulated in CMRL Low/High saw a 50-60% drop in islet yield. In contrast, islets encapsulated in HA gel Low/High showed similar islet yield to the FFI control. Reactive oxygen species (ROS) production (Figure 4.16B) by islets encapsulated in the HA gel Low/High was similar or lower than ROS production in FFI. ROS production in CMRL Low/High was increased. Islet fragmentation was highest in the CMRL Low/High with islet viability similar across all groups, and islets encapsulated in HA gel Low/High having the highest viability.

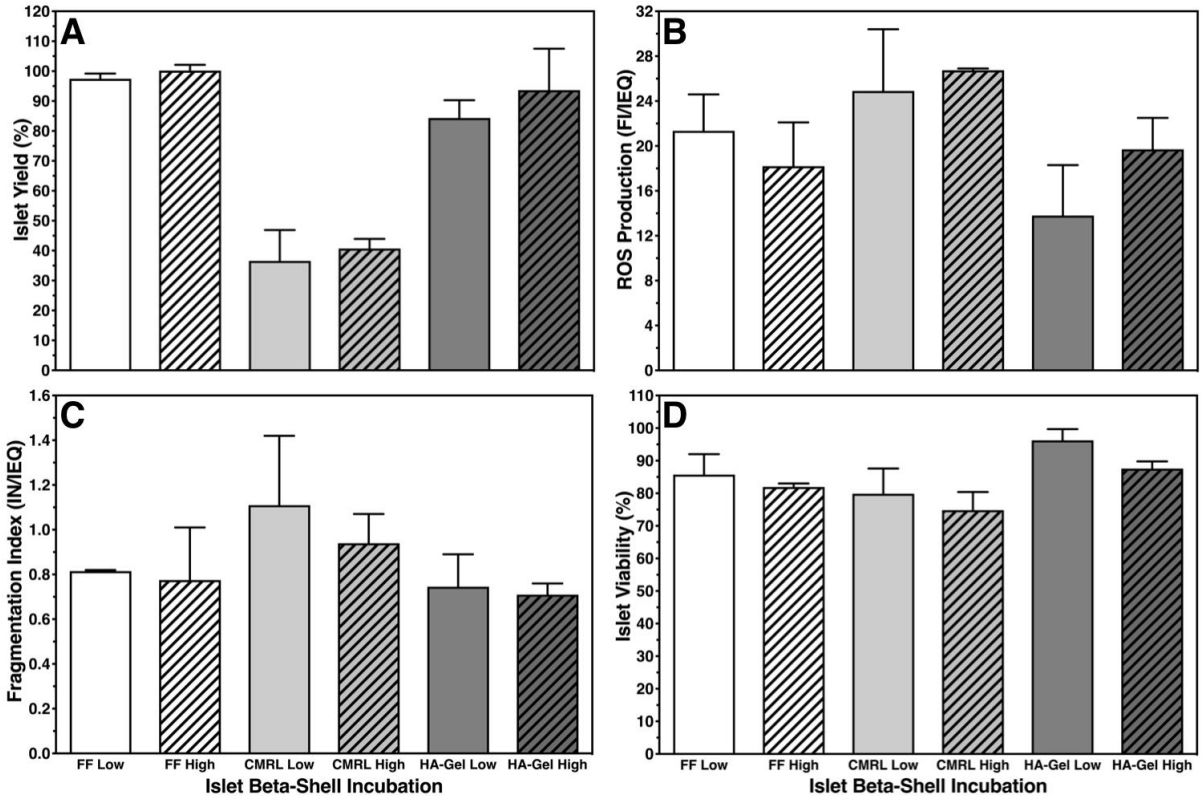

Figure 4.16 *Effect of differences in media (CMRL) against the natHA/PFD emulgel (HA-gel) as a vehicle/ECM for islets encapsulated in an immunoisolating shell and islet density (low and high) on (A) yield (%), (B) intra-islet ROS production (FI/IEQ), (C) fragmentation index (IN/IEQ), and (D) viability (%) of isolated human islets cultured for 4 – 5 days inside the devices. FF islets at a low and high density were used as a control.*

Islet morphology of the FF and encapsulated islets showed that islets encapsulated in the CMRL-1066 Low/High were highly fragmented and re-aggregated (Figure 4.17C and 4.17D). In contrast the islets encapsulated in HA-gel Low/High (Figure 4.17E and 4.17F) maintained the characteristic round morphology seen pre-culture and in the free-floating islets (Figure 4.17A and 4.17B).

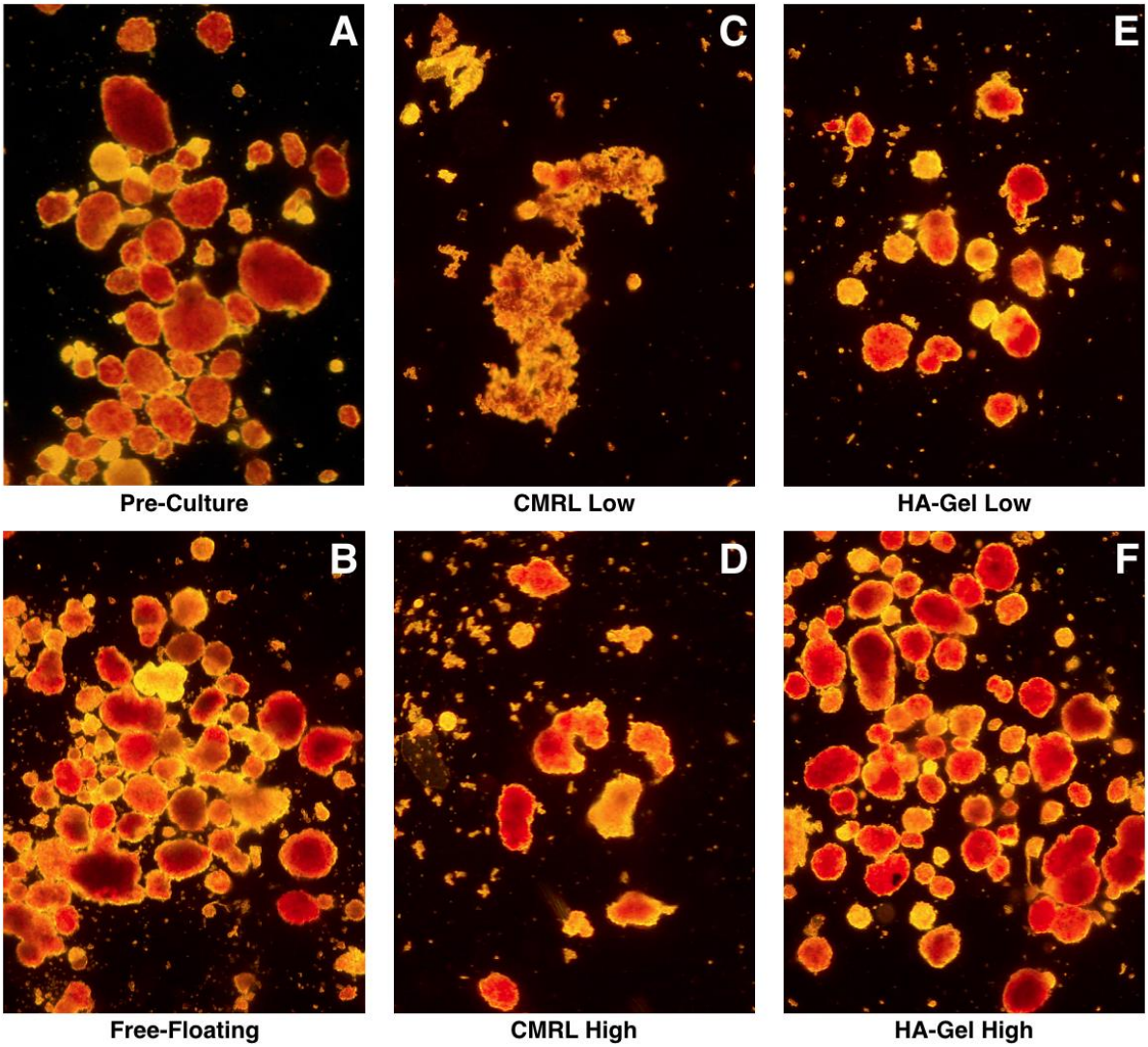

Figure 4.17 *Islets after 5 day culture in different encapsulation conditions. (A) Free-floating pre-culture, (B) Free-floating after culture, (C, D) encapsulation in β-shells filled with CMRL-1066 media, (E, F) encapsulation in β-shells filled with pre-oxygenated natHA/PFD emulgel (HA-gel).*

4.3.4 Acute *in vivo* filling study– July 2018

4.3.4.1 Radiopaque gel for July 2018 acute pig study

The rheogram of the steady state flow sweep of RGF1 and GF6 (Figure 4.18) showed that comparable resting viscosities were achieved; RGF1 shows resting viscosity of ~50 Pa.s, similar to the resting viscosity of GF6 of ~42 Pa.s. However RGF1 did not show the same degree of shear thinning as the GF6.

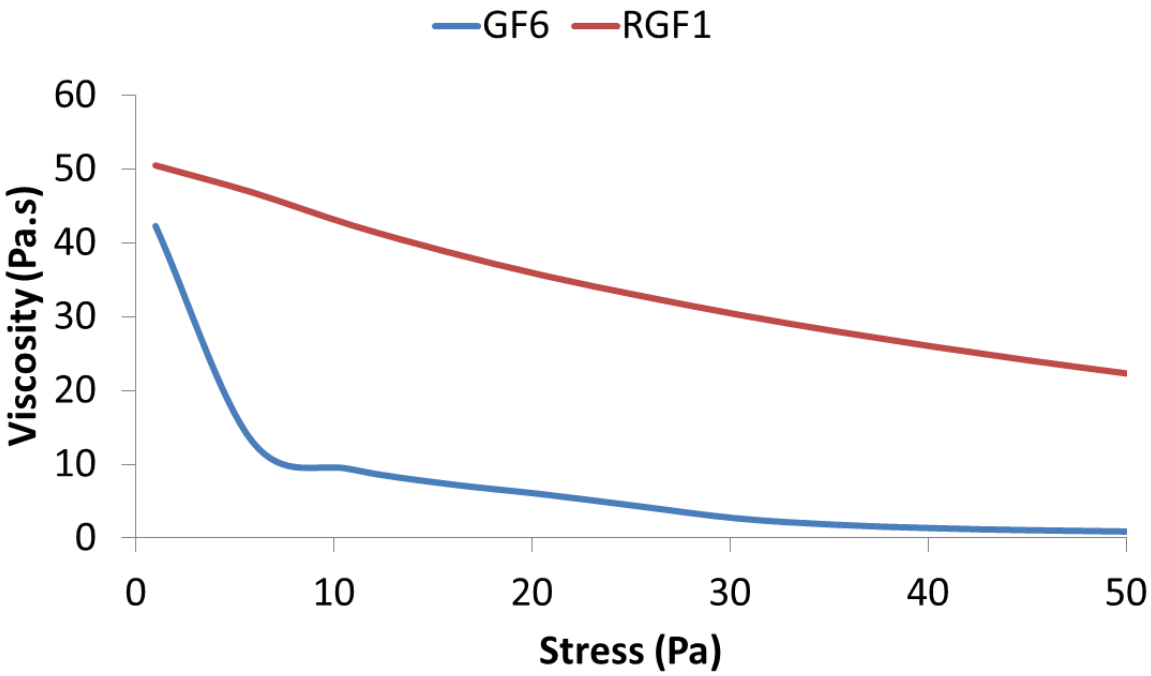

Figure 4.18 *Rheogram of steady state flow from 1-50 Pa of GF6 and RGF1, showing the resting viscosity of the RGF1is in an acceptable range compared to GF6. Data shown representative of the norm. (n=3)*

Figure 4.19 shows a microCT image from the preliminary RGF1 filling study. RGF1 was filled into the shell into Shell A and was clearly radiopaque through the β-shell material using microCT. Shell B was used as a control shell and an empty shell appears differently than a shell filled with the radiopaque gel.

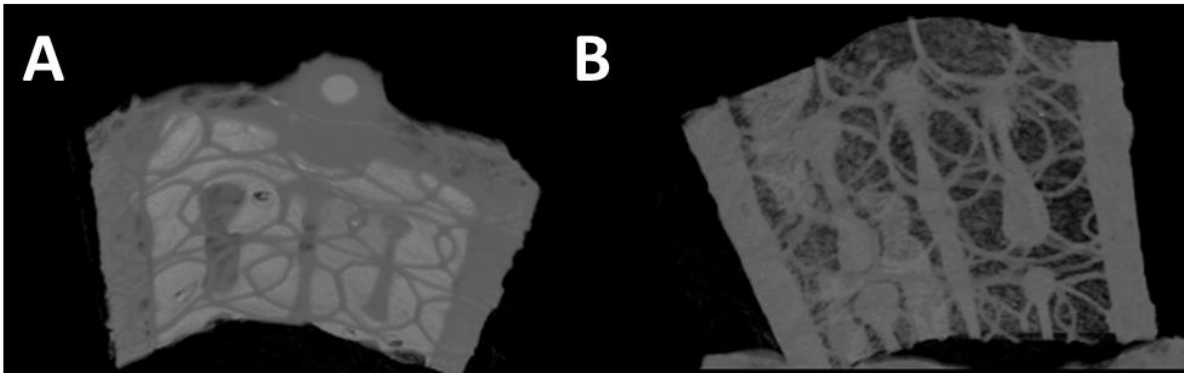

Figure 4.19 *MicroCT scans of (A) RGF1 filled into a 160µL β-shell and (B) an empty 160µL β-shell.*

4.3.4.2 Filling study – July 2018

2D x-ray was used to visualise the filling of the 20mL β-shells *in situ* in order to identify any issues with the filling protocol. Figure 4.20 below shows the filling of the first Shell, Shell A, with RGF1. It shows that as the shell was filling it was not spreading throughout the shell, and as the gel continued to be delivered to the shell it eventually burst just below the filling port, outlined in red.

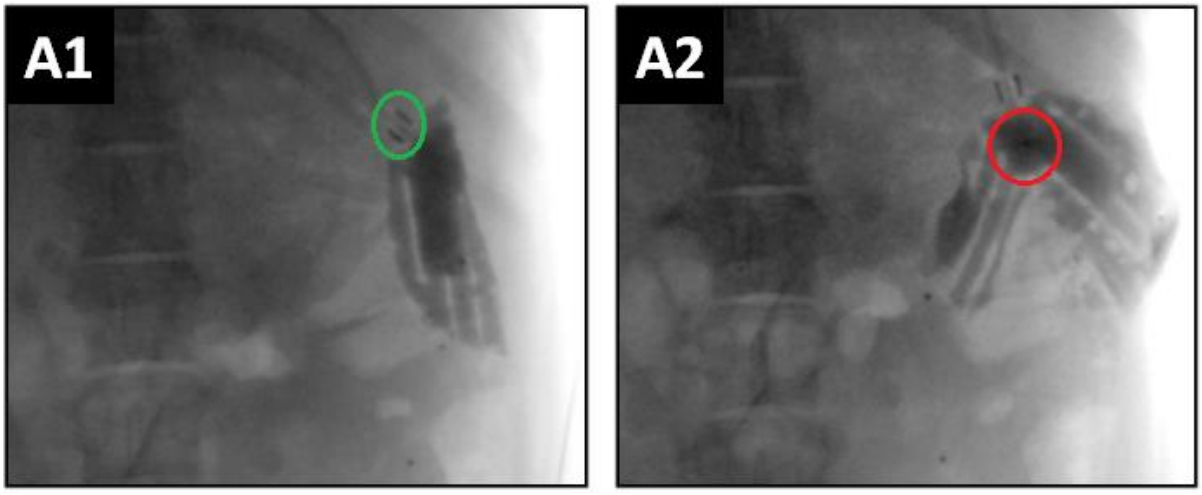

Figure 4.20 *CT scan images of Shell A taken while filling with RGF1, where A1 was taken before A2. (A1) – Shows the filling port outlined in green, with minimal spread of gel through the shell; the darker area below the filling port indicates the gel is accumulating. (A2) – Shows the gel spreading minimally through the shell and the black spot outlined in red shows where the shell has burst.*

Figure 4.21 below shows the filling of the second Shell, Shell B, with RGF1 showing the gel spreading through the shell. A number of small air bubbles can be seen clearly throughout the shell in addition to larger air bubbles and darker areas where the gel has accumulated.

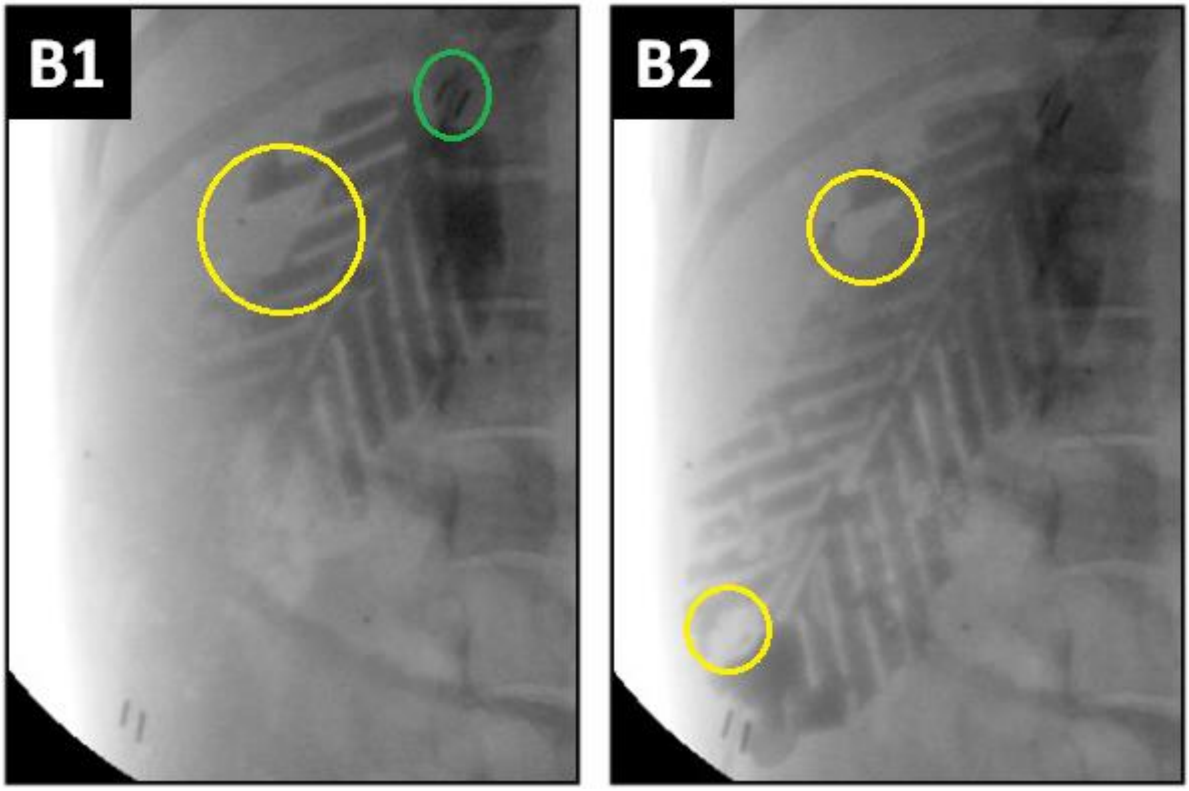

Figure 4.21 *CT scan images of Shell B taken while filling with RGF1, where A1 was taken before A2. (B1) – Shows the filling port outlined in green, and a section of the shell that has not filled outlined in yellow. (B2) – Shows the gel spreading throughout the shell, with multiple air bubbles and the largest air bubbles outlined in yellow.*

4.3.5 Acute *in vivo* filling study - December 2018

4.3.5.1 Radiopaque gel for December 2018 acute pig study

The rheogram of the steady state flow sweep of RGF2 and GF7 (Figure 4.22) showed comparable resting viscosities; RGF2 and GF7 both show a resting viscosity of ~4 Pa.s. RGF2 does not show the same degree of shear thinning under relatively low shear stress as GF7.

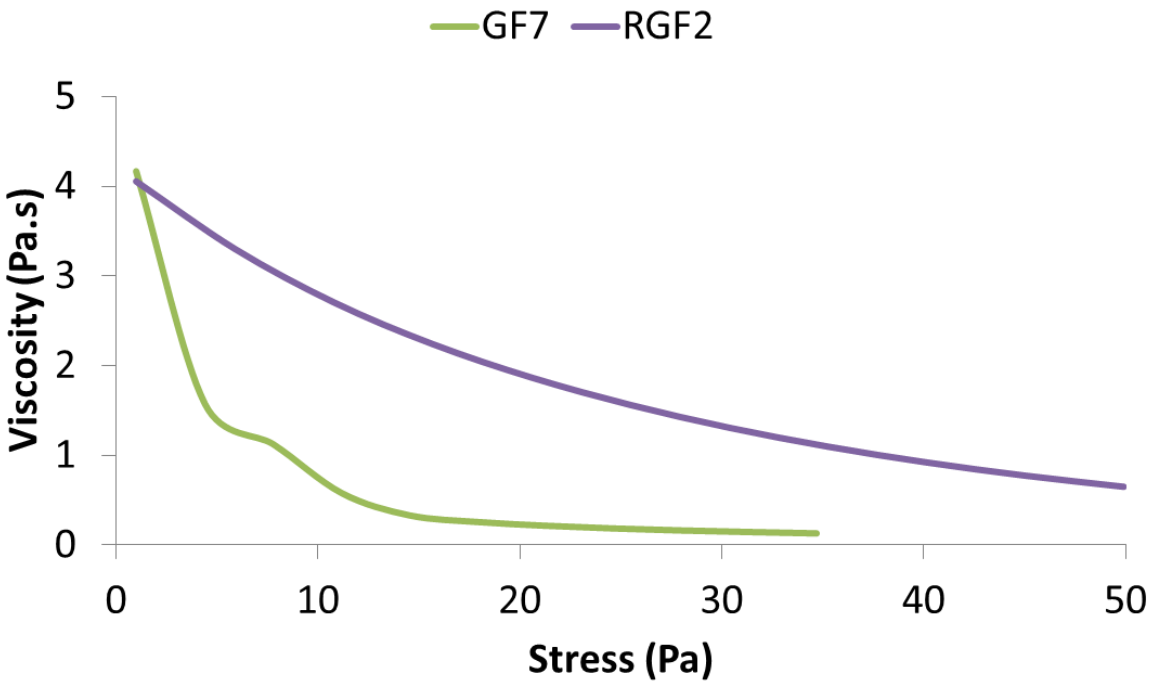

Figure 4.22 *Rheogram of steady state flow from 1-35 Pa of GF7 and 1-50 Ps of RGF2 showing the resting viscosity of RGF2 matches the resting viscosity of GF7. Data shown representative of the norm. (n=3)*

4.3.5.2 Filling study – December 2018

The 2D x-rays in Figure 4.23 below shows the filling of the first shell of the December acute pig study with RGF2. The new protocol combined with the reduced viscosity of RGF2 allowed for successful filling with minimal accumulation or bubbles. Figure 4.24 shows a second shell successfully filled with RGF2 using the new filling protocol.

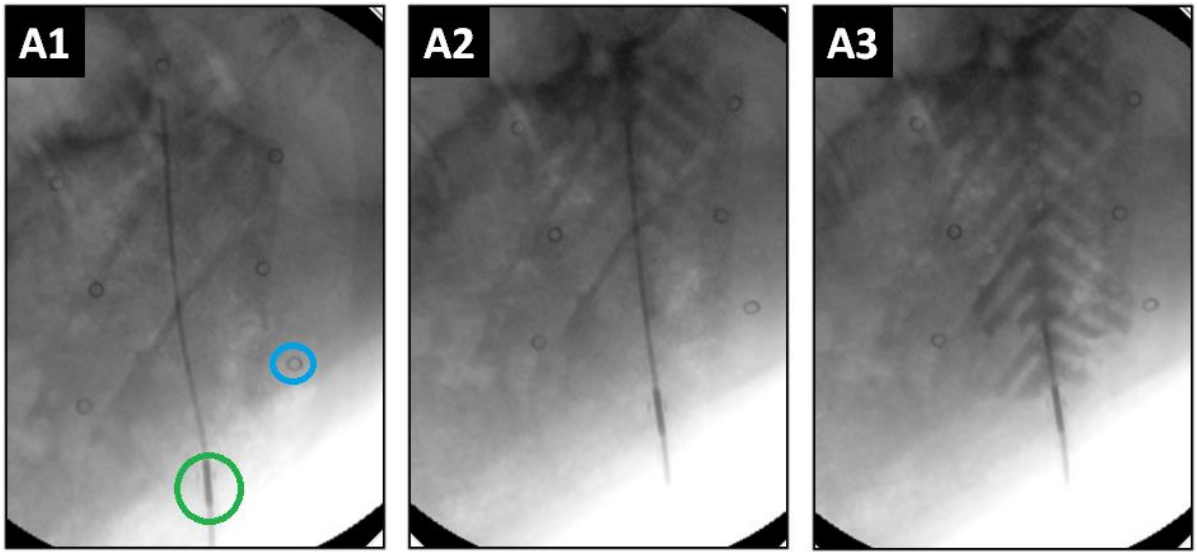

Figure 4.23 *2D x-ray images of Shell A taken while filling with RGF2, with A1, A2 and A3 images taken sequentially. (A1) – Shows the filling port outlined in green, and the dark line is a filling catheter extending through the length of the shell. Radiopaque suture rings are outlined in blue. (A2) – Shows the gel filling into the base of the shell and withdrawal of the catheter to facilitate filling. (A3) – Shows the shell filling completely and withdrawal of the filling catheter from the shell.*

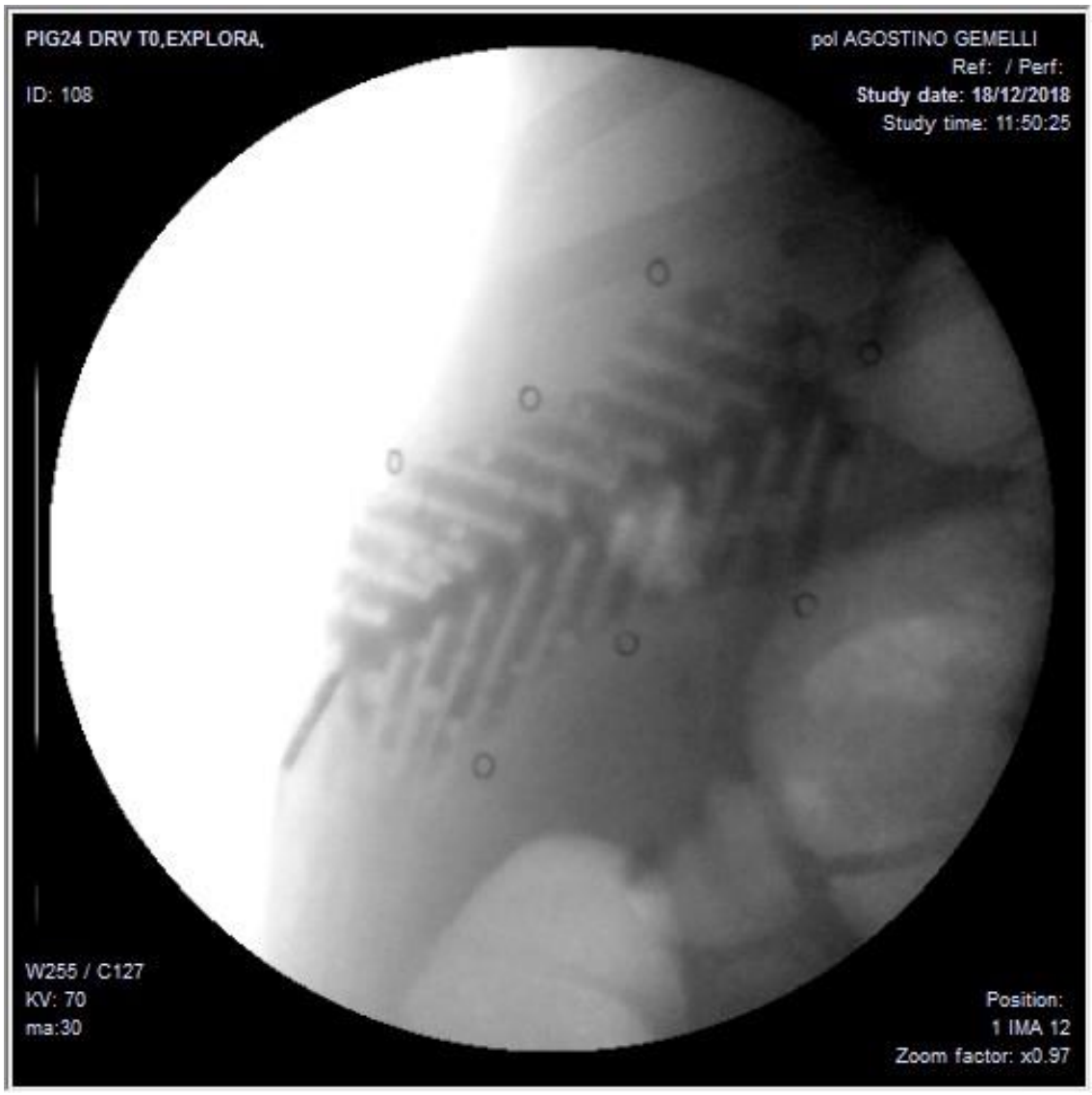

Figure 4.24 *2D x-ray image of a filled 10mL β-shell. RGF2 can be seen as the darker areas throughout the lighter shell structure.*

4.3.6 Small animal *in vivo* efficacy of the rat-βgel and β-shell

4.3.6.1 Small animal in vivo controls

Two control groups of animals were run alongside the experimental group for the first 4 weeks to show blood glucose response of healthy animals and to ensure that the STZ induction of diabetes was successful (Figure 4.25).

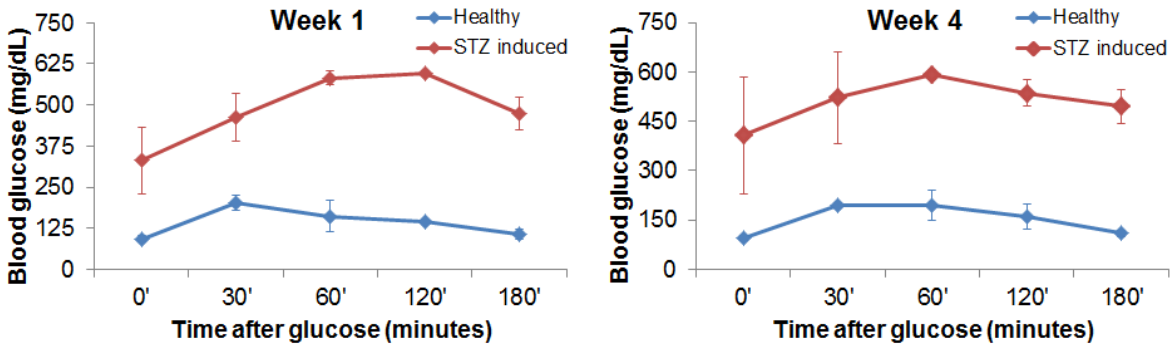

Figure 4.25 *Blood glucose levels of the control rats (healthy and STZ induced diabetes) for up to 4 weeks. At 0 min the healthy rats shows normoglycaemic blood glucose levels just before the administrations of the glucose challenge. Blood glucose levels rise for up to 30 min and show a drop in blood glucose by 60 min at both time-points (n=3). At 0 min the STZ induced diabetic rats show hyper glycaemia before the administration of the blood glucose challenge and at all time-points after (n=4)*

4.3.6.2 Small animal in vivo efficacy

Of 12 STZ induced diabetic wistar rats implanted with βgel, 6 (50%) showed a therapeutic response to a glucose challenge (Figure 4.26). The responder rats show a resting blood glucose below 125mg/dL, with an increase in blood glucose for up to 120 min after glucose administration to an average peak of ~350mg/dL, and a subsequent decrease in blood glucose by 180 min to ~270mg/dL, indicating insulin production in response to the increase in blood glucose concentration. The non-responders show a higher fasting blood glucose of >250mg/dL at all time-points and hyperglycemia for up to 3 h after administering glucose at all time-points.

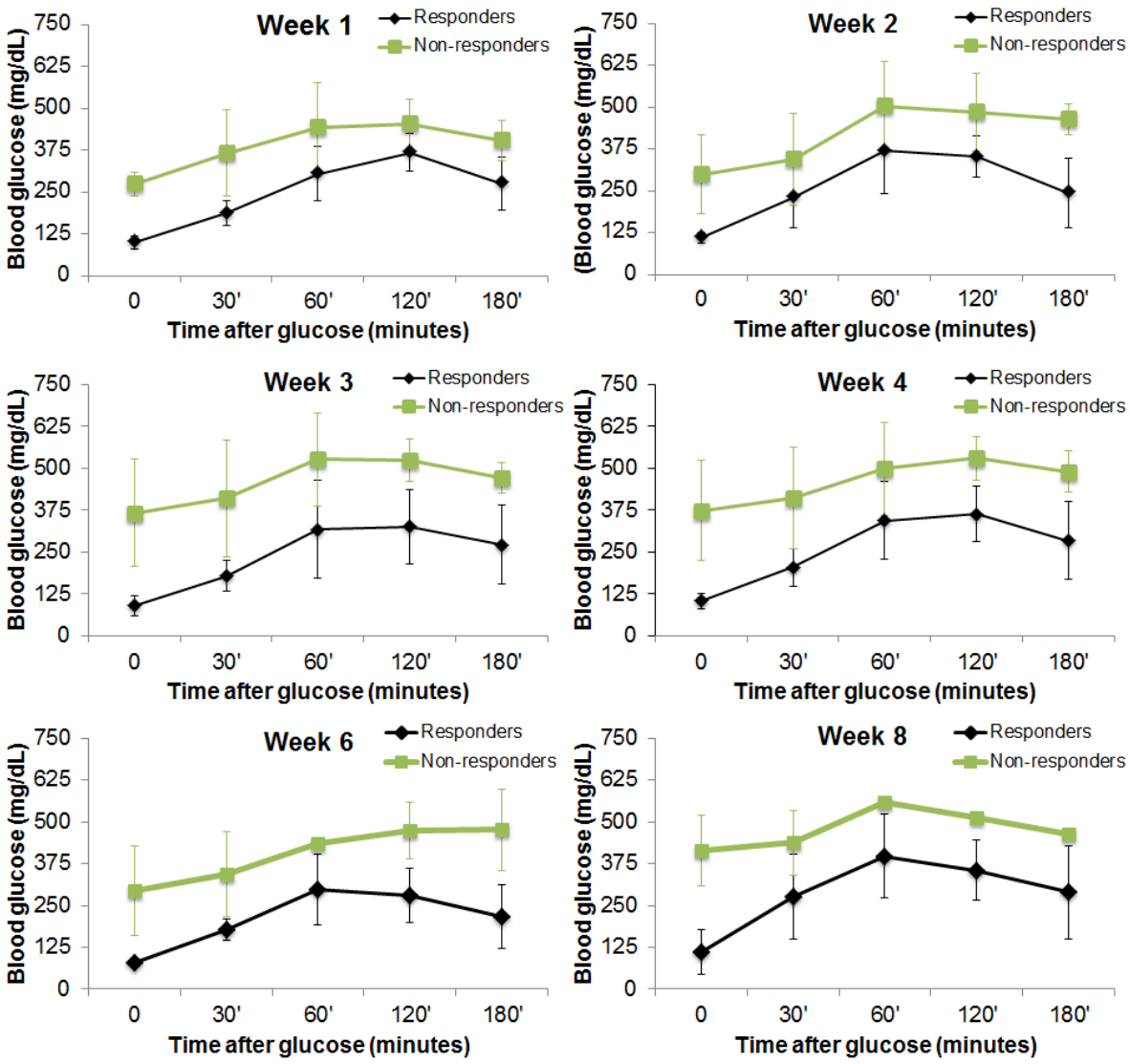

Figure 4.26 *Blood glucose levels of the responder and non-responder rats for up to 8 weeks. A fasting blood glucose <135mg/dL was used to indicate a response to the treatment. At 0 min the responder rats show normoglycaemic blood glucose levels just before the administrations of the glucose challenge. Blood glucose levels rise for up to 120 min and show a drop in blood glucose by 180 min (n=6) at all time-points. The non-responder rats show higher blood glucose at 0 min and hyperglycaemia for up to 180 min after glucose administration, n=6 Week 1-4 and n=2 Week 6+8.*

4.3.6.3 Small animal in vivo follow-up after Week 8

Following completion of the 8 week *in vivo* efficacy study, the implants were removed from four animals and these animals were maintained for a further 4 weeks to test their glycemic response. Three of the animals showed a worsened diabetic state with blood glucose levels remaining higher at 180 min following removal of the implant (Figure 4.27).

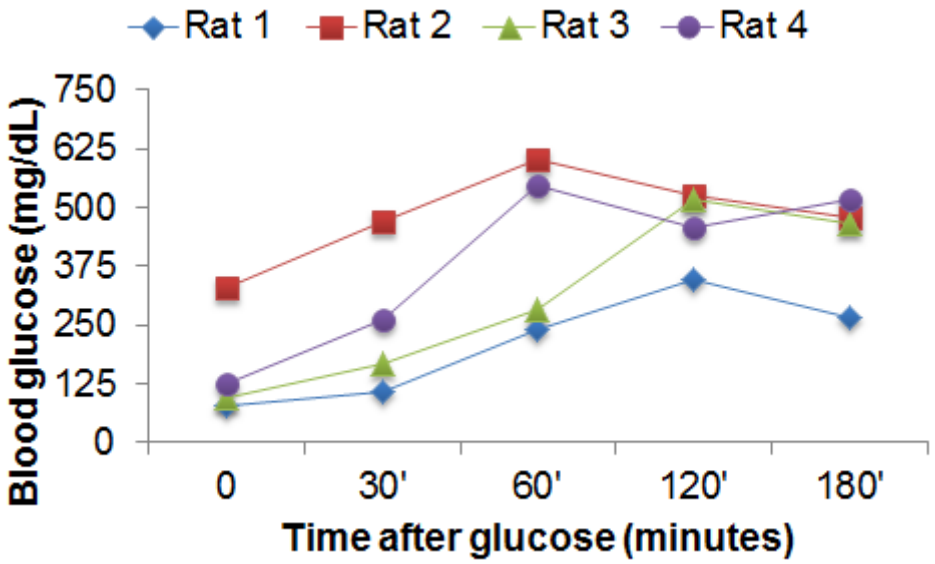

Figure 4.27 *Blood glucose levels of four of the responder rats 4 weeks following removal of the implanted devices. A blood glucose response similar to the response seen prior to the removal of the devices was used to indicate if there was a worsened diabetic state. At 0 min three rats show normoglycaemic blood levels (<135mg/dL) but two of these show higher blood glucose levels over the 180 min following blood glucose administration following the removal of the implant.*

The non-responders were euthanized at Week 4 and implants were removed for histological examination. Implants were removed from the responders at Week 8 for histological analysis. Figure 4.28 shows a gross examination of some of the implanted devices *in situ* before removal.

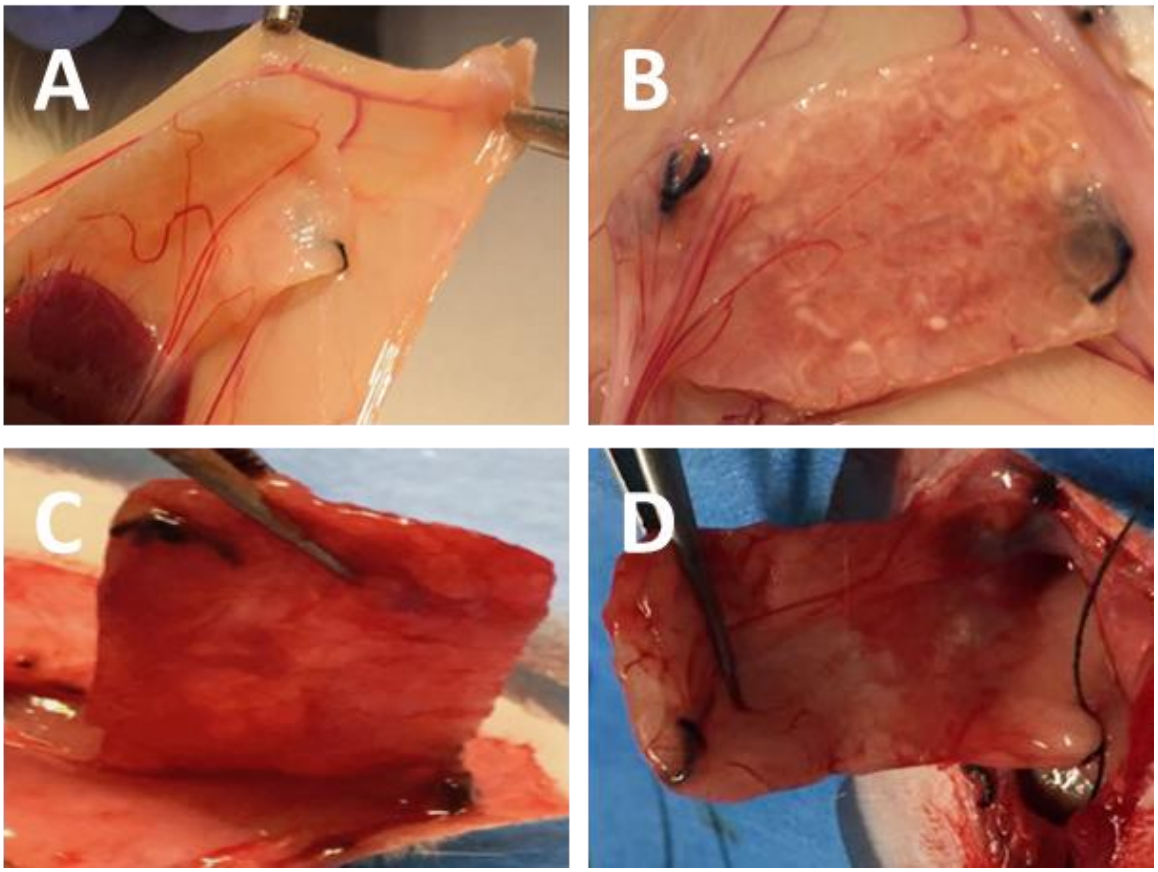

Figure 4.28 *An example of the gross examination of four of the implanted devices. The implanted devices show some tissue integration by growth of tissue on the devices, but both the non-responders (A+B) and the responders (C+D) are poorly vascularized, showing a small number of blood vessels on the surface of the shell.*

4.4 Discussion

The primary aim of this Chapter was to commence the process development and pre-clinical testing of the DRIVE technology required for clinical translation. A key challenge to overcome was the complexity of combining the multiple components of the DRIVE product: the natHA/PFD emulgel, the β-shell medical device, viable pancreatic islets, and the VEGF eluting microspheres. This required the integration of activities across multiple partners, and was achieved through the central co-ordination and development of processes and protocols at RCSI, which were then transferred to the pre-clinical testing sites. This chapter outlines these activities, as well as the results of preliminary pre-clinical *in vitro* and *in vivo studies* on the natHA/PFD emulgel system.

Protocols were designed to be an all-in-one traceable document, providing clear instructions for the reconstitution of the final product. In accordance with the requirements of ICH Q8 [Guidelines for preparing a Common Technical Document (CTD)] protocols were titled according to a standardised template to document the study they were intended for with traceability of all relevant factors such as operators, materials, processes included.

Under GMP guidelines, a reconstitution activity is only included if it can be justified that these steps cannot be performed as part of the manufacturing process. Reconstitution steps in our protocols can all be justified at this early stage of process development. Resuspension of the PFD emulsion and mixing into the natHA gel can be justified as the PFD emulsion is stable for up to 2 months but must be vortexed before use. Oxygenation must be performed on the day of the protocol to maximise oxygen levels in the emulgel. The incorporation of pancreatic islets and/or VEGF eluting microspheres must also be performed on site. The VEGF eluting microspheres must be kept dry until use to ensure a prolonged release of VEGF in the device. However it is important to acknowledge that further along the process pathway it is likely that further development of this system would be undertaken to reduce the current complexity of reconstitution.

In parallel to preparing protocols, a materials kit was also provided. The natHA was provided as a pre-filled syringe. In the early stages of testing, using the sterile lyophilised natHA gel was advantageous, as it facilitated flexibility in changing the

formulation of the final emulgel i.e. the different HA concentrations in GF6 and GF7. After the formulation was 'locked' it was decided for Contipro to almost exclusively supply moist heat sterilised, pre-filled syringes of natHA which ensured that manipulations were performed almost exclusively by a single operator. Reducing the number of manipulations reduces the risk of contamination. In addition, based on guidance from Contipro, pre-filled syringes are stable for at least one year under appropriate storage conditions. The one exception to this decision was the gel provided for human islet studies, where it was specifically requested that natHA be hydrated in CMRL-1066 media to minimise risks associated with losing human islets to poor nutrient diffusion. This procedure was performed using sterile components under aseptic conditions by a single operator, to minimise contamination risk.

For pre-clinical studies, PFD emulsion was provided as an aseptically compounded product in a sterile container. Using the EMA decision tree for aqueous products, it was clear that terminal sterilisation methods were not suitable for the PFD emulsion, as emulsion instability at high temperatures is well established in the literature (335-337). Filtration through a microbial retentive filter was also not feasible as the droplet size of the emulsion ranges above the 0.2µm pore size of the filters. Therefore for pre-clinical studies aseptic processing was deemed the most appropriate approach. In addition to aseptic preparation, the sonication step in the emulsion preparation may also act to lower the bioburden of the emulsion. The effect of sonication as a means of sterilisation in the food industry (338) and for hip implants (339) has been studied previously. Although it is not sufficient to use sonication alone, in combination with aseptic processing with sterile components it is likely to act to further reduce the bioburden of the PFD emulsion.

Protocol and kits were prepared and sent to a combination of six different collaborators and contractors for eleven different studies. Prior to commencing each study, the protocol was sent to confirm understanding. In addition, two training videos, one of the gel reconstitution and one of the oxygenation process, were prepared and two staff exchanges took place to facilitate protocol transfer. Out of the eleven studies to date, there has been one problem requiring intervention during processing. This related to the protocol not specifying whether the PBS to be used should be with or without Ca^{2+} and Mg^{2+}. This highlighted an oversight in not including PBS in kits where PBS was used to prepare the VEGF eluting microsphere

suspension, as it was assumed PBS would be available at all sites. There have been no infections caused by the natHA/PFD emulgel components in any of these studies. Successful transfer of protocols has enabled important preliminary pre-clinical data being obtained. Taking into consideration the complexity of the formulation and the protocol, the limited validation of the process, and the variety of successful applications of the protocol, the process development and transfer of the protocol has been successful.

To date there have been two studies to evaluate the biocompatibility of the natHA/PFD emulgel formulation. *In vitro* biocompatibility testing was performed at the Fraunhofer Institute IgB using GF6, in accordance with DIN EN ISO 10993-5: 2009, which contained the highest concentration of natHA in the emulgels studied. This formulation when compared to a negative for cytotoxicity control shows proliferation above 100% indicating that the extract is non-cytotoxic. Testing with human islets further confirmed biocompatibility of the natHA/PFD emulgel with indications that inclusion of the emulgel actually improves islet viability, compared to islets encapsulated without emulgel. Islet morphology was seen to be unchanged after being encapsulated in the β-shell with the emulgel. These preliminary results are positive, and future studies aim to investigate the function of encapsulated human islets by GSIS compared to free-floating counterparts.

The components and excipients of this formulation, namely the natHA, PFD and lipoid emulsifier, were selected because of their biocompatibility. NatHA is a naturally occurring polymer in the body and has been used as a cosmetic, as an active component, and as a biomaterial for many years (230-232, 340, 341), PFD is an FDA approved PFC which has previously seen use as a blood substitute (190, 217, 218), and phospholipid emulsifiers such as Lipoid E80 are well established for having excellent biocompatibility (342). While there has been research investigating the use of hydrogels supplemented with PFD emulsions for islet encapsulation (291, 343), and research investigating the use of HA as either a crosslinked hydrogel supplemented with collagen (113) or in combination as an alginate-HA hydrogel (110) we are not aware of any work to date that has investigated the use of a non-crosslinked HA hydrogel with or without an oxygen carrier (PFD) emulsion for islet encapsulation. Validation of the formulation biocompatibility *in vitro* justified this

formulation as the lead formulation for the project, and allowed us to move forward with *in vivo* studies.

The purpose of the two acute pig studies in July 2018 and December 2018 was to investigate filling of the β-shell with natHA/PFD emulgel, prior to chronic biocompatibility and efficacy studies. In order to visualise the filling process *in vivo* a radiopaque gel was formulated, which would enable monitoring of the filling process and any leakage of the gel.

For the July 2018 study, a radiopaque gel consisting of natHA and Visipaque® was developed (RGF1). The resting viscosity of GF6 was targeted, as this was the lead emulgel at this time. A minimum concentration of 21% w/w Visipaque was aimed for based on work done previously in the Duffy-Kelly group (333). Pilot work to validate visualisation of RGF1 filling a miniature 160µL via CR microCT was successful. Subsequently the process was scaled up for a 20mL β-shell.

In the first large animal study RGF1 was shown to be radiopaque and filling of the shell was readily visualised, however filling was not successful. In the first shell, the gel accumulated just below the filling port and did not spread adequately through the shell. As a result, the shell burst under the pressure of the accumulated gel. While filling was more successful with the second shell with the gel able to spread through the majority of the shells volume, a number of large air bubbles were visible through the shells structure, and accumulations of the gel were seen near the top and bottom of the shell.

While the July 2018 study demonstrated that a radiopaque gel had been successfully formulated the problems with filling also prompted a redesign of the β-shell, and a reformulation of the natHA/PFD emulgel. The accumulation that led to the shell bursting was a result of two factors; the high viscosity of the RGF1 and the design of the shell. The high viscosity of the RGF1 limited the spread of the gel through the β-shell structure. In addition, the design of the initial β-shell left the reservoir area just below the filling port weaker than the rest of the shell. Without internal structure to hold the shell to a specific thickness the gel could not enter and spread effectively from that part of the shell. These factors combined led to gel accumulation and eventual bursting of the shell at its weakest point and pointed to an important failure mode that required a re-design.

The aim of the December 2018 study was to investigate the filling of the reformulated hydrogel. For this study there were two important changes: the reformulation of the gel to RGF2 and the redesign of a stronger more structurally sound shell. Alongside the July 2018 filling study, the experiment looking at PI morphology after mixing experiment, from Chapter 3, Section 3.2.6.3 was performed. From this, we identified that to ensure islet morphology was retained after mixing we needed to reformulate the natHA/PFD emulgel to have lower viscosity. For this purpose we formulated GF7, and RGF2 was formulated to be a radiopaque gel that mimicked its resting viscosity. The UCD β-shell was scaled down to a 10mL volume design, and a filling catheter was introduced to facilitate the new filling protocol. Additionally, suture rings were integrated into the UCD β-shell design to facilitate suturing the β-shell in place to prevent it moving during and after the filling procedure.

Figure 4.23 and Figure 4.24 both show successful filling of the of the 10mL UCD β-shells. The combination of a new, improved filling protocol, a smaller more structurally robust shell design, and the reformulated lower viscosity gel facilitated a successful outcome

Small animal *in vivo* efficacy studies showed only a 50% response rate over 8 weeks. Four non-responders were euthanized and implants removed for histological examination after 4 weeks. Initial indications from these four non-responders were that there was only partial integration of the β-shell in to the tissue and there appeared to be poor vascularisation of implants. Based on this observation we hypothesised that a primary cause for non-response was the partial integration and poor vascularisation of the device. This was shown not to be the case however as the responder rats' implants showed a similarly poor vascularisation after 8 weeks, indicating that poor vascularisation over the first 4 weeks was not the cause of non-response. The control STZ induced diabetic rats (Figure 4.25) indicated that the STZ induction was successful. To further rule out the possibility that the responder rats were not diabetic, we saw that three of the four responder rats blood glucose levels at 180 min were higher following the removal of the implant, suggesting that the implant was improving the STZ induced diabetic state. Future histology work aims to investigate the contents of the retrieved β-shells to try to identify and explain the differences seen between the responder and non-responder groups.

For all 12 experimental rats, diabetes was induced by STZ before implantation of the device. For responder rats the mean fasting blood glucose (FBG) of the 6 responder rats was <135mg/dL at all the reported time-points, and individually one rat showed FBG levels >135mg/dL at week 3 (144mg/dL) and week 4 (149mg/dL).The mean PPBG after 120 min of the responder rats was >300mg/dL at all time-points. In the majority of the rats at all time-points blood glucose levels increased for up to 120 min and only started to decrease at 180 min, but remained >250mg/dL glucose (Figure 4.25). This indicates that the encapsulated islets are alive and functionally responding to increased blood glucose.

A 2010 paper by *Wang et al* (344) on the estimation of normal range of blood glucose in rats estimates that the criteria for normal or diabetic blood glucose levels in rats is similar to that seen in humans, with the upper limits for FBG in non-diabetic rats being ~135mg/dL and PPBG after 120 min being 180-190mg/dL. We confirmed these results with the healthy animal control group, showing <135mg/dL FBG and <180mg/dL PPBG. The FBG of the responder rats is in line with these results showing an improvement to the rats' diabetes, however the PPBG levels are above the non-diabetic levels within the reported times. The low FBG levels but high PPBG levels may indicate that there is a is a lag time to the response greater than is seen in endogenous insulin production or that there is not enough insulin produced to lower PPBG to normal levels in the measured timeframe.

Previous studies have shown cases of PPBG lowering to <180mg/dL within the 120 min limits in both a TheraCyte® device in STZ induced rats for up to 6 months (135) and in alginate macroencapsulated islets in STZ induced primates (112). This may suggest that glucose diffusion to the islets, increasing the time to GSIS, and insulin diffusion out of the shell, reducing systemic blood glucose response, is impeded by the therapy; the natHA/PFD emulgel and the shell. In Chapter 3 we discussed the potential issues with diffusion and the natHA/PFD emulgel which may be contributing to the lag seen in the therapy. The UCD β-shell may also be contributing to this by providing a further barrier to diffusion. The immunoisolating barrier is a 50-60µm thickness semi-permeable barrier and the shell is then further modified with a "rope-coiled" macroporous layer on the outside. This layer improves the shell structure and vascularisation of the device, but also covers the diffusion surface, limiting the surface area of diffusion and acting as an additional barrier to diffusion. It is also

possible that islet density is affecting the viability and function of encapsulated islets. Future histological analysis of the implanted β-shells and encapsulated islets will provide additional insight. However overall, this data is very positive, with results indicating that the natHA/PFD emulgel is biocompatible with the encapsulated islets.

Successful development and transfer of the protocols facilitated all *in vitro* and *in vivo* work in this Chapter. The *in vitro* studies showed biocompatibility of the natHA/PFD emulgel using both an ISO validated method with a cell line and with primary human islets. The successful scale-up of the natHA/PFD emulgel formulation, and formulation of appropriate radiopaque gel analogues enabled successful *in vivo* filling tests in a large animal model. These *in vivo* filling tests informed the reformulation of natHA/PFD emulgel to a lower viscosity, to improve filling and improve islet morphology as outlined in Chapter 3. The filling tests also identified problems in the design of the β-shell macroencapsulation device and informed a redesign to a more durable and structurally stable device. The preliminary *in vivo rat* results showed the potential efficacy of the rat-βgel and β-shell system in reversing diabetes in a small animal model. These results will form the basis for the future pre-clinical studies needed to translate the project to the clinic and first-in-man trials.

Chapter 5

Thesis Discussion

5.1 Overview

DM is a global disease, with a high prevalence and incidence worldwide. T1D is characterised by β-cell auto-immunity and the subsequent destruction of the insulin producing cells in the pancreas. Although T1D is the less prevalent of the two primary types of DM, the morbidity and mortality associated with T1D, combined with the substantial economic cost have made it a major public health issue that has attracted a great deal of interest for research into the treatment and prevention of the disease. One area of interest in the treatment of T1D has been the development of a system known as the bio-artificial pancreas. This three part system would consist of donor human islets, a biocompatible ECM to house them, and a semi-permeable immunoisolating shell to prevent graft rejection without the need for systemic immunosuppression.

Over the course of this thesis an oxygen carrier functionalised hydrogel, the natHA/PFD emulgel, has been formulated to act as a biomaterial ECM. In addition, processes and protocols were developed to support to transfer of materials and formulation to multiple sites to begin pre-clinical *in vitro* and *in vivo* testing. To date these studies have shown that the emulgel is biocompatible, both to ISO validated standards and with primary human islets, and the efficacy of the biomaterial has been shown in an *in vivo* small animal model. A means of assessing the filling of the hydrogel into shells *in situ* in a large animal model was also developed using a radiopaque hydrogel. These experiments mark the beginning of the extensive pre-clinical data required for translation of this project from the bench to bedside, but ultimately will inform all future work related to the clinical translation of the natHA/PFD emulgel as part of the DRIVE bio-artificial pancreas.

5.2 Thesis results discussion

5.2.1 Selection and formulation of the PFD emulsion

It has been well established that ensuring sufficient oxygen supply to the cells and tissues of the body is required for their function and survival. When formulating the functionalised biomaterial for this thesis we aimed to improve the oxygen supply to encapsulated cells, primarily aiming to supply cells in the time after encapsulation, to support their viability in the stressful period immediately following transplantation.

For this purpose we investigated PFCs, focusing on PFD and F6H8 based on their history of use in the preservation of donor pancreata, indicating biocompatibility. As the lead biomaterial, hyaluronic acid, was a hydrophilic material it was necessary to prepare the hydrophobic PFCs as an emulsion, to ensure they were homogenously incorporated into the material. Initially based on a paper by *Sanchez et al (246)*, the PFC emulsions were prepared by homogenisation. These emulsions showed relatively large, micro-sized droplets and were unstable, making them unsuitable for use. Sonicated emulsions were prepared using the same formulation but this method achieved smaller droplets sizes, and stability that extended for 3 weeks for the F6H8 emulsion and up to 2 months for the PFD emulsion.

Oxygen release profiles of the PFC emulsions were subsequently assessed, with pure PFCs and PBS used as a control. In theory PFCs have a higher solubility for oxygen than PBS, and therefore determining the time it took for oxygen to sustainably release to atmospheric levels after loading with oxygen would assist in identifying a lead PFC. It was observed that PFCs alone actually show a rapid release of loaded oxygen within a few hours, less than the PBS control, indicating that the oxygen diffusion coefficient of the PFCs was also higher. In contrast, when prepared as emulsions both PFCs gave a sustained and prolonged release of oxygen for up to 70-80 h. From these oxygen release profiles it was evident that the inclusion of the PFCs into the emulsion greatly improved the overall oxygen that could be loaded into a liquid volume. This was a positive result; however the data obtained from the oxygen release profiles has a number of limitations. Primarily, the oxygen release profiles alone did not identify a lead PFC, as both appeared equal when comparing the profiles of pure PFCs and PFC emulsions. Ultimately the PFD emulsion was selected based on its longer history of use with pancreatic tissue and its inclusion in a previously FDA approved product (199) increasing the ease of translation. Secondly, the oxygen release profiles gave us an indication of the increased oxygen capacity of the emulsions, but did not give us any indication of what would happen when pancreatic islets, cells with a high oxygen demand, were actively consuming the loaded oxygen. Finally, these oxygen release profiles did not show us properties that were seen only when the emulsions were incorporated into the gels; the effect on viscosity and the rheological properties of the functionalised hydrogels, and the effect on improved oxygen loading seen with natHA based gels.

5.2.2 HA-TA/PFD hydrogel

Having selected the PFD emulsion, the first hydrogels investigated were the HA-TA based hydrogels. Existing in a liquid state before crosslinking, HA-TA represented a promising option as it could be easily combined with the PFD emulsion, delivered to an immunoisolating shell via a catheter and crosslinked *in situ*. It was also shown that the HA-TA/PFD solution could be easily loaded with oxygen by bubbling 99.5% purity oxygen through the liquid. However numerous challenges soon became apparent with this approach.

The first challenge of the HA-TA formulation was the inclusion of H_2O_2 as a crosslinking agent. As outlined in Chapter 3 the cytotoxicity of H_2O_2 to the MIN6 cell line is established in the literature, however the degree of sensitivity observed was higher than anticipated resulting in a need to identify an alternative *in vitro* model. A primary rat pancreatic islet model was selected, which was felt to be more representative of the *in vivo* scenario. This model indicated there was a substantial decrease in the amount of insulin being released by the encapsulated islets when compared with a FFI control which led to an investigation of insulin diffusion through the gel. By investigating the insulin diffusion it was identified that the HA-TA based hydrogels were retarding the diffusion of insulin substantially and ultimately were not suitable for use as the functionalised biomaterial for this thesis.

5.2.3 natHA/PFD emulgel

The natHA/PFD emulgel was one of the two functionalised biomaterials that were investigated following the diffusion results obtained from the HA-TA based hydrogels. NatHA was selected as its biocompatibility is well established, and as a highly viscous liquid without a chemically crosslinked hydrogel matrix the same diffusion issues as the HA-TA hydrogels should not occur.

Due to time constraints associated with the work outlined in Chapter 4, the natHA/PFD emulgel was formulated and assessed on an iterative basis. GF6 was the first natHA/PFD emulgel formulated and tested, and the material and oxygen storage properties were very promising. It was sent to Fraunhofer IGB and shown to be biocompatible *in vitro* according to DIN EN ISO 10993-5: 2009 standards. Following this positive result, the first large animal model filling study was performed

in July 2018 with the RGF1 radiopaque hydrogel, at the same time that the INS-1E cell line was being established for *in vitro* testing.

The poor filling results and bursting of the shells from the July 2018 filling study indicated a need to reformulate the natHA/PFD emulgel. In addition we also wanted to investigate the effect of the mixing protocol on the morphology of encapsulated islets. It was shown that PIs encapsulated in 1.5% w/v natHA caused the breakdown of encapsulated PIs. This informed the reformulation of the natHA/PFD emulgel, as it was possible to determine a viscosity limit of ~2-6 Pa.s that the formulation should meet; a tighter range than the <40 Pa.s of the GF6 emulgel. GF7 was formulation of choice, with a lower resting viscosity than the 1.5% w/v natHA. The December 2018 filling study was performed with the RGF2 radiopaque hydrogel, which exhibited comparable viscosity to GF7and was successful.

This confirmed GF7 as the lead formulation, and *in vitro* human islet work followed this. Preliminary human islet experiments indicated that the emulgel was biocompatible with the human islets. Subsequent to this INS-1E *in vitro* experiments (Chapter 3) and small animal *in vivo* work (Chapter 4) were performed simultaneously and interestingly provided conflicting results. Results from in INS-1E experiments indicated that the natHA/PFD emulgel was not beneficial to encapsulated INS-1E cells in hypoxia, and also had a negative effect on cells in normoxia. In contrast, of the 12 rats implanted with the treatment of natHA/PFD emulgel encapsulated islets in a β-shell, 6 responded to the treatment, showing improved FBG and PPBG.

While *in vitro* results seen with the INS-1E cells would indicate that the natHA/PFD emulgel is not beneficial for encapsulated cells, human islet *in vitro* data and rat *in vivo* data contradicts this. The biocompatibility and efficacy data indicate that this treatment is potentially clinically relevant as a therapy for the treatment of T1D.

5.2.4 MCC/PFD hydrogel

In addition to the natHA/PFD emulgels, the thermoresponsive MCC/PFD hydrogel was also investigated as another potential alternative hydrogel for this project.

Initial oxygen release profile experiments were promising, the MCC/PFD hydrogel showing the most prolonged oxygen release of all the tested hydrogels and

emulgels. However when the rheological properties of the hydrogel were tested they were found to be too unstable to be viable for delivery via a catheter; the sol-gel transition temperature was too close to 37°C, risking a clog during catheter delivery, and its overall stability at 37°C was questionable.

Although the MCC/PFD hydrogel showed some promise as a biomaterial for this project, the success of the natHA/PFD emulgel overshadowed it. Future work could focus on optimising the hydrogel to have a higher and more stable sol-gel temperature.

5.2.5 Translation and protocol development

A key challenge working with the natHA based hydrogels was their high viscosity.

Simple processes such as incorporating the PFD emulsion into the natHA hydrogel were complicated as the emulsion could not be stirred into the hydrogel. Initially, the emulsion was incorporated through a combination of mixing, vortexing, and rolling on a roller. This was a time-consuming and inefficient process that was not translatable or transferable, and also could not be used to mix cells into the emulgel. The development of a method to mix the components through a luer-lok between two syringes, while very simple in principle, changed the process to being an accurate, consistent, and user friendly method of preparing the materials.

The high viscosity of the emulgel also affected oxygenation properties of the material. Low viscosity liquids i.e. PFD emulsion and HA-TA based hydrogels, could be oxygenated by a simple bubbling process. However for natHA, a specific oxygenation protocol had to be developed to ensure the natHA/PFD emulgels were oxygenated sufficiently. This process was more challenging to transfer to partner sites, as it required additional equipment, custom 3D printed consumables, and set-up time.

All of these considerations contributed to the development and transfer of the protocols. The development of these protocols was a deceptively large and integral piece of work, as these protocols formed the basis for a large body of work performed by the DRIVE consortium. This project was primarily responsible for the process development relating to the preparation of the natHA/PFD emulgels. This included collating the input from other partners and calculating the densities and

overages required for different parts of the emulgel e.g. incorporating the VEGF microspheres at the correct concentration, encapsulating islets at the agreed density, and ensuring the protocols outlined the excess that would be required for each experiment. The body of work that went into the process development and protocol development as part of this PhD was substantial, and yet it only represents the very beginnings of the pre-clinical required to translate the natHA/PFD emulgel and the DRIVE project to the clinic.

5.3 Clinical relevance

5.3.1 The challenges with cell models for T1D

While the MIN6 cell line is a well-established cell line for T1D research, it proved to be a very sensitive cell line requiring specific conditions such as low passage numbers and specific confluence ranges to remain glucose responsive. For our purposes, their high sensitivity to low concentrations of H_2O_2 meant they were not suitable for use with HA-TA hydrogels (300), and by the time we were investigating the other hydrogels their passage was too high meaning their glucose response was lost and we were unable to source lower passage numbers.

The INS-1E cell line, however, has been shown to work over a wide range of high passage numbers (277), in contrast to the MIN6 cell line. These cells had their own specific challenges, preferring a specific type of cell culture plastic to ensure optimal growth and function. The INS-1E cells appeared to be useful; having shown good glucose responsiveness following encapsulation in a control natHA hydrogel in normoxia. However looking at the INS-1E results alone indicated that encapsulation in the natHA/PFD emulgel was not beneficial and had a negative effect on their function. This conflicts with other *in vitro* and *in vivo* data obtained, with the natHA/PFD emulgel shown to be biocompatible with another cell line by an ISO validated method, and also biocompatible with primary human islets. We additionally saw in an *in vivo* rat model that it was successful at supporting encapsulated rat islets and improving the FBG and PPBG in 6 of 12 rats. These conflicting results show the importance of not relying on a single *in vitro* cell model and also highlight the challenges of mimicking complex 3D microenvironments in 2D settings.

A primary rat islet model was also established as part of this project. The primary challenge with this model was the limited supply of islets for the considerable time investment required. The density of 5,000 IEQ/mL identified as our translatable volume was difficult to achieve, requiring 6 rats per week to get enough islets to make 1-2 hydrogels. Between harvesting the rat pancreas and isolating encapsulated islets the entire protocol took up to 4-5 h minimum, repeated for 3 days in a row. In retrospect, there were a number of improvements that could have been made to the HA-TA protocol that may have improved the number of hydrogels from a single week of isolations but even then this practice is not cost or time efficient, and is not practical in the long-term.

The issue of scarcity is not limited only to the number of islets that can be isolated. Theoretically, the number of rats available to harvest islets from is unlimited, with cost and ethical concerns being the main limits on using the islets. In contrast, the number of human pancreases available for research is very limited. The supply of human is limited by the number of donor pancreases, and is further limited again by a % of donor pancreases not being suitable for whole pancreas or islet transplantation. It was fortunate therefore that a human pancreas became available at Oxford shortly after GF7 had been finalised as the lead formulation. Further human islet experiments were planned, but this work was unable to come to fruition as human islets were not available.

Developing a translatable cell-model is a challenge that has confronted almost every field of biomedical research. Although the primary islet model is a very useful and translatable model it is limited predominantly by the scarcity of islets. There are a number of groups working on developing unlimited iPSC lines for the treatment of T1D in a bio-artificial pancreas (85, 86), and these lines if achieved would eliminate the problems with scarcity of cells for research while also being the ideal model as they would also be the cells used for treatment.

5.3.2 DRIVE technology as a treatment for T1D

The primary objective of this thesis was to formulate a functionalised biomaterial to support cell viability for clinical applications, with a primary focus on islet encapsulation for diabetes. Ultimately, the primary objective of the DRIVE project was to develop an extravascular macroencapsulation device to act as a bio-artificial

pancreas. In the field of extravascular macroencapsulation, there are currently 3 main leaders in the field: Encaptra®, βair, and the Sernova Cell Pouch System™. All three companies have been in development longer, and all three have already started first-in-man trials.

This raises an important question: is there room in the market for another extravascular macroencapsulation bio-artificial pancreas? The preliminary *in vivo* results from the DRIVE project are promising, but can the technology compete with the existing technologies?

The Encaptra® Drug Delivery system, or the VC-01 product, utilises a proprietary and unlimited insulin producing cell line, overcoming the islet scarcity issue that presented significant challenges to DRIVE (141, 142). However the DRIVE product is flexible, and in the future when iPSC derived β-cells are available, the DRIVE product would be able to utilise those cells. Additionally, the VC-01 product is an immunoisolating device; however the company ViaCyte is also investigating the VC-02 product which aims to improve vascularisation of the encapsulated cells at the cost of the immunoisolation, requiring immunosuppression to prevent graft rejection. If the DRIVE product can maintain its immunoisolating shell, while also addressing vascularisation, it would be in a position to be able to compete with the VC-02 product. Similarly this is also the competitive advantage of the DRIVE product over the Sernova Cell Pouch System™.

The βair device is a novel device which utilises a replenishable O_2 reservoir to oxygenate encapsulated islets, and this is not a claim that the DRIVE product can compete with. However, if the DRIVE product can achieve the same results as the βair device, its main advantage is that it returns insulin production to the patient autonomously, without the need for daily refills of the O_2 reservoir (145).

However, while the bio-artificial pancreas represents an exciting frontier in diabetes treatment, in reality the next step in medical devices for the treatment of diabetes may not require endogenous insulin production at all. The concept of the artificial pancreas, the use of an insulin pump, a CGM device, and an insulin dosing algorithm may be the biggest competition to all macroencapsulation devices. Artificial pancreas products are in early stages, but show greatly improved blood glucose control (49). As CGM devices are improved over time, and the algorithms controlling insulin

dosing advance to become more patient specific or controlled by artificial intelligence, the need for patient input into monitoring blood glucose and administering insulin may be removed entirely. Although an artificial pancreas device will always need to have insulin reservoirs changed, many patients may find this to be an acceptable price to pay to avoid undergoing surgery for the same level of glucose control.

5.4 Future work

The preliminary data obtained throughout the course of this PhD have shown the natHA/PFD emulgel to show significant potential as a component of the macrovascular encapsulation system developed for DRIVE. A number of experiments are needed to complete the data set on the natHA/PFD emulgel and the DRIVE project, and future steps to turn this into a clinical reality would be predominantly focused on completing the pre-clinical work required to assemble a CTD or IND to start moving towards clinical trials.

Based on the work performed in this thesis, a summary of future steps to translate the product to the clinic are:

1. Developing validated sterilisation methods for all intermediates in the DRIVE product: As previously discussed, although efforts had been taken to sterilise components and ensure sterility for *in vitro* and *in vivo* work, validated methods would be required to translate to human trials.
2. Complete *in vitro* human islet testing: An experimental plan to compare human islets with and without VEGF was designed and approved before the end of the DRIVE project and this should be completed.
3. Repeat of rat *in vivo* study: 50% of the treated rats did not respond to treatment. When the samples from the first study have been analysed and the cause of the non-response has been elucidated the study should be repeated. Additionally, a control group of rats treated with rat islets encapsulated in a natHA hydrogel should be added as a suitable control; this will ensure the natHA/PFD emulgel encapsulation is more beneficial than a natHA hydrogel, as was seen in the INS-1E cells.
4. Biocompatibility and efficacy studies in a large animal model: This was planned by the DRIVE consortium, to first perform a biocompatibility study of

the natHA/PFD emulgel in the β-shell and to follow this with a chronic efficacy study.

5. Scale-up manufacture of the natHA/PFD emulgel: During the DRIVE project the protocol to prepare natHA/PFD emulgel was scaled up to a 12mL volume. Further scale-up to a final human sized volume, with a translatable preparation protocol, would be required.
6. Scalable oxygenation method for the natHA/PFD emulgel: The emulgel oxygenation protocol developed as part of this PhD project was designed for small volumes (1-3mL) of the emulgel and is not scalable to the final large volumes (>35mL) needed for a human sized volume of emulgel.

In addition to this, an important step to take is that the technology should apply for classification by the CAT. Classification is a free of charge service provided by the CAT, and it is a first step towards targeting a marketing authorisation (MA). As with all medicinal products, the requirements for a MA application are extensive, with the complexity of the technology increasing the complexity of requirements to attain an MA.

As the DRIVE product is a complex product, containing multiple factors that would need to be individually assessed in line with the Directives and Regulations laid out in the ATMP regulations it would take significant additional funding to achieve the requirements for a MA. The difficulty in applying for an MA can be exemplified by the fact that by October of 2017 the EMA had received eighteen MA applications, with nine applications being approved (345). In contrast, by this date 276 products had received a classification from CAT as an ATMP or non-ATMP (314).

EU regulations are evolving alongside the continuing development and clinical use of ATMPs and a number of accelerated pathways can be utilised by ATMPs, outlined in Figure 5.1.

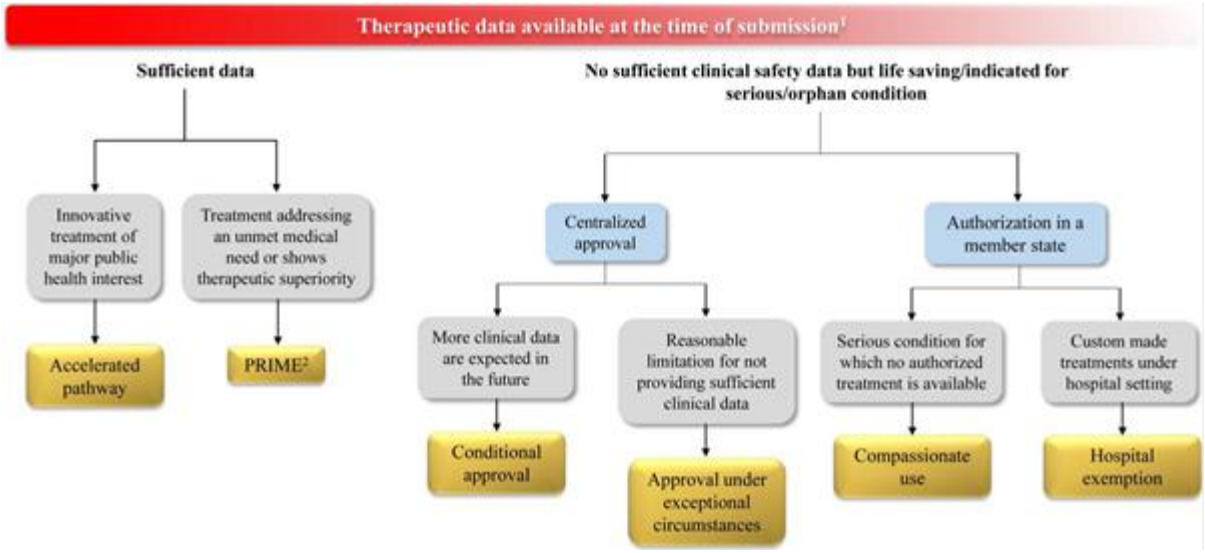

Figure 5.1 *Outline of expedited schemes available in the EU (346). [1]Refers to amount of therapeutic data available at time of submission, decreasing from left to right. [2]PRIME designated products are subject to accelerated assessment; of 41 PRIME medicines approved through PRIME, 14 of these have been ATMPs (347).*

The Hospital Exemption route was detailed in the ATMP regulation when it was first published. It details that ATMPs which are "*prepared on a non-routine basis according to specific quality standards, and used within the same Member State (MS) in a hospital under the exclusive professional responsibility of a medical practitioner, in order to comply with an individual medical prescription for a custom-made product for an individual patient" (309).* Under the regulation, the manufacturing of the product must first be authorised by the MS, and it is the responsibility of the MS to ensure traceability and pharmacovigilance requirements are met. The hospital exemption route is not intended as a means to bypass requirements needed for an MA, as use is limited to non-routine use in a single MS under direction supervision of a clinician. It is primarily intended for use of promising treatments in orphan or lifesaving indications, which also facilitates a faster route to first in man preliminary data, to support CTD and IND documents, helping applications for larger scale clinical trials.

The promise of the DRIVE project to return endogenous insulin production to the patient means it could utilise the Hospital Exemption route in the treatment of hypoglycaemia unawareness or 'brittle' diabetes. As outlined in the ATMP regulation, a product being used under Hospital Exemption must be custom prepared and used

within the same MS. The future work outlined in this Chapter and further process development will be necessary to ensure successful technology transfer to the hospital that would deliver the DRIVE device. This will be necessary to fulfil the requirements of the Hospital Exemption legislation and successfully translate the DRIVE project to the clinic.

5.5 Final Conclusion

Over the course of this project a lead functionalised biomaterial, the natHA/PFD emulgel was formulated, process development commenced and the material evaluated *in vitro* and *in vivo* with promising results. However a great deal of future work will be required to translate these results from animal models to first-in-man trials.

References

1. International_Diabetes_Federation. IDF Diabetes Atlas 8th edn. Brussels, Belgium: International Diabetes Federation; 2017.
2. WHO. Global report on diabetes http://apps.who.int/iris/bitstream/10665/204871/1/9789241565257_eng.pdf?ua=12016 [
3. Federation ID. IDF Diabetes Atlas. 2015.
4. Worldwide trends in diabetes since 1980: a pooled analysis of 751 population-based studies with 4·4 million participants. The Lancet. 2016;387(10027):1513-30.
5. Longnecker D. Anatomy and Histology of the Pancreas. Pancreapedia: Exocrine Pancreas Knowledge Base. 2014.
6. Laboratory TO. The Pancreas (Overview) [Available from: https://www.olivelab.org/the-pancreas-overview.html.
7. Yaginuma N, Takahashi T, Saito K, Kyoguku M. The Microvasculature of the Human Pancreas and Its Relation to Langerhans Islets and Lobules. Pathology - Research and Practice. 1986;181(1):77-84.
8. In't Veld P, Marichal M. Microscopic anatomy of the human islet of Langerhans. Advances in experimental medicine and biology. 2010;654:1-19.
9. Williams JA. Pancreatic Polypeptide. Pancreapedia: Exocrine Pancreas Knowledge Base. 2014.
10. Taylor MJ, Baicu SC. Nonenzymatic cryogenic isolation of therapeutic cells: novel approach for enzyme-free isolation of pancreatic islets using in situ cryopreservation of islets and concurrent selective freeze destruction of acinar tissue. Cell transplantation. 2014;23(11):1365-79.
11. Steiner DJ, Kim A, Miller K, Hara M. Pancreatic islet plasticity: Interspecies comparison of islet architecture and composition. Islets. 2010;2(3):135-45.
12. Arrojo e Drigo R, Ali Y, Diez J, Srinivasan DK, Berggren PO, Boehm BO. New insights into the architecture of the islet of Langerhans: a focused cross-species assessment. Diabetologia. 2015;58(10):2218-28.
13. Wilcox G. Insulin and Insulin Resistance. Clinical Biochemist Reviews. 2005;26(2):19-39.
14. Nathan DM. Diabetes: Advances in Diagnosis and Treatment. Jama. 2015;314(10):1052-62.
15. White SA, Shaw JA, Sutherland DER. Pancreas transplantation. The Lancet. 2009;373(9677):1808-17.
16. WHO. Definition and diagnosis of diabetes mellitus and intermediate hyperglycaemia http://www.who.int/diabetes/publications/Definition%20and%20diagnosis%20of%20diabetes_new.pdf2006 [
17. UK D. DIAGNOSTIC CRITERIA FOR DIABETES https://www.diabetes.org.uk/Professionals/Position-statements-reports/Diagnosis-ongoing-management-monitoring/New_diagnostic_criteria_for_diabetes/ [
18. Freeman AM PN. Insulin Resistance StatPearls: Treasure Island (FL): StatPearls Publishing; [updated 2018 Oct 27. Available from: https://www.ncbi.nlm.nih.gov/books/NBK507839/.
19. Aouacheri O, Saka S, Krim M, Messaadia A, Maidi I. The investigation of the oxidative stress-related parameters in type 2 diabetes mellitus. Canadian journal of diabetes. 2015;39(1):44-9.
20. Shi YC, Pan TM. Red mold, diabetes, and oxidative stress: a review. Applied microbiology and biotechnology. 2012;94(1):47-55.
21. Sami W, Ansari T, Butt NS, Hamid MRA. Effect of diet on type 2 diabetes mellitus: A review. International Journal of Health Sciences. 2017;11(2):65-71.
22. Zhou K, Pedersen HK, Dawed AY, Pearson ER. Pharmacogenomics in diabetes mellitus: insights into drug action and drug discovery. Nature reviews Endocrinology. 2016;12(6):337-46.
23. Li C, Ford ES, Zhao G, Tsai J, Balluz LS, Giles WH. Trends of insulin use among US adults with type 2 diabetes: the Behavioral Risk Factor Surveillance System, 1995-2007. Journal of diabetes and its complications. 2012;26(1):17-22.

24. Canivell S, Gomis R. Diagnosis and classification of autoimmune diabetes mellitus. Autoimmunity reviews. 2014;13(4-5):403-7.
25. Katsarou A, Gudbjörnsdottir S, Rawshani A, Dabelea D, Bonifacio E, Anderson BJ, et al. Type 1 diabetes mellitus. Nature Reviews Disease Primers. 2017;3:17016.
26. Xin GLL, Khee YP, Ying TY, Chellian J, Gupta G, Kunnath AP, et al. Current Status on Immunological Therapies for Type 1 Diabetes Mellitus. Current diabetes reports. 2019;19(5):22.
27. Michels A, Zhang L, Khadra A, Kushner JA, Redondo MJ, Pietropaolo M. Prediction and prevention of type 1 diabetes: update on success of prediction and struggles at prevention. Pediatric diabetes. 2015;16(7):465-84.
28. Evans M, Schumm-Draeger PM, Vora J, King AB. A review of modern insulin analogue pharmacokinetic and pharmacodynamic profiles in type 2 diabetes: improvements and limitations. Diabetes, Obesity & Metabolism. 2011;13(8):677-84.
29. Garg S, Moser E, Dain M-P, Rodionova A. Clinical Experience with Insulin Glargine in Type 1 Diabetes. Diabetes Technology & Therapeutics. 2010;12(11):835-46.
30. Coppolino R, Coppolino S, Villari V. Study of the aggregation of insulin glargine by light scattering. Journal of pharmaceutical sciences. 2006;95(5):1029-34.
31. Wilde MI, McTavish D. Insulin Lispro. Drugs. 1997;54(4):597-614.
32. Segal AR, Vootla T, Beaser RS. Insulin: Making Sense of Current Options. Endocrinology and metabolism clinics of North America. 2016;45(4):845-74.
33. Guettier J-M, Gorden P. Hypoglycemia. Endocrinology and Metabolism Clinics of North America. 2006;35(4):753-66.
34. Kittah NE, Vella A. MANAGEMENT OF ENDOCRINE DISEASE: Pathogenesis and management of hypoglycemia. European journal of endocrinology. 2017;177(1):R37-r47.
35. Koch B. Selected topics of hypoglycemia care. Canadian family physician Medecin de famille canadien. 2006;52:466-71.
36. Shapiro AM. Islet transplantation in type 1 diabetes: ongoing challenges, refined procedures, and long-term outcome. The review of diabetic studies : RDS. 2012;9(4):385-406.
37. Pancreas Islet Transplantation for Patients With Type 1 Diabetes Mellitus: A Clinical Evidence Review. Ontario health technology assessment series. 2015;15(16):1-84.
38. Hypoglycemia & Hypoglycemia Unawareness: Tulane University School of Medicine; 2017 [updated 2017/02/22. Available from: http://tmedweb.tulane.edu/pharmwiki/doku.php/hypoglycemia.
39. Kamoi K, Miyakoshi M, Maruyama R. A quality-of-life assessment of intensive insulin therapy using insulin lispro switched from short-acting insulin and measured by an ITR-QOL questionnaire: a prospective comparison of multiple daily insulin injections and continuous subcutaneous insulin infusion. Diabetes research and clinical practice. 2004;64(1):19-25.
40. Medtronic. Insulin pump therapy 2019 [Available from: https://www.medtronicdiabetes.com/treatments/insulin-pump-therapy.
41. Beck RW, Riddlesworth TD, Ruedy KJ, Kollman C, Ahmann AJ, Bergenstal RM, et al. Effect of initiating use of an insulin pump in adults with type 1 diabetes using multiple daily insulin injections and continuous glucose monitoring (DIAMOND): a multicentre, randomised controlled trial. The lancet Diabetes & endocrinology. 2017.
42. Sasaki M, Mogi T, Wada Y, Hirosawa I, Koizumi A. An endemic condition of biochemical hypoglycemia among male volunteers. Industrial health. 1996;34(4):323-33.
43. Clarke SF, Foster JR. A history of blood glucose meters and their role in self-monitoring of diabetes mellitus. British journal of biomedical science. 2012;69(2):83-93.
44. Patton SR, Clements MA. Continuous Glucose Monitoring Versus Self-monitoring of Blood Glucose in Children with Type 1 Diabetes- Are there Pros and Cons for Both? US endocrinology. 2012;8(1):27-9.

45. Rodbard D, Bailey T, Jovanovic L, Zisser H, Kaplan R, Garg SK. Improved quality of glycemic control and reduced glycemic variability with use of continuous glucose monitoring. Diabetes Technol Ther. 2009;11(11):717-23.
46. Reddy M, Jugnee N, Anantharaja S, Oliver N. Switching from Flash Glucose Monitoring to Continuous Glucose Monitoring on Hypoglycemia in Adults with Type 1 Diabetes at High Hypoglycemia Risk: The Extension Phase of the I HART CGM Study. Diabetes Technol Ther. 2018;20(11):751-7.
47. Lu M, Zuo Y, Guo J, Wen X, Kang Y. Continuous glucose monitoring system can improve the quality of glucose control and glucose variability compared with point-of-care measurement in critically ill patients: A randomized controlled trial. Medicine. 2018;97(36):e12138.
48. Heinemann L, Stuhr A, Brown A, Freckmann G, Breton MD, Russell S, et al. Self-measurement of Blood Glucose and Continuous Glucose Monitoring - Is There Only One Future? European endocrinology. 2018;14(2):24-9.
49. Jones RW, Gianni F, Despotou G, Katzis K. The Artificial Pancreas: Reducing Safety Risk via Intra-Peritoneal Insulin Delivery. Studies in health technology and informatics. 2017;238:56-9.
50. Weisman A, Bai JW, Cardinez M, Kramer CK, Perkins BA. Effect of artificial pancreas systems on glycaemic control in patients with type 1 diabetes: a systematic review and meta-analysis of outpatient randomised controlled trials. The lancet Diabetes & endocrinology. 2017;5(7):501-12.
51. What Is Living With An Artificial Pancreas Like? The Medical Futurist2016 [Available from: https://medicalfuturist.com/living-with-an-artificial-pancreas.
52. Allen N, Gupta A. Current Diabetes Technology: Striving for the Artificial Pancreas. Diagnostics (Basel, Switzerland). 2019;9(1).
53. Crabtree TSJ, McLay A, Wilmot EG. DIY artificial pancreas systems: here to stay? Practical Diabetes. 2019;36(2):63-8.
54. Hsu D, Katelaris C. Long-term management of patients taking immunosuppressive drugs2009. 68-71 p.
55. Holt CD. Overview of Immunosuppressive Therapy in Solid Organ Transplantation. Anesthesiology clinics. 2017;35(3):365-80.
56. Blondet NM, Healey PJ, Hsu E. Immunosuppression in the pediatric transplant recipient. Seminars in pediatric surgery. 2017;26(4):193-8.
57. Gallagher MP, Kelly PJ, Jardine M, Perkovic V, Cass A, Craig JC, et al. Long-term cancer risk of immunosuppressive regimens after kidney transplantation. Journal of the American Society of Nephrology : JASN. 2010;21(5):852-8.
58. Dean PG, Kukla A, Stegall MD, Kudva YC. Pancreas transplantation. BMJ (Clinical research ed). 2017;357:j1321.
59. Kim SS, Kim JH, Kim IJ. Current Challenges in Diabetic Nephropathy: Early Diagnosis and Ways to Improve Outcomes. Endocrinology and metabolism (Seoul, Korea). 2016;31(2):245-53.
60. Kandaswamy R, Skeans MA, Gustafson SK, Carrico RJ, Tyler KH, Israni AK, et al. OPTN/SRTR 2013 Annual Data Report: pancreas. American journal of transplantation : official journal of the American Society of Transplantation and the American Society of Transplant Surgeons. 2015;15 Suppl 2:1-20.
61. Weir GC, Bonner-Weir S. Islet beta cell mass in diabetes and how it relates to function, birth, and death. Annals of the New York Academy of Sciences. 2013;1281:92-105.
62. Bruni A, Gala-Lopez B, Pepper AR, Abualhassan NS, Shapiro AMJ. Islet cell transplantation for the treatment of type 1 diabetes: recent advances and future challenges. Diabetes, Metabolic Syndrome and Obesity: Targets and Therapy. 2014;7:211-23.
63. Qi M, Barbaro B, Wang S, Wang Y, Hansen M, Oberholzer J. Human Pancreatic Islet Isolation: Part I: Digestion and Collection of Pancreatic Tissue. Journal of Visualized Experiments : JoVE. 2009(27):1125.
64. Ricordi C, Lacy PE, Finke EH, Olack BJ, Scharp DW. Automated method for isolation of human pancreatic islets. Diabetes. 1988;37(4):413-20.

65. Bötticher G, Sturm D, Ehehalt F, Knoch KP, Kersting S, Grützmann R, et al. Isolation of Human Islets from Partially Pancreatectomized Patients. Journal of Visualized Experiments : JoVE. 2011(53):2962.
66. Kemp CB, Knight MJ, Scharp DW, Lacy PE, Ballinger WF. Transplantation of isolated pancreatic islets into the portal vein of diabetic rats. Nature. 1973;244(5416):447.
67. Ricordi C, Gray DW, Hering BJ, Kaufman DB, Warnock GL, Kneteman NM, et al. Islet isolation assessment in man and large animals. Acta diabetologica latina. 1990;27(3):185-95.
68. Huang H-H, Harrington S, Stehno-Bittel L. The Flaws and Future of Islet Volume Measurements. Cell transplantation. 2018;27(7):1017-26.
69. Ahearn AJ, Parekh JR, Posselt AM. Islet transplantation for Type 1 diabetes: where are we now? Expert review of clinical immunology. 2015;11(1):59-68.
70. Shapiro AM, Lakey JR, Ryan EA, Korbutt GS, Toth E, Warnock GL, et al. Islet transplantation in seven patients with type 1 diabetes mellitus using a glucocorticoid-free immunosuppressive regimen. The New England journal of medicine. 2000;343(4):230-8.
71. Agarwal A, Brayman KL. Update on Islet Cell Transplantation for Type 1 Diabetes. Seminars in Interventional Radiology. 2012;29(2):90-8.
72. Zeng Y, Ricordi C, Lendoire J, Carroll PB, Alejandro R, Bereiter DR, et al. The effect of prednisone on pancreatic islet autografts in dogs. Surgery. 1993;113(1):98-102.
73. Pepper AR, Gala-Lopez B, Ziff O, Shapiro AM. Revascularization of transplanted pancreatic islets and role of the transplantation site. Clinical & developmental immunology. 2013;2013:352315.
74. Hwang PT, Shah DK, Garcia JA, Bae CY, Lim DJ, Huiszoon RC, et al. Progress and challenges of the bioartificial pancreas. Nano convergence. 2016;3(1):28.
75. Kaddis JS, Danobeitia JS, Niland JC, Stiller T, Fernandez LA. Multicenter analysis of novel and established variables associated with successful human islet isolation outcomes. American journal of transplantation : official journal of the American Society of Transplantation and the American Society of Transplant Surgeons. 2010;10(3):646-56.
76. Berkova Z, Saudek F, Girman P, Zacharovova K, Kriz J, Fabryova E, et al. Combining Donor Characteristics with Immunohistological Data Improves the Prediction of Islet Isolation Success. Journal of diabetes research. 2016;2016:4214328.
77. HSE. Organ Donation Transplant Ireland Annual Report. Health Service Executive; 2018.
78. Dhanasekaran M, George JJ, Loganathan G, Narayanan S, Hughes MG, Williams SK, et al. Pig islet xenotransplantation. Current opinion in organ transplantation. 2017;22(5):452-62.
79. Groth CG, Korsgren O, Tibell A, Tollemar J, Moller E, Bolinder J, et al. Transplantation of porcine fetal pancreas to diabetic patients. Lancet (London, England). 1994;344(8934):1402-4.
80. Richter B, Neises G. 'Human' insulin versus animal insulin in people with diabetes mellitus. The Cochrane database of systematic reviews. 2002(3):Cd003816.
81. Kim A, Miller K, Jo J, Kilimnik G, Wojcik P, Hara M. Islet architecture: A comparative study. Islets. 2009;1(2):129-36.
82. Kemter E, Denner J, Wolf E. Will Genetic Engineering Carry Xenotransplantation of Pig Islets to the Clinic? Current diabetes reports. 2018;18(11):103.
83. Liu Z, Hu W, He T, Dai Y, Hara H, Bottino R, et al. Pig-to-Primate Islet Xenotransplantation: Past, Present, and Future. Cell transplantation. 2017;26(6):925-47.
84. Millman JR, Pagliuca FW. Autologous Pluripotent Stem Cell-Derived beta-Like Cells for Diabetes Cellular Therapy. Diabetes. 2017;66(5):1111-20.
85. Millman JR, Xie C, Van Dervort A, Gürtler M, Pagliuca FW, Melton DA. Generation of stem cell-derived β-cells from patients with type 1 diabetes. Nature communications. 2016;7:11463-.
86. Shahjalal HM, Abdal Dayem A, Lim KM, Jeon T-I, Cho S-G. Generation of pancreatic β cells for treatment of diabetes: advances and challenges. Stem cell research & therapy. 2018;9(1):355-.
87. Cierpka-Kmiec K, Wronska A, Kmiec Z. In vitro generation of pancreatic beta-cells for diabetes treatment. I. beta-like cells derived from human pluripotent stem cells. Folia histochemica et cytobiologica. 2019.

88. Kragl M, Lammert E. Basement membrane in pancreatic islet function. Advances in experimental medicine and biology. 2010;654:217-34.
89. Molina J, Rodriguez-Diaz R, Fachado A, Jacques-Silva MC, Berggren P-O, Caicedo A. Control of insulin secretion by cholinergic signaling in the human pancreatic islet. Diabetes. 2014;63(8):2714-26.
90. Wojtusciszyn A, Armanet M, Morel P, Berney T, Bosco D. Insulin secretion from human beta cells is heterogeneous and dependent on cell-to-cell contacts. Diabetologia. 2008;51(10):1843-52.
91. Stendahl JC, Kaufman DB, Stupp SI. Extracellular matrix in pancreatic islets: relevance to scaffold design and transplantation. Cell transplantation. 2009;18(1):1-12.
92. Yabe D, Seino Y, Seino Y. Incretin concept revised: The origin of the insulinotropic function of glucagon-like peptide-1 - the gut, the islets or both? Journal of diabetes investigation. 2018;9(1):21-4.
93. Dufour JM, Rajotte RV, Zimmerman M, Rezania A, Kin T, Dixon DE, et al. Development of an ectopic site for islet transplantation, using biodegradable scaffolds. Tissue Eng. 2005;11(9-10):1323-31.
94. Blomeier H, Zhang X, Rives C, Brissova M, Hughes E, Baker M, et al. Polymer scaffolds as synthetic microenvironments for extrahepatic islet transplantation. Transplantation. 2006;82(4):452-9.
95. Kin T, O'Neil JJ, Pawlick R, Korbutt GS, Shapiro AM, Lakey JR. The use of an approved biodegradable polymer scaffold as a solid support system for improvement of islet engraftment. Artificial organs. 2008;32(12):990-3.
96. Gibly RF, Zhang X, Lowe WL, Jr., Shea LD. Porous scaffolds support extrahepatic human islet transplantation, engraftment, and function in mice. Cell transplantation. 2013;22(5):811-9.
97. Riopel M, Wang R. Collagen matrix support of pancreatic islet survival and function. Frontiers in bioscience (Landmark edition). 2014;19:77-90.
98. Jalili RB, Moeen Rezakhanlou A, Hosseini-Tabatabaei A, Ao Z, Warnock GL, Ghahary A. Fibroblast populated collagen matrix promotes islet survival and reduces the number of islets required for diabetes reversal. Journal of cellular physiology. 2011;226(7):1813-9.
99. Yang XD, Li HM, Chen M, Zou XH, Zhu LY, Wei CJ, et al. Enhanced insulin production from murine islet beta cells incubated on poly(3-hydroxybutyrate-co-3-hydroxyhexanoate). Journal of biomedical materials research Part A. 2010;92(2):548-55.
100. Riopel M, Trinder M, Wang R. Fibrin, a Scaffold Material for Islet Transplantation and Pancreatic Endocrine Tissue Engineering. Tissue Engineering Part B: Reviews. 2014;21(1):34-44.
101. Hoare TR, Kohane DS. Hydrogels in drug delivery: Progress and challenges. Polymer. 2008;49(8):1993-2007.
102. Buwalda SJ, Vermonden T, Hennink WE. Hydrogels for Therapeutic Delivery: Current Developments and Future Directions. Biomacromolecules. 2017;18(2):316-30.
103. Ahmed EM. Hydrogel: Preparation, characterization, and applications: A review. Journal of Advanced Research. 2015;6(2):105-21.
104. Lee JH. Injectable hydrogels delivering therapeutic agents for disease treatment and tissue engineering. Biomaterials research. 2018;22:27-.
105. O'Neill HS, Gallagher LB, O'Sullivan J, Whyte W, Curley C, Dolan E, et al. Biomaterial-Enhanced Cell and Drug Delivery: Lessons Learned in the Cardiac Field and Future Perspectives. Advanced materials. 2016.
106. Perez-Luna VH, Gonzalez-Reynoso O. Encapsulation of Biological Agents in Hydrogels for Therapeutic Applications. Gels (Basel, Switzerland). 2018;4(3).
107. Hoffman AS. Hydrogels for biomedical applications. Advanced drug delivery reviews. 2002;54(1):3-12.
108. Bochenek MA, Veiseh O, Vegas AJ, McGarrigle JJ, Qi M, Marchese E, et al. Alginate encapsulation as long-term immune protection of allogeneic pancreatic islet cells transplanted into the omental bursa of macaques. Nature biomedical engineering. 2018;2(11):810-21.

109. Alagpulinsa DA, Cao JJL, Driscoll RK, Sirbulescu RF, Penson MFE, Sremac M, et al. Alginate-microencapsulation of human stem cell-derived beta cells with CXCL12 prolongs their survival and function in immunocompetent mice without systemic immunosuppression. American journal of transplantation : official journal of the American Society of Transplantation and the American Society of Transplant Surgeons. 2019.
110. Cañibano-Hernández A, Saenz del Burgo L, Espona-Noguera A, Orive G, Hernández RM, Ciriza J, et al. Hyaluronic acid enhances cell survival of encapsulated insulin-producing cells in alginate-based microcapsules. International journal of pharmaceutics. 2019;557:192-8.
111. Vegas AJ, Veiseh O, Gurtler M, Millman JR, Pagliuca FW, Bader AR, et al. Long-term glycemic control using polymer-encapsulated human stem cell-derived beta cells in immune-competent mice. Nature medicine. 2016;22(3):306-11.
112. Dufrane D, Goebbels RM, Gianello P. Alginate macroencapsulation of pig islets allows correction of streptozotocin-induced diabetes in primates up to 6 months without immunosuppression. Transplantation. 2010;90(10):1054-62.
113. Harrington S, Williams J, Rawal S, Ramachandran K, Stehno-Bittel L. Hyaluronic Acid/Collagen Hydrogel as an Alternative to Alginate for Long-Term Immunoprotected Islet Transplantation. Tissue engineering Part A. 2017.
114. McEwan K, Padavan DT, Ellis C, McBane JE, Vulesevic B, Korbutt GS, et al. Collagen-chitosan-laminin hydrogels for the delivery of insulin-producing tissue. Journal of tissue engineering and regenerative medicine. 2016;10(10):E397-e408.
115. Weaver JD, Headen DM, Hunckler MD, Coronel MM, Stabler CL, García AJ. Design of a vascularized synthetic poly(ethylene glycol) macroencapsulation device for islet transplantation. Biomaterials. 2018;172:54-65.
116. Phelps EA, Templeman KL, Thulé PM, García AJ. Engineered VEGF-releasing PEG-MAL hydrogel for pancreatic islet vascularization. Drug delivery and translational research. 2015;5(2):125-36.
117. Qi M. Transplantation of Encapsulated Pancreatic Islets as a Treatment for Patients with Type 1 Diabetes Mellitus. Advances in Medicine. 2014;2014:429710.
118. Scharp DW, Mason NS, Sparks RE. Islet immuno-isolation: The use of hybrid artificial organs to prevent islet tissue rejection. World Journal of Surgery. 1984;8(2):221-9.
119. Ohgawara H, Hirotani S, Miyazaki J, Teraoka S. Membrane immunoisolation of a diffusion chamber for bioartificial pancreas. Artificial organs. 1998;22(9):788-94.
120. Song S, Faleo G, Yeung R, Kant R, Posselt AM, Desai TA, et al. Silicon nanopore membrane (SNM) for islet encapsulation and immunoisolation under convective transport. Scientific reports. 2016;6:23679-.
121. O'Sullivan ES, Vegas A, Anderson DG, Weir GC. Islets Transplanted in Immunoisolation Devices: A Review of the Progress and the Challenges that Remain. Endocrine Reviews. 2011;32(6):827-44.
122. Colton CK. Oxygen supply to encapsulated therapeutic cells. Adv Drug Deliv Rev. 2014;67-68:93-110.
123. Krishnan R, Alexander M, Robles L, Foster 3rd CE, Lakey JRT. Islet and Stem Cell Encapsulation for Clinical Transplantation. The review of diabetic studies : RDS. 2014;11(1):84-101.
124. Berman DM, O'Neil JJ, Coffey LCK, Chaffanjon PCJ, Kenyon NM, Ruiz P, et al. Long-term survival of nonhuman primate islets implanted in an omental pouch on a biodegradable scaffold. American journal of transplantation : official journal of the American Society of Transplantation and the American Society of Transplant Surgeons. 2009;9(1):91-104.
125. de Vos P, Hamel AF, Tatarkiewicz K. Considerations for successful transplantation of encapsulated pancreatic islets. Diabetologia. 2002;45(2):159-73.
126. Polykandriotis E, Arkudas A, Euler S, Beier JP, Horch RE, Kneser U. [Prevascularisation strategies in tissue engineering]. Handchirurgie, Mikrochirurgie, plastische Chirurgie : Organ der

Deutschsprachigen Arbeitsgemeinschaft fur Handchirurgie : Organ der Deutschsprachigen Arbeitsgemeinschaft fur Mikrochirurgie der Peripheren Nerven und Gefasse 2006;38(4):217-23.
127. Scharp DW, Marchetti P. Encapsulated islets for diabetes therapy: history, current progress, and critical issues requiring solution. Adv Drug Deliv Rev. 2014;67-68:35-73.
128. Teramura Y, Iwata H. Bioartificial pancreas: Microencapsulation and conformal coating of islet of Langerhans. Advanced drug delivery reviews. 2010;62(7):827-40.
129. Kozlovskaya V, Zavgorodnya O, Kharlampieva E. Encapsulation and Surface Engineering of Pancreatic Islets: Advances and Challenges. 2012.
130. Omami M, McGarrigle JJ, Reedy M, Isa D, Ghani S, Marchese E, et al. Islet Microencapsulation: Strategies and Clinical Status in Diabetes. Current diabetes reports. 2017;17(7):47.
131. O'Cearbhaill ED, Ng KS, Karp JM. Emerging medical devices for minimally invasive cell therapy. Mayo Clinic proceedings. 2014;89(2):259-73.
132. Theracyte. The Technology 2019 [Available from: https://theracyte.com/technology/.
133. Josephs SF, Loudovaris T, Dixit A, Young SK, Johnson RC. In vivo delivery of recombinant human growth hormone from genetically engineered human fibroblasts implanted within Baxter immunoisolation devices. Journal of molecular medicine (Berlin, Germany). 1999;77(1):211-4.
134. Sweet IR, Yanay O, Waldron L, Gilbert M, Fuller JM, Tupling T, et al. Treatment of diabetic rats with encapsulated islets. Journal of cellular and molecular medicine. 2008;12(6b):2644-50.
135. Kumagai-Braesch M, Jacobson S, Mori H, Jia X, Takahashi T, Wernerson A, et al. The TheraCyte device protects against islet allograft rejection in immunized hosts. Cell transplantation. 2013;22(7):1137-46.
136. Boettler T, Schneider D, Cheng Y, Kadoya K, Brandon EP, Martinson L, et al. Pancreatic Tissue Transplanted in TheraCyte Encapsulation Devices Is Protected and Prevents Hyperglycemia in a Mouse Model of Immune-Mediated Diabetes. Cell transplantation. 2016;25(3):609-14.
137. Yang Z, Chen M, Fialkow LB, Ellett JD, Wu R, Nadler JL. Survival of pancreatic islet xenografts in NOD mice with the theracyte device. Transplantation proceedings. 2002;34(8):3349-50.
138. Elliott RB, Escobar L, Calafiore R, Basta G, Garkavenko O, Vasconcellos A, et al. Transplantation of micro- and macroencapsulated piglet islets into mice and monkeys. Transplantation proceedings. 2005;37(1):466-9.
139. Gabr MM, Zakaria MM, Refaie AF, Ismail AM, Khater SM, Ashamallah SA, et al. Insulin-producing Cells from Adult Human Bone Marrow Mesenchymal Stromal Cells Could Control Chemically Induced Diabetes in Dogs: A Preliminary Study. Cell transplantation. 2018;27(6):937-47.
140. Motte E, Szepessy E, Suenens K, Stange G, Bomans M, Jacobs-Tulleneers-Thevissen D, et al. Composition and function of macroencapsulated human embryonic stem cell-derived implants: comparison with clinical human islet cell grafts. American journal of physiology Endocrinology and metabolism. 2014;307(9):E838-46.
141. Agulnick AD, Ambruzs DM, Moorman MA, Bhoumik A, Cesario RM, Payne JK, et al. Insulin-Producing Endocrine Cells Differentiated In Vitro From Human Embryonic Stem Cells Function in Macroencapsulation Devices In Vivo. Stem cells translational medicine. 2015;4(10):1214-22.
142. Schulz TC. Concise Review: Manufacturing of Pancreatic Endoderm Cells for Clinical Trials in Type 1 Diabetes. Stem cells translational medicine. 2015;4(8):927-31.
143. FDA. A Safety, Tolerability, and Efficacy Study of VC-01™ Combination Product in Subjects With Type I Diabetes Mellitus 2019 [https://clinicaltrials.gov/ct2/show/study/NCT02239354?term=ViaCyte&rank=4].
144. Viacyte. Encaptra® Drug Delivery System 2019 [Available from: https://viacyte.com/technology/device-engineering.
145. Barkai U, Rotem A, de Vos P. Survival of encapsulated islets: More than a membrane story. World journal of transplantation. 2016;6(1):69-90.
146. Technologies B-O. Living with βAir 2019 [Available from: http://beta-o2.com/living-with-sair/.

147. Ludwig B, Zimerman B, Steffen A, Yavriants K, Azarov D, Reichel A, et al. A novel device for islet transplantation providing immune protection and oxygen supply. Horm Metab Res. 2010;42(13):918-22.
148. Ludwig B, Rotem A, Schmid J, Weir GC, Colton CK, Brendel MD, et al. Improvement of islet function in a bioartificial pancreas by enhanced oxygen supply and growth hormone releasing hormone agonist. Proceedings of the National Academy of Sciences of the United States of America. 2012;109(13):5022-7.
149. Neufeld T, Ludwig B, Barkai U, Weir GC, Colton CK, Evron Y, et al. The efficacy of an immunoisolating membrane system for islet xenotransplantation in minipigs. PloS one. 2013;8(8):e70150-e.
150. Ludwig B, Ludwig S, Steffen A, Knauf Y, Zimerman B, Heinke S, et al. Favorable outcome of experimental islet xenotransplantation without immunosuppression in a nonhuman primate model of diabetes. Proceedings of the National Academy of Sciences of the United States of America. 2017;114(44):11745-50.
151. Ludwig B, Reichel A, Steffen A, Zimerman B, Schally AV, Block NL, et al. Transplantation of human islets without immunosuppression. Proceedings of the National Academy of Sciences of the United States of America. 2013;110(47):19054-8.
152. FDA. An Open Label, Pilot Investigation, to Assess the Safety and Efficacy of Transplantation of Macro-encapsulated Human Islets Within the Bioartificial Pancreas Beta-Air in Patients With Type 1 Diabetes Mellitus 2018 [Available from: https://clinicaltrials.gov/ct2/show/NCT02064309.
153. Pepper AR, Pawlick R, Gala-Lopez B, MacGillivary A, Mazzuca DM, White DJG, et al. Diabetes Is Reversed in a Murine Model by Marginal Mass Syngeneic Islet Transplantation Using a Subcutaneous Cell Pouch Device. Transplantation. 2015;99(11):2294-300.
154. FDA. A Phase I/II Study of the Safety and Efficacy of Sernova's Cell PouchTM for Therapeutic Islet Transplantation. 2012.
155. FDA. A Safety, Tolerability and Efficacy Study of Sernova's Cell Pouch™ for Clinical Islet Transplantation. 2018.
156. Malda J, Klein TJ, Upton Z. The roles of hypoxia in the in vitro engineering of tissues. Tissue Eng. 2007;13(9):2153-62.
157. Stiers PJ, van Gastel N, Carmeliet G. Targeting the hypoxic response in bone tissue engineering: A balance between supply and consumption to improve bone regeneration. Mol Cell Endocrinol. 2016;432:96-105.
158. Moon JJ, West JL. Vascularization of engineered tissues: approaches to promote angio-genesis in biomaterials. Current topics in medicinal chemistry. 2008;8(4):300-10.
159. Papas KK, Pisania A, Wu H, Weir GC, Colton CK. A stirred microchamber for oxygen consumption rate measurements with pancreatic islets. Biotechnology and bioengineering. 2007;98(5):1071-82.
160. Dionne KE, Colton CK, Lyarmush M. Effect of Hypoxia on Insulin Secretion by Isolated Rat and Canine Islets of Langerhans. Diabetes. 1993;42(1):12-21.
161. Camci-Unal G, Alemdar N, Annabi N, Khademhosseini A. Oxygen Releasing Biomaterials for Tissue Engineering. Polymer international. 2013;62(6):843-8.
162. Ng SM, Choi JY, Han HS, Huh JS, Lim JO. Novel microencapsulation of potential drugs with low molecular weight and high hydrophilicity: hydrogen peroxide as a candidate compound. International journal of pharmaceutics. 2010;384(1-2):120-7.
163. Abdi SI, Ng SM, Lim JO. An enzyme-modulated oxygen-producing micro-system for regenerative therapeutics. International journal of pharmaceutics. 2011;409(1-2):203-5.
164. Mallepally RR, Parrish CC, Mc Hugh MA, Ward KR. Hydrogen peroxide filled poly(methyl methacrylate) microcapsules: potential oxygen delivery materials. International journal of pharmaceutics. 2014;475(1-2):130-7.
165. Li Z, Guo X, Guan J. An oxygen release system to augment cardiac progenitor cell survival and differentiation under hypoxic condition. Biomaterials. 2012;33(25):5914-23.

166. Pedraza E, Coronel MM, Fraker CA, Ricordi C, Stabler CL. Preventing hypoxia-induced cell death in beta cells and islets via hydrolytically activated, oxygen-generating biomaterials. Proceedings of the National Academy of Sciences of the United States of America. 2012;109(11):4245-50.
167. Coronel MM, Geusz R, Stabler CL. Mitigating hypoxic stress on pancreatic islets via in situ oxygen generating biomaterial. Biomaterials. 2017;129:139-51.
168. Gulden M, Jess A, Kammann J, Maser E, Seibert H. Cytotoxic potency of H2O2 in cell cultures: impact of cell concentration and exposure time. Free radical biology & medicine. 2010;49(8):1298-305.
169. Wang H, Zhao Y, Li T, Chen Z, Wang Y, Qin C. Properties of calcium peroxide for release of hydrogen peroxide and oxygen: A kinetics study. Chemical Engineering Journal. 2016;303:450-7.
170. Hopfner U, Schenck TL, Chavez MN, Machens HG, Bohne AV, Nickelsen J, et al. Development of photosynthetic biomaterials for in vitro tissue engineering. Acta biomaterialia. 2014;10(6):2712-7.
171. Lode A, Krujatz F, Brüggemeier S, Quade M, Schütz K, Knaack S, et al. Green bioprinting: Fabrication of photosynthetic algae-laden hydrogel scaffolds for biotechnological and medical applications. Engineering in Life Sciences. 2015;15(2):177-83.
172. Schenck TL, Hopfner U, Chavez MN, Machens HG, Somlai-Schweiger I, Giunta RE, et al. Photosynthetic biomaterials: a pathway towards autotrophic tissue engineering. Acta biomaterialia. 2015;15:39-47.
173. Cook CA, Hahn KC, Morrissette-McAlmon JB, Grayson WL. Oxygen delivery from hyperbarically loaded microtanks extends cell viability in anoxic environments. Biomaterials. 2015;52:376-84.
174. Henkel-Honke T, Oleck M. Artificial oxygen carriers: a current review. AANA journal. 2007;75(3):205-11.
175. Pilarek M. Liquid Perfluorochemicals as Flexible and Efficient Gas Carriers Applied in Bioprocess Engineering: An Updated Overview and Future Prospects. Chemical and Process Engineering. 2014;35(4).
176. Riess JG. Perfluorocarbon-based oxygen delivery. Artificial cells, blood substitutes, and immobilization biotechnology. 2006;34(6):567-80.
177. Riess JG. Oxygen carriers ("blood substitutes")--raison d'etre, chemistry, and some physiology. Chemical reviews. 2001;101(9):2797-920.
178. Brandhorst H, Asif S, Andersson K, Theisinger B, Andersson HH, Felldin M, et al. A new oxygen carrier for improved long-term storage of human pancreata before islet isolation. Transplantation. 2010;89(2):155-60.
179. White JC, Godsey ME, Bhatia SR. Perfluorocarbons enhance oxygen transport in alginate-based hydrogels. Polymers for Advanced Technologies. 2014;25(11):1242-6.
180. White JC, Stoppel WL, Roberts SC, Bhatia SR. Addition of perfluorocarbons to alginate hydrogels significantly impacts molecular transport and fracture stress. Journal of biomedical materials research Part A. 2013;101(2):438-46.
181. Khattak SF, Chin KS, Bhatia SR, Roberts SC. Enhancing oxygen tension and cellular function in alginate cell encapsulation devices through the use of perfluorocarbons. Biotechnology and bioengineering. 2007;96(1):156-66.
182. Li H, Wijekoon A, Leipzig ND. Encapsulated neural stem cell neuronal differentiation in fluorinated methacrylamide chitosan hydrogels. Annals of biomedical engineering. 2014;42(7):1456-69.
183. Douglas TEL, Pilarek M, Kalaszczyńska I, Senderek I, Skwarczyńska A, Cuijpers VMJI, et al. Enrichment of chitosan hydrogels with perfluorodecalin promotes gelation and stem cell vitality. Materials Letters. 2014;128:79-84.
184. Maillard E, Juszczak MT, Clark A, Hughes SJ, Gray DR, Johnson PR. Perfluorodecalin-enriched fibrin matrix for human islet culture. Biomaterials. 2011;32(35):9282-9.

185. Schaschkow A, Mura C, Bietiger W, Peronet C, Langlois A, Bodin F, et al. Impact of an autologous oxygenating matrix culture system on rat islet transplantation outcome. Biomaterials. 2015;52:180-8.
186. Muskula PR, Main ML. Safety With Echocardiographic Contrast Agents. Circulation Cardiovascular imaging. 2017;10(4).
187. Cosco D, Fattal E, Fresta M, Tsapis N. Perfluorocarbon-loaded micro and nanosystems for medical imaging: A state of the art. Journal of Fluorine Chemistry. 2015;171:18-26.
188. Yu Q, Liu K, Su L, Xia X, Xu X. Perfluorocarbon liquid: its application in vitreoretinal surgery and related ocular inflammation. BioMed research international. 2014;2014:250323.
189. Tognetto D, Lepori L, Lapasin R, Minutola D, Sanguinetti G, Michelone L, et al. A new heavy internal tamponade in vitreoretinal surgery: an in vitro study. Eye. 2008;22(8):1082-8.
190. Riess JG. Blood substitutes and other potential biomedical applications of fluorinated colloids. Journal of Fluorine Chemistry. 2002;114(2):119-26.
191. Damiano D, Wang SS. Novel use of a perfluorocarbon for supplying oxygen to aerobic submerged cultures. Biotechnology Letters. 1985;7(2):81-6.
192. Pilarek M, Grabowska I, Ciemerych MA, Dąbkowska K, Szewczyk KW. Morphology and growth of mammalian cells in a liquid/liquid culture system supported with oxygenated perfluorodecalin. Biotechnology Letters. 2013;35(9):1387-94.
193. Hosgood SA, Nicholson ML. The role of perfluorocarbon in organ preservation. Transplantation. 2010;89(10):1169-75.
194. Witkowski P, Liu Z, Guo Q, Poumian-Ruiz E, Cernea S, Herold K, et al. Two-layer method in short-term pancreas preservation for successful islet isolation. Transplantation proceedings. 2005;37(8):3398-401.
195. Brandhorst D, Iken M, Brendel MD, Bretzel RG, Brandhorst H. Long-term preservation of the pig pancreas by a one-layer method for successful islet isolation. Transplantation proceedings. 2005;37(1):229-30.
196. Keipert PE. Use of Oxygent, a perfluorochemical-based oxygen carrier, as an alternative to intraoperative blood transfusion. Artificial cells, blood substitutes, and immobilization biotechnology. 1995;23(3):381-94.
197. Kemming GI, Meisner FG, Wojtczyk CJ, Packert KB, Minor T, Thiel M, et al. Oxygent as a top load to colloid and hyperoxia is more effective in resuscitation from hemorrhagic shock than colloid and hyperoxia alone. Shock (Augusta, Ga). 2005;24(3):245-54.
198. Cho MH, Wang SS. Enhancement of oxygen transfer in Hybridoma cell culture by using a perfluorocarbon as an oxygen carrier. Biotechnology Letters. 1988;10(12):855-60.
199. Mitsuno T, Ohyanagi H, Naito R. Clinical studies of a perfluorochemical whole blood substitute (Fluosol-DA) Summary of 186 cases. Annals of Surgery. 1982;195(1):60-9.
200. Goh F, Gross JD, Simpson NE, Sambanis A. LIMITED BENEFICIAL EFFECTS OF PERFLUOROCARBON EMULSIONS ON ENCAPSULATED CELLS IN CULTURE: EXPERIMENTAL AND MODELING STUDIES. Journal of biotechnology. 2010;150(2):232-9.
201. Ju L-K, Lee JF, Armiger WB. Enhancing Oxygen Transfer in Bioreactors by Perfluorocarbon Emulsions. Biotechnology Progress. 1991;7(4):323-9.
202. Isaka M, Imamura M, Sakuma I, Shiiya N, Fukushima S, Nakai K, et al. Cardioprotective effect of perfluorochemical emulsion for cardiac preservation after six-hour cold storage. ASAIO journal (American Society for Artificial Internal Organs : 1992). 2005;51(4):434-9.
203. Maillard E, Juszczak MT, Langlois A, Kleiss C, Sencier MC, Bietiger W, et al. Perfluorocarbon emulsions prevent hypoxia of pancreatic beta-cells. Cell transplantation. 2012;21(4):657-69.
204. Amaral PF, Freire MG, Rocha-Leao MH, Marrucho IM, Coutinho JA, Coelho MA. Optimization of oxygen mass transfer in a multiphase bioreactor with perfluorodecalin as a second liquid phase. Biotechnology and bioengineering. 2008;99(3):588-98.
205. Lowe KC, Anthony P, Davey MR, Power JB. Culture of cells at perfluorocarbon-aqueous interfaces. Artificial cells, blood substitutes, and immobilization biotechnology. 1999;27(3):255-61.

206. Scott WE, 3rd, O'Brien TD, Ferrer-Fabrega J, Avgoustiniatos ES, Weegman BP, Anazawa T, et al. Persufflation improves pancreas preservation when compared with the two-layer method. Transplantation proceedings. 2010;42(6):2016-9.
207. Brandhorst H, Iken M, Scott WE, 3rd, Papas KK, Theisinger B, Johnson PR, et al. Quality of isolated pig islets is improved using perfluorohexyloctane for pancreas storage in a split lobe model. Cell transplantation. 2013;22(8):1477-83.
208. Tsujimura T, Suzuki Y, Takahashi T, Yoshida I, Fujino Y, Tanioka Y, et al. Successful 24-h preservation of canine small bowel using the cavitary two-layer (University of Wisconsin solution/perfluorochemical) cold storage method. American journal of transplantation : official journal of the American Society of Transplantation and the American Society of Transplant Surgeons. 2002;2(5):420-4.
209. Loehe F, Mueller C, Bittmann I, Messmer K, Schildberg FW. Influence of long-term preservation with endobronchially administered perfluorodecalin on pulmonary graft function. Transplantation. 2000;70(10):1417-24.
210. Asif S, Sedigh A, Nordstrom J, Brandhorst H, Jorns C, Lorant T, et al. Oxygen-charged HTK-F6H8 emulsion reduces ischemia-reperfusion injury in kidneys from brain-dead pigs. The Journal of surgical research. 2012;178(2):959-67.
211. Brandhorst H, Muehling B, Yamaya H, Henriksnaes J, Carlsson PO, Korsgren O, et al. New class of oxygen carriers improves islet isolation from long-term stored rat pancreata. Transplantation proceedings. 2008;40(2):393-4.
212. Brandhorst H, Theisinger B, Yamaya H, Henriksnas J, Carlsson PO, Korsgren O, et al. Perfluorohexyloctane improves long-term storage of rat pancreata for subsequent islet isolation. Transplant international : official journal of the European Society for Organ Transplantation. 2009;22(10):1017-22.
213. Stefaniotou MI, Aspiotis MV, Kitsos GD, Kalogeropoulos CD, Asproudis IC, Psilas KG. Our experience with perfluorohexyloctane (F6H8) as a temporary endotamponade in vitreoretinal surgery. European journal of ophthalmology. 2002;12(6):518-22.
214. Zeana D, Becker J, Kuckelkorn R, Kirchhof B. Perfluorohexyloctane as a long-term vitreous tamponade in the experimental animal. Experimental perfluorohexyloctane substitution. International ophthalmology. 1999;23(1):17-24.
215. Malchiodi-Albedi F, Matteucci A, Formisano G, Paradisi S, Carnovale-Scalzo G, Perilli R, et al. Perfluorohexyloctane (F6H8) induces structural modifications and increases apoptosis in rat primary retinal cultures. Journal of Biomedical Materials Research Part B: Applied Biomaterials. 2003;65B(1):133-6.
216. Stahle M, Foss A, Gustafsson B, Lempinen M, Lundgren T, Rafael E, et al. Evaluation of perfluorohexyloctane/polydimethylsiloxane for pancreas preservation for clinical islet isolation and transplantation. Cell transplantation. 2016.
217. Gould SA, Rosen AL, Sehgal LR, Sehgal HL, Langdale LA, Krause LM, et al. Fluosol-DA as a Red-Cell Substitute in Acute Anemia. New England Journal of Medicine. 1986;314(26):1653-6.
218. Bruno S, Ronda L, Faggiano S, Bettati S, Mozzarelli A, Abraham DJ. Oxygen Delivery via Allosteric Effectors of Hemoglobin and Blood Substitutes. Burger's Medicinal Chemistry and Drug Discovery: John Wiley & Sons, Inc.; 2003.
219. Matsumoto S, Kuroda Y. Perfluorocarbon for organ preservation before transplantation. Transplantation. 2002;74(12):1804-9.
220. Tamimi F, Comeau P, Le Nihouannen D, Zhang YL, Bassett DC, Khalili S, et al. Perfluorodecalin and bone regeneration. European cells & materials. 2013;25:22-36.
221. Dalmedico MM, Meier MJ, Felix JVC, Pott FS, Petz FdFC, Santos MC. Hyaluronic acid covers in burn treatment: a systematic review. Revista da Escola de Enfermagem da USP. 2016;50:522-8.
222. Stern R. Hyaluronan catabolism: a new metabolic pathway. European journal of cell biology. 2004;83(7):317-25.

223. Wu R-L, Huang L, Zhao H-C, Geng X-P. Hyaluronic acid in digestive cancers. Journal of Cancer Research and Clinical Oncology. 2016;143(1):1-16.
224. Nusgens BV. [Hyaluronic acid and extracellular matrix: a primitive molecule?]. Annales de dermatologie et de venereologie. 2010;137 Suppl 1:S3-8.
225. Price RD, Myers S, Leigh IM, Navsaria HA. The role of hyaluronic acid in wound healing: assessment of clinical evidence. American journal of clinical dermatology. 2005;6(6):393-402.
226. Vigetti D, Karousou E, Viola M, Deleonibus S, De Luca G, Passi A. Hyaluronan: biosynthesis and signaling. Biochimica et biophysica acta. 2014;1840(8):2452-9.
227. Tammi MI, Day AJ, Turley EA. Hyaluronan and homeostasis: a balancing act. The Journal of biological chemistry. 2002;277(7):4581-4.
228. Laurent TC, Laurent UB, Fraser JR. The structure and function of hyaluronan: An overview. Immunology and cell biology. 1996;74(2):A1-7.
229. Dicker KT, Gurski LA, Pradhan-Bhatt S, Witt RL, Farach-Carson MC, Jia X. Hyaluronan: a simple polysaccharide with diverse biological functions. Acta biomaterialia. 2014;10(4):1558-70.
230. Levillain A, Magoariec H, Boulocher C, Decambron A, Viateau V, Hoc T. Effects of a viscosupplementation therapy on rabbit menisci in an anterior cruciate ligament transection model of osteoarthritis. Journal of biomechanics. 2017;58:147-54.
231. Migliore A, Granata M. Intra-articular use of hyaluronic acid in the treatment of osteoarthritis. Clinical Interventions in Aging. 2008;3(2):365-9.
232. Nobile V, Buonocore D, Michelotti A, Marzatico F. Anti-aging and filling efficacy of six types hyaluronic acid based dermo-cosmetic treatment: double blind, randomized clinical trial of efficacy and safety. Journal of cosmetic dermatology. 2014;13(4):277-87.
233. Walimbe T, Panitch A, Sivasankar PM. A Review of Hyaluronic Acid and Hyaluronic Acid-based Hydrogels for Vocal Fold Tissue Engineering. Journal of voice : official journal of the Voice Foundation. 2017.
234. Zaviskova K, Tukmachev D, Dubisova J, Vackova I, Hejcl A, Bystronova J, et al. Injectable hydroxyphenyl derivative of hyaluronic acid hydrogel modified with RGD as scaffold for spinal cord injury repair. Journal of biomedical materials research Part A. 2018;106(4):1129-40.
235. Kurisawa M, Chung JE, Yang YY, Gao SJ, Uyama H. Injectable biodegradable hydrogels composed of hyaluronic acid-tyramine conjugates for drug delivery and tissue engineering. Chemical communications (Cambridge, England). 2005(34):4312-4.
236. Lee F, Chung JE, Kurisawa M. An injectable hyaluronic acid-tyramine hydrogel system for protein delivery. Journal of controlled release : official journal of the Controlled Release Society. 2009;134(3):186-93.
237. Xu K, Lee F, Gao S, Tan MH, Kurisawa M. Hyaluronidase-incorporated hyaluronic acid-tyramine hydrogels for the sustained release of trastuzumab. Journal of controlled release : official journal of the Controlled Release Society. 2015;216:47-55.
238. Ganesh N, Hanna C, Nair SV, Nair LS. Enzymatically cross-linked alginic-hyaluronic acid composite hydrogels as cell delivery vehicles. International journal of biological macromolecules. 2013;55:289-94.
239. Abu-Hakmeh A, Kung A, Mintz BR, Kamal S, Cooper JA, Lu XL, et al. Sequential gelation of tyramine-substituted hyaluronic acid hydrogels enhances mechanical integrity and cell viability. Medical & biological engineering & computing. 2016;54(12):1893-902.
240. Borreani J, Espert M, Salvador A, Sanz T, Quiles A, Hernando I. Oil-in-water emulsions stabilised by cellulose ethers: stability, structure and in vitro digestion. Food & function. 2017;8(4):1547-57.
241. Swartz ML. Citrucel (methylcellulose/bulk-forming laxative). Gastroenterology nursing : the official journal of the Society of Gastroenterology Nurses and Associates. 1989;12(1):50-2.
242. Rogers TL, Wallick D. Reviewing the use of ethylcellulose, methylcellulose and hypromellose in microencapsulation. Part 1: materials used to formulate microcapsules. Drug development and industrial pharmacy. 2012;38(2):129-57.

243. Kim JK, Yoo C, Cha YH, Kim YH. Thermo-reversible injectable gel based on enzymatically-chopped low molecular weight methylcellulose for exenatide and FGF 21 delivery to treat types 1 and 2 diabetes. Journal of controlled release : official journal of the Controlled Release Society. 2014;194:316-22.
244. Tang Y, Wang X, Li Y, Lei M, Du Y, Kennedy JF, et al. Production and characterisation of novel injectable chitosan/methylcellulose/salt blend hydrogels with potential application as tissue engineering scaffolds. Carbohydrate Polymers. 2010;82(3):833-41.
245. Payne C, Dolan EB, O'Sullivan J, Cryan SA, Kelly HM. A methylcellulose and collagen based temperature responsive hydrogel promotes encapsulated stem cell viability and proliferation in vitro. Drug Deliv Transl Res. 2017;7(1):132-46.
246. Sanchez Dominguez M, Maillard E, Krafft MP, Sigrist S, Belcourt A. Prevention of adhesion and promotion of pseudoislets formation from a beta-cell line by fluorocarbon emulsions. Chembiochem : a European journal of chemical biology. 2006;7(8):1160-3.
247. GmbH P. Firesting O2 Fiber-Optic Oxygen Meter, User Manual. Version 3.07.
248. Europe Co. European Pharmacopoeia. 2005;5.0.
249. Karthik P, Ezhilarasi PN, Anandharamakrishnan C. Challenges associated in stability of food grade nanoemulsions. Critical reviews in food science and nutrition. 2017;57(7):1435-50.
250. Daik R, Bidol S, Abdullah I. Effect of Molecular Weight on the Droplet Size and Rheological Properties of Liquid natural Rubber Emulsion2007.
251. Verwey EJW. Theory of the Stability of Lyophobic Colloids. The Journal of Physical and Colloid Chemistry. 1947;51(3):631-6.
252. O'Brien R, Langlais A, Seufert W. Diffusion coefficients of respiratory gases in a perfluorocarbon liquid. Science. 1982;217(4555):153-5.
253. Ju LK, Lee JF, Armiger WB. Effect of the interfacial surfactant layer on oxygen transfer through the oil/water phase boundary in perfluorocarbon emulsions. Biotechnology and bioengineering. 1991;37(6):505-11.
254. Mezger TG. The Rheology Handbook2014.
255. Schultz KM, Baldwin AD, Kiick KL, Furst EM. Gelation of Covalently Cross-Linked PEG–Heparin Hydrogels. Macromolecules. 2009;42(14):5310-6.
256. Kobayashi Y, Okamoto A, Nishinari K. Viscoelasticity of hyaluronic acid with different molecular weights. Biorheology. 1994;31(3):235-44.
257. Johnson AS, O'Sullivan E, D'Aoust LN, Omer A, Bonner-Weir S, Fisher RJ, et al. Quantitative assessment of islets of Langerhans encapsulated in alginate. Tissue engineering Part C, Methods. 2011;17(4):435-49.
258. Li S, Ma Y, Fu T, Zhu C, Li H. The viscosity distribution around a rising bubble in shear-thinning non-newtonian fluids. Brazilian Journal of Chemical Engineering. 2012;29:265-74.
259. Frank AM, Barker CF, Markmann JF. Comparison of Whole Organ Pancreas and Isolated Islet Transplantation for Type 1 Diabetes. Advances in Surgery. 2005;39:137-63.
260. Poitout V, Olson LK, Robertson RP. Insulin-secreting cell lines: classification, characteristics and potential applications. Diabetes & metabolism. 1996;22(1):7-14.
261. Miyazaki J, Araki K, Yamato E, Ikegami H, Asano T, Shibasaki Y, et al. Establishment of a pancreatic beta cell line that retains glucose-inducible insulin secretion: special reference to expression of glucose transporter isoforms. Endocrinology. 1990;127(1):126-32.
262. Ishihara H, Asano T, Tsukuda K, Katagiri H, Inukai K, Anai M, et al. Pancreatic beta cell line MIN6 exhibits characteristics of glucose metabolism and glucose-stimulated insulin secretion similar to those of normal islets. Diabetologia. 1993;36(11):1139-45.
263. Nakashima K, Kanda Y, Hirokawa Y, Kawasaki F, Matsuki M, Kaku K. MIN6 is not a pure beta cell line but a mixed cell line with other pancreatic endocrine hormones. Endocrine journal. 2009;56(1):45-53.

264. Hayashi H, Inoue K, Aung T, Tun T, Yuanjun G, Wenjing W, et al. Application of a novel B cell line MIN6 to a mesh-reinforced polyvinyl alcohol hydrogel tube and three-layer agarose microcapsules: an in vitro study. Cell transplantation. 1996;5(5 Suppl 1):S65-9.
265. Hirotani S, Eda R, Kawabata T, Fuchinoue S, Teraoka S, Agishi T, et al. Bioartificial endocrine pancreas (Bio-AEP) for treatment of diabetes: effect of implantation of Bio-AEP on the pancreas. Cell transplantation. 1999;8(4):399-404.
266. Wang WJ, Inoue K, Hayashi H, Aung T, Tun T, Gu YJ, et al. Efficacy of microencapsulation of a pancreatic B-cell line (MIN6) in an agarose/PSSa microbead as a bioartificial pancreas. Transplantation proceedings. 1996;28(2):1094-6.
267. Ohgawara H, Miyazaki J, Karibe S, Tashiro F, Akaike T, Hashimoto Y. Embedded-culture of pancreatic beta-cells derived from transgenic mouse insulinoma as a potential source for xenotransplantation using a diffusion chamber. Cell transplantation. 1995;4(3):307-13.
268. Barrientos R, Baltrusch S, Sigrist S, Legeay G, Belcourt A, Lenzen S. Kinetics of insulin secretion from MIN6 pseudoislets after encapsulation in a prototype device of a bioartificial pancreas. Horm Metab Res. 2009;41(1):5-9.
269. Hayashi H, Inoue K, Aung T, Tun T, Wenjing W, Gu YJ, et al. Long survival of xenografted bioartificial pancreas with a mesh-reinforced polyvinyl alcohol hydrogel bag employing a B-cell line (MIN6). Transplantation proceedings. 1996;28(3):1428-9.
270. Hayashi H, Inoue K, Aung T, Tun T, Wang WJ, Gu YJ, et al. Prolongation of survival of a xenografted bioartificial pancreas with amesh-reinforced polyvinyl alcohol hydrogel bag employing a B-cell line (MIN6). Transplantation proceedings. 1996;28(2):1097-8.
271. Kawakami Y, Inoue K, Hayashi H, Wang WJ, Setoyama H, Gu YJ, et al. Subcutaneous xenotransplantation of hybrid artificial pancreas encapsulating pancreatic B cell line (MIN6): functional and histological study. Cell transplantation. 1997;6(5):541-5.
272. Ohgawara H, Miyazaki J, Nakagawa Y, Sato S, Karibe S, Akaike T. Xenoimplantation using a diffusion chamber with a B-cell line (MIN6) as a bioartificial endocrine pancreas (Bio-AEP). Cell transplantation. 1996;5(5 Suppl 1):S71-3.
273. Skrzypek K, Barrera YB, Groth T, Stamatialis D. Endothelial and beta cell composite aggregates for improved function of a bioartificial pancreas encapsulation device. The International journal of artificial organs. 2018;41(3):152-9.
274. Asfari M, Janjic D, Meda P, Li G, Halban PA, Wollheim CB. Establishment of 2-mercaptoethanol-dependent differentiated insulin-secreting cell lines. Endocrinology. 1992;130(1):167-78.
275. Johnson AS, O'Sullivan E, D'Aoust LN, Omer A, Bonner-Weir S, Fisher RJ, et al. Quantitative Assessment of Islets of Langerhans Encapsulated in Alginate. Tissue Engineering Part C, Methods. 2011;17(4):435-49.
276. Skelin M, Rupnik M, Cencic A. Pancreatic beta cell lines and their applications in diabetes mellitus research. Altex. 2010;27(2):105-13.
277. Merglen A, Theander S, Rubi B, Chaffard G, Wollheim CB, Maechler P. Glucose Sensitivity and Metabolism-Secretion Coupling Studied during Two-Year Continuous Culture in INS-1E Insulinoma Cells. Endocrinology. 2004;145(2):667-78.
278. Espona-Noguera A, Ciriza J, Canibano-Hernandez A, Villa R, Saenz Del Burgo L, Alvarez M, et al. 3D printed polyamide macroencapsulation devices combined with alginate hydrogels for insulin-producing cell-based therapies. International journal of pharmaceutics. 2019;566:604-14.
279. Marchioli G, van Gurp L, van Krieken PP, Stamatialis D, Engelse M, van Blitterswijk CA, et al. Fabrication of three-dimensional bioplotted hydrogel scaffolds for islets of Langerhans transplantation. Biofabrication. 2015;7(2):025009.
280. Bloch K, Lozinsky VI, Galaev IY, Yavriyanz K, Vorobeychik M, Azarov D, et al. Functional activity of insulinoma cells (INS-1E) and pancreatic islets cultured in agarose cryogel sponges. Journal of biomedical materials research Part A. 2005;75(4):802-9.

281. Persaud SJ, Arden C, Bergsten P, Bone AJ, Brown J, Dunmore S, et al. Pseudoislets as primary islet replacements for research: report on a symposium at King's College London, London UK. Islets. 2010;2(4):236-9.
282. Kojima N. In vitro reconstitution of pancreatic islets. Organogenesis. 2014;10(2):225-30.
283. Jo YH, Nam BM, Kim BY, Nemeno JG, Lee S, Yeo JE, et al. Pseudoislet of hybrid cellular spheroids from commercial cell lines. Transplantation proceedings. 2013;45(8):3113-7.
284. Tsang WG, Zheng T, Wang Y, Tang J, Rind HB, Francki A, et al. Generation of functional islet-like clusters after monolayer culture and intracapsular aggregation of adult human pancreatic islet tissue. Transplantation. 2007;83(6):685-93.
285. Espona-Noguera A, Etxebarria-Elezgarai J, Saenz Del Burgo L, Canibano-Hernandez A, Gurruchaga H, Blanco FJ, et al. Type 1 Diabetes Mellitus reversal via implantation of magnetically purified microencapsulated pseudoislets. International journal of pharmaceutics. 2019;560:65-77.
286. Steiner DJ, Kim A, Miller K, Hara M. Pancreatic islet plasticity: interspecies comparison of islet architecture and composition. Islets. 2010;2(3):135-45.
287. Heller RS. The comparative anatomy of islets. Advances in experimental medicine and biology. 2010;654:21-37.
288. SCHER. Non-human primates in research and safety testing. 2009.
289. Zhu H-T, Wang W-L, Yu L, Wang B. Pig-Islet Xenotransplantation: Recent Progress and Current Perspectives. Frontiers in Surgery. 2014;1:7.
290. Kim H-I, Lee S-Y, Jin SM, Kim KS, Yu JE, Yeom S-C, et al. Parameters for successful pig islet isolation as determined using 68 specific-pathogen-free miniature pigs. Xenotransplantation. 2009;16(1):11-8.
291. Rodriguez-Brotons A, Bietiger W, Peronet C, Langlois A, Magisson J, Mura C, et al. Comparison of Perfluorodecalin and HEMOXCell as Oxygen Carriers for Islet Oxygenation in an In Vitro Model of Encapsulation. Tissue engineering Part A. 2016;22(23-24):1327-36.
292. Grodsky GM. A threshold distribution hypothesis for packet storage of insulin and its mathematical modeling. The Journal of clinical investigation. 1972;51(8):2047-59.
293. Gembal M, Detimary P, Gilon P, Gao ZY, Henquin JC. Mechanisms by which glucose can control insulin release independently from its action on adenosine triphosphate-sensitive K+ channels in mouse B cells. The Journal of clinical investigation. 1993;91(3):871-80.
294. Komatsu M, Takei M, Ishii H, Sato Y. Glucose-stimulated insulin secretion: A newer perspective. Journal of diabetes investigation. 2013;4(6):511-6.
295. Grill V, Adamson U, Cerasi E. Immediate and time-dependent effects of glucose on insulin release from rat pancreatic tissue. Evidence for different mechanisms of action. The Journal of clinical investigation. 1978;61(4):1034-43.
296. Carter JD, Dula SB, Corbin KL, Wu R, Nunemaker CS. A Practical Guide to Rodent Islet Isolation and Assessment. Biological Procedures Online. 2009;11:3-31.
297. Groot Nibbelink M, Marchioli G, Moroni L, Karperien M, Van Apeldoorn A. A Protocol to Enhance INS1E and MIN6 Functionality-The Use of Theophylline. International journal of molecular sciences. 2016;17(9):1532.
298. Sakata N, Egawa S, Sumi S, Unno M. Optimization of glucose level to determine the stimulation index of isolated rat islets. Pancreas. 2008;36(4):417-23.
299. Hou N, Torii S, Saito N, Hosaka M, Takeuchi T. Reactive Oxygen Species-Mediated Pancreatic β-Cell Death Is Regulated by Interactions between Stress-Activated Protein Kinases, p38 and c-Jun N-Terminal Kinase, and Mitogen-Activated Protein Kinase Phosphatases. Endocrinology. 2008;149(4):1654-65.
300. Inberg A, Linial M. Protection of pancreatic beta-cells from various stress conditions is mediated by DJ-1. The Journal of biological chemistry. 2010;285(33):25686-98.
301. Jeworrek C, Hollmann O, Steitz R, Winter R, Czeslik C. Interaction of IAPP and insulin with model interfaces studied using neutron reflectometry. Biophysical journal. 2009;96(3):1115-23.

302. Leverett LB, Hellums JD, Alfrey CP, Lynch EC. Red Blood Cell Damage by Shear Stress. Biophysical Journal. 1972;12(3):257-73.
303. Hua J, Erickson LE, Yiin T-Y, Glasgow LA. A Review of the Effects of Shear and Interfacial Phenomena on Cell Viability. Critical Reviews in Biotechnology. 1993;13(4):305-28.
304. Chisti Y. Hydrodynamic Damage to Animal Cells. Critical Reviews in Biotechnology. 2001;21(2):67-110.
305. Liu L, Zhou C, Xia X, Liu Y. Self-assembled lecithin/chitosan nanoparticles for oral insulin delivery: preparation and functional evaluation. International journal of nanomedicine. 2016;11:761-9.
306. Ansari MJ, Anwer MK, Jamil S, Al-Shdefat R, Ali BE, Ahmad MM, et al. Enhanced oral bioavailability of insulin-loaded solid lipid nanoparticles: pharmacokinetic bioavailability of insulin-loaded solid lipid nanoparticles in diabetic rats. Drug delivery. 2016;23(6):1972-9.
307. Detela G, Lodge A. Manufacturing process development of ATMPs within a regulatory framework for EU clinical trial & marketing authorisation applications. Cell and Gene Therapy Insights. 2016;2(4):425-52.
308. Directive 2001/83/EC of the European Parliament and of the Council of 6 November 2001 on the Community code relating to medicinal products for human use, (2001).
309. Regulation (EC) No 1394/2007 of the European Parliament and of the Council of 13 November 2007 on advanced therapy medicinal products and amending Directive 2001/83/EC and Regulation (EC) No 726/2004.
310. EMA. Committee for Advanced Therapies (CAT) [22/02/2019]. Available from: https://www.ema.europa.eu/en/committees/committee-advanced-therapies-cat.
311. EMA. Reflection paper on classification of advanced therapy medicinal products [22/02/2019]. Available from: https://www.ema.europa.eu/documents/scientific-guideline/draft-reflection-paper-classification-advanced-therapy-medicinal-products_en.pdf.
312. CAT. Scientific recommendation on classification of advanced therapy medicinal products - Suspension containing human islets of Langerhans, autologous or allogeneic. [22/02/2019]. Available from: https://www.ema.europa.eu/documents/report/scientific-recommendation-classification-advanced-therapy-medicinal-products-human-islets-langerhans_en.pdf.
313. CAT. Scientific recommendation on classification of advanced therapy medicinal products - Allogeneic pancreatic islets encapsulated by an elastin-like recombinamers [22/02/2019]. Available from: https://www.ema.europa.eu/documents/report/scientific-recommendation-classification-advanced-therapy-medicinal-products-allogeneic-pancreatic_en.pdf.
314. CAT. Summaries of scientific recommendations on classification of advanced therapy medicinal products [22/02/2019]. Available from: https://www.ema.europa.eu/en/human-regulatory/marketing-authorisation/advanced-therapies/advanced-therapy-classification/summaries-scientific-recommendations-classification-advanced-therapy-medicinal-products.
315. CAT. Scientific recommendation on classification of advanced therapy medicinal products - Alginate encapsulated porcine pancreatic islet cells [22/02/2019]. Available from: https://www.ema.europa.eu/documents/report/scientific-recommendation-classification-advanced-therapy-medicinal-products-alginate-encapsulated_en.pdf.
316. ICH. Mission 2019 [Available from: https://www.ich.org/about/mission.html.
317. Use ICfHoTRfPfH. PHARMACEUTICAL DEVELOPMENT Q8(R2) [Available from: https://www.ich.org/fileadmin/Public_Web_Site/ICH_Products/Guidelines/Quality/Q8_R1/Step4/Q8_R2_Guideline.pdf.
318. EMEA. Guideline on the sterilisation of the medicinal product, active substance, excipient and primary container 2014 [22/02/2019]. Available from: https://www.ema.europa.eu/documents/scientific-guideline/draft-guideline-sterilisation-medicinal-product-active-substance-excipient-primary-container_en.pdf.
319. Honek J. Preclinicalresearch in drug development. Medical Writing. 2017;26(4).

320. Lenzen S. Animal models of human type 1 diabetes for evaluating combination therapies and successful translation to the patient with type 1 diabetes. Diabetes/metabolism research and reviews. 2017;33(7).
321. Brito-Casillas Y, Melián C, Wägner AM. Study of the pathogenesis and treatment of diabetes mellitus through animal models. Endocrinología y Nutrición. 2016;63(7):345-53.
322. Al-Awar A, Kupai K, Veszelka M, Szűcs G, Attieh Z, Murlasits Z, et al. Experimental Diabetes Mellitus in Different Animal Models. Journal of diabetes research. 2016;2016:9051426-.
323. Sakata N, Yoshimatsu G, Tsuchiya H, Egawa S, Unno M. Animal models of diabetes mellitus for islet transplantation. Experimental diabetes research. 2012;2012:256707-.
324. Zhu H, Yu L, He Y, Wang B. Nonhuman Primate Models of Type 1 Diabetes Mellitus for Islet Transplantation. Journal of diabetes research. 2014;2014:9.
325. Bremer AA, Comuzzie AG, Kievit P, Havel PJ. Use and Importance of Nonhuman Primates in Metabolic Disease Research: Current State of the Field. ILAR journal. 2017;58(2):251-68.
326. THE NEED FOR NON-HUMAN PRIMATES IN BIOMEDICAL RESEARCH, PRODUCTION AND TESTING OF PRODUCTS AND DEVICES (UPDATE 2017) 2017 [Available from: https://ec.europa.eu/health/scientific_committees/non-human-primates-testing-9-conclusions_en.
327. King AJF. The use of animal models in diabetes research. British journal of pharmacology. 2012;166(3):877-94.
328. Schook LB, Collares TV, Darfour-Oduro KA, De AK, Rund LA, Schachtschneider KM, et al. Unraveling the swine genome: implications for human health. Annual review of animal biosciences. 2015;3:219-44.
329. Stice MJ, Dunn TB, Bellin MD, Skube ME, Beilman GJ. Omental Pouch Technique for Combined Site Islet Autotransplantation Following Total Pancreatectomy. Cell transplantation. 2018;27(10):1561-8.
330. Wiegand C, Hipler UC. Evaluation of biocompatibility and cytotoxicity using keratinocyte and fibroblast cultures. Skin pharmacology and physiology. 2009;22(2):74-82.
331. Standardisation IOf. ISO 10993-12:2012 [cited 22/02/2019. Available from: https://www.iso.org/standard/53468.html.
332. Standardisation IOf. ISO 10993-5:2009 [22/09/2019]. Available from: https://www.iso.org/standard/36406.html.
333. Rossi SM, Murray TE, Cassidy J, Lee MJ, Kelly HM. A Custom Radiopaque Thermoresponsive Chemotherapy-Loaded Hydrogel for Intratumoural Injection: An In Vitro and Ex Vivo Assessment of Imaging Characteristics and Material Properties. Cardiovascular and interventional radiology. 2019;42(2):289-97.
334. Fatimi A, Zehtabi F, Lerouge S. Optimization and characterization of injectable chitosan-iodixanol-based hydrogels for the embolization of blood vessels. Journal of biomedical materials research Part B, Applied biomaterials. 2016;104(8):1551-62.
335. Chansiri G, Lyons RT, Patel MV, Hem SL. Effect of surface charge on the stability of oil/water emulsions during steam sterilization. Journal of pharmaceutical sciences. 1999;88(4):454-8.
336. Chaturvedi PR, Patel NM, Lodhi SA. Effect of terminal heat sterilization on the stability of phospholipid-stabilized submicron emulsions. Acta pharmaceutica Nordica. 1992;4(1):51-5.
337. Pichot R, Watson RL, Norton IT. Phospholipids at the interface: current trends and challenges. Int J Mol Sci. 2013;14(6):11767-94.
338. Piyasena P, Mohareb E, McKellar RC. Inactivation of microbes using ultrasound: a review. International journal of food microbiology. 2003;87(3):207-16.
339. Monsen T, Lövgren E, Widerström M, Wallinder L. In vitro effect of ultrasound on bacteria and suggested protocol for sonication and diagnosis of prosthetic infections. Journal of clinical microbiology. 2009;47(8):2496-501.
340. Jianying Shen Yl, Yawei Xu, Lei Hou. Biocompatibility of an injectable gel composed of modified hyaluronic acid and adipose-derived mesenchymal cells. Int J Clin Exp Med. 2016;9(10):19567-73.

341. Ghosh K. 28 - Biocompatibility of hyaluronic acid: From cell recognition to therapeutic applications. In: Reis RL, Neves NM, Mano JF, Gomes ME, Marques AP, Azevedo HS, editors. Natural-Based Polymers for Biomedical Applications: Woodhead Publishing; 2008. p. 716-37.
342. Li J, Wang X, Zhang T, Wang C, Huang Z, Luo X, et al. A review on phospholipids and their main applications in drug delivery systems. Asian Journal of Pharmaceutical Sciences. 2015;10(2):81-98.
343. Lee SH, Park HS, Yang Y, Lee EY, Kim JW, Khang G, et al. Improvement of islet function and survival by integration of perfluorodecalin into microcapsules in vivo and in vitro. Journal of tissue engineering and regenerative medicine. 2018;12(4):e2110-e22.
344. Wang Z, Yang Y, Xiang X, Zhu Y, Men J, He M. [Estimation of the normal range of blood glucose in rats]. Wei sheng yan jiu = Journal of hygiene research. 2010;39(2):133-7, 42.
345. EMA. New action plan to foster development of advanced therapies [22/02/2019]. Available from: https://www.ema.europa.eu/en/news/new-action-plan-foster-development-advanced-therapies.
346. Elsanhoury A, Sanzenbacher R, Reinke P, Abou-El-Enein M. Accelerating Patients' Access to Advanced Therapies in the EU. Molecular therapy Methods & clinical development. 2017;7:15-9.
347. EMA. PRIME: priority medicines [22/02/2019]. Available from: https://www.ema.europa.eu/en/human-regulatory/research-development/prime-priority-medicines.

Appendices

Appendix 1

Appendix 1.1 KRB for rat islet GSIS

Chemical	MW	Final Concentration	g/L diH_2O
NaCl	58.44	137	8.0
KCl	74.55	4.7	0.44
KH_2PO_4	136.1	1.2	0.16
$MgSO_4$-$7H_2O$	246.48	1.2	0.3
$CaCl_2$-$2H_2O$	147	2.5	0.37
$NaHCO_3$	84.01	25	2.1
BSA	-	0.5mg/mL	0.5

Appendix 1.2 KRB for INS-1E GSIS

Chemical		MW		Final Concentration	g/L diH_2O	
NaCl		58.44		115mM	6.72	
KCL		74.55		5mM	0.37	
$NaHCO_3$		84.01		24mM	2	
$CaCl_2$	$CaCl_2.2H_2O$	110.98	147	2.2mM	0.24	0.32
$MgCL_2$	$MgCL_2.6H_2O$	95.211	203.31	1mM	0.1	0.21
HEPES		238.3		20mM	4.766	
BSA		-		2mg/mL	2	

Appendix 2

β-Gel preparation procedure for Human Islet study – UCD Shell

To be completed by operator;

Operator & date.	Initials: ⌊__⌋⌊__⌋⌊__⌋ Paraph: _____ ⌊__⌋⌊__⌋/⌊__⌋⌊__⌋/⌊__⌋⌊__⌋ (dd/mm/yy)

Kit contents

Materials

Material description	Supplied by :	Delivery date (dd/mm/yy)
Component A • 1x 1.2mL Native-HA (1.845% w/v) solution in CMRL-1066 in capped 3mL syringe (**Syringe A**) Lot No:	RCSI	⌊__⌋⌊__⌋/⌊__⌋⌊__⌋/⌊__⌋⌊__⌋
Component B • 1x 2mL PFD emulsion (66.78% w/v) in 15mL Falcon tube (**Component B)** Lot No:	RCSI	⌊__⌋⌊__⌋/⌊__⌋⌊__⌋/⌊__⌋⌊__⌋
8x UCD β-shells + 8x Shell caps Lot no: Jan2019	UCD	⌊__⌋⌊__⌋/⌊__⌋⌊__⌋/⌊__⌋⌊__⌋

Consumables

Consumable description	Product/ lot reference	Expiry date (dd/mm/yy)	QC status
8x 3mL Syringe Luer-lok tip BD	8140553 CAV04	30/04/23	**Conform** ☐ **Not conform** ☐ **R&D use only** ☐
4x Combifix Adapter (female-female luer)	18L02A8151	01/10/23	**Conform** ☐ **Not conform** ☐ **R&D use only** ☐
5x 18G 1.2x40mm needles BD Microlance	1807 05	01/01/23	**Conform** ☐ **Not conform** ☐ **R&D use only** ☐
3x Luer lock cap UHS (RED)	32362354	01/08/19	**Conform** ☐ **Not conform** ☐ **R&D use only** ☐

Preparative actions

A Laminar Air Flow is available	yes / no
CMRL 1066 complete medium available (40% serum)	yes / no
8400 IEQ available	_____ IEQ used
Syringe pump available	yes / no
Oxygenation syringe available	yes / no
Qosina Oxyview oxygen flow meter	yes / no
BSL Y-mixer available	yes / no
UCD bracket available	yes / no
All materials stored at 4°C before use	yes / no
VEGF microspheres available (stored at -20°C)	yes / no

Gel Preparation

To prepare β-gel for 4 UCD shells	
1. Vortex **Component B,** the PFD emulsion, for 30 seconds **Confirm Component B selected []**	yes / no Time vortexed : _____
2. Draw 1.5mL PFD emulsion into a 3mL syringe using an 18G needle– **Syringe B**	yes / no PFD emulsion volume :_____ mL
3. Remove the red cap from **Syringe A** and connect it to the female-female luer connector. Fill the air volume of the connector with **Native-HA** from **Syringe A**. **Confirm Syringe A selected []**	yes / no
4. Connect **Syringe B** to the other end of the female-female luer connector.	yes / no
5. Vigorously mix the contents of **Syringe A** into **Syringe B** and then transfer the contents back to **Syringe A.** Repeat this 20-30 times until the mixture appears homogenous and milky.	yes / no Times mixed : _____ Volume **Syringe A** : _____
6. Remove **Syringe B** and the female-female luer connector from **Syringe A**.	yes / no
7. **Oxygenate the emulgel by the oxygenation protocol (Appendix A)**	yes / no
8. Transfer 0.6mL to two fresh syringes: **Syringe C1** and **Syringe C2**	yes / no Volume **Syringe C1** : _____ Volume **Syringe C2** : _____
To prepare β-Gel WITHOUT VEGF	
9. Resuspend 2400 IEQ in 0.2mL of complete medium and transfer to a 3mL syringe – **Syringe D1**	yes / no _____ IEQ used Volume of islet suspension : _____
10. Connect **Syringe C1** to a female-female luer connector and fill the air volume with oxygenated emulgel.	yes / no
11. Connect **Syringe D1** to the female-female luer connector with **Syringe C1**	yes / no

12. First mix the contents of **Syringe C1** into **Syringe D1** and then transfer the contents back to **Syringe C1.** Repeat this 15-20 times, until homogenous +5 additional mixes.	yes / no Times mixed : _____
13. Disconnect the empty **Syringe D1** from the female-female luer.	yes / no Volume **Syringe C1** : _____
14. **Syringe C1** can now be used to fill 2 UCD shells **(Appendix B).**	yes / no
To prepare β-Gel WITH VEGF	
15. Prepare a suspension of 25mg/mL VEGF microspheres in the eppendorf using complete media.	yes / no
16. Resuspend 2400 IEQ in 0.2mL of the VEGF microsphere suspension and transfer to a 3mL syringe – **Syringe D2**	yes / no _____ IEQ used Volume of islet suspension : _____
17. Connect **Syringe C2** to a female-female luer connector and fill the air volume with oxygenated emulgel.	yes / no
18. Connect **Syringe D2** to the female-female luer connector with **Syringe C2.**	yes / no
19. First mix the contents of **Syringe C2** into **Syringe D2** and then transfer the contents back to **Syringe C2.** Repeat this 15-20 times, until homogenous +5 additional mixes.	yes / no Times mixed : _____
20. Disconnect the empty **Syringe D2** from the female-female luer.	yes / no Volume **Syringe C1** : _____
21. **Syringe C2** can now be used to fill 2 UCD shells **(Appendix B).**	yes / no

Comments

The final concentrations for these protocols are:

	Emulgel
Nat-HA	0.615% w/v
PFD	27.8% w/v
Lipoid	3.33…% w/v

Appendix A:

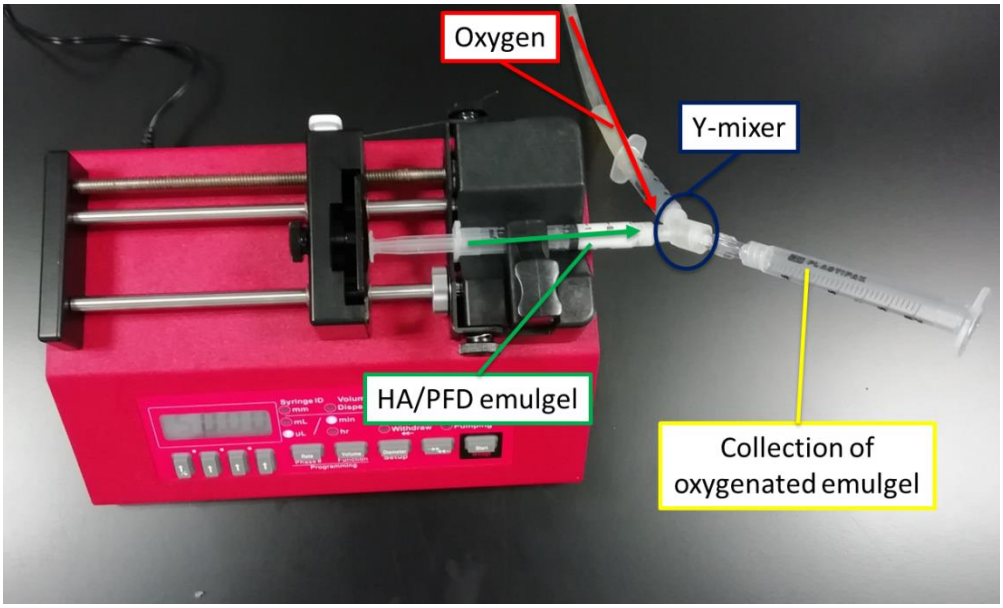

Oxygenation Method	
1. **Syringe A** is connected to the BSL Y-mixer.	yes / no
2. The oxygen supply is connected to the other input of the Y-mixer using a 3mL syringe and tubing	yes / no
3. Remove the plunger from a 3mL syringe (**Syringe C**). Connect a female-female luer to **Syringe C** and connect it to the static mixer opposite the oxygen supply and **Syringe A.**	yes / no
4. Setup in the syringe pump as shown in the image above. **Syringe C** should be angled upwards to prevent the gel from flowing out.	yes / no
5. Set the syringe diameter to 8.66mm on the syringe pump.	yes / no
6. Set the oxygen flow to 1.5L/min	yes / no
7. Start the syringe pump at a rate of 50uL/minute until the content of the syringe is depleted or you have collected ~1.5mL of oxygenated gel (minimum).	yes / no
8. Replace plunger in **Syringe C** and remove remaining air gaps. Return to Step 8 of Gel Preparation protocol.	yes / no

Appendix B:

A

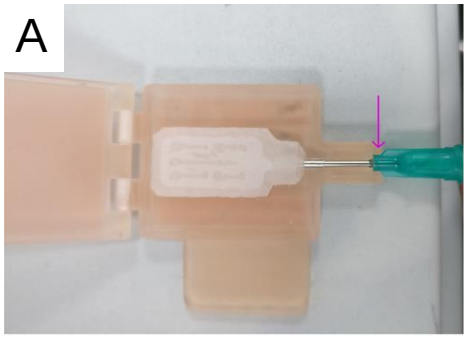

B

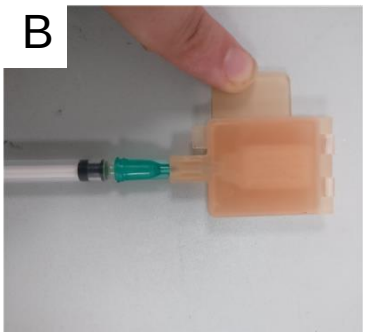

C

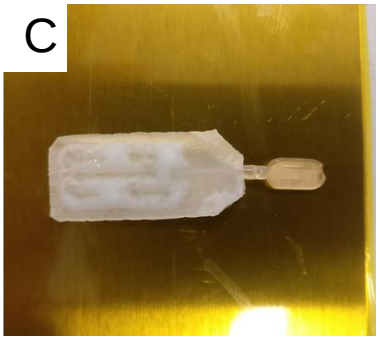

Filling the UCD Shell	
9. Set the syringe diameter to 8.66mm on the syringe pump.	yes / no
10. Set the volume to be dispensed to 0.2mL	yes / no
11. Attach a UCD shell to **Syringe C.**	yes / no
12. Attach the UCD bracket to the green luer lock and close. The bracket should grip the green luer as indicated by the arrow in Figure A	yes / no
13. Start the syringe pump at a rate of 100uL/minute	yes / no
14. When the 0.2mL of gel has been dispensed ensure the syringe pump has stopped.	yes / no
15. Detach the shell from the **Syringe C**, and remove the filling tip. Seal the inlet port with the UCD Shell cap. Once sealed the tab can be snapped off (Figure C).	yes / no
16. Place in a 6 well plate with enough media to cover the body of the shell (6mL).	yes / no
17. Mix the gel in **Syringe C** 5-10 times before filling another shell.	yes / no
18. Repeat Steps 2 – 9 for each shell.	

Appendix C:

Emptying the UCD Shell	
19. Cut off the perimeter of the shell to open the shell	yes / no
20. Wash the insides of the shell using media and collect into a Falcon Tube.	yes / no
21. The islets can now be centrifuged and collected for analysis.	yes / no

Appendix 3

Appendix 3.1

The base formulation used for the protocols was originally calculated for preliminary *in vitro* and *in vivo* studies. These experiments required gel to fill n=3 shells, 0.16mLfill volume and ~0.09-0.1mL dead space.

$$(0.16mL + 0.09mL) \times 3 = 0.75mL$$

Early shell designs could not be filled as reliably as newer designs, and lack of a standardised filling protocol meant shells were prone to bursting. An overage of an additional shell fill was account for in the protocol to overcome this. An additional overage of 0.2mL was included to account for gel loss in female-female luers used of mixing and needle dead spaces, giving a final formulation volume of 1.2mL.

The final gel mixing protocol occurred in two steps:

- Step 1 mixes the natHA and PFD emulsion together to give an intermediate natHA/PFD emulgel
- Step 2 incorporates additional components of the gel such as the cell component or VEGF, diluting the intermediate to the final concentration
- It was decided that ¼ of the final volume (0.3mL) would be made up of the cell/VEGF suspension to give sufficient volume to manipulate the component
- The PFD emulsion starting concentration was set at 66.78% w/v
- The target PFD concentration was 30% w/v PFD
- The target HA concentration was 0.615% w/v natHA

The calculation to determine starting volumes of PFD emulsion and natHA volume and concentration are detailed below.

$$Dilution\ equation: Concentration_1 \times Volume_1 = Concentration_2 \times Volume_2$$

$$C1V1 = C2V2$$

For PFD emulsion volume:

$$(\text{Final Volume})(\text{Target PFD Conc})(\text{Intermediate dilution})(\text{Intermediate PFD Conc})$$

$$1.2mL \times 30\%w/v = 0.9mL \times A$$

$$A = \frac{1.2 \times 30}{0.9}$$

$$A = 40\%w/v$$

$$(\text{Stock PFD Volume})(\text{Stock PFD Conc})(\text{Intermediate dilution})(\text{Intermediate PFD Conc})$$

$$B \times 6678\%w/v = 0.9mL \times 40\%w/v$$

$$B = \frac{0.9 \times 40}{6678}$$

$$B = 0.54mL$$

The equipment used for mixing and measuring in these experiments was 3mL syringes, which limited the volumes that could be used to 0.1mL graduations. Rounding down the starting PFD volume to 0.5mL gives a final concentration:

$$(\text{Stock PFD Volume})(\text{Stock PFD Conc})(\text{Intermediate dilution})(\text{Intermediate PFD Conc})$$

$$0.5mL \times 6678\%w/v = 0.9mL \times C$$

$$C = \frac{0.5 \times 6678}{0.9}$$

$$C = 3710\%w/v$$

$$(\text{Final Volume})(\text{Final PFD Conc})(\text{Intermediate dilution})(\text{Intermediate PFD Conc})$$

$$1.2mL \times D = 0.9mL \times 3710\%w/v$$

$$D = \frac{0.9 \times 3710}{1.2}$$

$$D = 2783\%w/v$$

Knowing the target natHA concentration at 0.615%, and the available volume remaining in the intermediate step (0.4mL) the starting concentration of HA can be calculated as below:

For natHA starting concentration:

(Final Volume)(Target natHA %)(Intermediate Volume)(Intermediate natHA %)

$$1.2mL \times 0.615\%w/v = 0.9mL \times A$$

$$A = \frac{1.2 \times 0.615}{0.9}$$

$$A = 0.82\%w/v$$

(Stat Vol)(Stat %)(Intermediate vol)(Intermediate %)

$$0.4mL \times B = 0.9mL \times 0.82\%w/v$$

$$B = \frac{0.9 \times 0.82}{0.4}$$

$$B = 1.845\%w/v$$

Appendix 3.2

The overages provided for this protocol allow for the preparation of three times the amount of natHA/PFD emulgel intermediate to be prepared for the oxygenation step. This is done to ensure that there is enough intermediate available after oxygenation step.

This protocol requires a total of 1.2mL of oxygenated intermediate (0.6mL of oxygenated emulgel transferred to two fresh syringes), and so the base formulation is not suitable as only 0.9mL of intermediate is prepared, before accounting for any loss. Double of the base formulation gives 1.8mL before any loss. This volume could be sufficient for the protocol before loss; however there are a number of dead volumes associated with the protocol up to this point in the protocol. These are:

- 0.05mL loss per female-female luer used: 1. Mixing the intermediate natHA/PFD emulgel, 2. During the oxygenation protocol, 3. Transfer to the fresh syringes.
- The y-mixer used in the oxygenation protocol has a 0.25-0.3mL dead space.

$$(0.6mL \times 2) + (0.05mL \times 3) + 0.3mL = 1.65mL$$

It is possible that this protocol could have been completed using double the volume of the base formulation, however as this protocol was using scarcely available human islets, and the cost of the natHA/PFD emulgel components are moderately low, providing sufficient excess to account for any loss was deemed acceptable.

Appendix 3.3

To minimise waste of human islets, the overages were minimised as much as possible.

The shells used for this study, in combination with a defined filling protocol need 0.2mL per fill, accounting for 0.16mL fill volume and 0.04mL dead space, and two shells were needed per experimental group. To prepare enough of the final natHA/PFD emulgel to fill the n=2 shells, plus one extra fill for potential burst shells, plus excess, the protocol makes up 0.8mL of final natHA/PFD emulgel.

The final natHA/PFD emulgels for this study needed 480 IEQ/shell and 1mg VEGF microspheres/shell

<u>For IEQ density:</u>

The final fill volume of the shells is 0.16mL:

$$480\ IEQ/0.16mL$$
$$2{,}400\ IEQ/0.8mL$$

The protocol details that 2,400 IEQ should be suspended in 0.2mL and transferred to the syringe, and this will then be mixed with the 0.6mL intermediate and diluted to the final concentration of 2,400 IEQ/0.8mL. Although this leaves no overages, discussion with the DRIVE partners in Oxford were confident this could be done in order to minimise waste of human islets. The protocol also includes a section to record deviations if they were deemed necessary on the day of the experiment.

<u>For VEGF concentration:</u>

$$1mg/0.16mL$$
$$5mg/0.8mL$$
$$5mg\ /\ 0.2mL = 25mg/mL$$

By preparing a 25mg/mL VEGF microsphere suspension, 0.2mL of this can be used to resuspend the islets to give the final concentration when mixed with the 0.6mL intermediate. At this density and islet count the size of the islet pellet should not affect the final concentrations; however this will need to be considered when entering studies using larger volumes with higher islet counts.